The Biosynthetic Pathway of Kainoids

by

Una Patricia Ramsey

Submitted in partial fulfilment of the requirements for the degree of Doctor of Philosophy

at

Dalhousie University
Halifax, Nova Scotia

Sept, 1994

ISBN 0-315-98928-9

Name UNA PATRICIA RAMSEY

Dissertation Abstracts International is arranged by broad, general subject categories. Please select the one subject which most nearly describes the content of your dissertation. Enter the corresponding four-digit code in the spaces provided.

BIOCHEMISTRY — SUBJECT TERM

0487 — SUBJECT CODE

U·M·I

Subject Categories

THE HUMANITIES AND SOCIAL SCIENCES

COMMUNICATIONS AND THE ARTS
Architecture 0729
Art History 0377
Cinema 0900
Dance 0378
Fine Arts 0357
Information Science 0723
Journalism 0391
Library Science 0399
Mass Communications 0708
Music 0413
Speech Communication 0459
Theater 0465

EDUCATION
General 0515
Administration 0514
Adult and Continuing 0516
Agricultural 0517
Art 0273
Bilingual and Multicultural 0282
Business 0688
Community College 0275
Curriculum and Instruction 0727
Early Childhood 0518
Elementary 0524
Finance 0277
Guidance and Counseling 0519
Health 0680
Higher 0745
History of 0520
Home Economics 0278
Industrial 0521
Language and Literature 0279
Mathematics 0280
Music 0522
Philosophy of 0998
Physical 0523
Psychology 0525
Reading 0535
Religious 0527
Sciences 0714
Secondary 0533
Social Sciences 0534
Sociology of 0340
Special 0529
Teacher Training 0530
Technology 0710
Tests and Measurements 0288
Vocational 0747

LANGUAGE, LITERATURE AND LINGUISTICS
Language
- General 0679
- Ancient 0289
- Linguistics 0290
- Modern 0291

Literature
- General 0401
- Classical 0294
- Comparative 0295
- Medieval 0297
- Modern 0298
- African 0316
- American 0591
- Asian 0305
- Canadian (English) 0352
- Canadian (French) 0355
- English 0593
- Germanic 0311
- Latin American 0312
- Middle Eastern 0315
- Romance 0313
- Slavic and East European 0314

PHILOSOPHY, RELIGION AND THEOLOGY
Philosophy 0422
Religion
- General 0318
- Biblical Studies 0321
- Clergy 0319
- History of 0320
- Philosophy of 0322

Theology 0469

SOCIAL SCIENCES
American Studies 0323
Anthropology
- Archaeology 0324
- Cultural 0326
- Physical 0327

Business Administration
- General 0310
- Accounting 0272
- Banking 0770
- Management 0454
- Marketing ..... [illegible]

Canadian Studies ..... [illegible]
Economics
- General 0501
- Agricultural 0503
- Commerce-Business 0505
- Finance 0508
- History 0509
- Labor 0510
- Theory 0511

Folklore 0358
Geography 0366
Gerontology 0351
History
- General 0578
- Ancient 0579
- Medieval 0581
- Modern 0582
- Black 0328
- African 0331
- Asia, Australia and Oceania 0332
- Canadian 0334
- European 0335
- Latin American 0336
- Middle Eastern 0333
- United States 0337

History of Science 0585
Law 0398
Political Science
- General 0615
- International Law and Relations 0616
- Public Administration 0617

Recreation 0814
Social Work 0452
Sociology
- General 0626
- Criminology and Penology 0627
- Demography 0938
- Ethnic and Racial Studies 0631
- Individual and Family Studies 0628
- Industrial and Labor Relations 0629
- Public and Social Welfare 0630
- Social Structure and Development 0700
- Theory and Methods 0344

Transportation 0709
Urban and Regional Planning 0999
Women's Studies 0453

THE SCIENCES AND ENGINEERING

BIOLOGICAL SCIENCES
Agriculture
- General 0473
- Agronomy 0285
- Animal Culture and Nutrition 0475
- Animal Pathology 0476
- Food Science and Technology 0359
- Forestry and Wildlife 0478
- Plant Culture 0479
- Plant Pathology 0480
- Plant Physiology 0817
- Range Management 0777
- Wood Technology 0746

Biology
- General 0306
- Anatomy 0287
- Biostatistics 0308
- Botany 0309
- Cell 0379
- Ecology 0329
- Entomology 0353
- Genetics 0369
- Limnology 0793
- Microbiology 0410
- Molecular 0307
- Neuroscience 0317
- Oceanography 0416
- Physiology 0433
- Radiation 0821
- Veterinary Science 0778
- Zoology 0472

Biophysics
- General 0786
- Medical 0760

EARTH SCIENCES
Biogeochemistry 0425
Geochemistry 0996
Geodesy 0370
Geology 0372
Geophysics 0373
Hydrology 0388
Mineralogy 0411
Paleobotany 0345
Paleoecology 0426
Paleontology 0418
Paleozoology 0985
Palynology 0427
Physical Geography 0368
Physical Oceanography 0415

HEALTH AND ENVIRONMENTAL SCIENCES
Environmental Sciences 0768
Health Sciences
- General 0566
- Audiology 0300
- Chemotherapy 0992
- Dentistry 0567
- Education 0350
- Hospital Management 0769
- Human Development 0758
- Immunology 0982
- Medicine and Surgery 0564
- Mental Health 0347
- Nursing 0569
- Nutrition 0570
- Obstetrics and Gynecology 0380
- Occupational Health and Therapy 0354
- Ophthalmology 0381
- Pathology 0571
- Pharmacology 0419
- Pharmacy 0572
- Physical Therapy 0382
- Public Health 0573
- Radiology 0574
- Recreation 0575
- Speech Pathology 0460
- Toxicology 0383

Home Economics 0386

PHYSICAL SCIENCES
Pure Sciences

Chemistry
- General 0485
- Agricultural 0749
- Analytical 0486
- Biochemistry 0487
- Inorganic 0488
- Nuclear 0738
- Organic 0490
- Pharmaceutical 0491
- Physical 0494
- Polymer 0495
- Radiation 0754

Mathematics 0405
Physics
- General 0605
- Acoustics 0986
- Astronomy and Astrophysics 0606
- Atmospheric Science 0608
- Atomic 0748
- Electronics and Electricity 0607
- Elementary Particles and High Energy 0798
- Fluid and Plasma 0759
- Molecular 0609
- Nuclear 0610
- Optics 0752
- Radiation 0756
- Solid State 0611

Statistics 0463

Applied Sciences

Applied Mechanics 0346
Computer Science 0984

Engineering
- General 0537
- Aerospace 0538
- Agricultural 0539
- Automotive 0540
- Biomedical 0541
- Chemical 0542
- Civil 0543
- Electronics and Electrical 0544
- Heat and Thermodynamics 0348
- Hydraulic 0545
- Industrial 0546
- Marine 0547
- Materials Science 0794
- Mechanical 0548
- Metallurgy 0743
- Mining 0551
- Nuclear 0552
- Packaging 0549
- Petroleum 0765
- Sanitary and Municipal 0554
- System Science 0790

Geotechnology 0428
Operations Research 0796
Plastics Technology 0795
Textile Technology 0994

PSYCHOLOGY
General 0621
Behavioral 0384
Clinical 0622
Developmental 0620
Experimental 0623
Industrial 0624
Personality 0625
Physiological 0989
Psychobiology 0349
Psychometrics 0632
Social 0451

DEDICATION

This thesis is dedicated to my grandfather:

ROBERT THOMAS REGINALD ALLEN

28 July 1895 - 13 March 1981

Tempo, Co. Fermanagh, Northern Ireland

For encouraging my curiosity and drive to understand the world.

He is remembered with great fondness.

TABLE OF CONTENTS

Table of Contents.....v

List of Figures.....viii

List of Tables.....xiv

Abstract.....xv

Abbreviations and Symbols used.....xvi

Acknowledgements.....xix

INTRODUCTION.....1

CHAPTER ONE: THE PATHWAY OF DOMOIC ACID BIOSYNTHESIS IN THE PENNATE DIATOM *PSEUDONITZSCHIA PUNGENS F. MULTISERIES*.....21

Introduction.....22

Methods and Materials.....30

Culturing and growth of phytoplankton.....30

Label preparation, addition to culture, and harvest.....32

Domoic acid sample analyses and purification.35

Nuclear magnetic resonance spectroscopy.....37

Statistical tests.....39

Results.....41

Stable isotope labelling experiments.....41

Growth curves.....41

[1-^{13}C]-acetate labelling experiment.....48

[1,2-^{13}C]-acetate labelling experiment...48

Timed labelling experiments with [1,2-^{13}C]-acetate.....58

[2-^{13}C,$^{2}H_3$]-acetate labelling experiment.....58

Radioactive isotope labelling experiments....62

Growth curves.....62

[1,5-^{14}C]-citric acid, [1-^{14}C]-α-ketoglutarate and L[1-^{14}C]-glutamate labelling experiments.....66

Discussion.....73

CHAPTER TWO: THE SEARCH FOR INTERMEDIATES IN THE BIOSYNTHESIS OF DOMOIC ACID AND KAINIC ACID.....97

Introduction.....98

Methods and Materials.....108

Algal cultures.....108

Extraction of free amino acids from plankton.....110

Isolation of 1'-hydroxydihydrokainic acid from *P. palmata*.....111

Nuclear magnetic resonance spectroscopy.....114

Mass spectrometry and infrared spectroscopy.....115

Results.....116

Amino acid profiles of *Pseudonitzschia* spp..116

Amino acid profiles of the *Palmaria palmata* mutant.....129

Isolation and identification of 1'-hydroxydihydrokainic acid.....129

Discussion.....148

CHAPTER THREE: PRELIMINARY ENZYME STUDIES IN THE BIOSYNTHESIS OF KAINOIDS.....151

Introduction.....152

Methods and Materials.....164

Dimethylallylpyrophosphate and geranyl-pyrophosphate synthesis and purification....164

Kainic acid prenyltransferase enzyme assays.164

Gliotoxin and (+)-limonene experiments.....167

Results..... 169

DMAPP and GPP synthesis and purification....169

Kainic acid prenyltransferase enzyme assays.169

Gliotoxin and (+)-limonene experiments.....175

Discussion.....184

CONCLUSION.....189

APPENDIX: THE CONSTRUCTION OF A cDNA LIBRARY FROM *PSEUDONITZSCHIA PUNGENS* F. *MULTISERIES*.....194

BIBLIOGRAPHY.....197

LIST OF FIGURES

FIGURE 1: The Kainoids.....3

FIGURE 2: The Structure of Saxitoxin and Neosaxitoxin...8

FIGURE 3: The Putative Pathway of Saxitoxin Synthesis...9

FIGURE 4: The Incorporation of Stable Isotopes into Neosaxitoxin.....11

FIGURE 5: The Structures of Brevetoxin A and B.....12

FIGURE 6: Acetate Incorporation Pattern and Putative Precursors of Brevetoxin.....14

FIGURE 7: The Incorporation of [2-^{13}C]-Acetate into Putative Precursors of Brevetoxin B.....15

FIGURE 8: Proposed Method of Ring Closure in Brevetoxin B Synthesis.....16

FIGURE 9: The Incorporation of Acetate into Okadaic Acid and The Proposed Precursors.....18

FIGURE 10: The Structure of Ciguatoxin.....19

FIGURE 11: Three Putative Pathways of Domoic Acid Biosynthesis.....23

FIGURE 12: The Incorporation of Acetate into an Isoprenoid Chain.....24

FIGURE 13: Incorporation of Acetate in Glutamate Biosynthesis.....26

FIGURE 14: The Incorporation of Acetate in Proline Biosynthesis.....27

FIGURE 15: The Incorporation of Acetate in Fatty Acid Biosynthesis.....29

FIGURE 16: Calculation of Probabilities of ^{13}C at Carbon B when ^{13}C at Carbon A.....40

FIGURE 17: Growth Curve and Domoic Acid Production by *Pseudonitzschia pungens* f. *multiseries* Strain 13CC with [1-^{13}C]-Acetate Added on Days 13, 14 and 15.....42

FIGURE 18: Growth Curve and Domoic Acid Production by *Pseudonitzschia pungens* f. *multiseries* Strain 13CC with [1,2-^{13}C]-Acetate Added on Days 6, 7 and 8....43

FIGURE 19: Growth Curve and Domoic Acid Production by *Pseudonitzschia pungens* f. *multiseries* Strain KP59/2 with [1,2-^{13}C]-Acetate Added Early in Growth of Culture on Day 4.....45

FIGURE 20: Growth Curve and Domoic Acid Production by *Pseudonitzschia pungens* f. *multiseries* Strain KP59/2 with [1,2-^{13}C]-Acetate Added Late in Growth of Culture on Day 7.....46

FIGURE 21: Growth Curve and Domoic Acid Production by *Pseudonitzschia pungens* f. *multiseries* Strain KP59/2 with [2-^{13}C,$^{2}H_3$]-Acetate Added.....47

FIGURE 22: An Expansion of the ^{13}C-NMR Spectrum for Domoic Acid Labelled with [1,2-^{13}C]-Acetate.....51

FIGURE 23: [1,2-^{13}C]-Acetate Labelling Pattern of Domoic Acid from *Pseudonitzschia pungens* f. *Multiseries* Strain 13CC.....57

FIGURE 24: An Expansion of the ^{13}C-NMR Spectrum for Domoic Acid Labelled with [2-^{13}C,$^{2}H_3$]-Acetate.....60

FIGURE 25: Growth Curve and Domoic Acid Production by *Pseudonitzschia pungens* f. *multiseries* Strain KP59/2 with [1,5-^{14}C]-Citrate Added Just Prior to the Stationary Phase of Growth.....63

FIGURE 26: Growth Curve and Domoic Acid Production by *Pseudonitzschia pungens* f. *multiseries* Strain KP59/2 with [1-^{14}C]-α-Ketoglutarate Added Just Prior to the Stationary Phase of Growth.....64

FIGURE 27: Growth Curve and Domoic Acid Production by *Pseudonitzschia pungens* f. *multiseries* Strain KP59/2 with L[1-^{14}C]-Glutamate Added Just Prior to the Stationary Phase of Growth.....65

FIGURE 28: Total Amount of Domoic Acid Synthesized in Cultures of *Pseudonitzschia pungens* f. *multiseries* with [1,5-^{14}C]-Citrate, [1-^{14}C]-α-Ketoglutarate and L[1-^{14}C]-Glutamate.....67

FIGURE 29: % Incorporation of [1,5-^{14}C]-Citrate, [1-^{14}C]-α-Ketoglutarate or L[1-^{14}C]-Glutamate into *Pseudonitzschia pungens* f. *multiseries* Cells.....68

FIGURE 30: Incorporation of [1,5-^{14}C]-Citrate, [1-^{14}C]-α-Ketoglutarate or L[1-^{14}C]-Glutamate into Domoic Acid.....69

FIGURE 31: The Incorporation of Acetate into an Isoprenoid Chain.....75

FIGURE 32: Labelling of Domoic Acid with [1,2-^{13}C]-Acetate During One Round of the Citric Acid Cycle.....77

FIGURE 33: Labelling of Domoic Acid with [1,2-^{13}C]-Acetate During the Second Round of the Citric Acid Cycle.....78

FIGURE 34: Labelling of Domoic Acid with [1,2-^{13}C]-Acetate During the Three Rounds of the Citric Acid Cycle.....79

FIGURE 35: [2-^{13}C,$^{2}H_3$]-Acetate Labelling of an Isoprenoid Chain.....88

FIGURE 36: Labelling of Domoic Acid with [2-^{13}C,$^{2}H_3$]-Acetate During the First Round of the Citric Acid Cycle.....89

FIGURE 37: Labelling of Domoic Acid with [2-^{13}C,$^{2}H_3$]-Acetate During the Second Round of the Citric Acid Cycle.....90

FIGURE 38: Formation of Furan and Pyran Rings from Prenyl Group.....100

FIGURE 39: The Incorporation of the Prenyl Group in the Biosynthesis of Ergoline and Indole Alkaloids.....101

FIGURE 40: The Attachment of Linear Prenyl Groups onto O, N, S Atoms of Compounds Originating from Different Biogenetic Sources.....102

FIGURE 41: Putative Steps in Domoic Acid Biosynthesis.....104

FIGURE 42: Biogenesis of the Kainoids.....105

FIGURE 43: Putative Pathways of Acromelic Acid Biosynthesis.....107

FIGURE 44: Amino Acid Profile of Axenic *Pseudonitzschia pungens* f. *multiseries* Strain 13CC During Late Exponential Growth.....117

FIGURE 45: Amino Acid Profile of Axenic *Pseudonitzschia australis*.....118

FIGURE 46: Amino Acid Profile of Xenic *Pseudonitzschia pungens* f. *multiseries* Strain KP72 Grown with $NaNO_3$ as the Sole N Source.....119

FIGURE 47: Amino Acid Profile of Xenic *Pseudonitzschia pungens* f. *multiseries* Strain KP76 Grown with $NaNO_3$ as the Sole N Source.....120

FIGURE 48: Amino Acid Profile of Xenic *Pseudonitzschia pungens* f. *multiseries* Strain KP82 Grown with $NaNO_3$ as the Sole N Source.....121

FIGURE 49: Amino Acid Profile of Xenic *Pseudonitzschia pungens* f. *multiseries* Strain KP82 Grown with NH_4Cl as the Sole N Source.....123

FIGURE 50: Amino Acid Profile of Xenic *Pseudonitzschia pungens* f. *pungens* Strain KP42 Grown with $NaNO_3$ as the Sole N Source.....124

FIGURE 51: Amino Acid Profile of Xenic *Pseudonitzschia pungens* f. *pungens* Strain KP43 Grown with $NaNO_3$ as the Sole N Source.....125

FIGURE 52: Amino Acid Profile of Xenic *Pseudonitzschia pungens* f. *pungens* Strain KP42 Grown with NH_4Cl as the Sole N Source.....126

FIGURE 53: Amino Acid Profile of Xenic *Pseudonitzschia pungens* f. *pungens* Strain KP55 Grown with $NaNO_3$ as the Sole N Source.....127

FIGURE 54: Amino Acid Profile of Xenic *Pseudonitzschia pungens* f. *pungens* Strain KP57 Grown with $NaNO_3$ as the sole N Source.....128

FIGURE 55: Amino Acid Profile of Xenic *Pseudonitzschia pungens* f. *pungens* Strain KP57 Grown with NH_4Cl as the Sole N Source.....130

FIGURE 56: Amino Acid Profile of *Palmaria palmata* Mutant (GM).....131

FIGURE 57: X-Ray SEM Analyses of (A) the Chelex-100 Spheres Before 1'-Hydroxydihydrokainic Acid Was Added to the Top of the Column and (B) the Resulting Blue Spheres After 1'-Hydroxydihydrokainic Acid Was Eluted.....133

FIGURE 58: X-Ray SEM Analyses of (A) the Carbon Planchet Sample Holder and (B) the Carbon Planchet with the Pre-chelex-100 1'-Hydroxydihydrokainic Acid Added.....134

FIGURE 59: The ^{13}C-NMR Spectrum of 1'-Hydroxydihydrokainic Acid at pD 1.76.....136

FIGURE 60: HMQC Spectrum of 1'-Hydroxydihydrokainic acid at pD 1.76.....138

FIGURE 61: The ^{1}H-NMR Spectrum of 1'-Hydroxydihydrokainic Acid at pD 1.76.....139

FIGURE 62: 2D-COSY NMR Spectrum of 1'-Hydroxydihydrokainic Acid at pD 1.76.....141

FIGURE 63: HMBC NMR Spectrum of 1'-Hydroxydihydrokainic Acid at pD 1.76.....142

FIGURE 64: 2D-NOESY NMR Spectrum of 1'-Hydroxydihydrokainic Acid at pD 4.12.....144

FIGURE 65: Several Kainoid Structures.....145

FIGURE 66: Interactions Among Protons of 1'-Hydroxydihydrokainic Acid Based on NOESY Data pD 4.12.....146

FIGURE 67: The Reactions Mediated by the Prenyltransferase in Glyceollin and Phaseollin Synthesis.....153

FIGURE 68: The Reactions Mediated by the Prenyltransferases in the Synthesis of Furocoumarins and *O*-prenylated Coumarins.....154

FIGURE 69: The Reactions Mediated by the Prenyltransferases in the Prenylation of tRNA, Proteins and in Strictosidine Synthesis.....157

FIGURE 70: Structures of Gliotoxin and (+)-Limonene...162

FIGURE 71: ^{1}H-NMR Spectrum of Purified DMAPP.....170

FIGURE 72: ^{1}H-NMR Spectrum of Purified GPP.....171

FIGURE 73: The Autoradiograph of the Kainic Acid Prenyltransferase Assay After 1 h.....172

FIGURE 74: The Autoradiograph of the Kainic Acid Prenyltransferase Assay After 24 h.....173

FIGURE 75: The Effect of Gliotoxin on the Growth of *Pseudonitzschia pungens* f. *multiseries* Strain KP59/2.....176

FIGURE 76: The Effect of Gliotoxin on Domoic Acid Production by *Pseudonitzschia pungens* f. *multiseries* Strain KP59/2.....177

LIST OF TABLES

TABLE 1: Culture Volumes, Labelled Precursors and Strains of Axenic *Pseudonitzschia pungens* f. *multiseries* Used in Feeding Experiments.....31

TABLE 2: The % Absolute ^{13}C Enrichment in Domoic Acid.....49

TABLE 3: DPM Values for Domoic Acid Purified from *Pseudonitzschia pungens* f. *multiseries* Cells Grown with Added [1,5-^{14}C]-Citrate, [1-^{14}C]-α-Ketoglutarate or L[1-^{14}C]-Glutamate Normalized to the Amount of Domoic Acid Produced by the Cultures.....70

TABLE 4: DPM Values for Domoic Acid Purified from *Pseudonitzschia pungens* f. *multiseries* Cells Grown with Added [1,5-^{14}C]-Citrate, [1-^{14}C]-α-Ketoglutarate or L[1-^{14}C]-Glutamate Normalized to the Cellular DPM.....72

TABLE 5: Xenic *Pseudonitzschia* spp.Cultures Provided by Dr. J. Smith.....109

TABLE 6: NMR Data for 1'-Hydroxydihydrokainic Acid.....135

TABLE 7: 1D-^{1}H NMR Data for Kainic Acid and 1'-Hydroxydihydrokainic Acid.....140

TABLE 8: The Effects of Gliotoxin on the Growth of *Pseudonitzschia pungens* f. *multiseries* Strain KP59/2.....179

TABLE 9: The Effects of Gliotoxin on Domoic Acid Production by *Pseudonitzschia pungens* f. *multiseries* Strain KP59/2.....180

TABLE 10: The Effects of (+)-Limonene on the Growth of *Pseudonitzschia pungens* f. *multiseries* Strain KP59/2.....181

TABLE 11: The Effects of (+)-Limonene on Domoic Acid Production by *Pseudonitzschia pungens* f. *multiseries* Strain KP59/2.....183

ABSTRACT

Domoic acid and kainic acid are neurotoxic amino acids that belong to a group of compounds called the kainoids. The pathway of domoic acid biosynthesis was investigated in the photosynthetic single-celled plankton or diatom *Pseudonitzschia pungens* f. *multiseries* using both ^{13}C- and ^{14}C-labelled precursors. Labelling with [1,2-^{13}C]-acetate revealed that domoic acid is biosynthesized by the condensation of an isoprenoid chain with a citric acid cycle product. The addition of [1,2-^{13}C]-acetate early and late during exponential growth did not affect the resulting ^{13}C enrichment pattern. Further studies with [2-^{13}C,$^{2}H_3$]-acetate showed that the hydroxyl group of isocitrate is converted to a carbonyl group before the transamination reaction, suggesting that the citric acid cycle product is a derivative of glutamate. [1,5-^{14}C]-Citrate, [1-^{14}C]-α-ketoglutarate and L[1-^{14}C]-glutamate were incorporated into domoic acid at low levels.

The *Palmaria palmata* mutant GM, a known producer of kainic acid, was examined for possible intermediates of kainic acid biosynthesis. An unknown secondary amino acid was isolated and identified as 1'-hydroxydihydrokainic acid. This compound is probably formed by hydration of kainic acid and is unlikely to be a precursor of kainic acid. 1'-Hydroxy-dihydrokainic acid is able to chelate both calcium and copper and may function as a metal detoxifier within the cells.

Two protein prenylation inhibitors, gliotoxin and (+)-limonene did not inhibit domoic acid biosynthesis in *P. pungens* f. *multiseries*. (+)-Limonene at a final concentration of 0.5 μM did result in an increase in domoic acid production. Preliminary kainic acid prenyltransferase assays with [1,5-^{14}C]-citrate, [1-^{14}C]-α-ketoglutarate or L[1-^{14}C]-glutamate added did not produce ^{14}C-labelled kainic acid.

LIST OF ABBREVIATIONS AND SYMBOLS USED

A	angstrom
ACP	acyl carrier protein
amp	ampere
ASP	amnesic shellfish poisoning
AVG	average
BK	background
C_{DMSO}	moles dimethylsulfoxide
C_{DA}	moles domoic acid
°C	degrees Celsius
cDNA	complementary deoxyribonucleic acid
CFP	ciguatera fish poisoning
Ci	Curie
cm	centimetre
CoA	Coenzyme A
COSY	correlation spectroscopy
CPM	counts per minute
δ	chemical shift in parts per million
d	distilled
D	deuterium
1D	one dimensional
2D	two dimensional
DA	domoic acid
DEPT	distortionless enhancement by polarization transfer
DC	direct current
DMAPP	dimethylallylpyrophosphate
DMSO	dimethylsulfoxide
DOPA	dihydroxyphenylalanine
DPM	disintegration per minute
DSP	diarrhetic shellfish poisoning
DTT	dithiothreitol
E_{DA}	absolute ^{13}C enrichment of domoic acid
F., f.	forma
Fig.	figure
Figs.	figures
FMOC-Cl	9-fluorenylmethyl-chloroformate
g	grams
GGT	geranylgeranyltransferase
GPP	geranylpyrophosphate
GTP	guanosine 5'-triphosphate
h	hour
HMBC	heteronuclear multiple bond correlation
HMG	hydroxymethylglutarate
HMQC	heteronuclear multiple quantum correlation
HPLC	high performance liquid chromatography
HVPE	high voltage paper electrophoresis
Hz	hertz

I_{DA}	average integral per carbon of domoic acid
I_{DMSO}	average integral per carbon of DMSO
IPP	isopentenylpyrophosphate
J_{cc}	coupling constants
kb	kilobase
kDa	kilodalton
kg	kilogram
K_m	Michaelis-Menten constant
L	litre
Log	logarithm
LSIMS	liquid secondary ion mass spectroscopy
m	metre
M	molar
µE	microEinstein
mg	milligram
MHz	megahertz
min	minute
µL	microlitre
mL	millilitre
µm	micrometre
µM	micromolar
mm	millimetre
mM	millimolar
mRNA	messenger ribonucleic acid
MVA	L-mevalonic acid
m/z	mass-to-charge ratio
N	north
NAD+	β-nicotinamide-adenine dinucleotide
NADH	β-nicotinamide-adenine dinucleotide, reduced
NADP+	β-nicotinamide-adenine dinucleotide phosphate
nCi	nanoCurie
ng	nanogram
nm	nanometre
NMR	nuclear magnetic resonance spectroscopy
NOE	nuclear overhauser effect
NOESY	nuclear overhauser effect spectroscopy
OPP	pyrophosphate
P	probability
PMSF	phenylmethylsulfonyl fluoride
PolyA	poly adenylated
ppm, PPM	parts per million
PSP	paralytic shellfish poisoning
R_f	ratio to front
RNA	ribonucleic acid
rpm	revolutions per minute
RT	retention time
s	seconds
SEM	scanning electron microscope
sp.	species (singular)
spp.	species (plural)
STD	standard deviation
SWM	seawater media

TLC	thin layer chromatography
tRNA	transfer ribonucleic acid
UV	ultraviolet
W	west
xg	times force of gravity

ACKNOWLEDGEMENTS

I acknowledge and thank the following people at the Institute for Marine Biosciences, National Research Council: David Tappen for showing me how to make F/2 media. Dr. D. Douglas for providing me with axenic strains of *Pseudonitzschia* spp. Patricia LeBlanc, Cheryl Craft and Dr. M. Laycock for providing me with advice and guidance during the chemical purification of domoic acid and 1'-hydroxydihydrokainic acid. Robert Richards for introducing me to the amino acid analyzer. Don Leek for recording the NMR spectra and Dr. J. Walter for his patience and guidance in my quest to understand NMR. Denise LeBlanc for Mass Spectroscopy of 1'-hydroxydihydrokainic acid. David O'Neil for X-ray SEM metal analyses. Jeff Gallant and Cindy Leggiadro for help with the photography and Dr. A. McCulloch for critical review of the thesis. I would like to thank all those still at IMB and some who have moved on to other endeavours for their advice, encouragement and friendship over the past four years.

Thanks to Dr. J. Smith at the Department of Fisheries and Oceans, Moncton for several samples of *Pseudonitzschia* spp. for amino acid analysis. I gratefully acknowledge the contribution of Jeffery Wright, Krista Pronk, and Dr. R.

Pocklington for domoic acid analyses at the Bedford Institute of Oceanography.

I would like to sincerely thank my supervisor, Dr. J.L.C. Wright, for introducing me to the fascinating world of secondary metabolites and for his guidance and encouragement during this research project. I appreciate the advice of my committee members Dr. L. Vining, Dr. S. Douglas and Dr. M. Gray. I gratefully acknowledge the financial support of NSERC during the past four years and the Sumner Fellowship during my final year of study.

The unwavering support of my family over the past four years is greatly appreciated. Lastly, loving thanks go to my husband, Bruce, for his love, encouragement, advice and understanding which made completion of my research possible.

INTRODUCTION

Domoic acid, kainic acid and acromelic acids A and B are all members of a group of neurologically active amino acids called the kainoids (Fig 1; Laycock et al., 1989; Konno et al., 1988). All of these compounds are structurally similar to glutamic acid, which has long been known as a neurotransmitter (Shinozaki et al., 1986; Olney, 1990). The neurotoxicities of both domoic acid and kainic acid result from their selective binding to kainate receptor sites on nerve endings in the central nervous system (Debonnel et al., 1990; Hampson et al., 1990). Domoic acid and kainic acid have also been shown to have insecticidal and anthelmintic properties (Maeda et al., 1984; Lincoln et al., 1990).

Domoic acid was first identified in the marine red alga *Chondria armata* Okam. from coastal Japan and later in other red algae *Chondria baileyana* and *Alsidium corallinum* (Takemoto and Daigo, 1958; Bates et al., 1988; Impellizzeri et al., 1975). α-Kainic acid has also been reported in red algae but in the species *Digenea simplex* (Wulf.) C.Ag., *Alsidium helminthocorton*, *Centroceras clavulatum*, and the Chinese and Mediterranean isolates of *Calglossa leprieurii* (Murakami et al., 1953; Nitta et al., 1958; Balansard et al., 1982; Impellizzeri et al., 1975; Pie-Gen and Shan-Lin, 1986). More recently it has been reported in a spontaneous mutant of *Palmaria palmata* collected from the Atlantic coastline of Canada (Laycock et al., 1989).

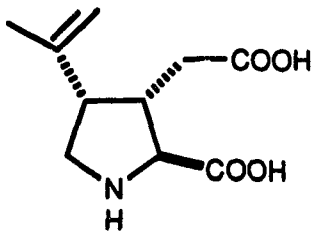

KAINIC ACID

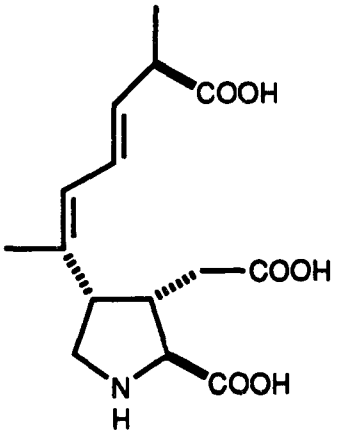

DOMOIC ACID

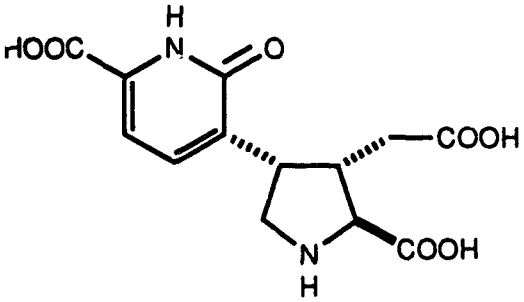

ACROMELIC ACID A

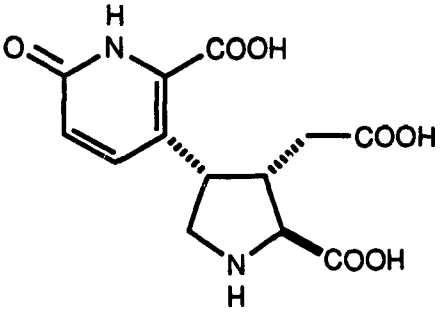

ACROMELIC ACID B

FIGURE 1: THE KAINOIDS

An outbreak of human poisoning occurred in Canada in 1987 resulting from the ingestion of blue mussels (*Mytilus edulis* L.) from the Cardigan Bay area of eastern Canada that were contaminated with domoic acid (Wright et al., 1989). Three deaths resulted along with 153 cases of intoxication (Bates et al., 1988; Perl et al., 1990). Due to the neurological symptoms, which included memory loss, disorientation and coma, the illness caused by domoic acid was named Amnesic Shellfish Poisoning (ASP) (Quilliam and Wright, 1989; Waldichuk, 1989; Perl et al., 1990). Later, the organism producing the domoic acid toxin was discovered to be the marine diatom *Pseudonitzschia pungens* forma *multiseries* (formerly *Nitzschia pungens* Grunow forma *multiseries* Hasle) (Bates et al., 1988; Rao et al., 1988). Diatoms are single-celled photosynthetic algae that are known to grow seasonally to high densities (bloom) in coastal areas (Burckle, 1978; Smayda, 1990). In this case, a dense bloom of the domoic acid-producing diatom *Pseudonitzschia pungens* f. *multiseries* in Cardigan Bay, P.E.I. was filtered from the water column by local mussels, which concentrated the neurotoxin to levels of *ca.* 1000 ppm. This was the first reported case of a diatom producing a toxic metabolite. The reoccurrence of seasonal toxic blooms of *Pseudonitzschia pungens* f. *multiseries* have been reported in P.E.I. in subsequent years, suggesting that this was not an isolated incident (Bates et al., 1989a; Smith et al., 1989).

Later research has shown that isolates of *Pseudonitzschia pungens* f. *multiseries* from the Gulf of Mexico are also able to produce domoic acid (Dickey et al., 1992). The diatom *Pseudonitzschia pseudodelicatissima* (formerly *Nitzschia pseudodelicatissima*) has also been implicated in the production of domoic acid discovered in soft-shell clams and blue mussels in the Bay of Fundy, N.B., Canada in both 1988 and 1990 (Martin et al., 1993).

In 1991 on the Pacific coast, in the Monterey Bay area of California, deaths of brown pelicans and Brandt's cormorants were believed to be caused by the ingestion of domoic acid-containing northern anchovies (Wright, 1992; Work et al., 1993). The source of the domoic acid was another diatom, *Pseudonitzschia australis* Frenguelli (previously *Nitzschia pseudoseriata* Hasle; Fritz et al., 1992; Garrison et al., 1992). This bloom was apparently widespread on the west coast, extending from Monterey Bay, California, to Alaska (Horner et al., 1994). Domoic acid poisoning of humans in Washington due to ingestion of toxic razor clams led to further investigations in both Washington and Oregon, that revealed that Dungeness crabs also contained domoic acid (Wright, 1992). Domoic acid has also been found in marine invertebrates along the coast of British Columbia since 1992, with the majority of domoic acid-containing samples from the Barkley, Clayoquot, and Quatsino Sound areas on the west coast

of Vancouver Island (Forbes and Chiang, 1994; Whyte et al., 1994).

Incidences of ASP have also been reported outside of North America. The first report of ASP in New Zealand was in 1993, when numerous cases of human poisoning occurred due to ingestion of contaminated mussels (Chang et al., 1993). Two potential ASP-producing organisms, *Pseudonitzschia pungens* and *P. australis,* were both present in the water column at the time of the ASP outbreak (Chang et al., 1993). Isolates of *Pseudonitzschia* spp. shown to produce domoic acid have also been recovered from the coastal waters of Denmark (Lundholm et al., 1994). *Pseudonitzschia pungens* is widely distributed and in high abundance in Chinese coastal waters, although it is not clear if these isolates have the ability to produce domoic acid (Zou et al., 1993).

The problem of toxic algal blooms resulting in toxic shellfish is not a recent occurrence. Cases of Paralytic Shellfish Poisoning (PSP) have been documented on the north-west Pacific coast of Canada for centuries (Kao, 1993). Symptoms of PSP include numbness in the lips and mouth, prickly sensations in the fingertips and toes, headaches, dizziness and distinct muscular weakness resulting from the blockage of cellular voltage-gated sodium channels (Kao, 1993). Saxitoxin, a tetrahydropurine, was the first water

soluble PSP toxin identified (Fig. 2). Since its isolation, 18 structurally related compounds have been classified as PSP toxins; these are generally divided into the saxitoxin or neosaxitoxin structural groups (Fig. 2; Kao, 1993). These general structures are further modified by the presence of 11-O-sulfate or N-sulfate groups, the absence of oxygen at C-13 and the absence of the carbamoyl group (for review see Shimizu, 1993). PSP toxins are produced by blooms of unicellular biflagellate algae or dinoflagellates from the genus *Alexandrium*, including *A. acatenella*, *A. catenella*, *A. excavatum*, *A. fundyense* and *A. tamarense*, as well as *Gymnodinium catenatum* and the South Pacific dinoflagellate *Pyrodinium bahamense* var. *compressa* (Anderson, 1989; Shimizu, 1993; Cembella and Todd, 1993). In addition, saxitoxin and neosaxitoxin are also produced by the freshwater cyanobacterium *Aphanizomenon flos-aquae* and are found in the tropical or subtropical calcareous red algae *Jania* spp. (Shimizu, 1988).

The biosynthesis of neosaxitoxin has been investigated in *Aphanizomenon flos-aquae* (for review see Shimizu, 1993). The results of labelling experiments suggest that the tricyclic skeleton is formed by the condensation of acetate with the α-carbon of arginine and, the subsequent loss of arginine's carboxyl group, followed by amidation and cyclization (Fig. 3; Shimizu, 1988). Labelling experiments revealed the

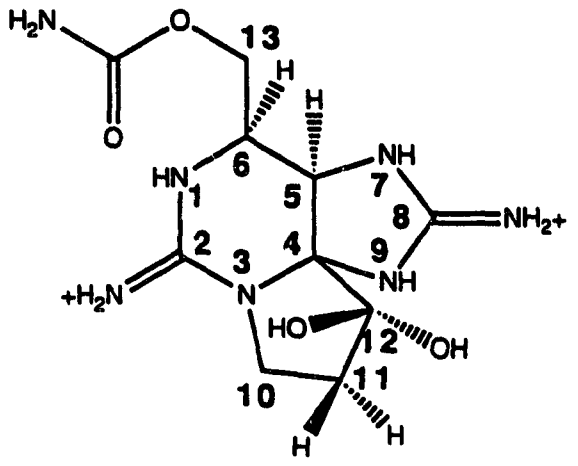

SAXITOXIN

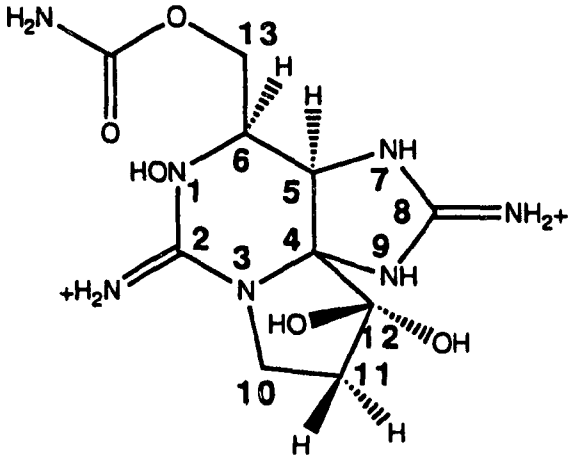

NEOSAXITOXIN

FIGURE 2: THE STRUCTURES OF SAXITOXIN AND NEOSAXITOXIN

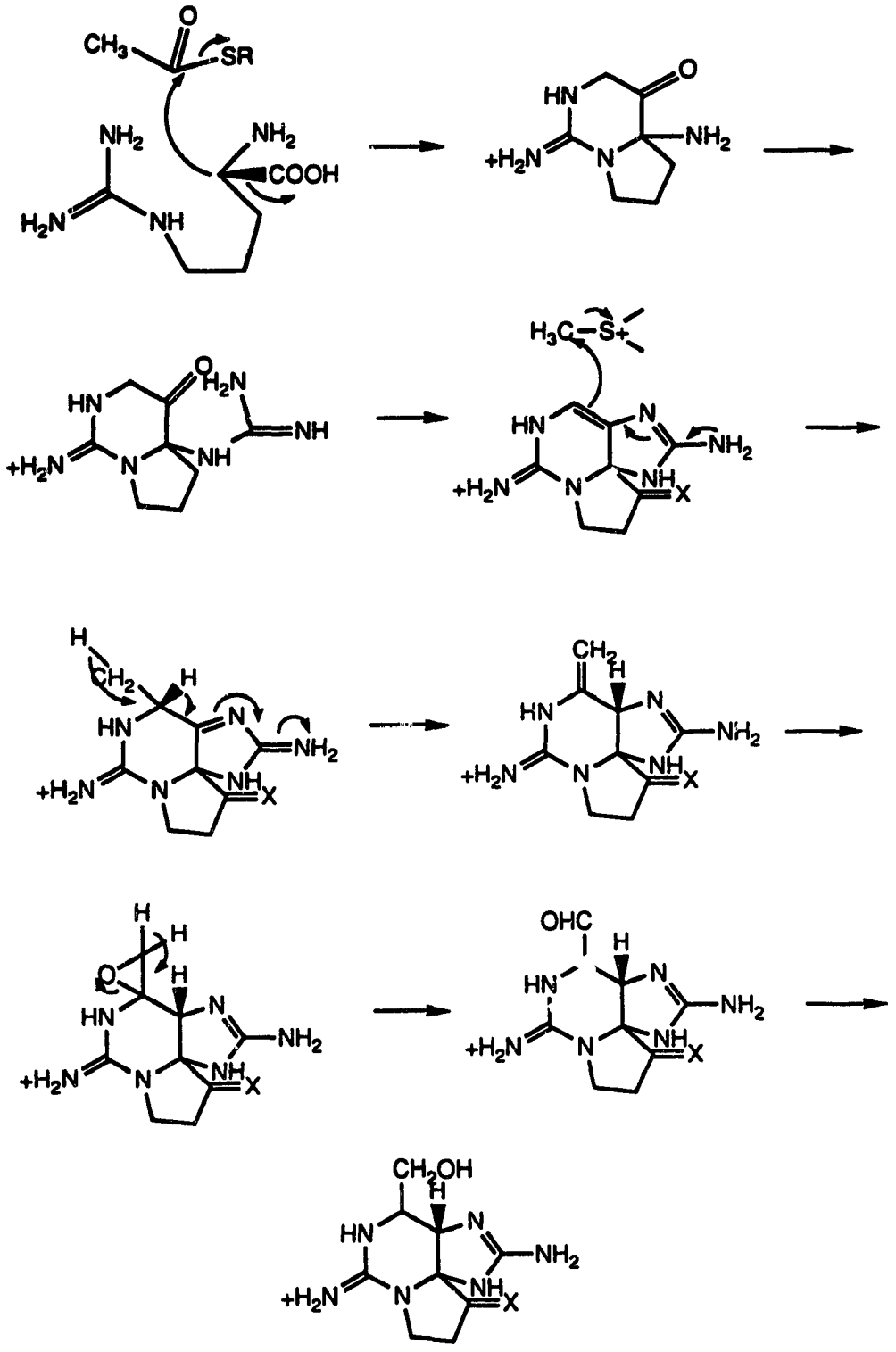

FIGURE 3: THE PUTATIVE PATHWAY OF SAXITOXIN SYNTHESIS (modified from Shimizu, 1993)

incorporation of [1,2-^{13}C]-acetate at positions C5 and C6 and of [2-^{13}C, 2-^{15}N]-arginine at C4 and C9 with the ^{13}C-^{15}N bond intact (Fig 4; Shimizu et al., 1984). Biosynthetic experiments with [1,2-^{13}C,$^{2}H_3$]-acetate revealed the presence of one deuterium at C5 probably originating from the acetate methyl group at C6 by a 1,2-hydride shift (Gupta et al., 1989). Feeding of [methyl-^{13}C,$^{2}H_3$]-methionine resulted in enrichment at C13 of neosaxitoxin with only one deuterium attached, suggesting that C13 originates from methionine via *S*-adenosylmethionine but that the methyl group undergoes subsequent oxidation (Gupta et al., 1989). The resulting terminal methylene group may then be converted to an epoxide, which opens to an aldehyde with subsequent reduction producing the terminal carbinol group (Fig 3; Shimizu, 1993).

Brevetoxins A and B, produced by the dinoflagellate *Gymnodinium breve*, are responsible for both human poisoning due to the consumption of contaminated shellfish and also fish kills (Fig. 5; Lee et al., 1986). Brevetoxins A and B both function by inducing cellular sodium channels (Baden and Trainer, 1993). Originally, it was thought that the brevetoxin polyether structure originated from a single polyketide chain derived from acetate with the methyl branches resulting either from the substitution of propionate for acetate or from methionine via methylation by *S*-adenosylmethionine (for review see Garson, 1993 and Shimizu,

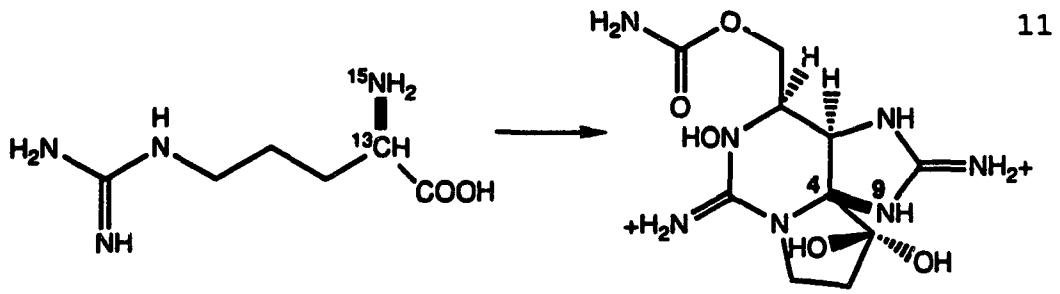

[2-^{13}C, 2-^{15}N]-ARGININE NEOSAXITOXIN

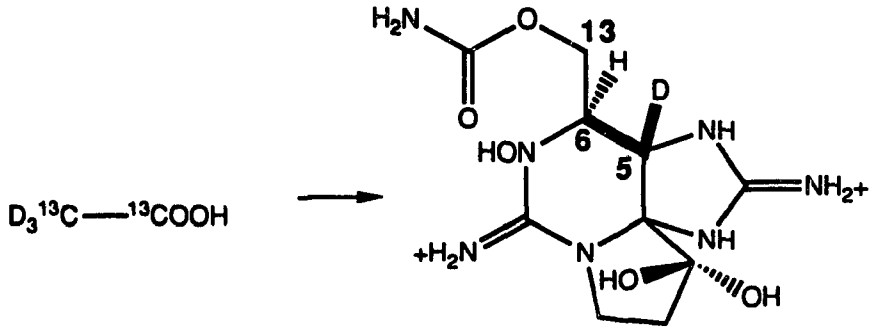

[1,2-^{13}C,$^{2}H_3$]-ACETATE NEOSAXITOXIN

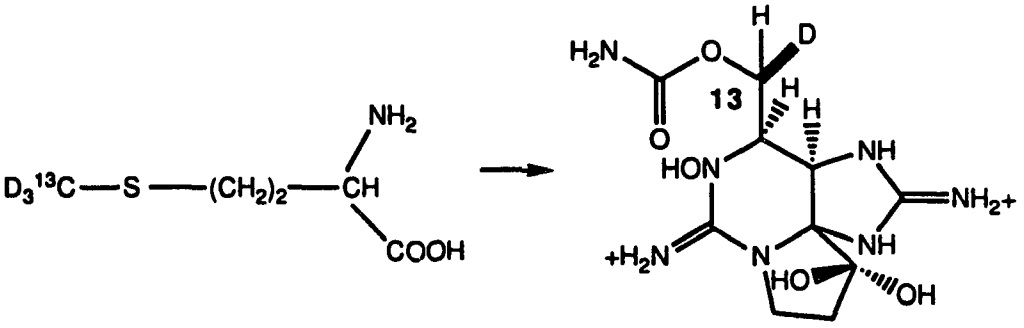

[*methyl*-^{13}C,$^{2}H_3$]-METHIONINE NEOSAXITOXIN

FIGURE 4: THE INCORPORATION OF STABLE ISOTOPES IN NEOSAXITOXIN (modified from Shimizu, 1993)

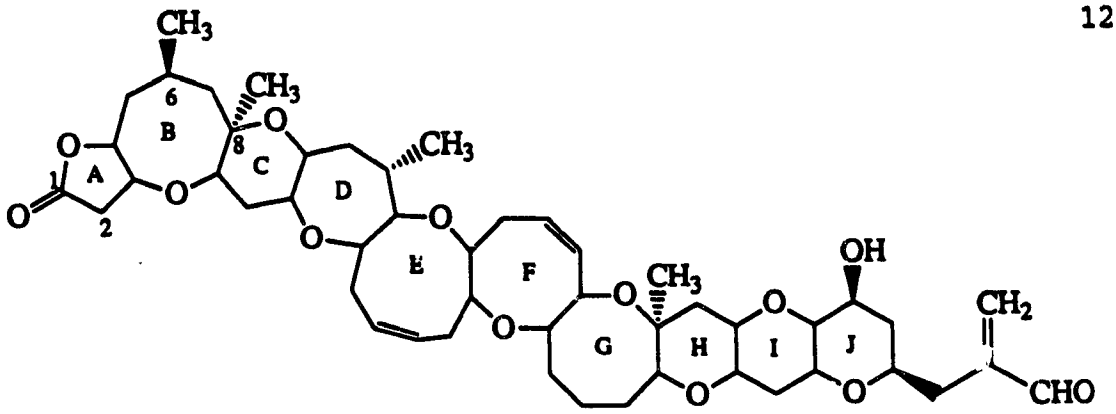

BREVETOXIN A

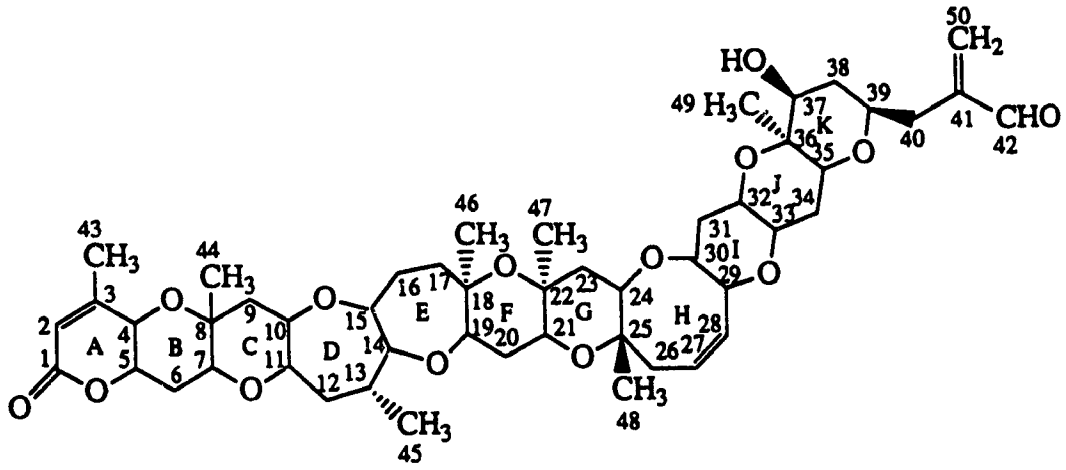

BREVETOXIN B

FIGURE 5: THE STRUCTURES OF BREVETOXIN A AND B

1993). Initial biosynthetic studies of Brevetoxin B with acetate and methionine revealed a pattern of incorporation which suggested the polyketide was instead synthesized from precursors originating from mixed biogenetic sources (Fig. 6; Chou and Shimizu, 1987). The methyl groups at C8, C22, C25 and C36 were derived from methionine whereas those at C3 and C18 appeared to be derived from acetate units followed by decarboxylation (Lee et al., 1989). The presence of ^{13}C-^{13}C couplings in brevetoxin from feeding experiments with [2-^{13}C]-acetate was explained by the involvement of dicarboxylic acids (such as succinate) originating from the citric acid cycle (Fig. 7; Lee et al., 1989). The labelling pattern also suggested the involvement of another dicarboxylic acid, hydroxymethylglutarate (HMG), an intermediate in isoprenoid synthesis (Fig. 7; Chou and Shimizu, 1987). It was proposed that the polyketide chain was formed by a new pathway in which C_4 and C_5 dicarboxylic acids condense followed by decarboxylation. Finally a novel cyclization process has been proposed in which the *trans*-double bonds of the polyene undergo epoxidation, and the final all-*trans* cyclic structure is formed by an epoxide-opening cascade (Fig. 8; Lee et al., 1989).

Another group of toxins produced by algal blooms are those that are responsible for Diarrhetic Shellfish Poisoning (DSP). The symptomatology includes diarrhea, nausea, vomiting

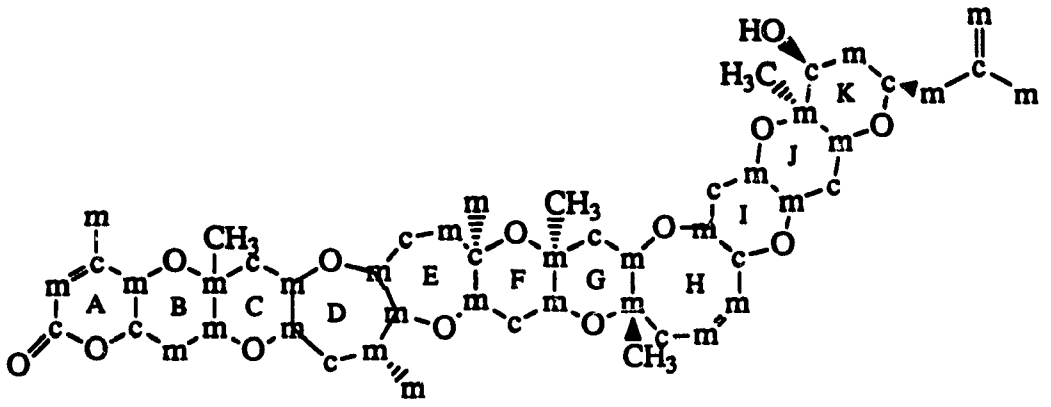

m - acetate methyl group
c - acetate carboxyl group

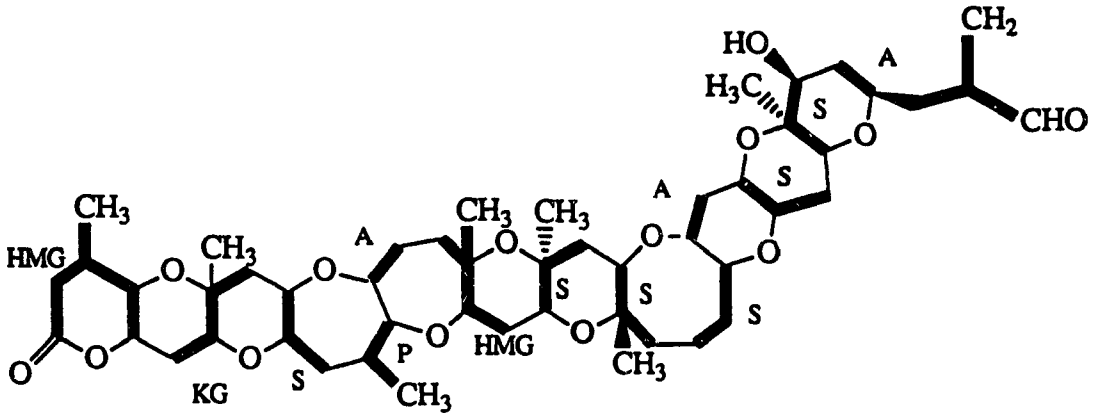

S - dicarboxylic acid such as succinate
HMG - hydroxymethylglutarate
P - propionate
A - acetate
KG- α-ketoglutarate

FIGURE 6: ACETATE INCORPORATION PATTERN AND PUTATIVE PRECURSORS OF BREVETOXIN (modified from Shimizu, 1993)

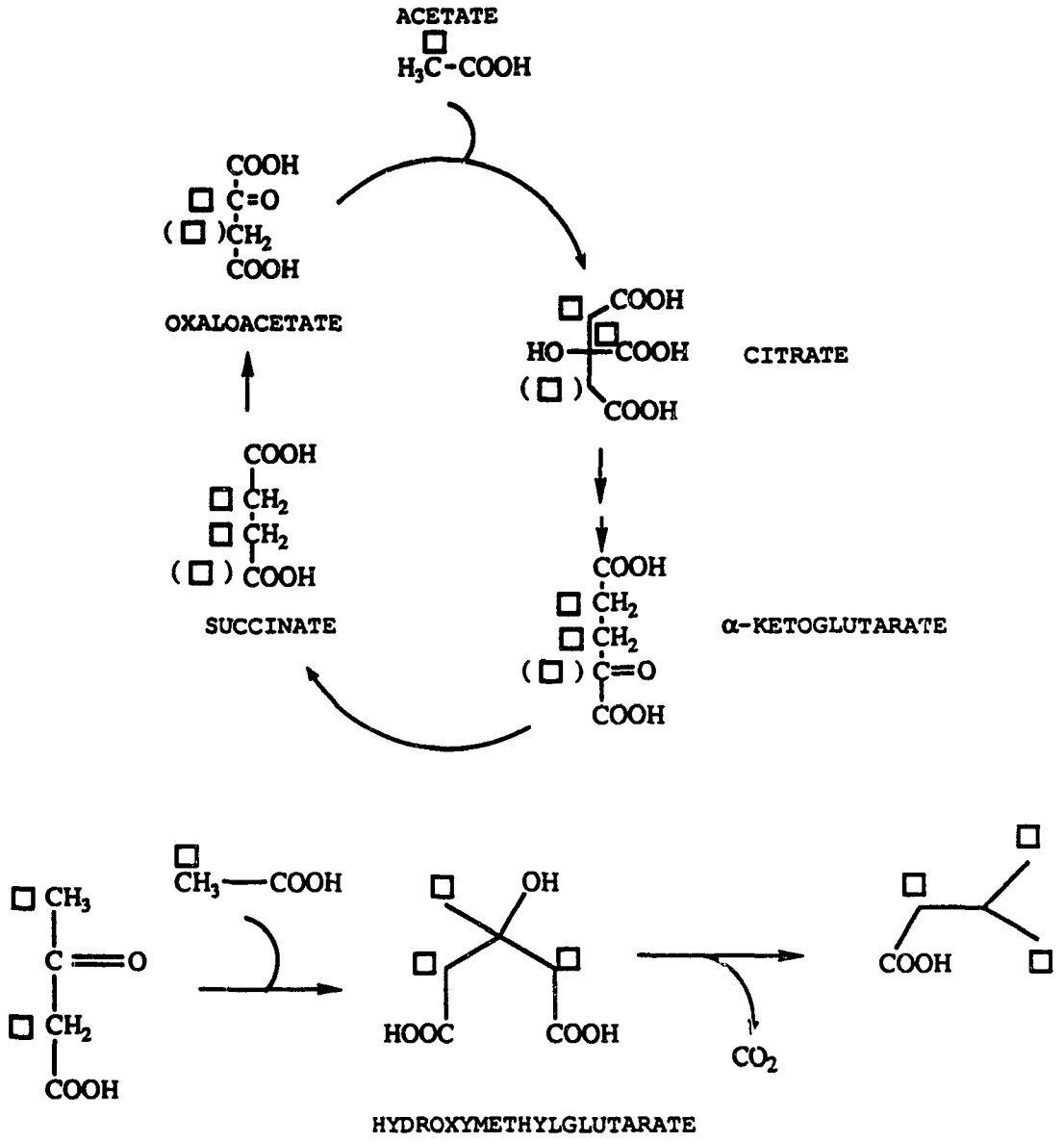

FIGURE 7: THE INCORPORATION OF [2-^{13}C]-ACETATE INTO PUTATIVE PRECURSORS OF BREVETOXIN B.
(The square represents the methyl group of acetate; modified from Shimizu, 1993)

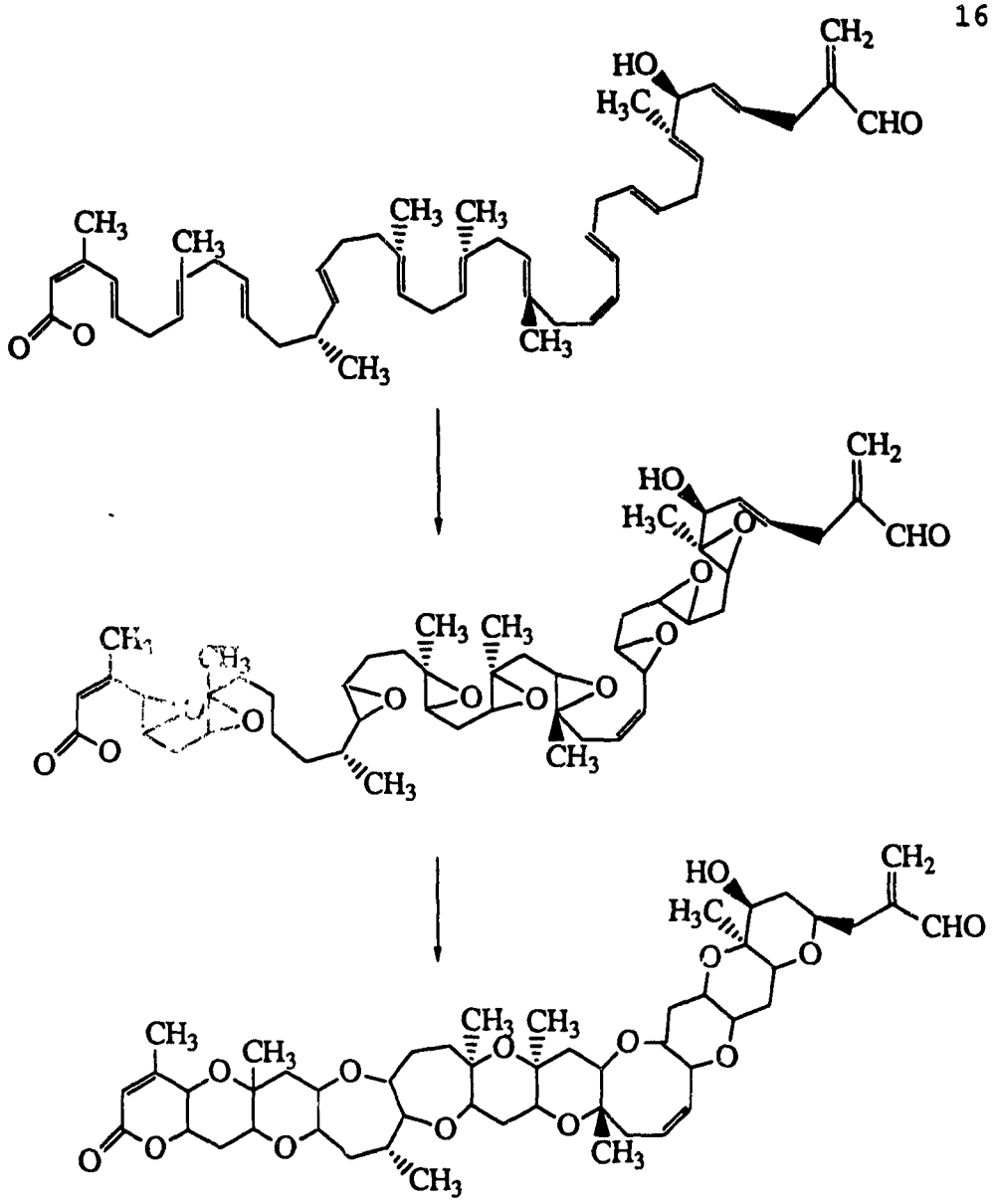

FIGURE 8: PROPOSED METHOD OF RING CLOSURE IN BREVETOXIN B SYNTHESIS (modified from Lee et al., 1989; Garson, 1993)

and abdominal pain (Aune and Yndestad, 1993). Okadaic acid and related compounds probably produce DSP symptoms by stimulating the phosphorylation of proteins that control sodium secretion by intestinal cells or those that regulate solute permeability, thus resulting in passive loss of fluids (Fig. 9; Aune and Yndestad, 1993). The location of okadaic acid in the fatty tissue of shellfish is due to lipophilic properties conferred by its polyether structure (Aune and Yndestad, 1993). Dinoflagellates from the genera *Dinophysis* (*D. fortii, D. norvegica, D. acuta, D. mitra, D. rotundata, D. tripes* and *D. acuminata)* and *Prorocentrum* (*P. lima* and *P. concavum*) are known producers of okadaic acid (Aune and Yndestad, 1993; Cembella and Todd, 1993; Shimizu, 1993). The biosynthesis of okadaic acid has been studied in *P. lima* where initial ^{13}C-labelled acetate feeding experiments suggested the involvement of acetate, citrate, succinate and hydroxymethylglutarate (Fig. 9; see for review Garson, 1993 and Shimizu, 1993), and this was confirmed by later studies (Norte et al., 1994). The pattern of labelling in okadaic acid suggests a similar pathway to that in brevetoxin biosynthesis.

Ciguatoxin, another polyether toxin, was identified as the compound responsible for ciguatera fish poisoning (CFP), which results from ingestion of fish from tropical waters (Fig. 10; for review see Garson, 1993). The suspected

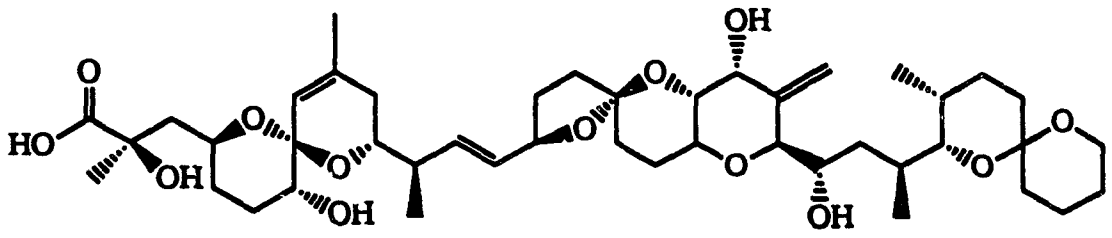

OKADAIC ACID

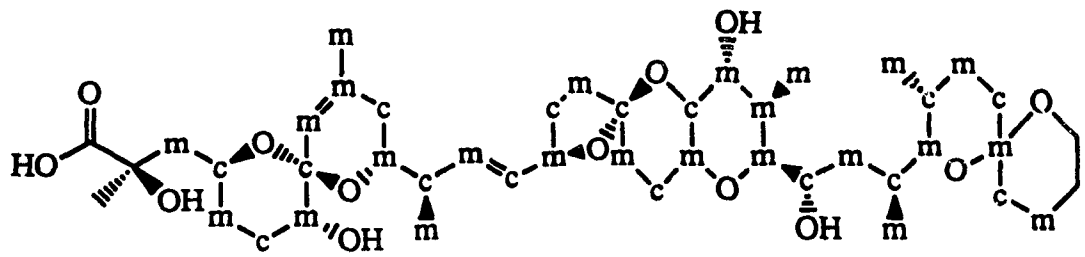

m-acetate methyl group
c-acetate carboxyl group

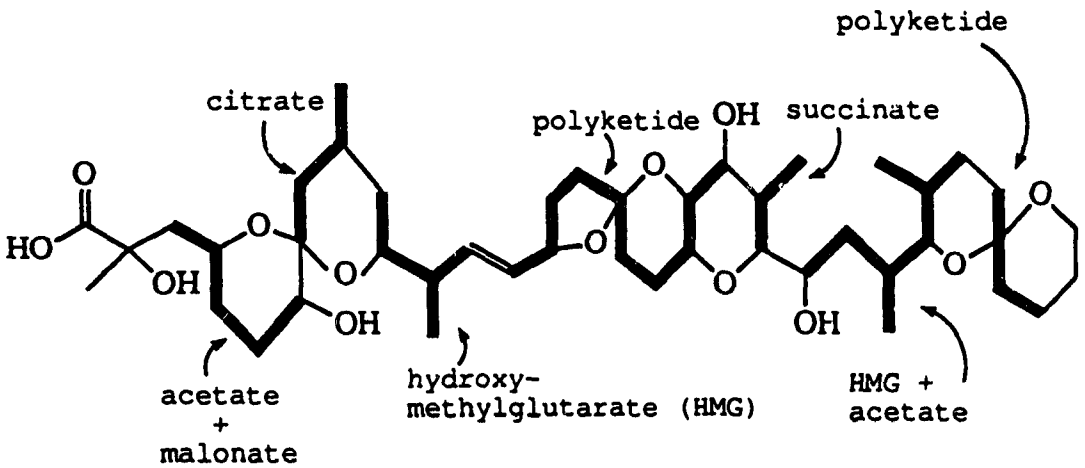

FIGURE 9: THE INCORPORATION OF ACETATE INTO OKADAIC ACID AND THE PROPOSED PRECURSORS (modified from Schmitz and Yasumoto, 1991; Shimizu, 1993)

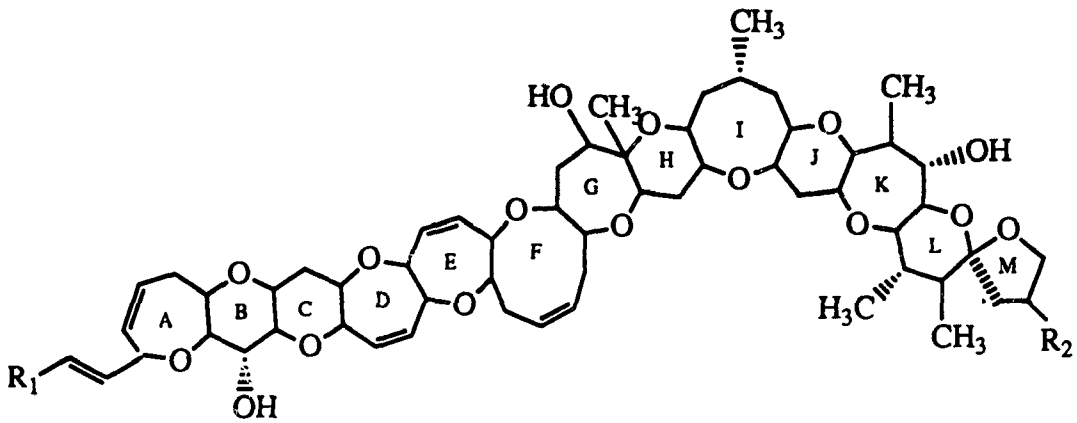

CIGUATOXIN (R_1=$HOCH_2CH(OH)$; R_2=OH)

GT4b (R_1=CH_2=CH ; R_2=H)

FIGURE 10: THE STRUCTURE OF CIGUATOXIN (modified from Garson, 1993)

causative organism is the dinoflagellate *Gambierdiscus toxicus* (Murata et al., 1990). The structurally similar gambiertoxin-4b (GT4b) has been proposed as a biosynthetic intermediate (Fig. 10; Murata et al., 1990). Biosynthetic studies have not been reported for ciguatoxin, although it might be expected to be derived by a mechanistic path similar to that observed for the brevetoxins.

The increasing frequency and distribution of toxic phytoplankton blooms suggests that this problem is reaching a global scale, yet basic biological questions remain to be answered (Smayda, 1989; Smayda, 1990). The research described in this thesis was designed to investigate the pathway of domoic acid and kainic acid biosynthesis and the biosynthetic enzymes involved in the process. The first chapter discusses the elucidation of the pathway of domoic acid biosynthesis in *Pseudonitzschia pungens* f. *multiseries* using precursor compounds labelled with stable isotopes and radioisotopes. The second chapter examines several producers of domoic acid and kainic acid for possible intermediates in the pathway of kainoid synthesis. The final chapter discusses preliminary enzyme studies.

CHAPTER ONE

THE PATHWAY OF DOMOIC ACID BIOSYNTHESIS IN THE PENNATE DIATOM *PSEUDONITZSCHIA PUNGENS* f. *MULTISERIES*

INTRODUCTION

Until work described in this thesis was begun the biosynthetic pathway of kainoids remained unknown. The structural similarity of members of this group, in particular domoic acid and kainic acid, suggests a common biosynthetic pathway for this group of compounds (Laycock et al., 1989). This chapter examines the biosynthesis of one of the kainoids, domoic acid, by the pennate diatom *Pseudonitzschia pungens* f. *multiseries* using isotopically labelled precursors. Several pathways of domoic acid biosynthesis have been proposed based on the structure of the molecule. Three putative pathways will be examined in more detail.

In the first putative pathway, an isoprenoid chain condenses with an activated C5 unit, possibly a derivative of a citric acid cycle product, to produce the proline ring system (see Pathway 1 in Fig. 11; Laycock et al., 1989). The putative biosynthetic precursors, although originating from different biogenetic sources, are both originally derived from acetate (Mann, 1987). The isoprenoid chain in this pathway is most likely synthesized from acetate in the usual way (Fig. 12). Acetyl-SCoenzyme A (SCoA) and acetoacetyl-SCoA condense together to form 3-hydroxy-3-methylglutaryl-SCoA, which is subsequently converted to L-mevalonic acid (MVA). MVA undergoes phosphorylation to produce MVA-5-pyrophosphate,

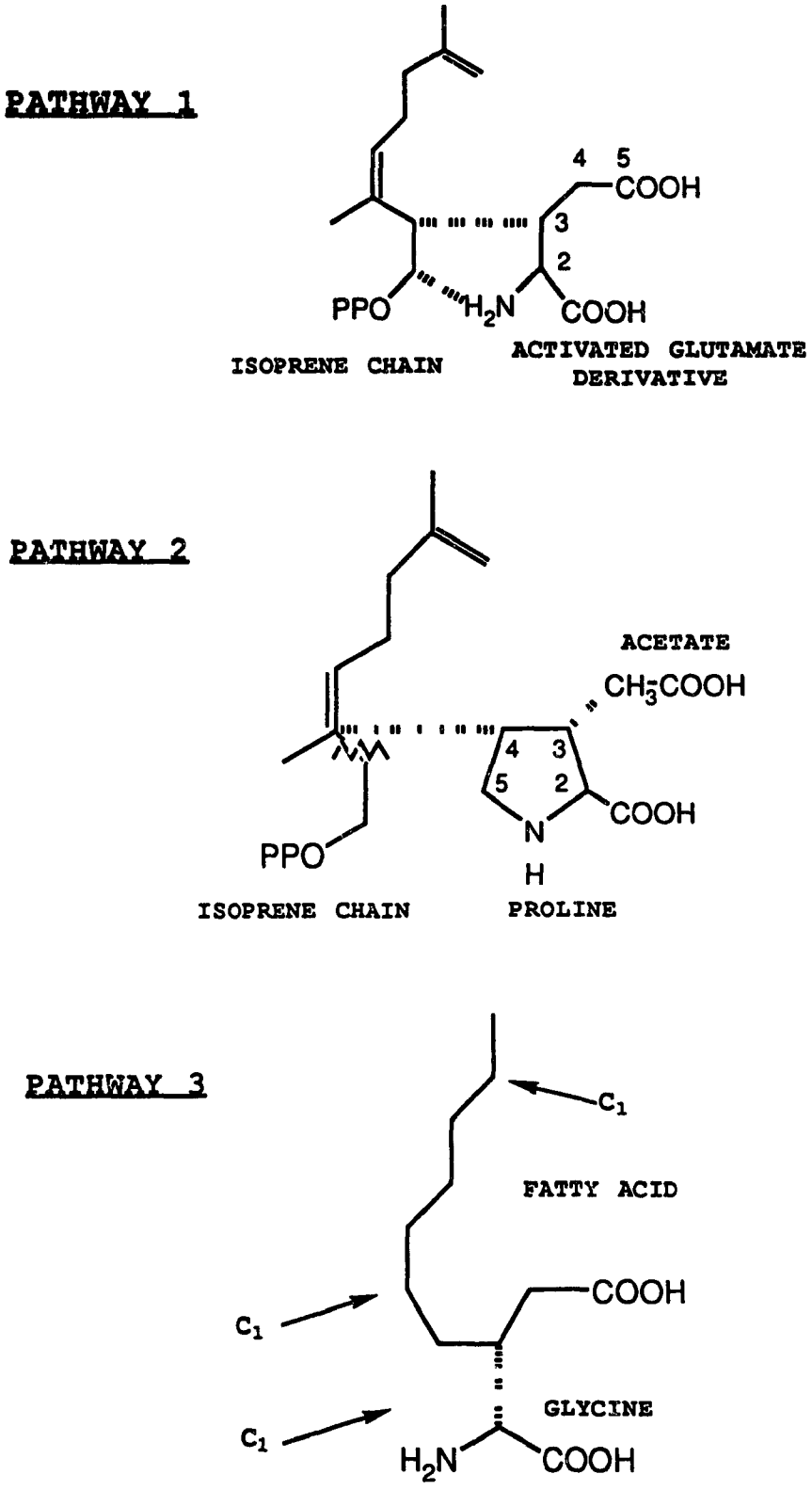

FIGURE 11: THREE PUTATIVE PATHWAYS OF DOMOIC ACID BIOSYNTHESIS

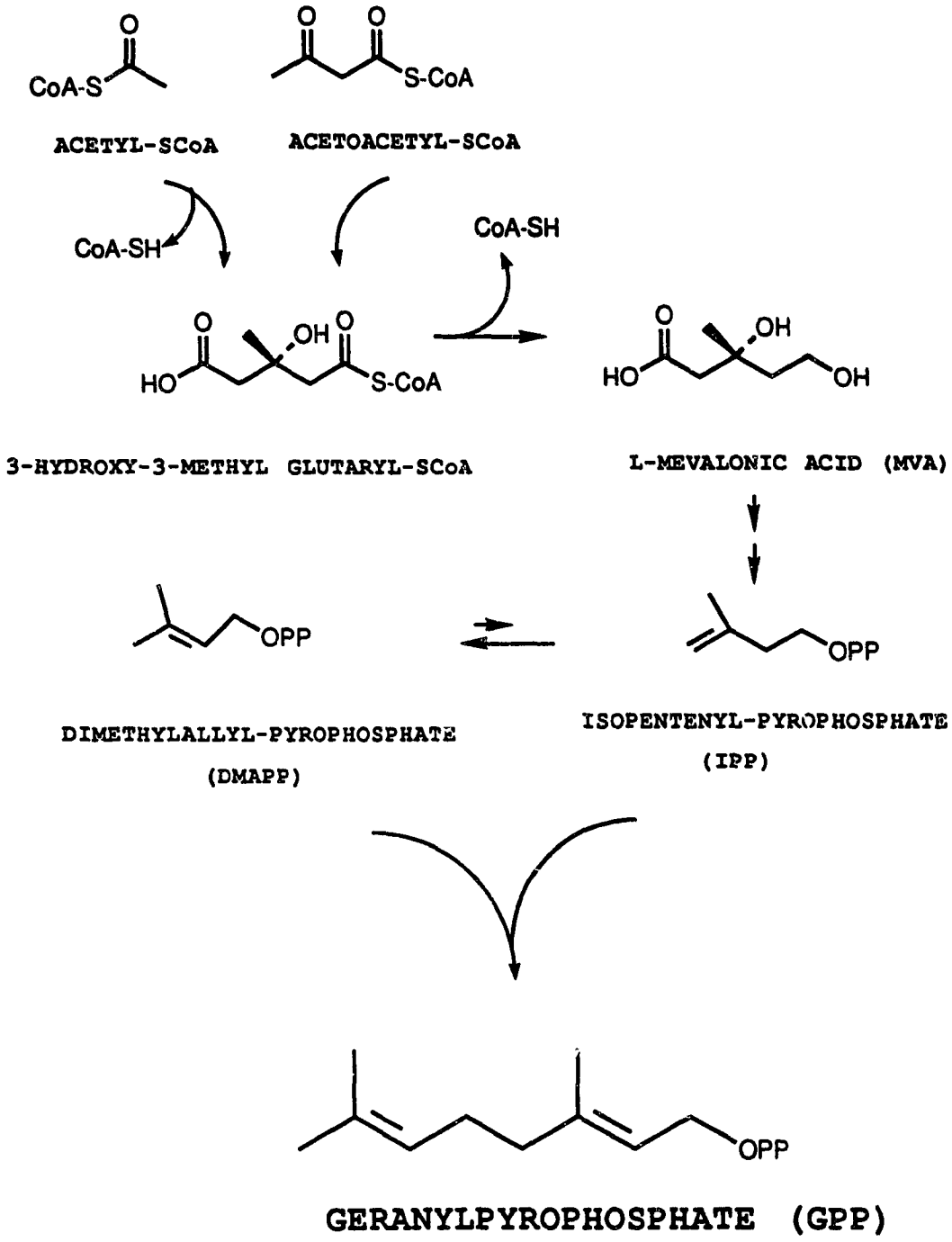

FIGURE 12: THE INCORPORATION OF ACETATE INTO AN ISOPRENOID CHAIN

which is subsequently decarboxylated and dehydrated to create isopentenylpyrophosphate (IPP). IPP is converted to dimethylallylpyrophosphate (DMAPP) by an isomerase enzyme (Mann, 1987). In many organisms this reaction is essentially irreversible. The pyrophosphate group on the tail of the isoprenoid is a good leaving group and makes both DMAPP and IPP very reactive (Mann, 1987). Longer chained isoprenoids such as geranyl and farnesyl pyrophosphate are generated by the head-to-tail condensation of IPP and DMAPP. Glutamate is also derived from acetate, but via the citric acid cycle (Fig. 13; Goodwin and Mercer, 1983). Acetate condenses with oxaloacetate to generate citrate, which is converted to cis-aconitate, isocitrate, and then to α-ketoglutarate. The transamination of α-ketoglutarate produces glutamate (Fig. 13; Goodwin and Mercer, 1983).

In the second hypothetical pathway, glutamic acid cyclizes via the semi-aldehyde to generate a proline ring (Fig. 14; Goodwin and Mercer, 1983), which then condenses with acetate and a cleaved isoprene chain to form C-C bonds at two inactivated positions in the ring system (Pathway 2 in Fig. 11). The biosynthesis of isoprenoid chains from acetate is discussed above.

In the third putative pathway, a fatty acid chain condenses with glycine. This pathway requires the addition of

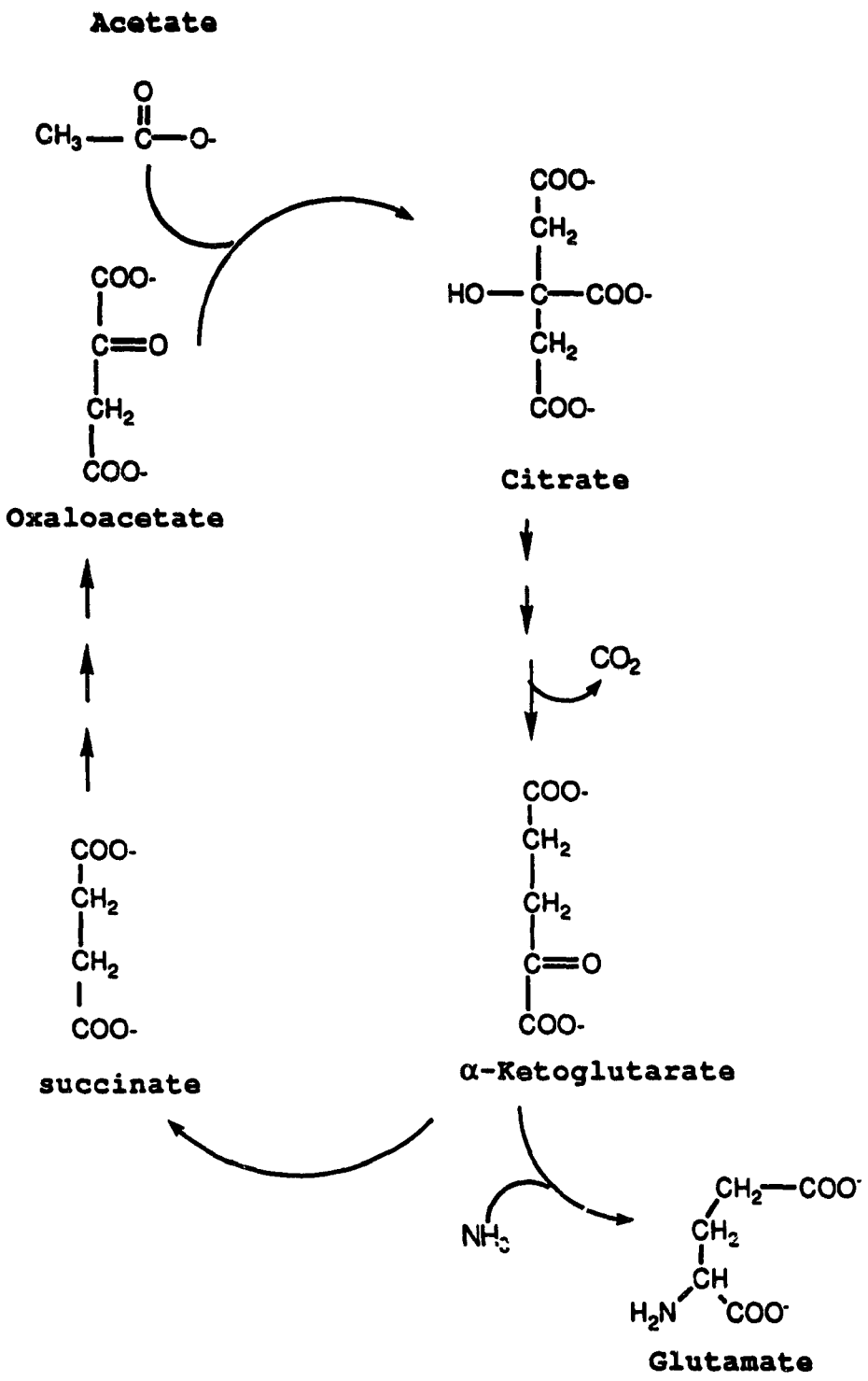

FIGURE 13: INCORPORATION OF ACETATE IN GLUTAMATE BIOSYNTHESIS

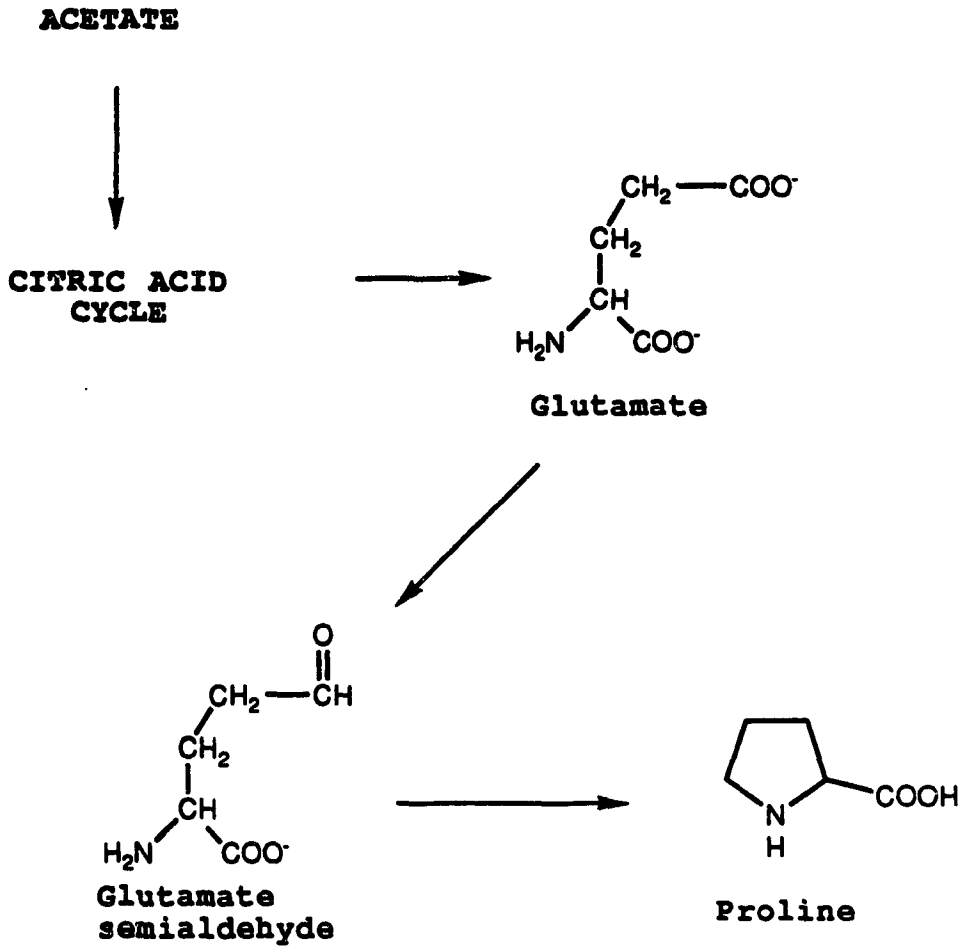

FIGURE 14: THE INCORPORATION OF ACETATE IN PROLINE BIOSYNTHESIS

three C_1 units at unreactive carbons in the fatty acid chain to generate the final structure of domoic acid (Pathway 3 in Fig. 11). In the common pathway of fatty acid biosynthesis, acetyl-SCoA condenses with carbon dioxide to generate malonyl-SCoA, which is transferred to the acyl carrier protein (ACP) (Mann, 1987). Acetyl-SCoA is transferred to ACP by the acetyl-SCoA:ACP transacylase and then to the acyl-ACP:malonyl-ACP-condensing enzyme, probably within a multienzyme complex, for the condensation reaction with malonyl-ACP during the elongation phase (Fig. 15; Mann, 1987; Goodwin and Mercer, 1983). The product is then converted to a saturated acyl-ACP via an hydroxylated intermediate (Fig. 15; Mann, 1987). In photosynthetic organisms glycine is commonly derived from a product of the Calvin cycle and is thus not biosynthesized from acetate (Goodwin and Mercer, 1983).

This chapter describes the results of both ^{13}C and ^{14}C precursor feeding experiments using the pennate diatom *Pseudonitzschia pungens* f. *multiseries*. The resulting domoic acid labelling patterns are examined in order to elucidate the pathway of domoic acid biosynthesis.

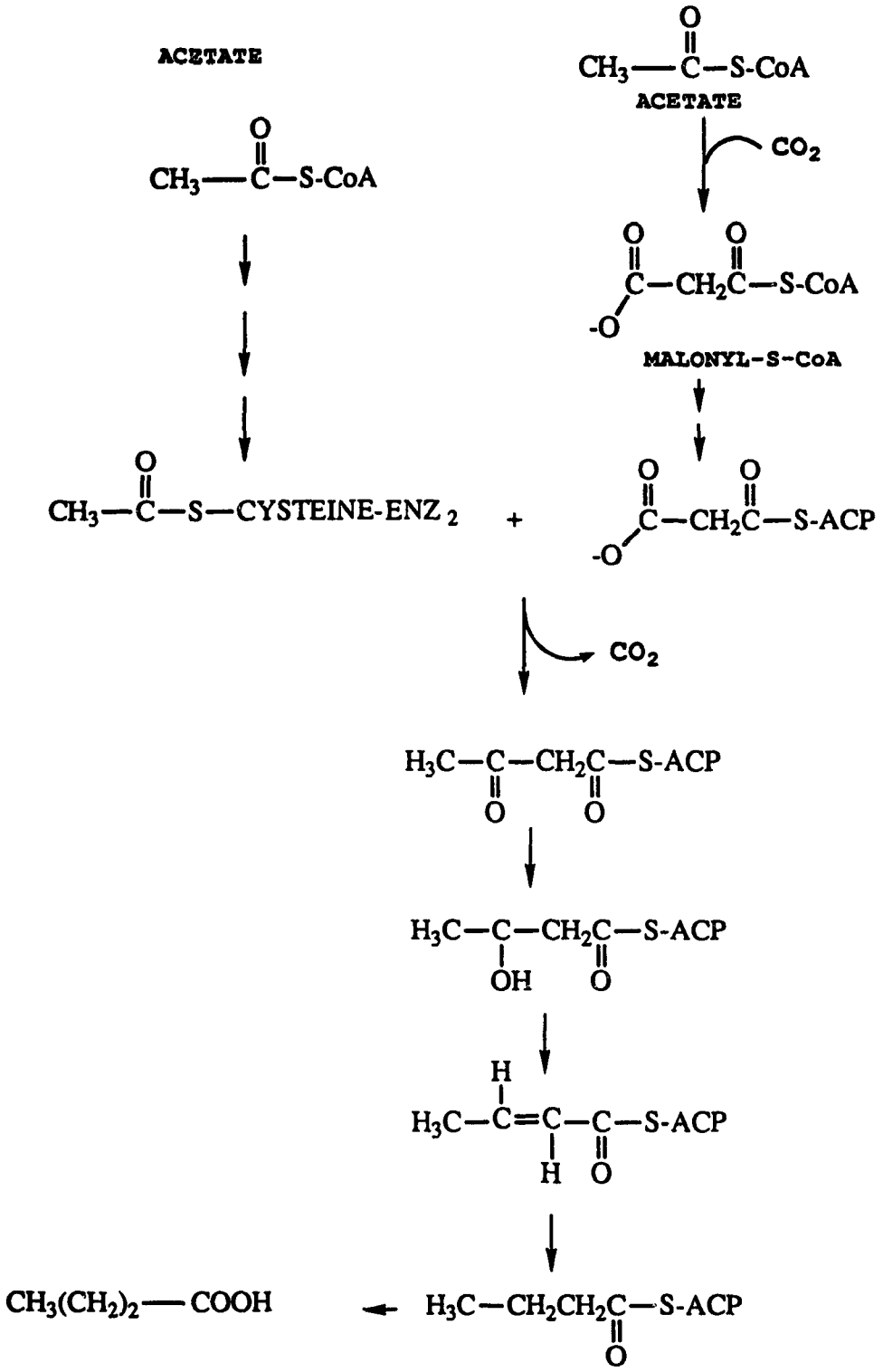

FIGURE 15: THE INCORPORATION OF ACETATE IN FATTY ACID BIOSYNTHESIS (ENZ_2- refers to the acyl-ACP-malonyl-ACP condensing enzyme)

METHODS AND MATERIALS

CULTURING AND GROWTH OF PHYTOPLANKTON

Two axenic strains of *Pseudonitzschia pungens* f. *multiseries* were obtained from Donald Douglas, Institute for Marine Biosciences, National Research Council, Halifax, N.S. (Douglas and Bates, 1992). The first strain, 13CC, was originally isolated in Galveston Channel, TX (clone TKA-2) (Fryxell et al., 1990) and the second strain KP59/2 was originally isolated in Cardigan Bay, P.E.I. by K. Pauley, Fisheries and Oceans, Moncton, N.B. Cultures were grown in batch system using F/2 media (Guillard, 1975) with 4.1 mM Tris buffer. The cultures were maintained at 15°C with a light intensity of 30-50 $\mu E \cdot m^{-2} \cdot s^{-1}$ measured using a 4π sensor (model QSL-100, Biospherical Instruments, San Diego, CA) and a 12:12 h light:dark cycle. The cultures and volumes used in each isotope experiment are listed in Table 1. The 12L-fermentor system (Microferm, New Brunswick Scientific, NJ) used in the first two experiments was modified to allow supply and measurement of light intensity (Douglas and Bates, 1992). The remaining experiments were performed in 1L or 1.5L media per Fernbach with rotation at 80 rpm.

Culture samples (100 mL fermentor samples; 5 mL Fernbach samples) were routinely removed to monitor the growth of the culture. *P. pungens* f. *multiseries* cell numbers were

TABLE 1: CULTURE VOLUMES, LABELLED PRECURSORS AND STRAINS OF AXENIC *PSEUDONITZSCHIA PUNGENS* F. *MULTISERIES* USED IN FEEDING EXPERIMENTS.

LABELS	CULTURE SIZE	STRAIN
[1-^{13}C]-acetate	12L	13CC
[1,2-^{13}C]-acetate	12L	13CC
[1,2-^{13}C]-acetate (early feeding)	8X1.5L	KP59/2
[1,2-^{13}C]-acetate (late feeding)	8X1.5L	KP59/2
[2-^{13}C,$^{2}H_3$]-acetate	10X1.5L	KP59/2
[1,5-^{14}C]-citrate	3X1L	KP59/2
[1-^{14}C]-α-ketoglutarate	3X1L	KP59/2
L[1-^{14}C]-glutamate	3X1L	KP59/2

determined for three 5 µL culture replicas using a microscope (Ortholux II, Leitz Wetzlar, Germany). The % transmittance of culture samples was measured at 750 nm (model PC 800 colorimeter, Brinkmann Instruments, Westbury. NY) and then converted to optical density using the following formula:
optical density = -log(% transmittance/100).
The samples were then stored at -20°C (two 30 mL fermentor samples or one 5 mL Fernbach sample) for later domoic acid analysis. All culture inoculations and transfers were performed in a laminar flow hood using aseptic techniques. The bacteria-free nature of the culture was routinely tested during inoculation and harvest by spotting 0.5 mL of culture onto nutrient-enriched marine agar plates (2216 Marine Agar, Difco Laboratories, Detroit, MI).

LABEL PREPARATION, ADDITION TO CULTURE, AND HARVEST

The ^{13}C-labelled acetate precursors, dissolved in dH_2O, were [1-^{13}C]-acetate (99.7% ^{13}C; 1.65 g per 10 mL) and [1,2-^{13}C]-acetate (99.7% ^{13}C, 1.68 g per 30 mL with strain 13CC; 90% ^{13}C, 4.03 g per 48 mL with stain KP59/2) (source: MSD Isotopes, Canada). The [2-^{13}C,$^{2}H_3$]-acetate (99% ^{13}C and >99.8% D) (supplied by C. Craft, Institute for Marine Biosciences, National Research Council, Halifax, N.S.) precursor was dissolved in deuterium oxide (99.9% D; Cambridge Isotope Lab, Woburn, MA) to give a solution (2.58 g per 30 mL) that was autoclaved. After autoclaving (15 min) the precursor solution

was added to the cultures immediately before the stationary phase of growth and thereafter at 24 and 48 h (0.67 mM in culture per pulse) to give a final concentration in the medium of 2.0 mM. For the early and late feeding experiments with [1,2-^{13}C]-acetate, the precursor was added in a single pulse. In the early-feeding experiment, it was added on day 4 during the early stages of exponential growth; in the late-feeding experiment it was added on day 7 after the onset of the stationary phase of growth. In the case of the ^{14}C-labelled compounds, [1,5-^{14}C]-citric acid, [1-^{14}C]-α-ketoglutarate, and L[1-^{14}C]-glutamic acid (NEN Research Products, DuPont Company, Ont.), each precursor was added separately to three 1-L cultures in three pulses (1.1 µCi/pulse) immediately before the stationary phase of growth and thereafter at 24 and 48 h.

Several days after the final label was added in each experiment, when culture domoic acid levels were generally greater than 40 ng/mL, a final 5 mL sample was removed and filtered through a 0.2 µm sterile filter unit (Millipore, Bedford, MA) and the filtrate frozen at -20°C to later determine the amount of domoic acid present in the media. For the stable isotope experiments, the cells were transferred into a dispensing pressure vessel that passed the culture into a filtration apparatus (293 mm; Millipore) equipped with a 0.3 µm filter membrane (Millipore). The cells were then washed from the membrane using seawater and centrifuged for 10 to 15

min at a maximum of 3800 xg in a Beckman J2-21 centrifuge in a 250 mL Nalgene bottle to pellet the cells (Nalge Co., NY). The supernatant was decanted from the Nalgene bottle and the cell pellet then stored at -70°C until later domoic acid purification. Samples (5 mL) of the post-filtration medium and the post-centrifugation supernatant were routinely taken and stored at -20°C in order to later determine losses of domoic acid during the harvesting procedure. For the ^{14}C-experiments, the culture in each Fernbach was separately filtered through a 0.3 µm filter membrane in a Buchner funnel and washed twice with seawater. The membrane with the cells was then transferred to a Nalgene bottle and stored at -20°C until domoic acid was purified. In the radiotracer experiments two samples (5 mL) were removed from the culture before filtration. One sample was passed through a Millipore filter unit containing a 0.3 µm membrane, and the cells were washed twice with seawater. The membrane was transferred to a scintillation vial as were the filtrate, the two washes and a sample (5 mL) of the original culture. Scintillation fluid (5 mL; Beckman Ready Safe, Beckman Instruments Inc., CA) was added and the radioactivity was measured on a Beckman scintillation counter (Beckman Instruments Inc., CA). The blank consisted of seawater (5 mL). Quenching was accounted for in each sample using the H numbers determined by the scintillation counter. A standard quench curve of counting efficiencies, generated by dividing the counts per minute

(CPM) for each standard by its known disintegrations per minute (DPM), versus H number was prepared. DPMs for each sample were calculated by dividing CPM by the counting efficiencies, determined from the standard curve. Cellular incorporation of the [1,5-^{14}C]-citrate, [1-^{14}C]-α-ketoglutarate or [1-^{14}C]-glutamate was calculated by dividing the cellular DPM by the total of cellular DPM plus DPMs for the media and two washes after background DPM had been subtracted.

DOMOIC ACID SAMPLE ANALYSES AND PURIFICATION

The culture samples stored at -20°C were analyzed for domoic acid by K. Pronk, J.H.D. Wright and Dr. R. Pocklington at the Department of Fisheries and Oceans, Bedford Institute of Oceanography, Dartmouth, N.S. All samples were sonicated before analysis. The domoic acid was reacted with 9-fluorenylmethyl-chloroformate (FMOC-Cl) and analysed with a High Performance Liquid Chromatography (HPLC) system equipped with a fluorescence detector (Pocklington et al., 1990). The FMOC procedure is sensitive within the range of 2×10^{-9} to 1×10^{-6} g·mL^{-1} domoic acid in seawater. For those samples that exceeded 1×10^{-6} g·mL^{-1} domoic acid, an HPLC-UV system equipped with a diode array detector was used instead (Quilliam et al., 1989). Domoic acid concentrations given were determined using the FMOC system unless otherwise stated.

Domoic acid purification is based on the procedure of

Wright et al. (1989). The frozen cell pellet stored at -70°C was transferred from the Nalgene bottle into a 250 mL beaker and suspended in aqueous 60% methanol (100 mL). The cells were then sonicated at 7 DC amp in a Branson Sonifier (Branson, Danbury, CN) for 1 min prior to centrifugation at 15,700 xg in a Beckman centrifuge to remove cellular debris. The supernatant was decanted and the cells re-extracted. The resulting supernatants were pooled and dried. If the harvest centrifugation supernatant contained high levels of domoic acid due to leakage from the cells then it was also dried and pooled with the cell extract. In the radiotracer experiments, 200 µg of a nonradioactive domoic acid solution (1 mg/mL) was added at this stage to act as a carrier of the radioactive domoic acid. Methanol was then added until the sample was dissolved. Reversed phase C18 (55-105 µm particle size; 125 A pore size; Waters, Millipore Corp., MA) was added and the sample dried. The sample was resuspended in dH_2O and dried twice to remove any traces of methanol. The dried sample was applied to the top of an activated reversed phase C18 column and eluted with increasing percentage of aqueous acetonitrile (four column volumes each of; 2%, 5%, 7%, 10%, 13%, 15%, 30% and 50%) containing acetic acid (0.2%). The fractions were dried and resuspended in dH_2O for analysis on the analytical HPLC system (Analytical VYDAC column 201TP52, Separations Group, CA; HP1090 LC, Hewlett Packard, Ont.), and fractions containing domoic acid were pooled and dried. The pooled

fractions were resuspended in dH_2O (1 mL) and if necessary, filtered through a 0.2 µm filter unit (Millipore) before preparative HPLC. Finally domoic acid was obtained following preparative HPLC (C18 VYDAC column 201TP1010) and elution with 8% acetonitrile containing trifluoroacetic acid (0.2%). The eluate was monitored at 242 nm and the domoic acid peak (RT 50 min) was collected and pooled from several injections (flow rate 2 mL/min). The pooled material was dried and resuspended twice in deuterium oxide before nuclear magnetic resonance (NMR) analysis.

NUCLEAR MAGNETIC RESONANCE SPECTROSCOPY

NMR spectroscopy of the purified domoic acid samples was performed at 500.13 MHz (^1H) or 125.77 MHz (^{13}C) on a Bruker AMX-500 Spectrometer in 5 mm sample tubes at 20°C (spectra were recorded by D.M. Leek and J.A. Walter, Marine Chemistry Section, Institute for Marine Biosciences, National Research Council, Halifax, N.S.). The purified domoic acid (DA), dissolved in D_2O, was acidified by addition of DCl to pH 1.5 to 1.7. The ^1H and ^{13}C spectra had both been previously assigned in this pH range (Walter et al., 1992). To measure the absolute ^{13}C-enrichment at each position, integrated areas of domoic acid ^{13}C resonances were compared with those of natural ^{13}C abundance dimethyl sulfoxide (DMSO; $(CH_3)_2SO$) added to the sample before the spectra were recorded. The molar ratio of DMSO/DA had been previously established from the ^1H

NMR spectrum of the mixture, obtained under conditions of complete spin lattice relaxation. Concentrations of DA and DMSO were also determined by comparison of the integrated resonance intensities with those of a standard sucrose/D_2O solution obtained under identical conditions including probe tuning and matching, flip angle (40°), temperature (20°C), probe geometry, and tube diameter (precision tubes with 0.01 mm tolerance). Knowing the natural abundance enrichment of the DMSO to be 1.108% ^{13}C, the absolute enrichment F_{DA} of the DA ^{13}C at each position was calculated using the following formula:

$$E_{DA} = I_{DA}/I_{DMSO} \times 1.108 \times C_{DMSO}/C_{DA}$$

where I_{DMSO} and I_{DA} are the average integrals of DMSO and DA carbon resonances, respectively, and C_{DMSO}/C_{DA} is the molar ratio of DMSO/DA.

The percent incorporation of intact doubly labelled units or single labels originating from [1,2-^{13}C]-acetate were calculated using expanded ^{13}C proton or deuterium decoupled spectra. If two ^{13}C are adjacent then spin-spin coupling will occur and the resonance will be split into a central peak and satellites (Marshall, 1983). If satellites overlap with the central peak or with the other satellites then probability equations can be used to determine the integrals of each peak

alone. By substituting in the integrals for the overlapping peaks in the probability equations it is possible to solve for p and q (see example in Fig. 16). Coupling constants, Jcc, were generally measured directly from expanded spectra. Bruker PANIC simulation was used in the [2-^{13}C, $^{2}H_3$]-acetate experiment to interpret satellite patterns due to isotope shifts.

STATISTICAL TESTS

All tests of statistical significance were performed using a pairwise T-test. Significance was defined as $P<0.05$.

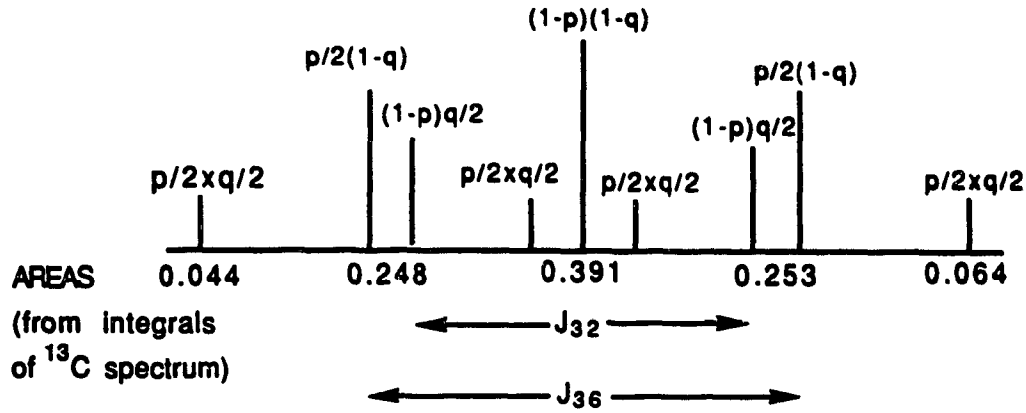

pq/4 = (0.044 + 0.064)/2=0.054 therefore p=0.216/q

(1-p)(1-q)= 0.391-(2X0.054)=0.283

solve for q, substitute in p=0.216/q

p= 0.51 or 0.42 q= 0.42 or 0.51

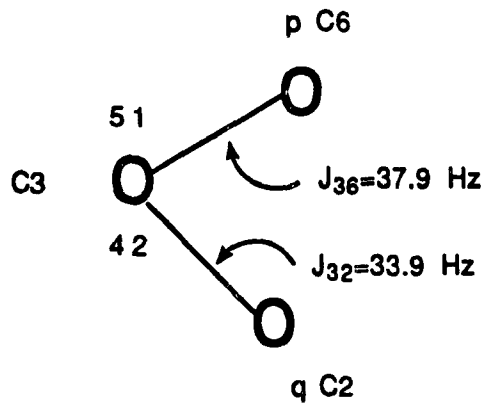

p= probability of ^{13}C at C6 when C3 is ^{13}C

q= probability of ^{13}C at C2 when C3 is ^{13}C

FIGURE 16: CALCULATION OF PROBABILITIES OF ^{13}C AT CARBON B WHEN ^{13}C AT CARBON A. (Probabilities given in percent. The coupling constants J_{cc} are also shown).

RESULTS

STABLE ISOTOPE LABELLING EXPERIMENTS:

GROWTH CURVES

The growth curves and domoic acid levels in each labelling experiment were used to determine the optimum time for precursor addition. The growth curves for *Pseudonitzschia pungens* f. *multiseries* strain 13CC grown in a fermentor system with either [1-^{13}C]-acetate or [1,2-^{13}C]-acetate added during the late exponential growth phase are shown in Figs. 17 and 18. The [1-^{13}C]-acetate was added on days 13, 14, and 15 and [1,2-^{13}C]-acetate was added to a separate culture on days 6, 7, and 8. The [1-^{13}C]-acetate-fed culture entered an initial lag phase of growth in comparison to the [1,2-^{13}C]-acetate-fed culture, which entered immediately into the exponential phase of growth. The inoculum for the [1-^{13}C]-acetate labelling experiment was grown to day 7, and in the [1,2-^{13}C]-acetate labelling experiment the inoculum was grown to day 9. In neither case had the inoculum started producing domoic acid. Domoic acid production began only after the onset of the stationary phase of growth for the [1-^{13}C]-acetate feeding experiment while production began earlier during the late exponential phase of growth in the [1,2-^{13}C]-acetate feeding experiment.

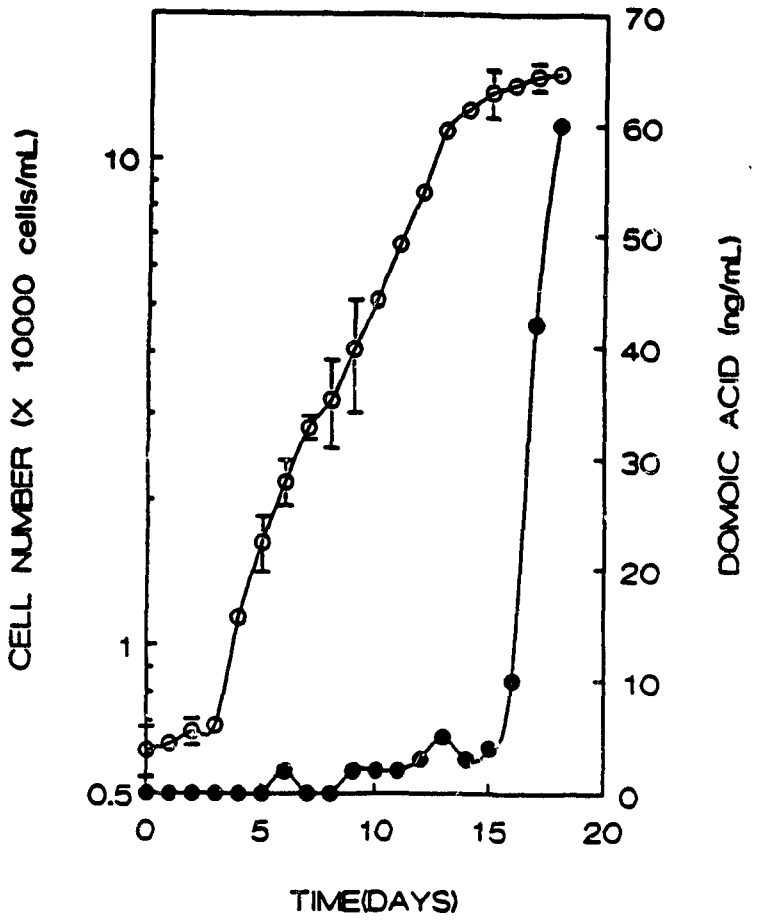

FIGURE 17: GROWTH CURVE AND DOMOIC ACID PRODUCTION BY *PSEUDONITZSCHIA PUNGENS* F. *MULTISERIES* STRAIN 13CC WITH [1-^{13}C]-ACETATE ADDED ON DAYS 13, 14 AND 15. ERROR BARS BASED ON TRIPLICATE SAMPLES (open circles represent cell numbers and closed circles represent domoic acid levels)

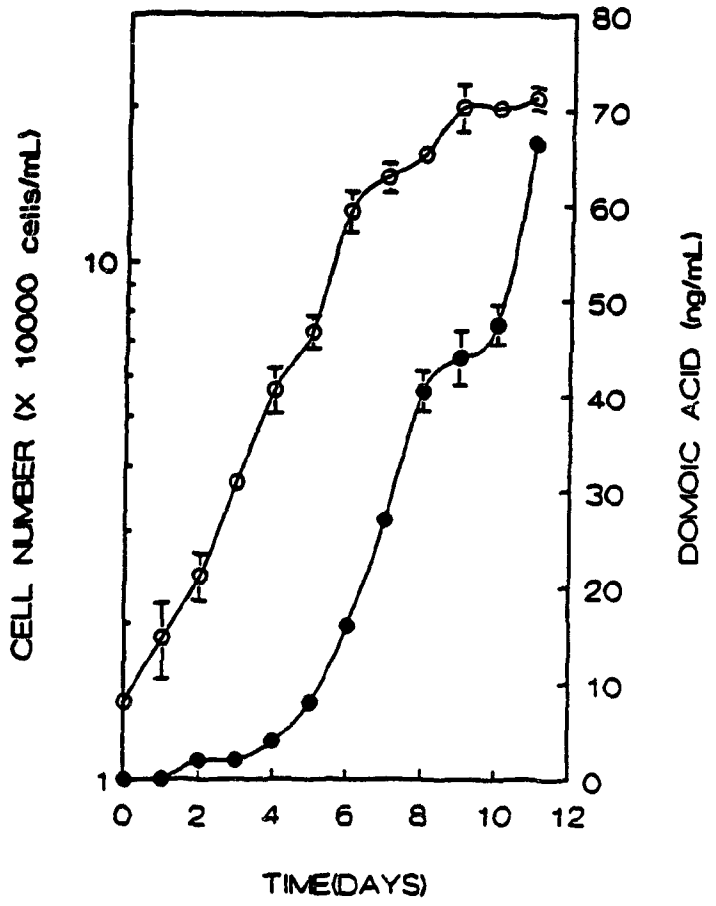

FIGURE 18: GROWTH CURVE AND DOMOIC ACID PRODUCTION BY *PSEUDONITZSCHIA PUNGENS* F. *MULTISERIES* STRAIN 13CC WITH [1,2-^{13}C]-ACETATE ADDED ON DAYS 6, 7, and 8. ERROR BARS BASED ON TRIPLICATE SAMPLES (open circles represent cell numbers and closed circles represent domoic acid levels)

The growth curves of *P. pungens* f. *multiseries* strain KP59/2 for both the early and late feeding experiments with [1,2-^{13}C]-acetate are shown in Figs. 19 and 20. These curves show the average optical densities and domoic acid levels for eight Fernbachs with associated standard deviations. In both cases domoic acid production began during the stationary phase of growth. Large domoic acid concentration variations were present between Fernbachs as indicated by the large error bars. The [1,2-^{13}C]-acetate precursor was added to the early feed Fernbach cultures in one pulse on day four during mid-exponential growth when domoic acid production had not commenced. The labelled compound was added to the late feed Fernbach cultures in one pulse on day seven during the late exponential growth phase just prior to the stationary phase and the start of domoic acid production.

The growth curve for *Pseudonitzschia pungens* f. *multiseries* strain KP59/2 cultures fed [2-^{13}C, $^{2}H_3$]-acetate is shown in Fig. 21. In this experiment 10 Fernbachs with 1.5L each of culture were used. Domoic acid production commenced during the late exponential phase of growth. Variations in growth rates and in the rates of domoic acid production were similar to those observed in the early and late [1,2-^{13}C]-acetate labelling experiments. The precursor was generally added to the Fernbachs in three pulses on days nine, ten and eleven. However, Fernbachs 3 and 6 lagged in growth and

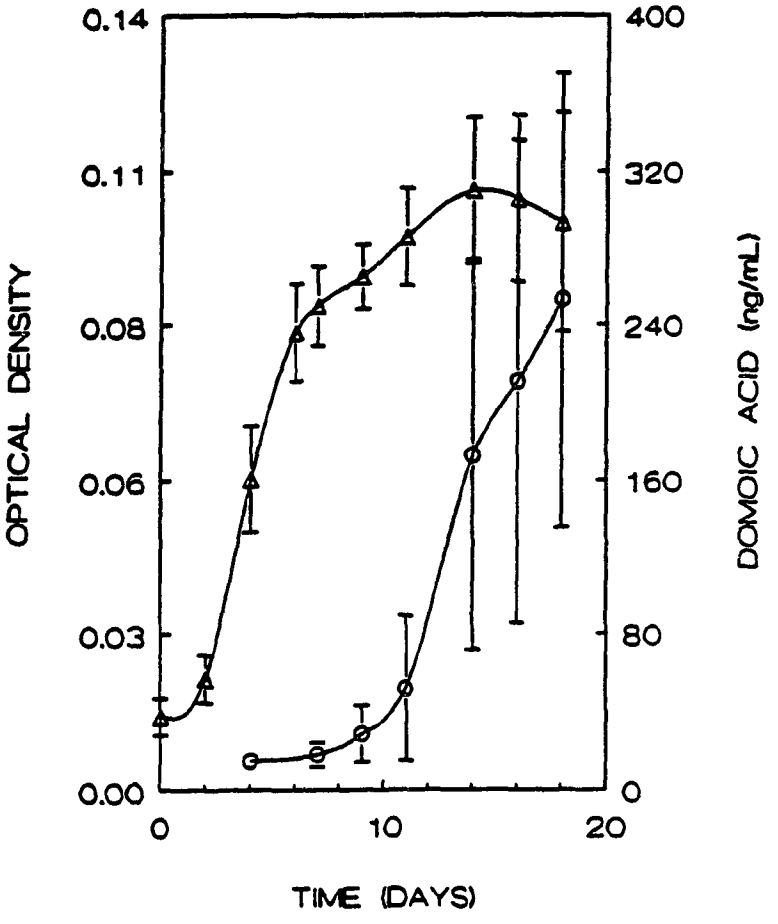

FIGURE 19: GROWTH CURVE AND DOMOIC ACID PRODUCTION BY *PSEUDONITZSCHIA PUNGENS* F. *MULTISERIES* STRAIN KP59/2 WITH [1,2-^{13}C]-ACETATE ADDED EARLY IN GROWTH OF CULTURE ON DAY 4. DATA POINTS REPRESENT THE AVERAGE OF 8 FERNBACHS WITH ERROR BARS BASED ON SAMPLE STANDARD DEVIATION CALCULATIONS. (open triangles represent optical density values and open circles represent domoic acid levels)

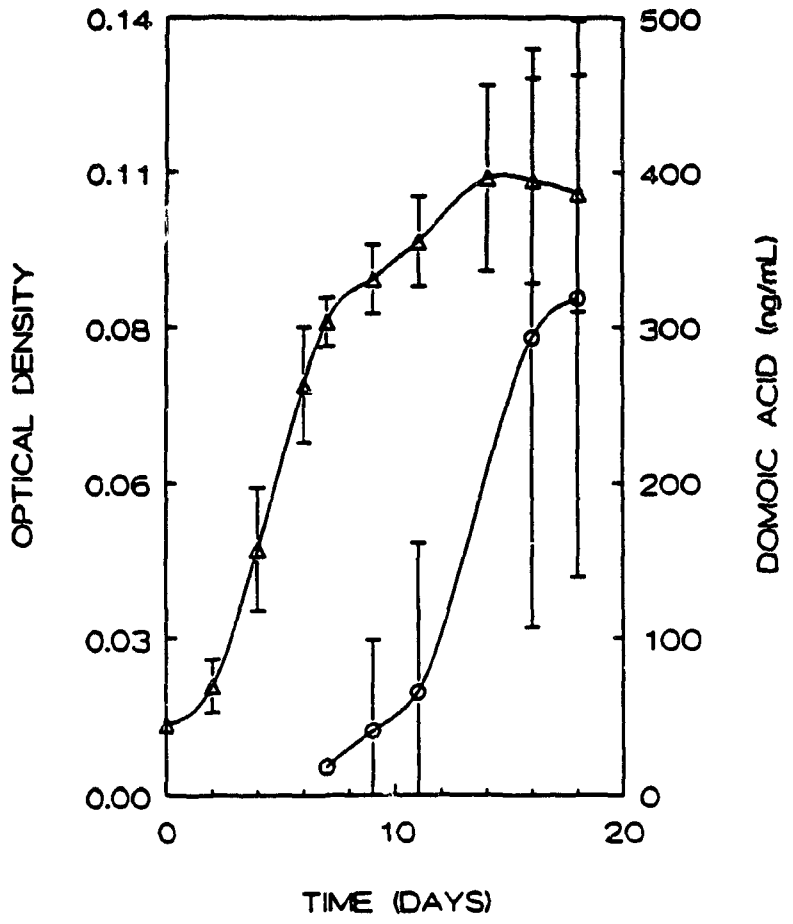

FIGURE 20; GROWTH CURVE AND DOMOIC ACID PRODUCTION BY *PSEUDONITZSCHIA PUNGENS* F. *MULTISERIES* STRAIN KP59/2 WITH [1,2-^{13}C]-ACETATE ADDED LATE IN GROWTH OF CULTURE ON DAY 7. DATA POINTS REPRESENT THE AVERAGE OF 8 FERNBACHS WITH ERROR BARS BASED ON SAMPLE STANDARD DEVIATION CALCULATIONS. (open triangles represent optical density values and open circles represent domoic acid levels

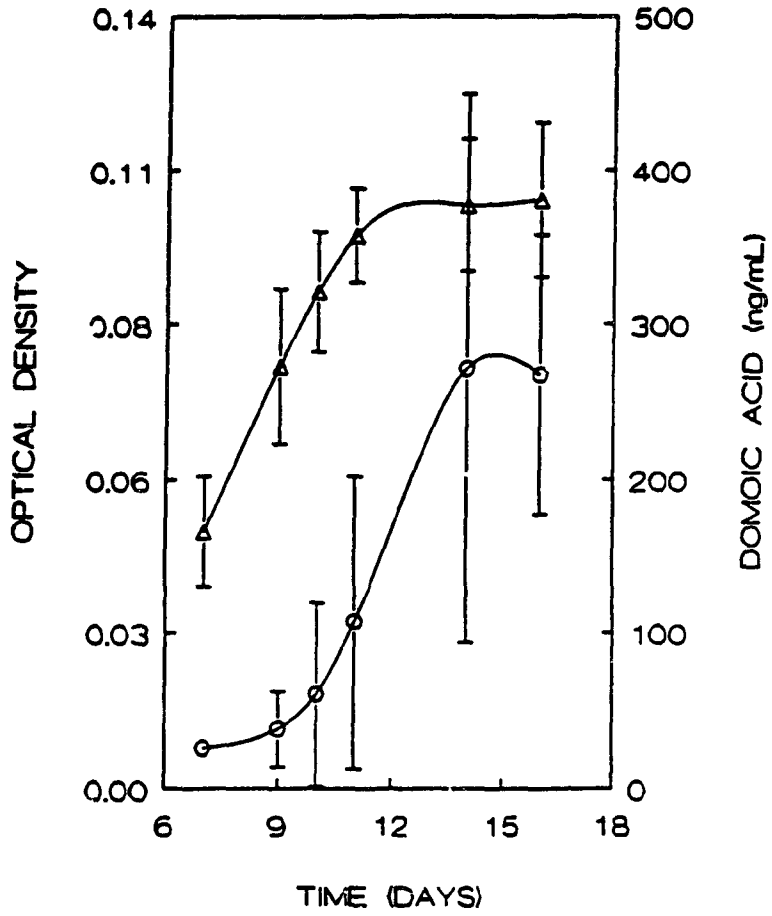

FIGURE 21: GROWTH CURVE AND DOMOIC ACID PRODUCTION BY *PSEUDONITZSCHIA PUNGENS* F. *MULTISERIES* STRAIN KP59/2 WITH [2-^{13}C,^{2}H$_3$]-ACETATE ADDED. DATA POINTS REPRESENT THE AVERAGE OF 10 FERNBACHS WITH ERROR BARS BASED ON SAMPLE STANDARD DEVIATION CALCULATIONS. (open triangles represent optical density values and open circles represent domoic acid levels)

precursor was therefore added on days ten, eleven and twelve, whereas Fernbach 10 grew quickly, so that the precursor was added on days eight, nine and ten.

[1-^{13}C]-ACETATE LABELLING EXPERIMENT

Purified domoic acid (*ca* 100 µg from ^{1}H NMR analysis) was obtained from *Pseudonitzschia pungens* f. *multiseries* strain 13CC cells fed with [1-^{13}C]-acetate. The ^{13}C NMR spectrum of the labelled domoic acid showed significant isotope enrichment at the carboxyl carbon C7 (>9% ^{13}C) and lesser enrichment at the carboxyl carbon C8 (>3% ^{13}C); no other positions showed detectable isotope enrichment above natural abundance levels (1.1% ^{13}C; Table 2).

[1,2-^{13}C]-ACETATE LABELLING EXPERIMENT

In the [1,2-^{13}C]-acetate labelling experiment purified domoic acid (*ca* 108 µg from ^{1}H NMR analysis) was isolated from *Pseudonitzschia pungens* f. *multiseries* strain 13CC cells. The isotope enrichment following incorporation of [1,2-^{13}C]-acetate is shown in Table 2. The positions C6 and C7 showed a similar level of enrichment with absolute ^{13}C values of 30.6% and 29.2%, respectively. This enrichment is approximately twice that at positions C2, C3 and C8 with ^{13}C enrichment of 17.4%, 15.6%, and 14.5%, respectively. The carbons C4 and C5 of the

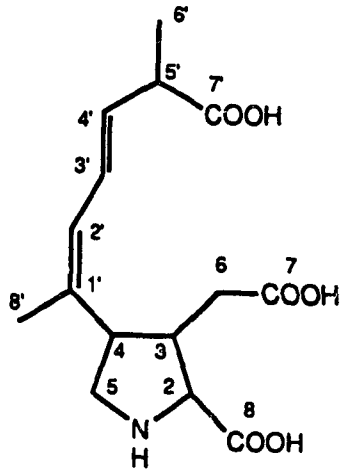

TABLE 2: THE % ABSOLUTE ^{13}C ENRICHMENT IN DOMOIC ACID

	CARBON POSITION						
LABEL	**C2**	**C3**	**C4**	**C5**	**C6**	**C7**	**C8**
[1-^{13}C]-ACETATE[a]	<2	<2	<2	<2	<2	>9	>3
[1,2-^{13}C]-ACETATE[b]	17.4	15.6	3.6	3.2	30.6	29.2	14.5
EARLY FEEDING: [1,2-^{13}C]-ACETATE[c]	9.2	9.1	5.1	4.3	18.1	20.3	10.6
LATE FEEDING: [1,2-^{13}C]-ACETATE[d]	11.0	9.3	4.4	4.4	17.1	18.1	10.1
[2-^{13}C,$^{2}H_3$]-ACETATE[e]	3.9	3.8	1.4	1.5	14.0	1.0	2.3

	CARBON POSITION							
LABEL	**C1'**	**C2'**	**C3'**	**C4'**	**C5'**	**C6'**	**C7'**	**C8'**
[1-^{13}C]-acetate[a]	<2	<2	<2	<2	<2	<2	<2	<2
[1,2-^{13}C]-acetate[b]	4.3	2.8	2.8	3.0	3.8	3.0	2.7	3.7
EARLY FEEDING: [1,2-^{13}C]-acetate[c]	4.5	4.0	4.5	3.4	5.5	6.0	4.4	5.9
LATE FEEDING: [1,2-^{13}C]-acetate[d]	4.2	4.7	3.7	3.4	4.1	5.4	3.8	4.4
[2-^{13}C,$^{2}H_3$]-ACETATE[e]	1.6	0.8	1.2	1.7	1.9	1.9	1.3	2.1

[a]Growth curve Fig.17, [b]Growth curve Fig. 18, [c]Growth curve Fig. 19, [d]Growth curve Fig. 20, [e]Growth curve Fig. 21. Error *ca* 2.5% for C2, C3, C6, C7 and C8; 1% for C-4, C-5 and C-1' to C-8'.

proline ring and those from positions C1′ to C8′ in the side chain have a similar level of enrichment ranging from 2.7 to 4.3%.

An expansion of the ^{13}C-NMR spectrum for [1,2-^{13}C]-acetate labelled domoic acid with the coupling constants, J_{cc}, between adjacent ^{13}C indicated is shown in Fig. 22. Coupling occurs between C2, C8; C2, C3; C3, C6; C6, C7; C4, C5; C8′, C1′; C3′, C4′; C5′, C6′. The intensity distribution of multiplets due to ^{13}C-^{13}C coupling was used to calculate the probabilities P_{AB} (%) that when the indicated carbon A is ^{13}C, the adjacent carbon B is also ^{13}C (Fig. 23). The high probabilities of P_{67} (96%) and P_{76} (94%) and P_{28} (69%) and P_{82} (72%) show that intact doubly-labelled acetate units were incorporated at the C6, C7 and C2, C8 positions approximately 95% and 71% of the time, respectively.

Doubly-labelled units were also observed between C4, C5; C1′, C8′; C3′, C4′; and C5′, C6′. Satellites were observed around the C7′ resonance, but no corresponding ones were present around C5′ so it was not clear if there was a double-labelled unit between C5′ and C7′. The intensity of the satellites relative to the central peaks when compared to the absolute ^{13}C enrichments showed that approximately 1% (mole fraction 0.978) originated from natural abundance material, approximately 1% (mole fraction 0.008 +/- 0.005) from doubly

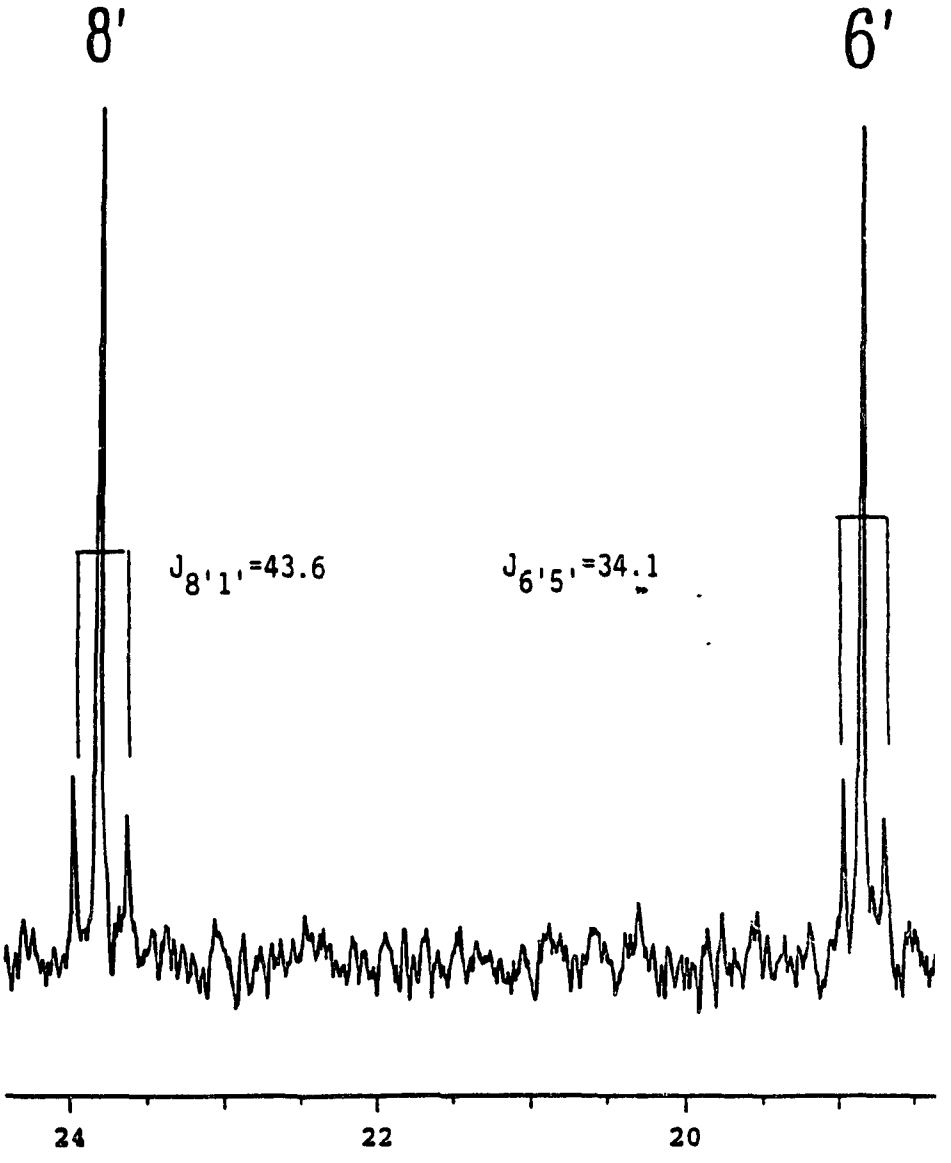

FIGURE 22: AN EXPANSION OF THE ^{13}C-NMR SPECTRUM FOR DOMOIC ACID LABELLED WITH [1,2-^{13}C]-ACETATE.
EACH CARBON RESONANCE IS NUMBERED AND THE COUPLING CONSTANTS, J_{CC} ARE GIVEN.
(baseline is in PPM)

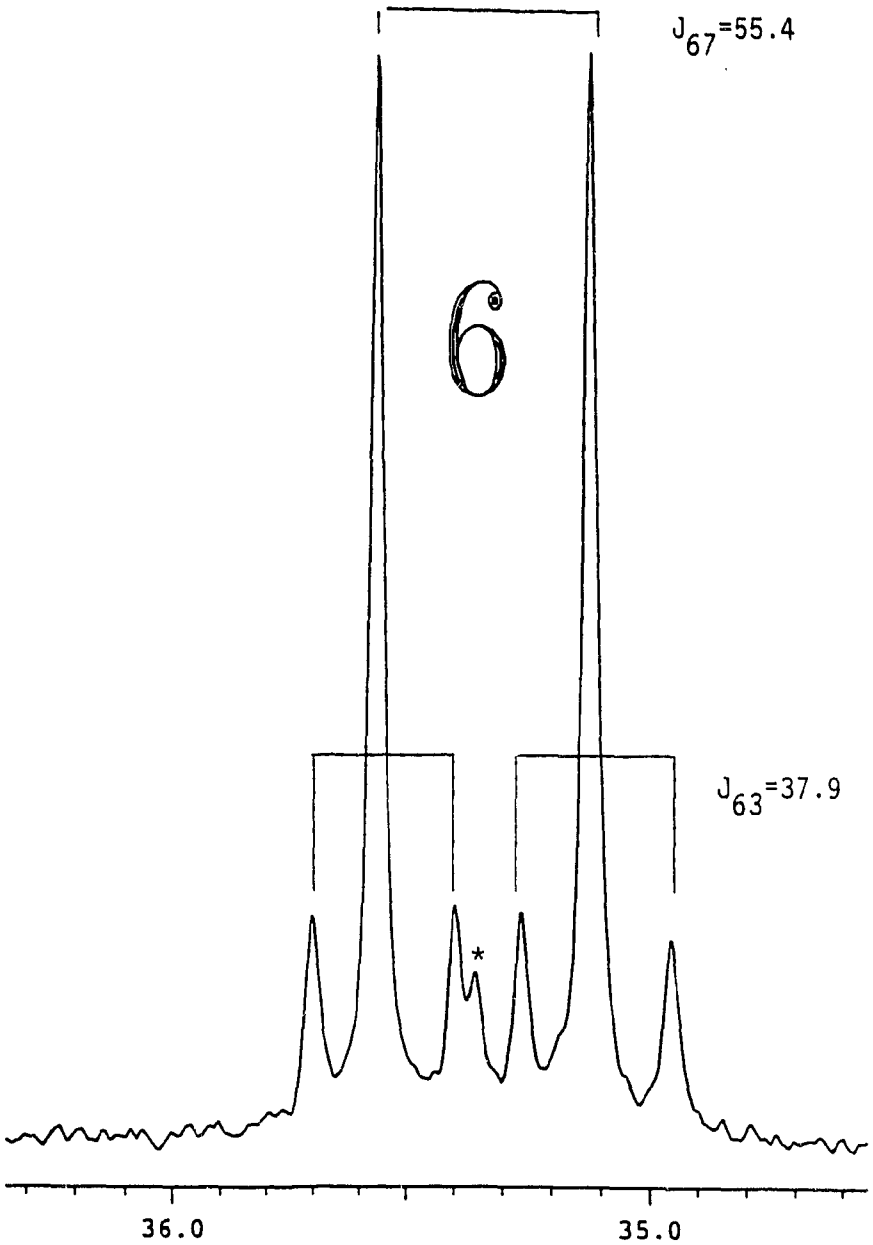

FIGURE 22: (continued)
(* Natural abundance peak)

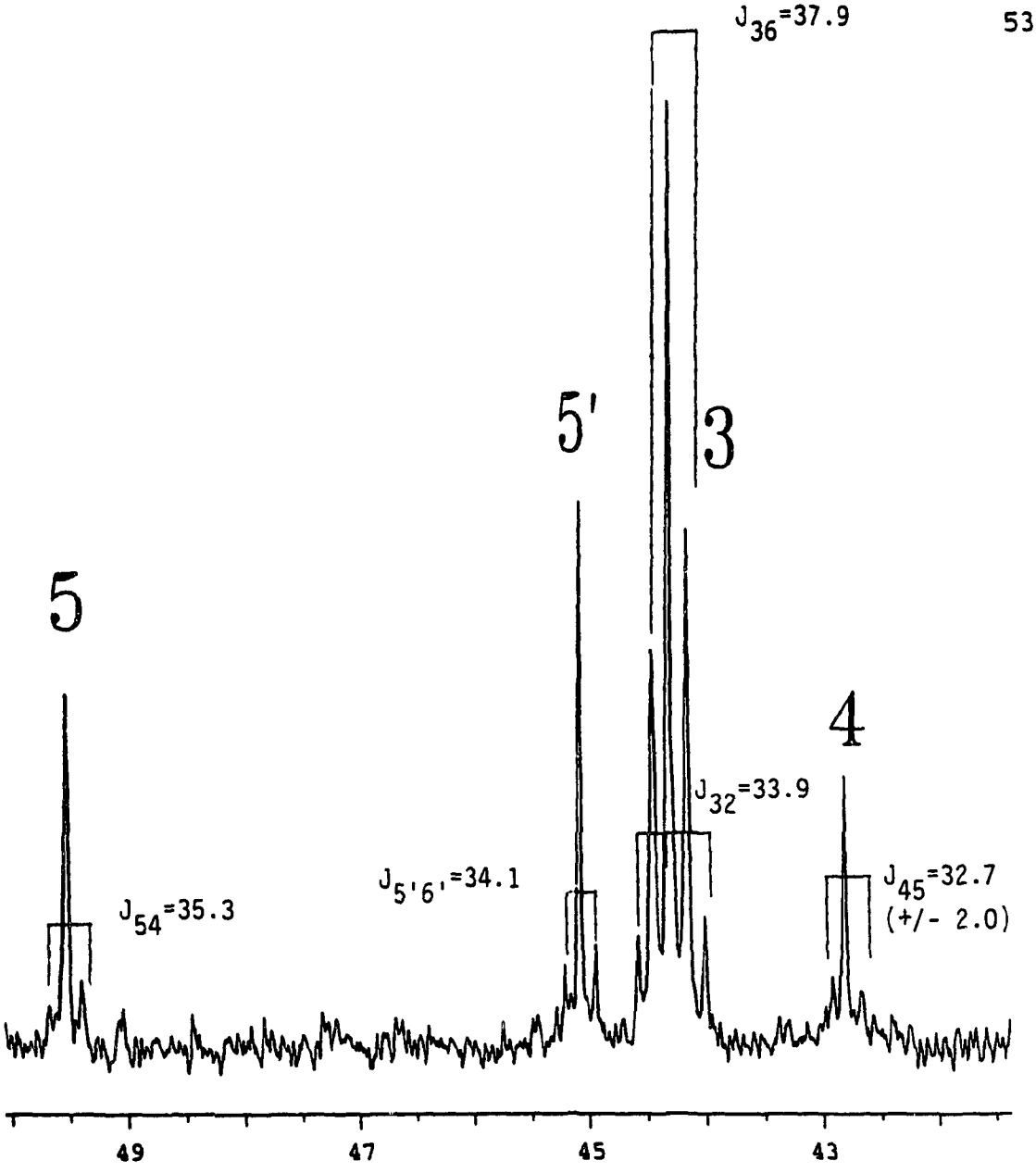

FIGURE 22: (continued)

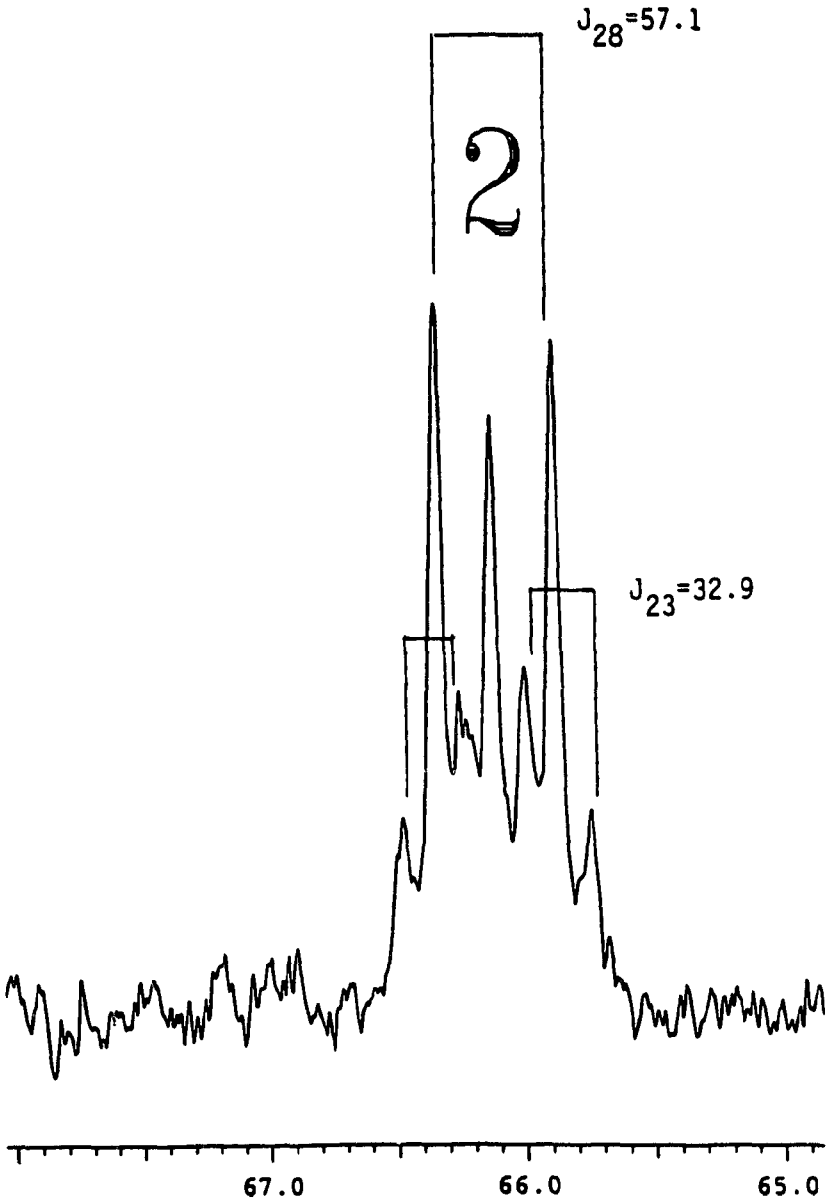

FIGURE 22: (continued)

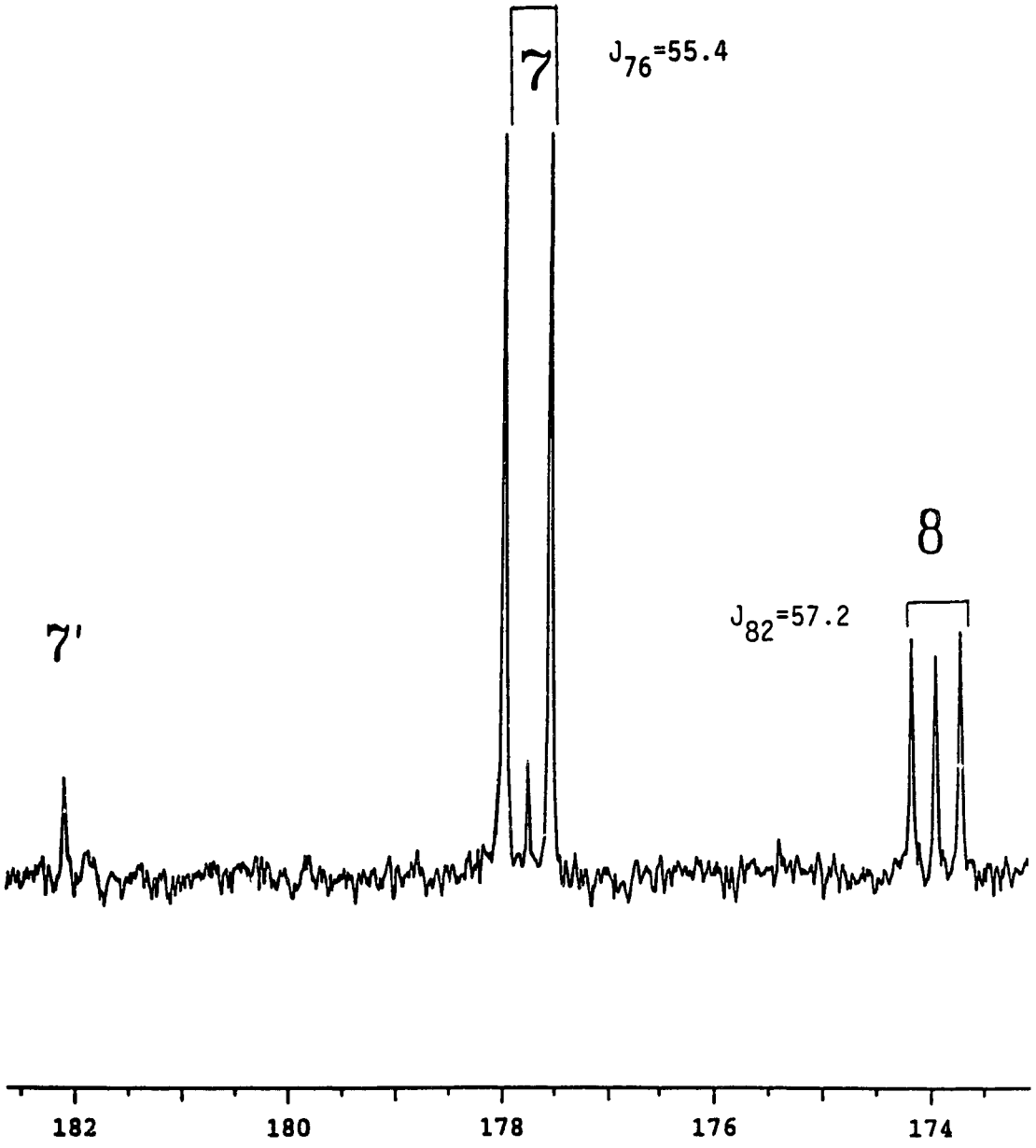

FIGURE 22: (continued)

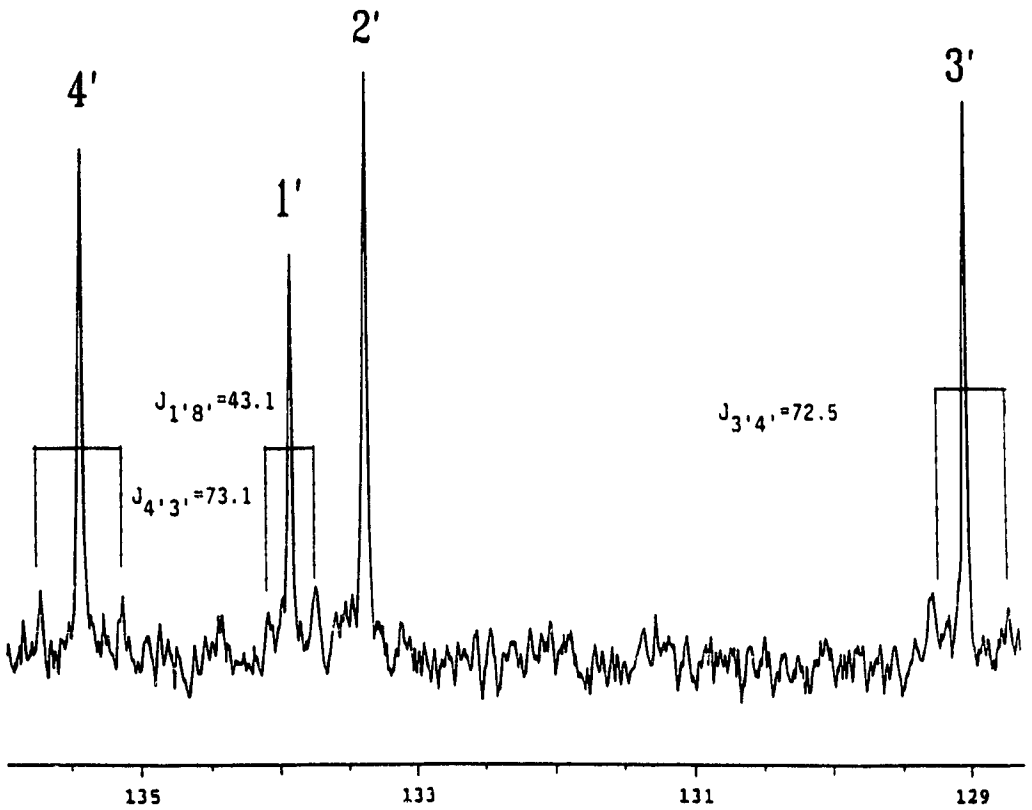

FIGURE 22: (continued)

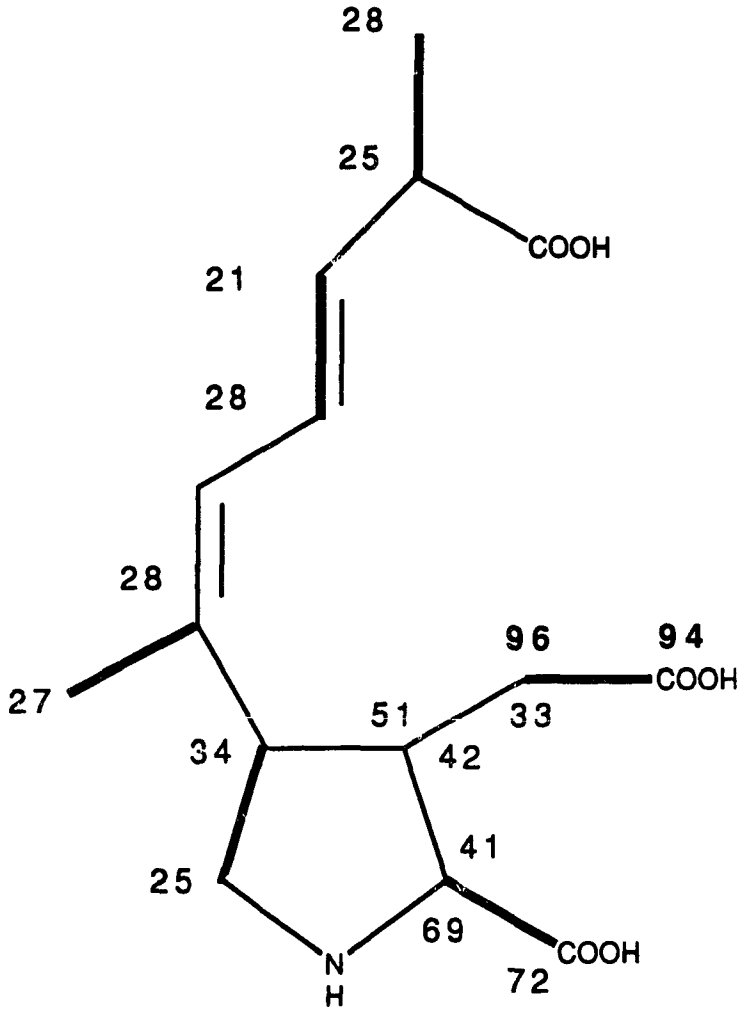

FIGURE 23: [1,2-^{13}C]-ACETATE DERIVED LABELLING PATTERN OF DOMOIC ACID FROM *PSEUDONITZSCHIA PUNGENS* F. *MULTISERIES* STRAIN 13CC. NUMBERS REPRESENT P_{AB} (%) WHEN INDICATED CARBON A IS ^{13}C THE ADJACENT CARBON B IS ALSO ^{13}C. BOLD LINES REPRESENT POSITIONS OF DOUBLE-LABELLED ACETATE INCORPORATION. ERROR *CA.* +/- 5% EXCEPT P_{36} *CA.* +/- 7%

labelled acetate units and approximately 1% (mole fraction 0.014) from scrambled single label. Satellites due to coupling between adjacent doubly-labelled units were not observed, possibly due to their low intensity.

TIMED LABELLING EXPERIMENTS WITH [1,2-^{13}C]-ACETATE

In the [1,2-^{13}C]-acetate early and late feeding experiments 335 µg and 330 µg of purified domoic acid were isolated from *P. pungens* f. *multiseries* strain KP59/2 cells, respectively. The % incorporation of ^{13}C in the toxin from these experiments is shown in Table 2. The labelling patterns for C6 and C7 versus C2, C8 and C3 showed a 2:1 ratio similar to that seen in the previous [1,2-^{13}C]-acetate labelling experiment with *P. pungens* f. *multiseries* strain 13CC. The levels of enrichment in this part of the molecule, however, were lower in the early and late feeding experiments conducted with *P. pungens* f. *multiseries* strain KP59/2 . The proline ring carbons C4 and C5 and the side chain carbons C1′ to C8′ showed a similar low level of ^{13}C enrichment. The time of label addition to the culture did not significantly affect the ^{13}C enrichment results.

[2-^{13}C, $^{2}H_3$]-ACETATE LABELLING EXPERIMENT

The ^{13}C isotopic enrichments in the 364 µg of purified

domoic acid obtained following incorporation of [2-^{13}C,$^{2}H_3$]-acetate are shown in Table 2. Position C6 showed the highest level of ^{13}C enrichment (14%), which is 3 to 4 times the enrichment values for C2 (3.9%) and C3 (3.8%). The level of ^{13}C incorporation at C8 (2.3%) was less than the enrichment at C2 and C3. The proline ring carbons C4 and C5 and the sidechain carbons C1′, C4′, C5′, C6′ and C8′ had very low levels of ^{13}C enrichment. Positions C2′, C3′ and C7′ were not detectably enriched with ^{13}C above the natural abundance level of 1.1%.

The {^{1}H, ^{2}H} decoupled ^{13}C-NMR spectrum of domoic acid derived from [2-^{13}C,$^{2}H_3$]-acetate revealed the presence of only one deuterium-labelled position, and this was at C6. This was recognized by the appearance of an isotope-shifted signal upfield of the ^{13}C resonance (Fig. 24). The isotope shift between $^{13}CH_2$ and ^{13}CHD is approximately 0.3 ppm, with a similar shift for ^{13}CHD to $^{13}CD_2$; an isotope shift of 0.3 to 0.6 ppm is generally observed for each D on a ^{13}C (Vederas, 1987). The presence of the two ^{13}CHD peaks in a 1:1 ratio is likely due to the chirality now present at this carbon caused by the presence of one H and one D (Fig. 24). A comparison of the intensities of the $^{13}CH_2$, ^{13}CHD and $^{13}CD_2$ peaks showed that when C6 is ^{13}C, 73% of the time it is in the form $^{13}CD_2$, 9% in the form ^{13}CHD and 18% in the form $^{13}CH_2$.

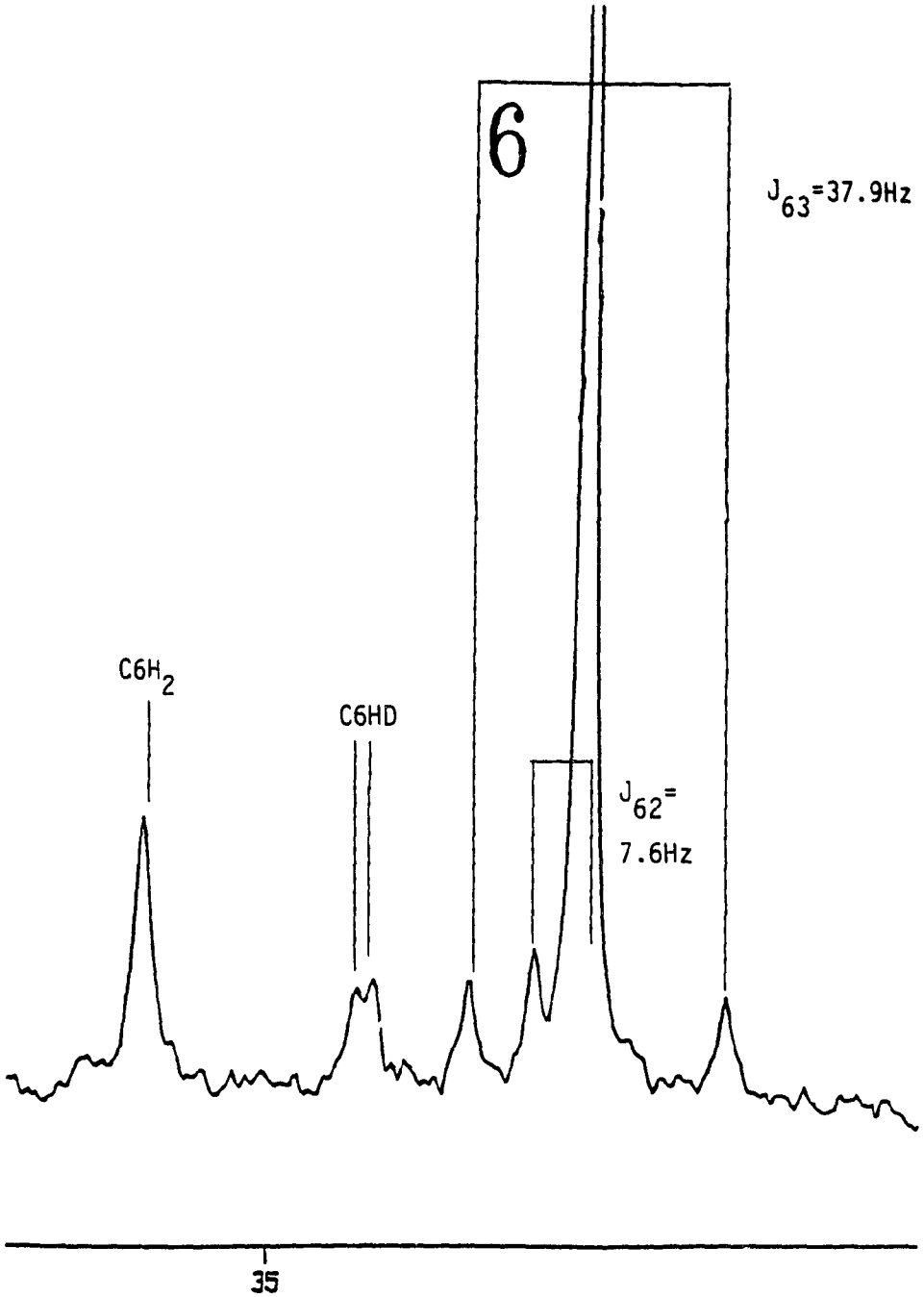

FIGURE 24: AN EXPANSION OF THE ^{13}C-NMR SPECTRUM FOR DOMOIC ACID LABELLED WITH [2-^{13}C,$^{2}H_3$]-ACETATE
EACH CARBON RESONANCE IS NUMBERED AND THE COUPLING CONSTANTS, J_{CC} ARE GIVEN.
(baseline is in PPM)

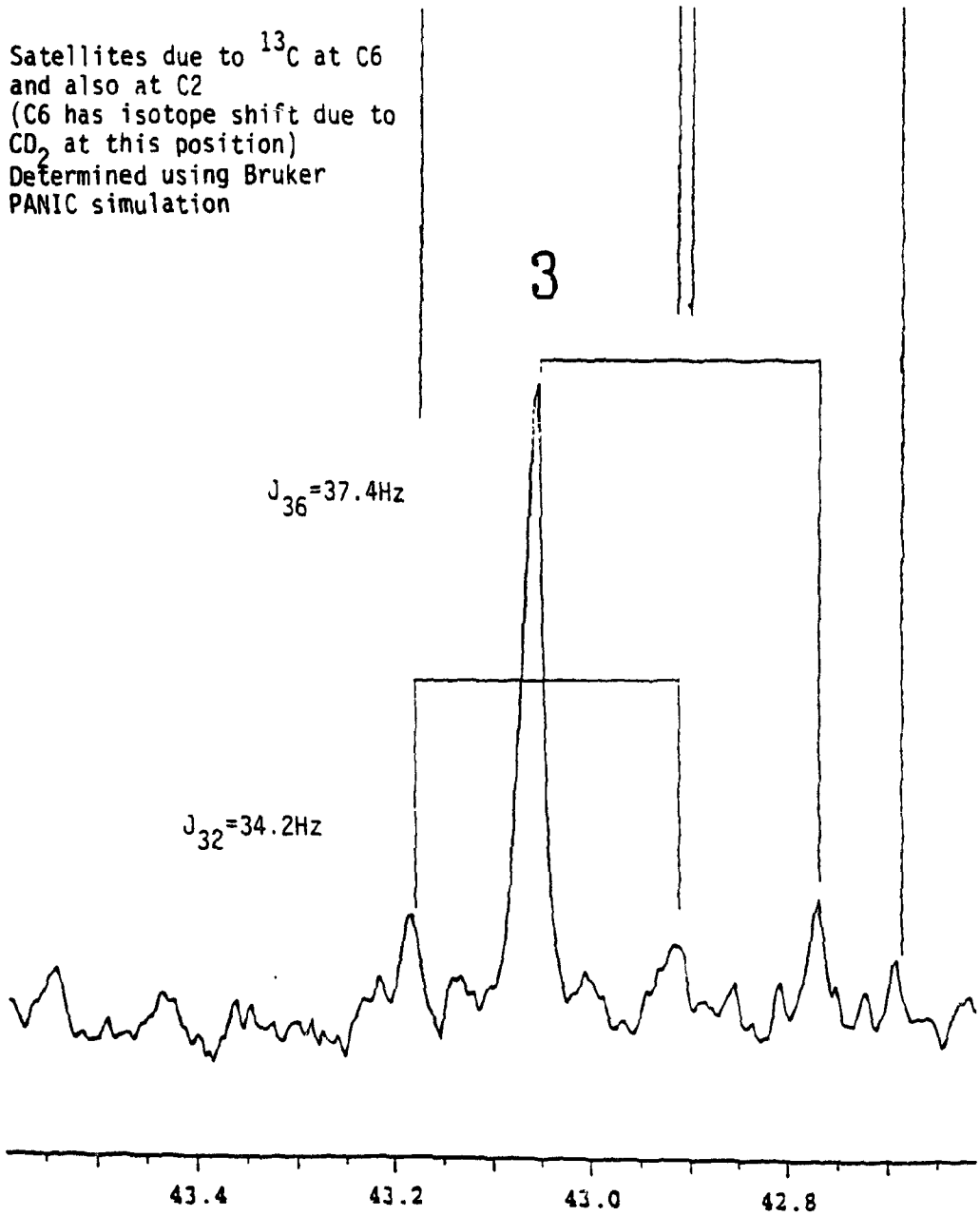

FIGURE 24: (continued)

The expansion of the ^{13}C-NMR spectrum for domoic acid labelled with [2-^{13}C,$^{2}H_3$]-acetate also shows the coupling constants J_{32} and J_{36} (Fig. 24). The ^{13}C-^{13}C satellites resulting from the coupling between C3 and C6 had undergone an isotope shift due to the >70% CD_2 at C6. Satellites also resulted from the presence of ^{13}C at both C6 and at C2 but were shifted upfield due to the CD_2 at C6 (Fig. 24). No isotope shifts were observed for either C2 or C3.

RADIOACTIVE ISOTOPE LABELLING EXPERIMENTS:

GROWTH CURVES

The growth curves of *Pseudonitzschia pungens* f. *multiseries* strain KP59/2 for each of the [1,5-^{14}C]-citrate, [1-^{14}C]-α-ketoglutarate and L[1-^{14}C]-glutamate feeding experiments are shown in Figs. 25, 26, and 27, respectively. In all cases domoic acid production began during late exponential growth phase just prior to the onset of the stationary phase of growth. Each precursor was added in three pulses at the onset of domoic acid production. The [1,5-^{14}C]-citrate was added to Fernbach 1 on days 7, 8 and 9 and to Fernbachs 2 and 3 on days 9, 10 and 11. The [1-^{14}C]-α-ketoglutarate was added to Fernbach 1 on days 10, 11 and 12 and to Fernbachs 2 and 3 on days 11, 12 and 13. The L[1-^{14}C]-glutamate was added to Fernbach 1 on days 9, 10 and 11, to

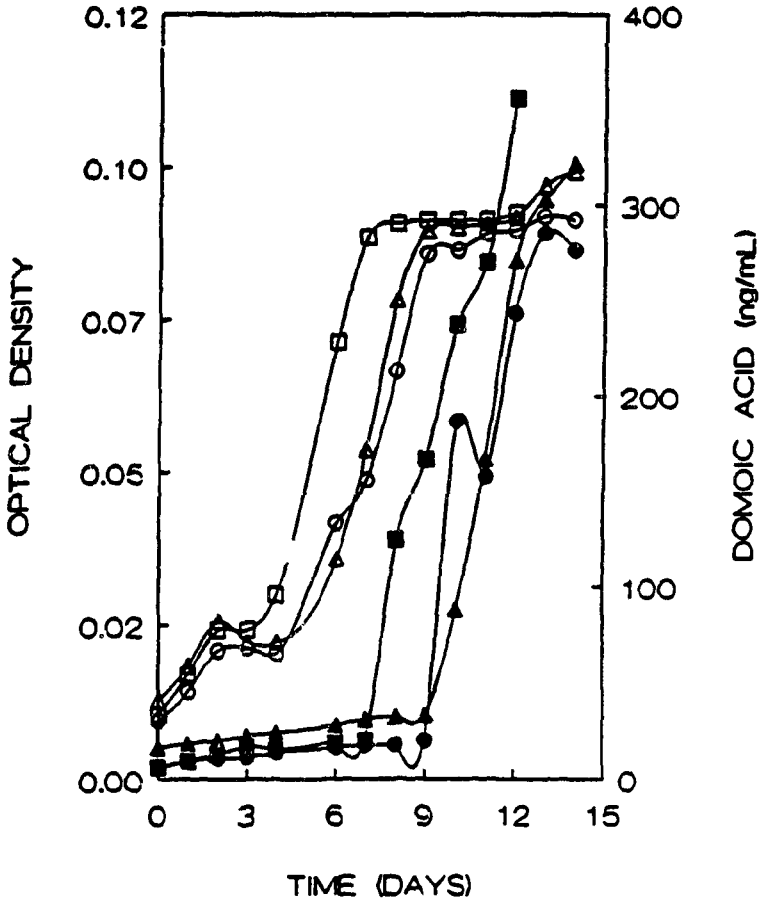

FIGURE 25: GROWTH CURVE AND DOMOIC ACID PRODUCTION BY *PSEUDONITZSCHIA PUNGENS* F. *MULTISERIES* STRAIN KP59/2 WITH [1,5-^{14}C]-CITRATE ADDED JUST PRIOR TO THE STATIONARY PHASE OF GROWTH.
(open symbols represent optical densities and closed symbols represent domoic acid levels; squares for Fernbach 1, triangles for Fernbach 2, and circles for Fernbach 3)

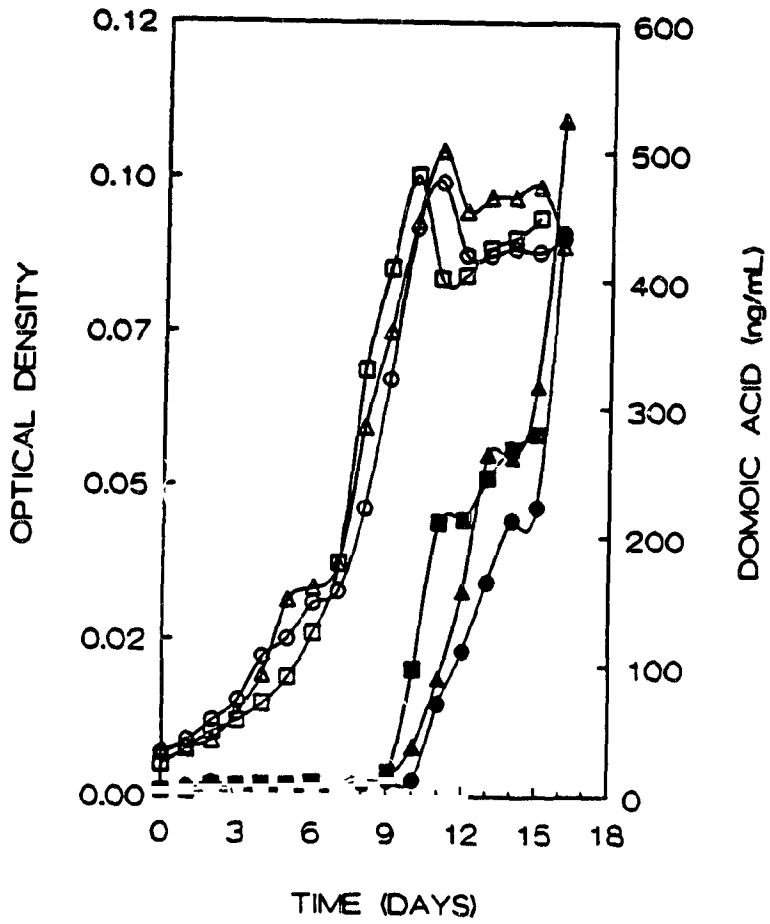

FIGURE 26: GROWTH CURVE AND DOMOIC ACID PRODUCTION BY *PSEUDONITZSCHIA PUNGENS* F. *MULTISERIES* STRAIN KP59/2 WITH [1-^{14}C]-α-KETOGLUTARATE ADDED JUST PRIOR TO THE STATIONARY PHASE OF GROWTH.
(open symbols represent optical densities and closed symbols represent domoic acid levels; squares for Fernbach 1, triangles for Fernbach 2, and circles for Fernbach 3)

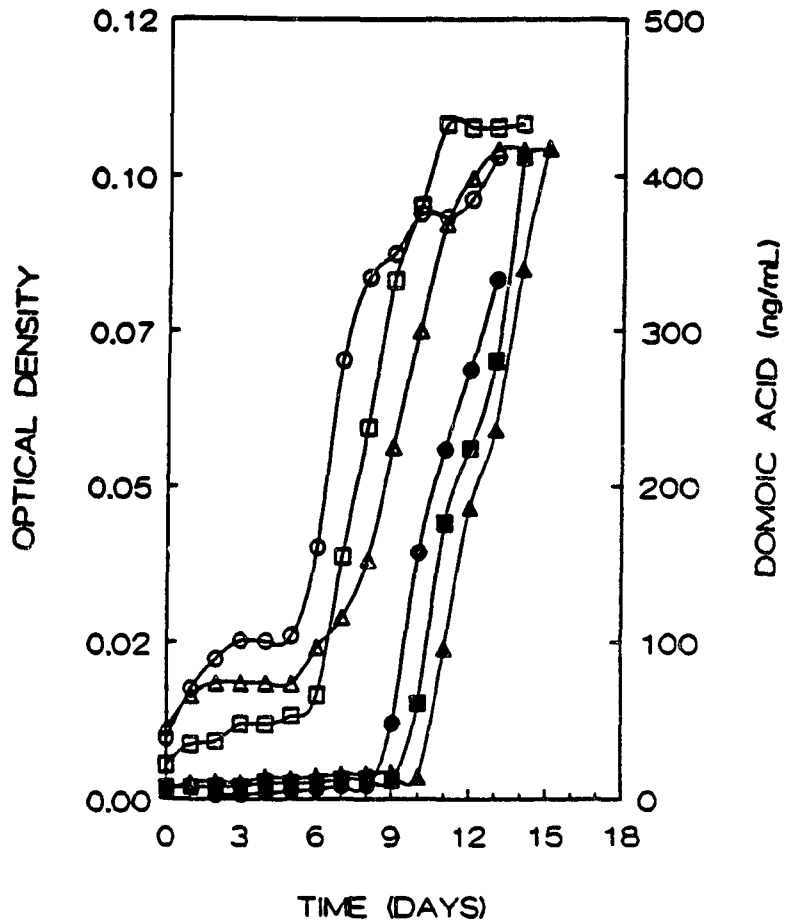

FIGURE 27: GROWTH CURVE AND DOMOIC ACID PRODUCTION BY *PSEUDONITZSCHIA PUNGENS* F. *MULTISERIES* STRAIN KP59/2 WITH L[1-^{14}C]-GLUTAMATE ADDED JUST PRIOR TO THE STATIONARY PHASE OF GROWTH.
(open symbols represent optical densities and closed symbols represent domoic acid levels; squares for Fernbach 1, triangles for Fernbach 2, and circles for Fernbach 3)

Fernbach 2 on days 10, 11 and 12 and to Fernbach 3 on days 8, 9 and 10.

[1,5-^{14}C]-CITRATE, [1-^{14}C]-α-KETOGLUTARATE AND L[1-^{14}C]-GLUTAMATE LABELLING EXPERIMENTS

The amount of domoic acid produced for each Fernbach with [1,5-^{14}C]-citrate, [1-^{14}C]-α-ketoglutarate and L[1-^{14}C]-glutamate added was not significantly different ($P>0.05$) and thus the addition of each of these precursors did not appear to affect the level of domoic acid produced (Fig. 28).

The average cellular incorporation of each of [1,5-^{14}C]-citrate, [1-^{14}C]-α-ketoglutarate and L[1-^{14}C]-glutamate in three Fernbach cultures was not significantly different ($p>0.05$) at 0.63%, 0.53%, and 0.69%, respectively (Fig. 29).

The average incorporations of [1,5-^{14}C]-citrate, [1-^{14}C-α-ketoglutarate, and L[1-^{14}C]-glutamate into domoic acid were low in each case and did not differ significantly ($P>0.05$) (Fig. 30). Large variations between Fernbachs for each precursor were also noted. When the amount of labelled domoic acid was normalized to the total amount of domoic acid produced for each Fernbach, the differences between the labelled compounds were not significant ($P>0.05$) (Table 3). Of the [1,5-^{14}C]-citrate, [1-^{14}C]-α-ketoglutarate and L[1-^{14}C]-glutamate label

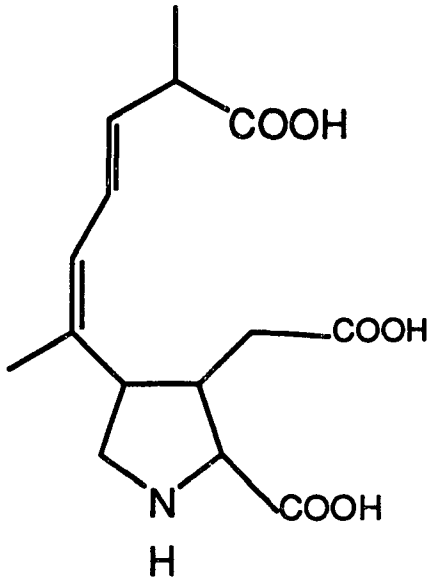

DA (mg)	DA(mg)	DA (mg)
C1 0.294	K1 0.207	G1 0.344
C2 0.270	K2 0.323	G2 0.343
C3 0.231	K3 0.263	G3 0.281
AVG 0.264	AVG 0.264	AVG 0.323
STD 0.231	STD 0.058	STD 0.036

PAIRWISE T-TEST:

C1-C3	K1-K3	NOT SIGNIFICANT
C1-C3	G1-G3	NOT SIGNIFICANT
K1-K3	G1-G3	NOT SIGNIFICANT

FIGURE 28: TOTAL AMOUNT OF DOMOIC ACID SYNTHESIZED IN CULTURES OF *PSEUDONITZSCHIA PUNGENS* F. *MULTISERIES* WITH [1,5-^{14}C]-CITRATE, [1-^{14}C]-α-KETOGLUTARATE OR L[1-^{14}C]-GLUTAMATE ADDED.
(C1, C2 and C3 refer to Fernbachs 1, 2 and 3 with [1,5-^{14}C]-citrate added. Likewise, K1-K3 and G1-G3 refer to Fernbachs with [1-^{14}C]-α-ketoglutarate or L[1-^{14}C]-glutamate added. AVG = average, STD = sample standard deviation)

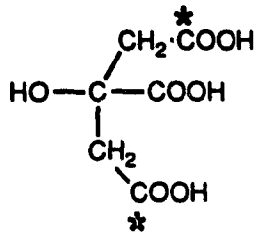

[1,5- ^{14}C]-CITRATE

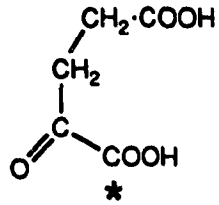

[1-^{14}C]-α-KETOGLUTARATE

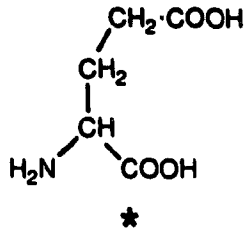

[1-^{14}C]-GLUTAMATE

% CELLULAR INCORPORATION OF ^{14}C COMPOUNDS:

C1 0.83	K1 0.83	G1 0.32
C2 0.5	K2 0.38	G2 1.2
C3 0.55	K3 0.38	G3 0.55
AVG 0.63	AVG 0.53	AVG 0.69
STD 0.18	STD 0.26	STD 0.46
99.4% OUTSIDE CELL	99.5% OUTSIDE CELL	99.3% OUTSIDE CELL

PAIRWISE T-TEST:

C1-C3	K1-K3	NOT SIGNIFICANT
C1-C3	G1-G3	NOT SIGNIFICANT
K1-K3	G1-G3	NOT SIGNIFICANT

FIGURE 29: % INCORPORATION OF [1,5-^{14}C]-CITRATE, [1-^{14}C]-α-KETOGLUTARATE OR L[1-^{14}C]-GLUTAMATE INTO *PSEUDONITZSCHIA PUNGENS* F. *MULTISERIES* CELLS. (C1, C2 and C3 refer to Fernbachs 1, 2 and 3 with [1,5-^{14}C]-citrate added. Likewise, K1-K3 and G1-G3 refer to Fernbachs with [1-^{14}C]-α-ketoglutarate or L[1-^{14}C]-glutamate added. AVG = average, STD = sample standard deviation. Star represents sites of ^{14}C.)

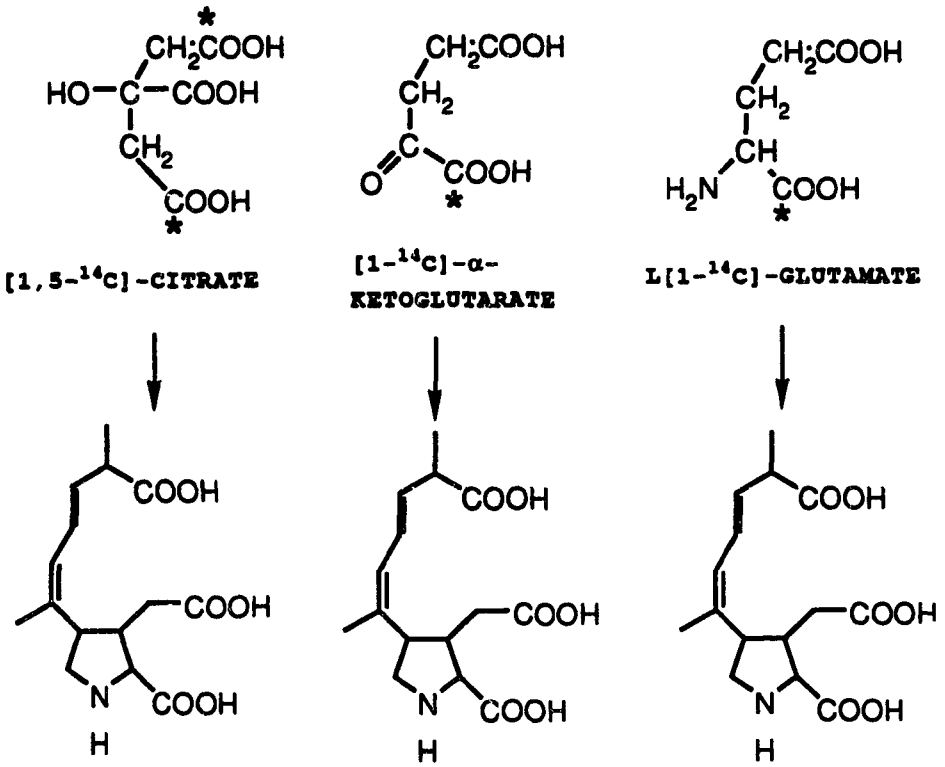

DPM	DPM	DPM
C1 59.21	K1 55.64	G1 54.4
C2 41.33	K2 42.51	G2 135.35
C3 55.01	K3 78.10	G3 70.32
AVG 51.9	AVG 58.6	AVG 86.7
STD 9.4	STD 18.0	STD 42.9

BACKGROUND DPM
38.15
38.56
36.96 AVG 37.6 STD 0.8

PAIRWISE T-TEST:

C1-C3	K1-K3	NOT SIGNIFICANT
C1-C3	G1-G3	NOT SIGNIFICANT
K1-K3	G1-G3	NOT SIGNIFICANT

FIGURE 30: INCORPORATION OF [1,5-^{14}C]-CITRATE, [1-^{14}C]-α-KETOGLUTARATE OR L[1-^{14}C]-GLUTAMATE INTO DOMOIC ACID.

(C1, C2 and C3 represent Fernbachs 1, 2 and 3 with [1,5-^{14}C]-citrate added. Likewise, K1-K3 and G1-G3 refer to Fernbachs with [1-^{14}C]-α-ketoglutarate and L[1-^{14}C]-glutamate. AVG = average, STD = sample standard deviation. Star represents site of ^{14}C).

TABLE 3: DPM VALUES FOR DOMOIC ACID PURIFIED FROM *PSEUDONITZSCHIA PUNGENS* F. *MULTISERIES* CELLS GROWN WITH ADDED [1,5-^{14}C]-CITRATE, [1-^{14}C]-α-KETOGLUTARATE OR L[1-^{14}C]-GLUTAMATE NORMALIZED TO THE AMOUNT OF DOMOIC ACID PRODUCED BY THE CULTURES. AVG = AVERAGE, STD= SAMPLE STANDARD DEVIATION.

FERNBACH NUMBER	DPM/mg DA
[1,5-^{14}C]-CITRATE:	
C1	202.77
C2	153.07
C3	238.14
AVG	197.9
STD	42.8
[1-^{14}C -α-KETOGLUTARATE:	
K1	268.79
K2	131.61
K3	296.96
AVG	232.4
STD	88.4
L[1-^{14}C]-GLUTAMATE:	
G1	158.14
G2	394.61
G3	249.93
AVG	267.6
STD	119.3

PAIRWISE T-TEST:

C1-C3	K1-K3	NOT SIGNIFICANT
K1-K3	G1-G3	NOT SIGNIFICANT
C1-C3	G1-G3	NOT SIGNIFICANT

that entered the cells, 0.035%, 0.08% and 0.11%, respectively, was incorporated into domoic acid (Table 4). The difference between [1,5-^{14}C]-citrate and L[1-^{14}C]-glutamate was significant ($p<0.05$) whereas the differences between [1,5-^{14}C]-citrate and [1-^{14}C]-α-ketoglutarate and between [1-^{14}C]-α-ketoglutarate and L[1-^{14}C]-glutamate were not significant ($P>0.05$).

TABLE 4: DPM VALUES FOR DOMOIC ACID PURIFIED FROM *PSEUDONITZSCHIA PUNGENS* F. *MULTISERIES* CELLS GROWN WITH ADDED [1,5-^{14}C]-CITRATE, [1-^{14}C]-α-KETOGLUTARATE OR L[1-^{14}C]-GLUTAMATE NORMALIZED TO THE CELLULAR DPMs. AVG = AVERAGE, STD = SAMPLE STANDARD DEVIATION, BK = AVERAGE BACKGROUND DPM

FERNBACH	DPM-BK	CELLULAR DPMS	DA DPM/CELL DPM (%)
[1,5-^{14}C]-CITRATE:			
C1	21.31	54959.80	0.039
C2	3.43	27470.10	0.012
C3	17.11	32491.60	0.053
AVG			0.04
STD			0.02
[1-^{14}C]-α-KETOGLUTARATE:			
K1	17.74	47662.16	0.037
K2	4.61	24139.97	0.019
K3	40.20	21712.76	0.185
AVG			0.08
STD			0.09
L[1-^{14}C]-GLUTAMATE:			
G1	16.50	18519.60	0.089
G2	97.45	69960.80	0.139
G3	32.33	31261.60	0.103
AVG			0.11
STD			0.03

PAIRWISE T-TEST:

C1-C3	K1-K3	NOT SIGNIFICANT
C1-C3	G1-G3	SIGNIFICANT
K1-K3	G1-G3	NOT SIGNIFICANT

DISCUSSION

Domoic acid production generally began during the onset of the stationary phase of growth and dramatically increased during the stationary phase as reported in the literature for both non-axenic and axenic cultures of *Pseudonitzschia pungens* f. *multiseries* (Bates et al., 1989a; Douglas and Bates, 1992). The only exception was the production of domoic acid during the late exponential phase in the [1,2-^{13}C]-acetate labelling experiment with *P. pungens* f. *multiseries* strain 13CC grown in a fermentor system. The reason for this deviation is not understood. The media used consistently contained an excess of nitrogen and had a plentiful supply of light, both known requirements for domoic acid production (Bates et al., 1989b).

Unlike the first two labelling experiments with [1-^{13}C]-acetate and [1,2-^{13}C]-acetate which were conducted in a 12 L fermentor system, the early and late [1,2-^{13}C]-acetate feeding experiments and the [2-^{13}C,$^{2}H_3$]-acetate labelling experiments were performed in several 1.5 L Fernbachs. Although all the Fernbach cultures began producing domoic acid after the onset of the stationary phase of growth as usual, the rates varied considerably among the individual Fernbachs. Differences in growth rates among Fernbachs may account for some of this variation in domoic acid production.

The significant isotope enrichment of domoic acid from [1-^{13}C]-acetate at the carboxyl carbon C7(>9%) and C8(>3%) showed that acetate was efficiently taken up by the diatom cells and utilized in domoic acid biosynthesis. There was no measurable isotope enrichment of any other position in the molecule, but the enrichment at C7 and C8 clearly indicates an important role for acetate in domoic acid biosynthesis.

The incorporation of [1,2-^{13}C]-acetate into domoic acid revealed a high level of enrichment of C6 and C7 which was twice that of C2, C3 and C8. In addition C4 and C5 of the proline ring and C1′ to C8′ of the side chain had similar levels of enrichment ranging from 2.7 to 4.3% (average 3.3 +/- 0.6%) (Table 2), suggesting incorporation of acetate into domoic acid through a different intermediate precursor. In the first putative pathway of domoic acid biosynthesis (Fig. 11), in which an isoprenoid chain condenses with an activated citric acid cycle intermediate, a similar level of isotope enrichment would be expected for C4 and C5 of the proline ring and C1′ to C8′ of the side chain since these carbons would be derived from a single biosynthetic source, an intact C10 isoprenoid chain (Fig. 31). A similar level of enrichment with [1,2-^{13}C]-acetate has also been reported in the synthesis of polyterpenes (Stoessl et al., 1978). In this proposed pathway for domoic acid biosynthesis, the other half of the

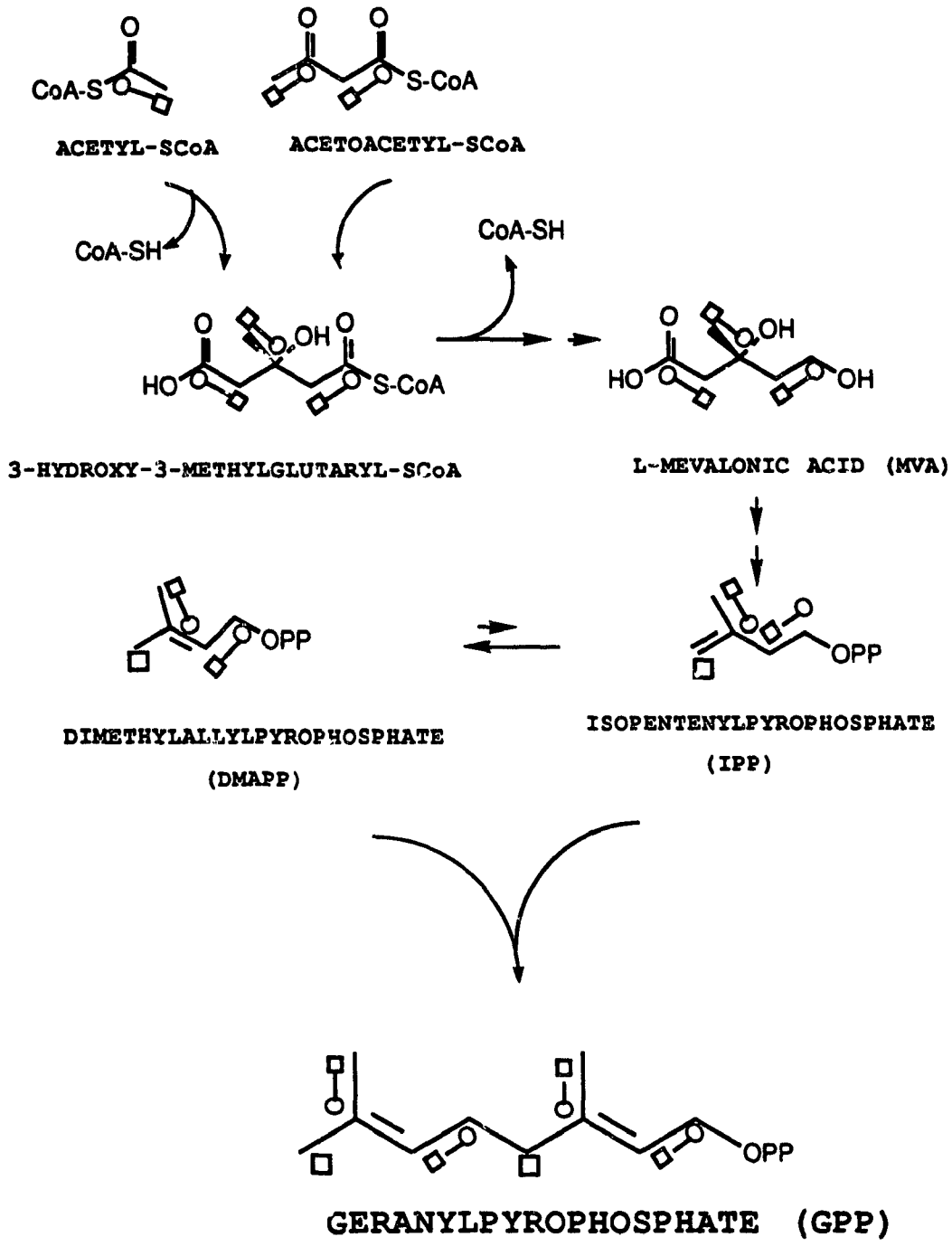

FIGURE 31: THE INCORPORATION OF ACETATE INTO AN ISOPRENOID CHAIN

(□—O represents a CH_3-COOH unit)

molecule is derived from an activated citric acid cycle intermediate, and hence C2, C3, C6, C7, and C8 should show a labelling pattern similar to that expected for an intermediate such as α-ketoglutarate or glutamate. [1,2-^{13}C]-Acetate entering the first round of the citric acid cycle would result in ^{13}C labelling at positions C6 and C7 of domoic acid only (Fig. 32), but after two rounds, two isotopically labelled species of domoic acid would be obtained with a different isotope distribution resulting from passage of the labelled precursor through the cycle (see Fig. 33). In both these isotopic species C6 and C7 are labelled, whereas C2 and C8, or C3, are labelled in only one of the species. The observed enrichment at positions C6 and C7 (approximately 30%) is significantly higher than that at C2, C3 and C8 (approximately 15%), as expected from passage of the precursor through more than one round of the citric acid cycle.

The high probabilities P_{67} and P_{76} (approximately 95%) indicate incorporation of an intact acetate unit at C6-C7 of domoic acid and are consistent with the condensation of acetate with oxaloacetate in the citric acid cycle. The high proportion of doubly-labelled units present at positions C2 and C8, based on probabilities P_{28} and P_{82} of approximately 71%, and the approximately 1/3 single-labelled units at C2 and C8, would result from multiple rounds of the citric acid cycle (Fig 34). The P_{32} and P_{23} values are the same, suggesting that

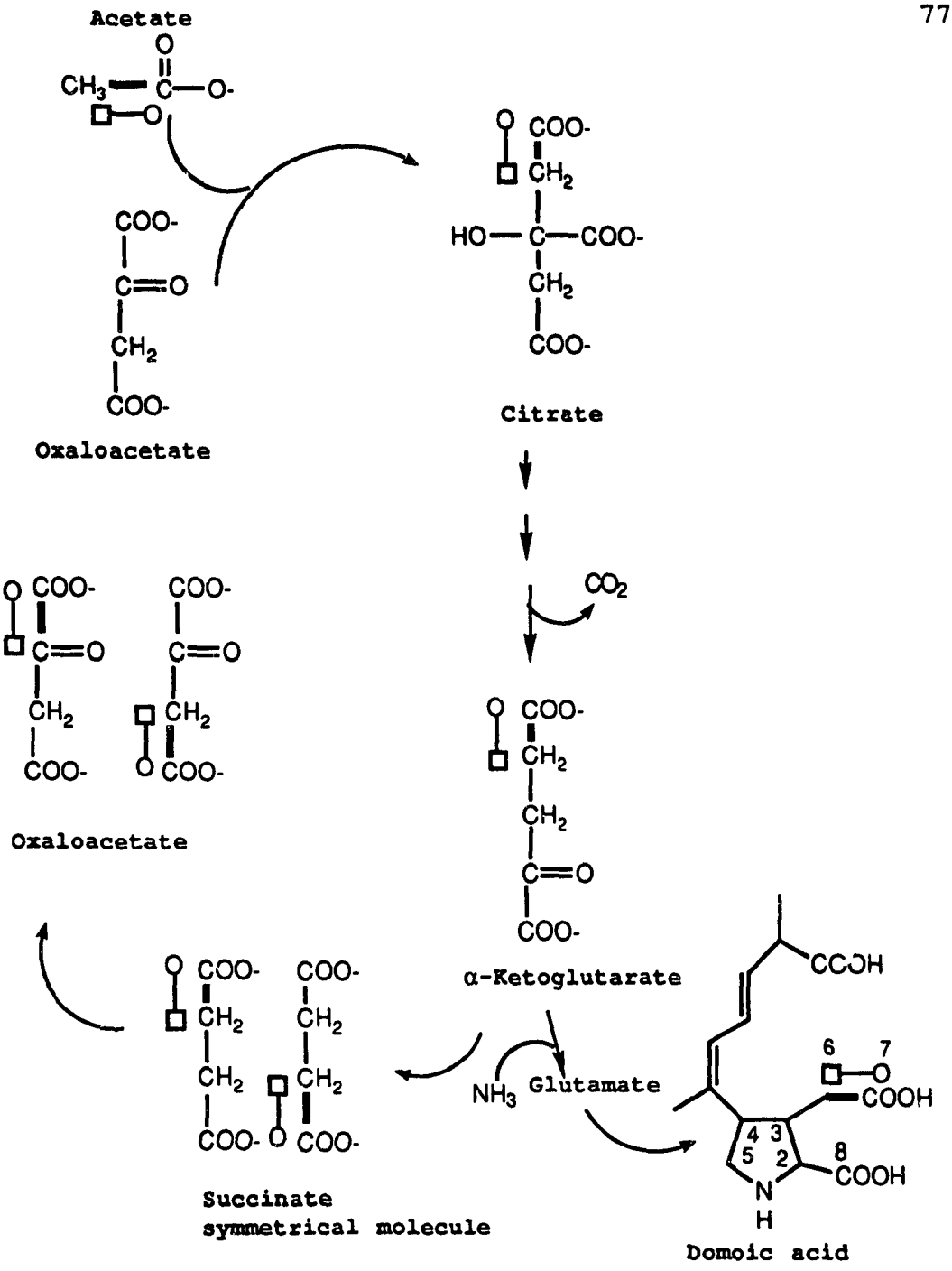

FIGURE 32: LABELLING OF DOMOIC ACID WITH [1,2-^{13}C]-ACETATE DURING ONE ROUND OF THE CITRIC ACID CYCLE (□—○ represents CH_3-COOH)

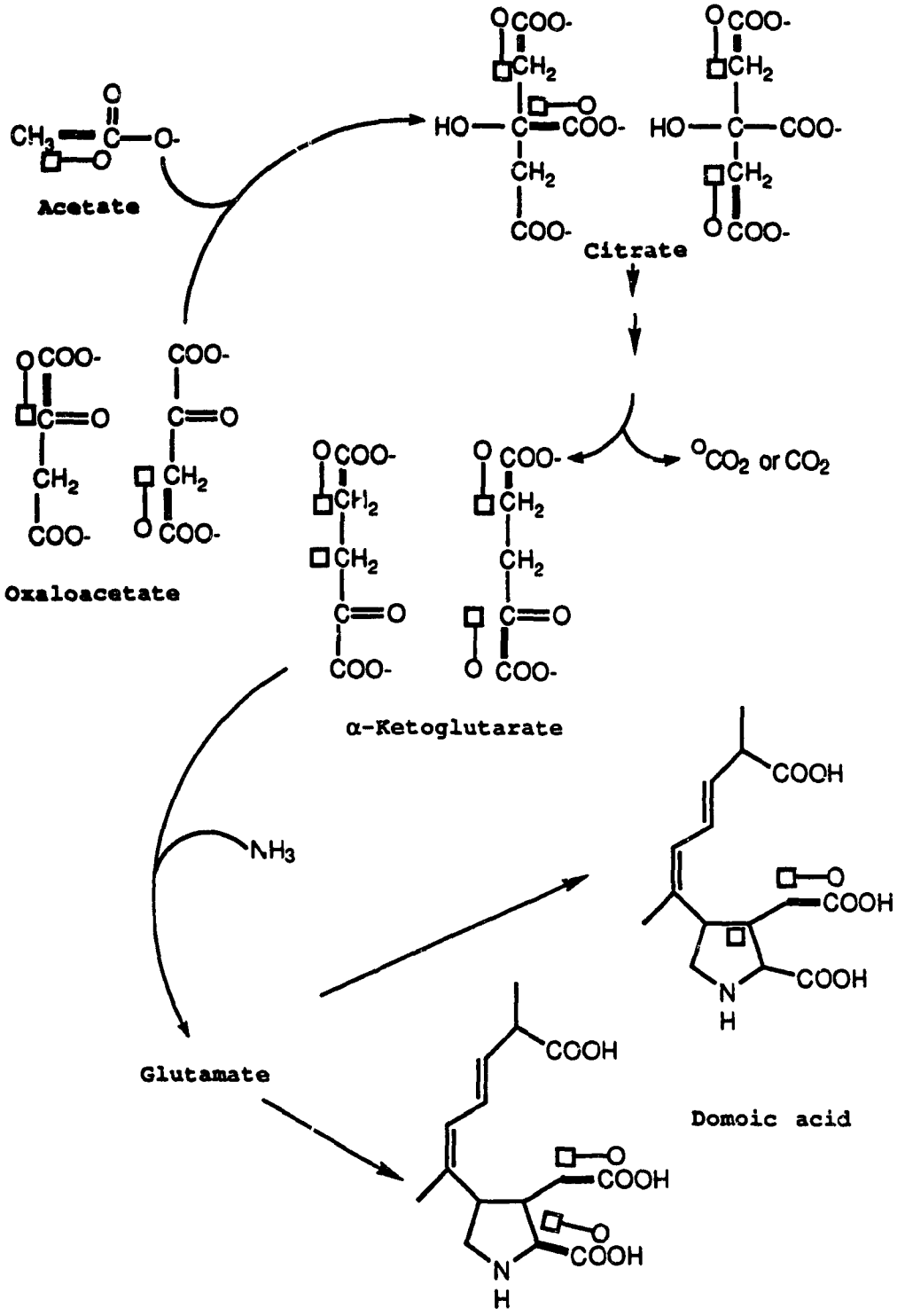

FIGURE 33: LABELLING OF DOMOIC ACID WITH [1,2-^{13}C]-ACETATE DURING THE SECOND ROUND OF THE CITRIC ACID CYCLE

(□—O represents CH_3-COOH)

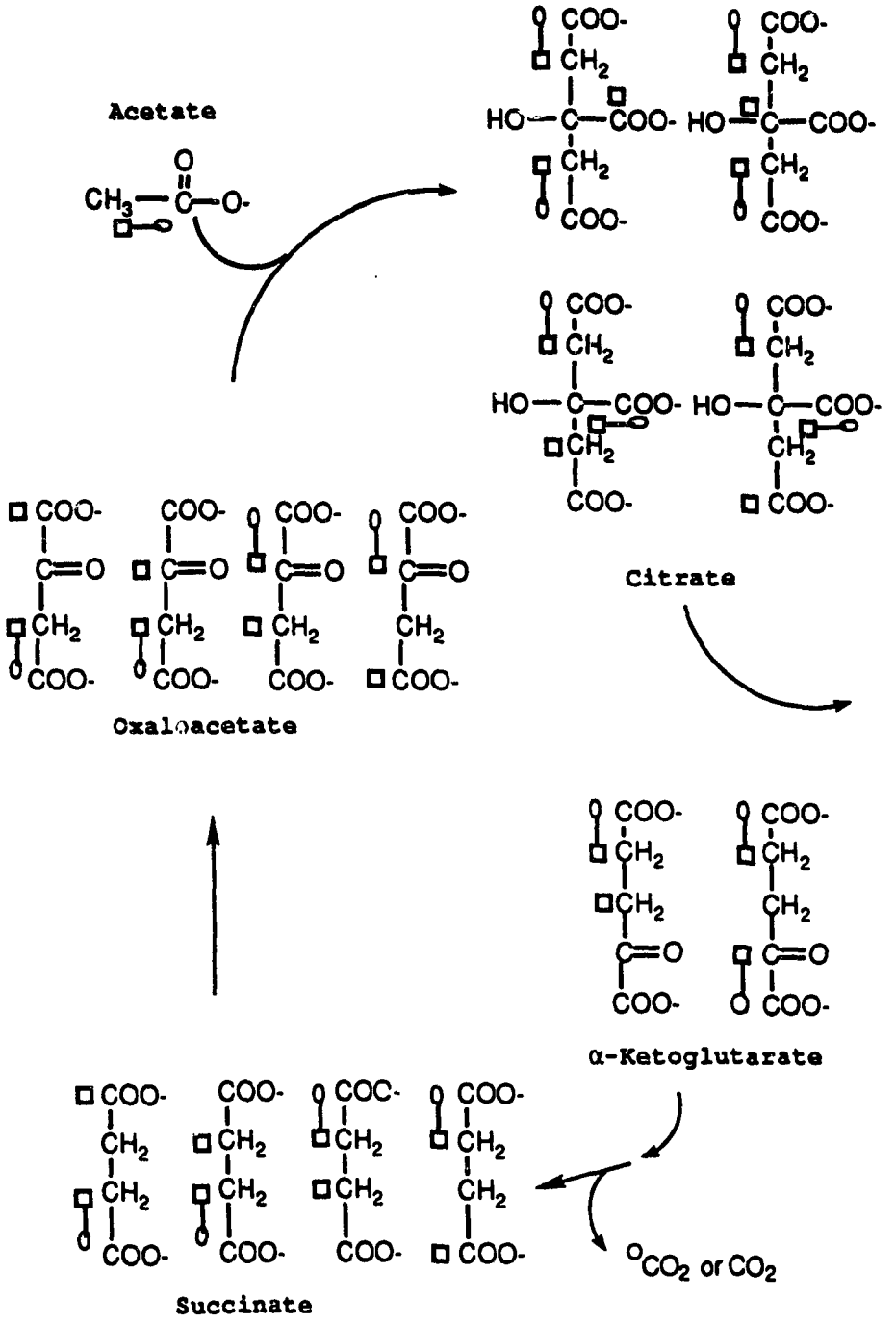

FIGURE 34: LABELLING OF DOMOIC ACID WITH [1,2-^{13}C]-ACETATE DURING THE THREE ROUNDS OF THE CITRIC ACID CYCLE

(□—O represents CH_3-COOH)

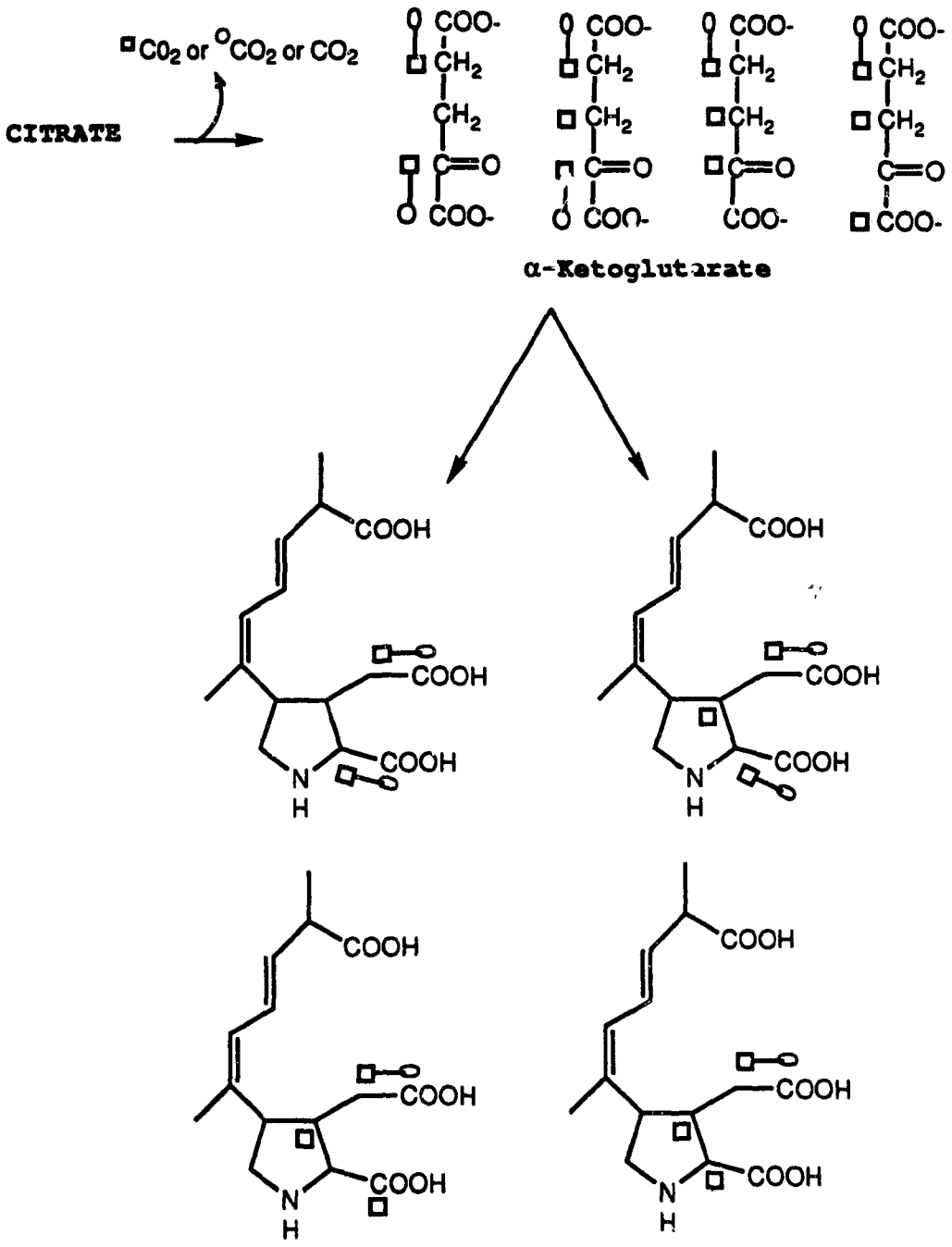

FIGURE 34: (CONTINUED)

when the bond was formed between C2 and C3 the citric acid cycle intermediates were approximately 42% enriched with ^{13}C. The presence of ^{13}C at both C2 and C3 indicates the precursor had completed more than one round of the citric acid cycle (Figs. 33 and 34). Based on the P_{36} and P_{63} values (Fig. 23) it is possible to show that the average ^{13}C enrichment of the C3, C2, C8 unit was diluted to approximately 33% in the oxaloacetate pool at the time of condensation with the 51% enriched pool of acetate. Further dilution with an equal amount of natural abundance product occurred after the formation of the C3, C6 bond resulting in the enrichment values obtained (Table 2).

The incorporation of intact doubly-labelled units at C4, C5; C1′, C8′; C3′, C4′ and C5′, C6′ coincide with the predicted pattern if the side-chain is derived from the isoprenoid pathway. The ambiguity of ^{13}C coupling between C5′ and C7′ and the clear observation of an intact unit between C5′ and C6′ suggests that the end methyl groups of the isoprenoid chain are biosynthetically distinguishable and therefore there is no rotation about the C4′- C5′ bond before oxidation of C7′ to a carboxyl group. Although C2′ was enriched it is formed from a cleaved acetate unit and consequently no satellites were observed.

The lower incorporation of acetate in the isoprenoid

chain compared with the citrate-derived portion, and the presence of single label due to scrambling, suggests that the acetate for isoprenoid synthesis is from a different acetate pool than that used by the citric acid cycle. One explanation for this is that the geranylpyrophosphate derivative was synthesized early before the acetate precursor was added, and later utilized for domoic acid biosynthesis when the citric acid cycle derivative was produced. Another explanation is that the geranylpyrophosphate is synthesized in another portion of the cell less accessible to acetate. Yet a third explanation is that the isoprenoid skeleton is assembled from an alternate pathway, such as from isoleucine (Mann, 1987). However, few cases of isoprenoid synthesis from isoleucine have been reported (Mann, 1987).

In the second proposed pathway of domoic acid biosynthesis (Fig. 11), a cleaved isoprenoid chain condenses with proline. Proline results from the cyclization of glutamate via the semi-aldehyde and thus from the citric acid cycle. Based on the expected results of one or two rounds of the citric acid cycle as previously described, C4 and C5 should be more highly enriched than C2, C8, and C3 if the former are derived from proline. The lower level of enrichment at C4 and C5 in contrast to C2, C8 and C3 thus argues against this alternative pathway of domoic acid biosynthesis.

In the third putative pathway of domoic acid biosynthesis (Fig. 11), a fatty acid chain condenses with glycine and addition of three C_1 groups is required to complete the toxin structure. If the molecule is derived from this pathway a similar level of ^{13}C isotope enrichment would be expected for C6'-C1', C4, C3, C6 and C7 since these carbons would be derived from the same fatty acid chain and thus a common pool of acetate. An examination of the [1,2-^{13}C]-acetate labelling results of domoic acid reveals that ^{13}C enrichment levels are not consistent with this pattern and show significantly higher levels of ^{13}C enrichment at C3, C6 and C7 in contrast to the low levels of C1' to C6'.

In the [1,2-^{13}C]-acetate labelling experiment described above, the lower incorporation of acetate in C4 and C5 and C1' to C8' in contrast to the higher levels of incorporation of acetate units at C2, C8 and C6, C7 led to the suggestion that the geranyl unit may be synthesized early and is only utilized for domoic acid biosynthesis when the citric acid derivative becomes available. If the isoprenoid chain was synthesized early then a higher level of ^{13}C enrichment in this chain would be expected when the labelled acetate was added early rather than later in the growth cycle. In order to test this theory [1,2-^{13}C]-acetate was added to cultures either early or late during exponential growth. The % incorporation of ^{13}C in domoic acid from both experiments did not differ greatly from

each other, revealing that the time of precursor addition has little effect. This result suggests that acetate is stored in a pool that is utilized during the growth period for biosynthesis, including the synthesis of the isoprenoid chain. The low levels of enrichment in the isoprenoid chain may then result from a greater dilution of the acetate pool with natural abundance material in comparison to the acetate pool used in the citric acid cycle-derived portion of domoic acid.

Another possible explanation for the lower level of incorporation of [1,2-^{13}C]-acetate in the isoprenoid sidechain in comparison to the citric acid cycle-derived portion, is a reduced level of accessibility of acetate to the site of isoprenoid synthesis. Many isoprenoid compounds in plants, especially those involved in photosynthesis such as the chlorophyll pigments, are synthesized in the plastid (Kleinig and Beyer, 1985). In diatoms the plastid is surrounded by four membranes, the inner two being the membranes of the organelle itself and the outer two representing the plastid endoplasmic reticulum (Round et al., 1990). The permeability of the plastid endoplasmic reticulum membranes to acetate or acetyl-SCoA is not known. The outer chloroplast membrane in plants is freely permeable to low molecular weight compounds while the inner membrane is less permeable and transport is generally facilitated by translocator proteins located within

the membrane (Lehner and Heldt, 1978; Goodwin and Mercer, 1983; Flugge and Heldt, 1991). The chloroplast inner membrane is permeable to acetate but not to acetyl-SCoA. Acetate, a relatively metabolically inert molecule, is transported into the chloroplast where it is converted by acetyl-SCoA synthetase into acetyl-SCoA, the more reactive form (Stumpf, 1980).

If the isoprenoid chain in domoic acid is synthesized in the chloroplast then its enzymes must compete with enzymes from other pathways that draw from the acetyl-SCoA pool, such as those involved in lipid biosynthesis (Goodwin and Mercer, 1983). Lipid synthesis, which occurs in the chloroplast, generally increases when diatoms are limited in growth by a deficiency of Si (Taguchi et al., 1987; Roessler, 1988). In cultures of *P. pungens* f. *multiseries* grown under Si-limiting conditions with an excess of N, free fatty acid levels increased while overall lipid levels decreased (Parrish et al., 1990). The catabolism of acetate-derived products may also add scrambled label back into the acetyl-SCoA pool, which may then be incorporated during further isoprenoid synthesis.

In these early and late [1,2-^{13}C]-acetate feeding experiments a different axenic strain of *Pseudonitzschia pungens* f. *multiseries* was used. In the first two labelling experiments strain 13CC, originating from Galveston, Texas,

was used. However, over time 13CC produced lower levels of domoic acid and was no longer useful for biosynthetic studies. Another axenic strain, KP59/2, originating from Cardigan Bay, P.E.I., was therefore used for all subsequent experiments. Consequently it was essential to ensure that the labelling pattern of domoic acid from [1,2-^{13}C]-acetate was consistent between the two strains. Strain KP59/2 indeed yielded domoic acid with a similar 2:1 ratio for C6 and C7 versus C2, C8 and C3 and low levels of ^{13}C enrichment in the proline ring carbons C4 and C5 and the side chain carbons C1′ to C8′. The only difference was significantly lower levels of ^{13}C enrichment in C2, C3, C6, C7 and C8 in strain KP59/2 as compared to strain 13CC. This difference may result from addition of the labelled acetate in one pulse to the Fernbachs used in the early and late feeding experiments. The labelled acetate was added in three pulses separated by 24 h in the previous [1,2-^{13}C]-acetate experiment grown in the fermentor system. Nevertheless the experiments revealed an important observation that these geographically separate strains both employ a similar pathway for domoic acid biosynthesis.

Further information on the mechanisms of domoic acid biosynthesis can be obtained by using precursors labelled with both ^{13}C and ^{2}H. The [2-^{13}C, $^{2}H_3$]-acetate-derived domoic acid showed low levels of ^{13}C enrichment in C4, C5 and C1′ to C8′, similar to those of the other labelling experiments, and

evidence of scrambling of some of the label was indicated by the presence of ^{13}C at sites where it would not be predicted if synthesized directly from [2-^{13}C, $^{2}H_3$]-acetate (Fig. 35). Significantly, deuterium was also not detected at C4, C5 and C1' to C8', which may be further evidence of scrambling of the label. The low levels of enrichment may, however, preclude the identification of deuterium from the incorporation of intact label.

As expected, the % incorporation of ^{13}C in domoic acid from [2-^{13}C,$^{2}H_3$]-acetate is much higher at positions C2, C3, C6, C7, and C8, proposed to originate from a citric acid cycle intermediate (Table 2). In the first round of the cycle, only C6 is labelled (Fig. 36) and in the second round C6 as well as C2 or C3 are labelled (Fig. 37). In the third round, the ^{13}C label from the methyl group of acetate is present at C6, C2, C3 and at the carboxyl carbon C8 (see Fig 34). The enrichment at C6(9.1%) is three times the enrichments of C3(3.0%) and C2 (2.7%). This differs from the 2:1 ratio seen for the [1,2-^{13}C] acetate labelling experiments. This difference is probably due to size variations within the pools of acetate and citric acid cycle intermediates. The probability of C2 being ^{13}C when C3 was ^{13}C was 30% but upon bond formation between C3 and C6, the probability was reduced to 14%, likely due to dilution of the citric acid cycle intermediate pool with an equal amount of natural abundance material before the bond formed. This is

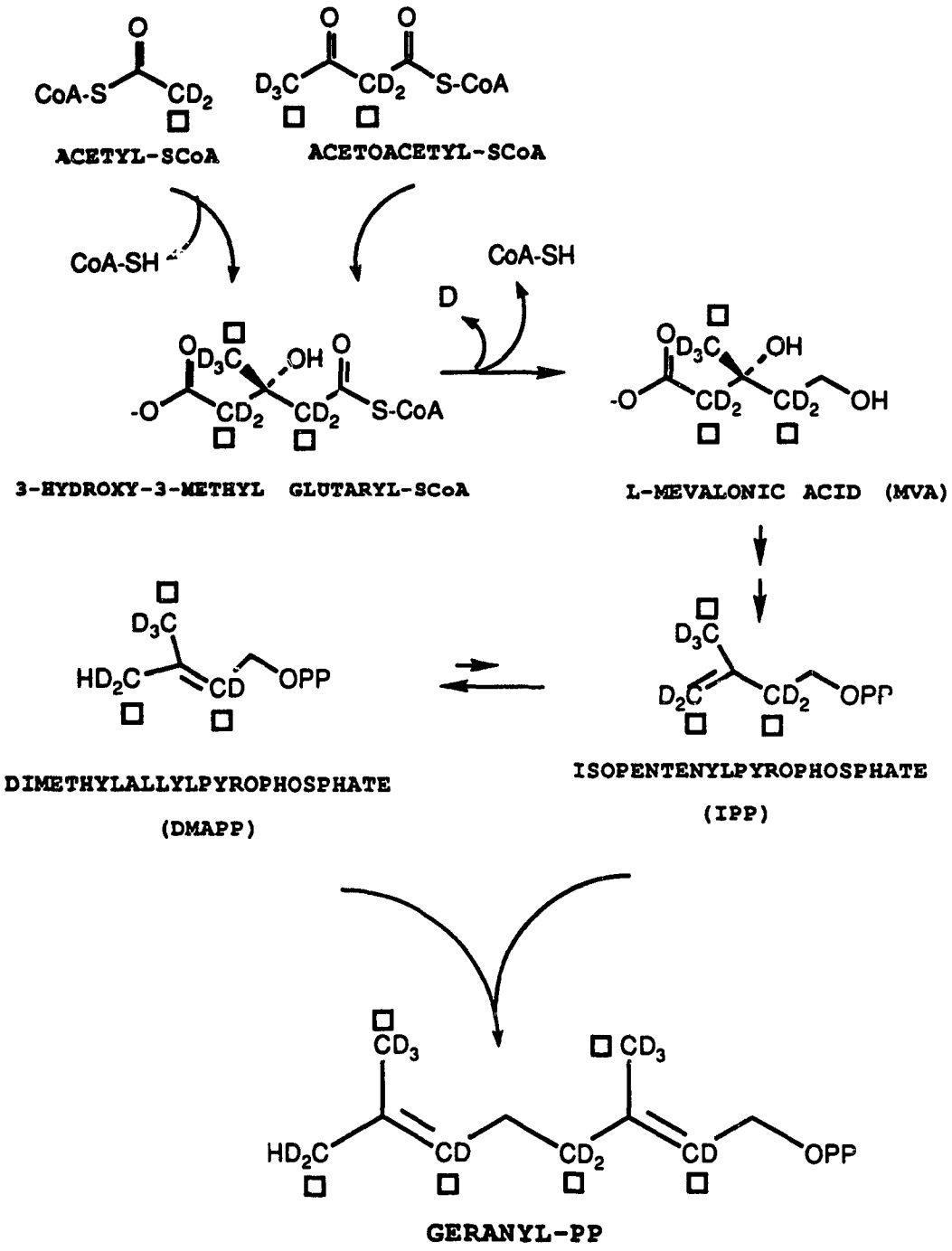

FIGURE 35: [2-^{13}C, $^{2}H_3$]-ACETATE LABELLING OF AN ISOPRENOID CHAIN

(□ represents the methyl group of acetate)

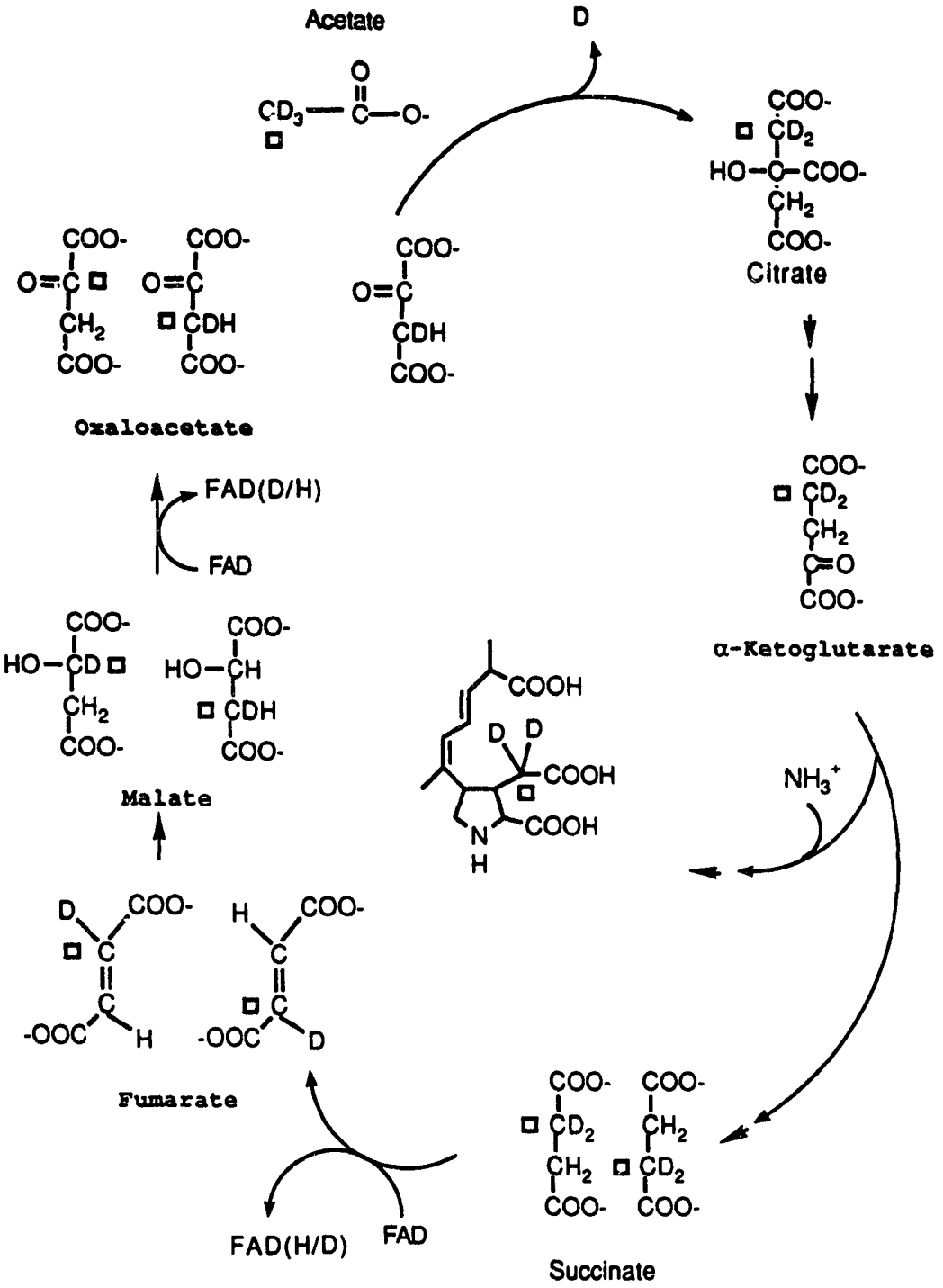

FIGURE 36: LABELLING OF DOMOIC ACID WITH [2-^{13}C,^{2}H$_3$]-ACETATE DURING THE FIRST ROUND OF THE CITRIC ACID CYCLE. D = DEUTERIUM

(□ represents methyl group of acetate)

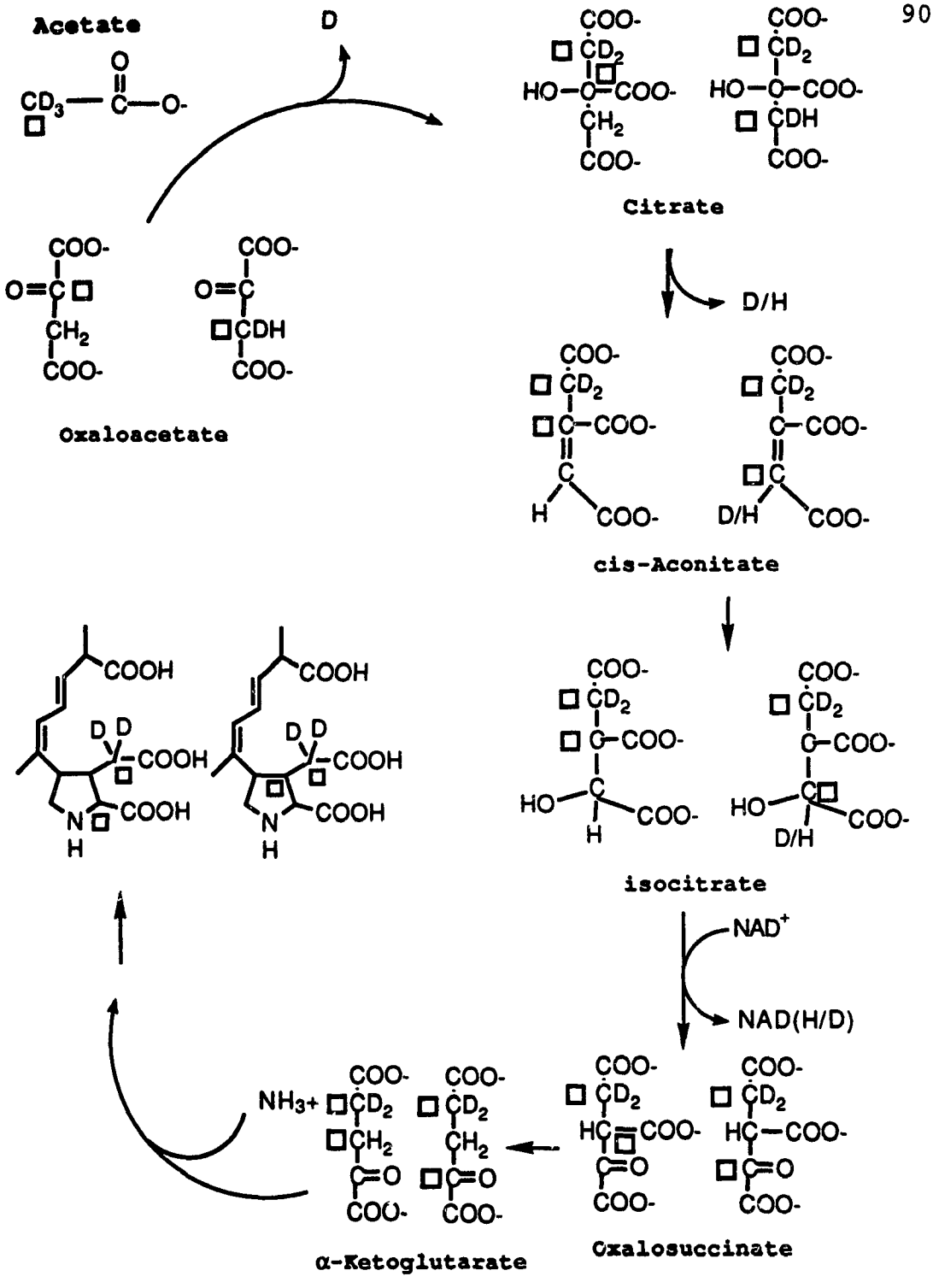

FIGURE 37: LABELLING OF DOMOIC ACID WITH [2-^{13}C,^{2}H$_3$]-ACETATE DURING THE SECOND ROUND OF THE CITRIC ACID CYCLE D= DEUTERIUM
(□ represents the methyl group of acetate)

substantiated by the 12% probability that when ^{13}C was at C6, there was also ^{13}C at C3. This probability (P_{63} 12%) is approximately a quarter of the probability P_{36} of 52% that when ^{13}C was at C3 there was also ^{13}C at C6. This pool was then diluted with 5 times the amount of natural abundance material resulting in the % incorporation values observed (Table 2). Kinetic isotope effects may result from the increase in energy required to break the C-D bond due to the decreased bond length in comparison to the C-H bond (Sedgewick and Cornforth, 1977). In the present situation the kinetic isotope effect would result in a decrease in the ^{13}C enrichment ratio of C6, C7 to C3,C2 and C8 due to the presence of deuterium at C6 and the lack of deuterium at C2 and C3. In fact an increase in this ratio was observed, suggesting that kinetic isotope effects can be excluded.

The total retention of deuterium at C6 was 77.5%. When position C6 was ^{13}C, 73% of the time it was in the form $^{13}CD_2$, 9% in the form ^{13}CHD and 18% in the form $^{13}CH_2$. This suggests that the labelled acetate unit condensing with oxaloacetate in the citric acid cycle has undergone minimal scrambling.

No isotope shifts were observed for either C2 or C3, confirming the absence of deuterium at these positions and supporting the role of a citric acid cycle intermediate in the biosynthesis of domoic acid. The deuterium present at C2 in

citrate, cis-aconitate and isocitrate would be removed during the oxidation of the hydroxyl group in isocitrate to a ketone group in the production of α-ketoglutarate. Oxalosuccinate is an intermediate in the conversion of isocitrate to α-ketoglutarate by the enzyme isocitrate dehydrogenase and usually remains bound to the enzyme during the reaction. The centric diatom *Cyclotella cryptica* grown under Si starvation conditions showed a 2/3 reduction in the α-ketoglutarate and L-glutamate pool sizes (Werner, 1978). It was speculated that the enzyme isocitrate dehydrogenase was regulated by an effector that is itself a silicon compound or is affected by silicon metabolism (Werner, 1978). Perhaps oxalosuccinate is synthesized without the final decarboxylation reaction necessary to generate α-ketoglutarate. Domoic acid production in *P. pungens* f. *multiseries* has been documented to occur when Si is limiting (Bates et al., 1989), although an excess of nitrogen is also required. At the moment it is not known if *P. pungens* f. *multiseries* responds to Si-limited conditions with an excess of nitrogen in the same manner as *Cyclotella cryptica* when Si is lacking.

Based on the examination of the ^{13}C enrichment results from the labelled acetate experiments it appears that domoic acid is synthesized from an isoprenoid chain condensing with an activated citric acid cycle derivative. Further details of the pathway of synthesis were required, such as the identity

of the activated citric acid cycle derivative. Labelling experiments with [1,5-^{14}C]-citrate, [1-^{14}C]-α-ketoglutarate and L[1-^{14}C]-glutamate were performed in order to gain more information about this derivative, since the levels of incorporation of these labelled compounds into domoic acid might suggest the point of exit from the citric acid cycle of the product which condenses with the isoprenoid chain.

The average incorporations of [1,5-^{14}C]-citrate, [1-^{14}C]-α-ketoglutarate, and L[1-^{14}C]-glutamate into domoic acid were low in each case and did not significantly differ ($P>0.05$). The low incorporation of dicarboxylic acids and tricarboxylic acids has been reported in biosynthetic studies of other marine algal metabolites, such as brevetoxin (Shimizu, 1993).

The low cellular incorporation level of less than 1% for [1,5-^{14}C]-citrate, [1-^{14}C]-α-ketoglutarate and L[1-^{14}C]-glutamate suggests that an active form of transport for citrate, α-ketoglutarate and glutamate is not present in the diatom *Pseudonitzschia pungens* f. *multiseries* strain KP59/2. These compounds appear to be passively diffusing through the cell wall and cell membrane. The low incorporation of these ^{14}C-labelled compounds suggests that experiments with stable ^{13}C-labelled citrate, α-ketoglutarate and glutamate are not feasible.

The addition of [1,5-^{14}C]-citrate, [1-^{14}C]-α-ketoglutarate or L[1-^{14}C]-glutamate to the cultures did not affect the level of domoic acid production. Although the amount of domoic acid produced between Fernbachs was not significantly different, large variations did occur in the amount of labelled domoic acid that was formed. Results from both [1,2-^{13}C]-acetate and [2-^{13}C,$^{2}H_3$]-acetate labelling experiments suggested that acetate entering the citric acid cycle undergoes multiple rounds of the cycle. If [1,5-^{14}C]-citric acid, [1-^{14}C]-α-ketoglutarate and deaminated L[1-^{14}C]-glutamate entered multiple rounds of the citric acid cycle, then the ^{14}C label would be lost as $^{14}CO_2$. A high degree of variation in labelled domoic acid between the Fernbachs would result depending on the number of rounds of the citric acid cycle and the pool sizes of each intermediate.

Less than 1% of the ^{14}C-labelled precursors that entered the cells were incorporated into domoic acid. This may result from the inaccessibility of the enzymes in domoic acid biosynthesis to the labelled precursors. The activated citric acid cycle derivative suggested to condense with the isoprenoid chain is most likely derived from the citric acid cycle within the mitochondria. Although the chloroplasts in many plant species contain enzymes from the citric acid cycle, such as isocitrate dehydrogenase, it is not clear if enzymes required for a complete citric acid cycle are present (Chen

and Gadal, 1990; Graham, 1980). In the mitochondria, the enzymes of the citric acid cycle, with the exception of succinate dehydrogenase which is integrated into the inner membrane, are located in the mitochondrial matrix, which is bound by a double membrane system (Goodwin and Mercer, 1983). The outer membrane functions as a physical barrier to large solutes while the inner membrane functions as the permeability barrier (Wiskich, 1977). In many plants, including the alga *Scenedesmus* sp., labelled acetate (possibly in the form of acetyl-SCoA) is incorporated into intermediates of the citric acid cycle, suggesting that the inner membrane of the mitochondria is permeable to acetate or acetyl-SCoA (Graham, 1980).

The transport of the ^{14}C-labelled compounds across the mitochondrial membrane, the proposed site of synthesis of the citric acid cycle intermediate in domoic acid biosynthesis, is regulated by the concentration of organic acids within the mitochondria (Wiskich, 1980). Most of the mitochondrial tricarboxylic acids are present as citrate instead of isocitrate because of the equilibrium characteristics of aconitase (Wiskich, 1980). This results in an increase in citrate concentrations within the mitochondria and thus an efflux of this citric acid cycle intermediate into the cytoplasm (Wiskich, 1980). This may affect the rate of influx of [1,5-^{14}C]-citrate or the exchange with other tricarboxylic

acids in the mitochondrial matrix. The α-ketoglutarate carrier in plant mitochondria appears to be different from the tricarboxylic acid carrier but its regulation is not clearly understood (Wiskich, 1980). Glutamate transport into the mitochondria is less specific and can exchange with either dicarboxylic or tricarboxylic ions within the mitochondria (Wiskich, 1980).

The amount of cellular [1-^{14}C]-glutamic acid incorporated into domoic acid was significantly higher than that of [1,5-^{14}C]-citrate. This result suggests that glutamic acid may be a more direct precursor to the activated citric acid cycle derivative which condenses with the isoprenoid chain. The incorporation of α-ketoglutarate, which is an intermediate in the conversion of citrate to glutamate, was not significantly different from either of the other ^{14}C precursors, as expected if glutamate is closer to the end of the pathway that synthesizes the activated derivative. If glutamate is a precursor, then the low levels of incorporation suggest that the activation of C3 may be necessary before glutamate undergoes the condensation reaction with the isoprenoid chain. The cellular site of activation of glutamate may be inaccessible to the [1-^{14}C]-glutamic acid added to the cells.

CHAPTER TWO

THE SEARCH FOR INTERMEDIATES IN THE BIOSYNTHESIS OF DOMOIC ACID AND KAINIC ACID

INTRODUCTION

Many compounds of both primary and secondary metabolism are modified by the attachment of isoprenoid chains. The process is called prenylation and once attached the isoprenoid chain is called a prenyl group. In some cases the prenyl group remains in its linear form while in others it cyclizes to produce a ring system. This introduction will examine the general process of prenylation in compounds from different biogenetic sources. The process of prenylation in kainoid biosynthesis will also be discussed. The discovery of intermediates provides insights into the biosynthetic pathway of a secondary metabolite; this chapter will speculate on and describe the search for such intermediates in kainoid biosynthesis.

Many compounds from very diverse biochemical origins are prenylated in plants. Within a molecule, the prenyl group may be attached through one of several activated atoms including carbon, oxygen, nitrogen or sulphur. In many cases carbon atoms within phenolic ring systems are prenylated. A phenolic hydroxyl group activates the benzene ring and enhances the probability of a second substitution in the ring at the *ortho*- or *para*-positions (Fessenden and Fessenden, 1982; Ege, 1989). Consequently, prenylation of a phenol occurs at the *ortho*- or *para*-positions as found in the prenylation of isoflavonoids,

coumarins, and quinolines. In many cases the presence of an adjacent phenolic group results in cyclization of the prenyl group to form either a furan or a pyran ring system such as is found in the isoflavonoid glyceollin, the coumarin psoralen, and the furoquinoline alkaloid dictamnine (Fig. 38; Welle and Grisebach, 1988; Austin and Brown, 1973; Hamerski and Matern, 1988; Grundon, 1988). In other carbon-prenylated compounds the isoprenoid origins of the prenyl group are further obscured when it is incorporated into the backbone of the final structure, as exemplified by the ergoline alkaloid elymoclavine or the indole alkaloid strictosidine (Fig. 39; Robinson, 1981; Kutchan et al., 1991).

In the prenylation of oxygen, nitrogen and sulphur, nucleophilic groups such as -OH , $-NH_2$ and -SH displace the pyrophosphate group of the isoprenoid unit to produce the prenylated product. In these cases subsequent cyclization of the prenyl group is less likely to occur, as seen in the prenyl groups attached to the oxygen of coumarins, the nitrogen of adenine within tRNA, or the sulphur of cysteine residues within proteins (Fig. 40, Chiang et al., 1982; Hamerski et al., 1990a; Letham and Palni, 1983; Connolly and Winkler, 1989; Rilling et al., 1989).

The biosynthesis of domoic acid is an exception to this general trend since the prenyl group attached to the nitrogen

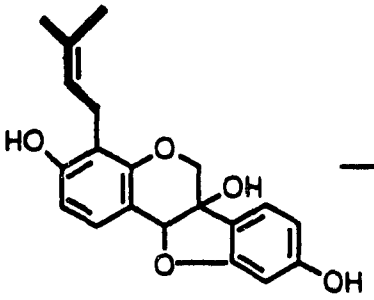

4-DIMETHYLALLYLGLYCINOL

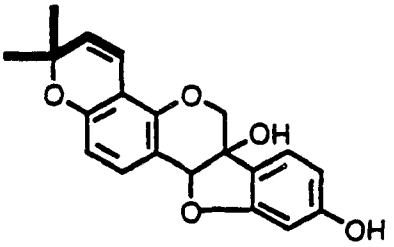

GLYCEOLLIN I

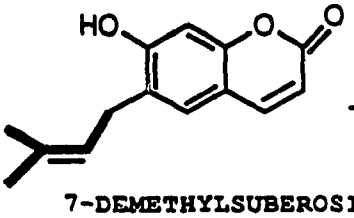

7-DEMETHYLSUBEROSIN

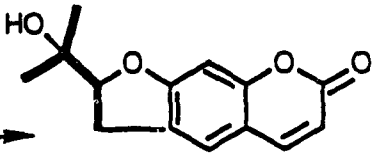

MARMESIN

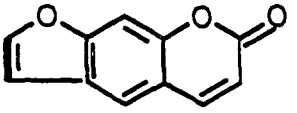

PSORALEN

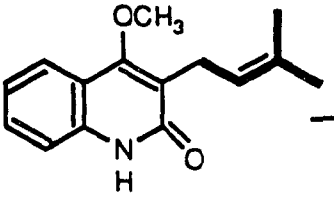

4-METHOXY-3-PRENYLQUINOLINE

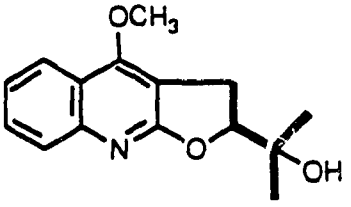

PLATYDESMINE

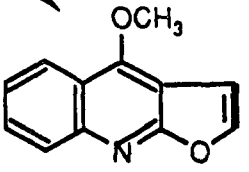

DICTAMNINE

FIGURE 38: FORMATION OF FURAN AND PYRAN RINGS FROM PRENYL GROUP SHOWN IN BOLD (modified from: Welle and Grisebach, 1988; Hamerski and Matern, 1988; Grundon, 1988)

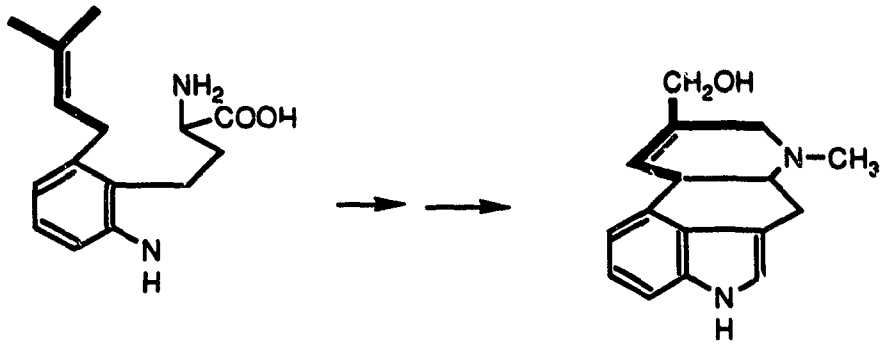

4-DIMETHYLALLYL TRYPTOPHAN

ELYMOCLAVINE

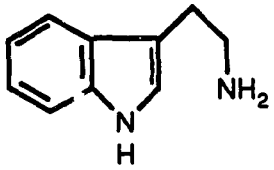

TRYPTAMINE

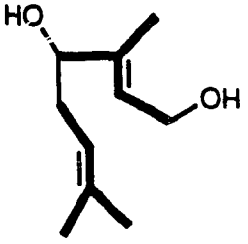

4-HYDROXYGERANIOL

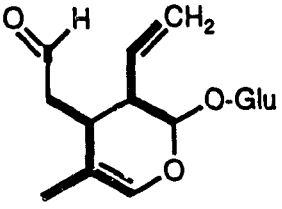

SECOLOGANIN

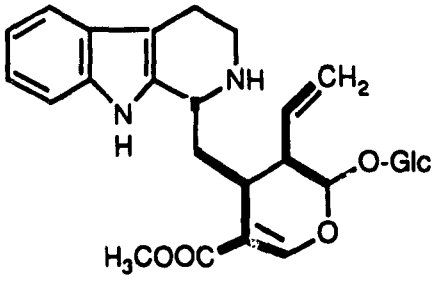

STRICTOSIDINE

FIGURE 39: THE INCORPORATION OF THE PRENYL GROUP SHOWN IN BOLD IN THE BIOSYNTHESIS OF ERGOLINE AND INDOLE ALKALOIDS (modified from Robinson, 1981; Kutchan et al., 1991).

PRENYLATED COUMARINS:

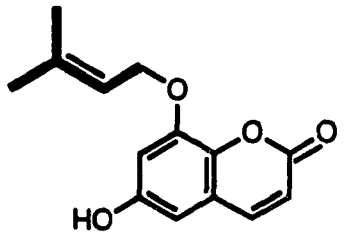

PRENYLETIN

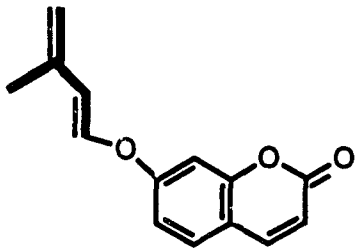

BUTENYL ETHER

PRENYLATED ADENINE

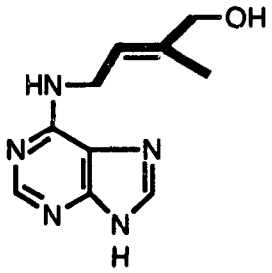

trans-ZEATIN

PRENYLATED tRNA

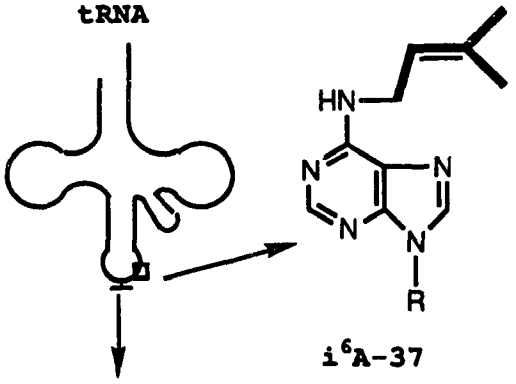

i^6A-37

PRENYLATED PROTEINS

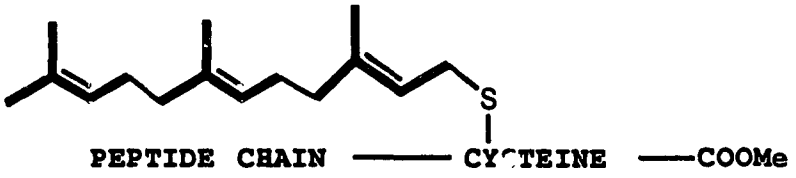

FIGURE 40: THE ATTACHMENT OF LINEAR PRENYL GROUPS SHOWN IN BOLD ONTO O, N OR S ATOMS OF COMPOUNDS ORIGINATING FROM DIFFERENT BIOGENETIC SOURCES

is partially incorporated into the backbone of the structure resulting in the production of the proline ring system. The pyrophosphate group on the isoprenoid chain is a good leaving group and would readily react with the amino group on the citric acid cycle product. The formation of the other bond to close the ring requires a suitable leaving group that activates the third carbon in the glutamic acid derivative. It is not clear which is the first step in the process (Fig. 41). If both steps occur simultaneously there will be no buildup of intermediates from this pathway. If either step occurs with a delay before the final ring closure several possible intermediates may be present. If the prenylation of $-NH_2$ is the first step of the reaction, the intermediate will be a secondary amino acid. However, if the carbon-carbon bond is the first one formed, the intermediate will be a primary amino acid (Fig. 41). It has been suggested that the biosynthesis of kainic acid follows a very similar pathway in which DMAPP instead of geranylpyrophosphate condenses with the activated glutamic acid derivative (Fig. 42; Laycock et al., 1989).

The poisonous mushroom *Clitocybe acromelalga* is a known producer of the kainoids acromelic acids A and B (Shinozaki et al., 1986). It has been proposed that both acromelic acids A and B are synthesized through the condensation of stizolobic acid, derived from dihydroxyphenylalanine (DOPA), with an

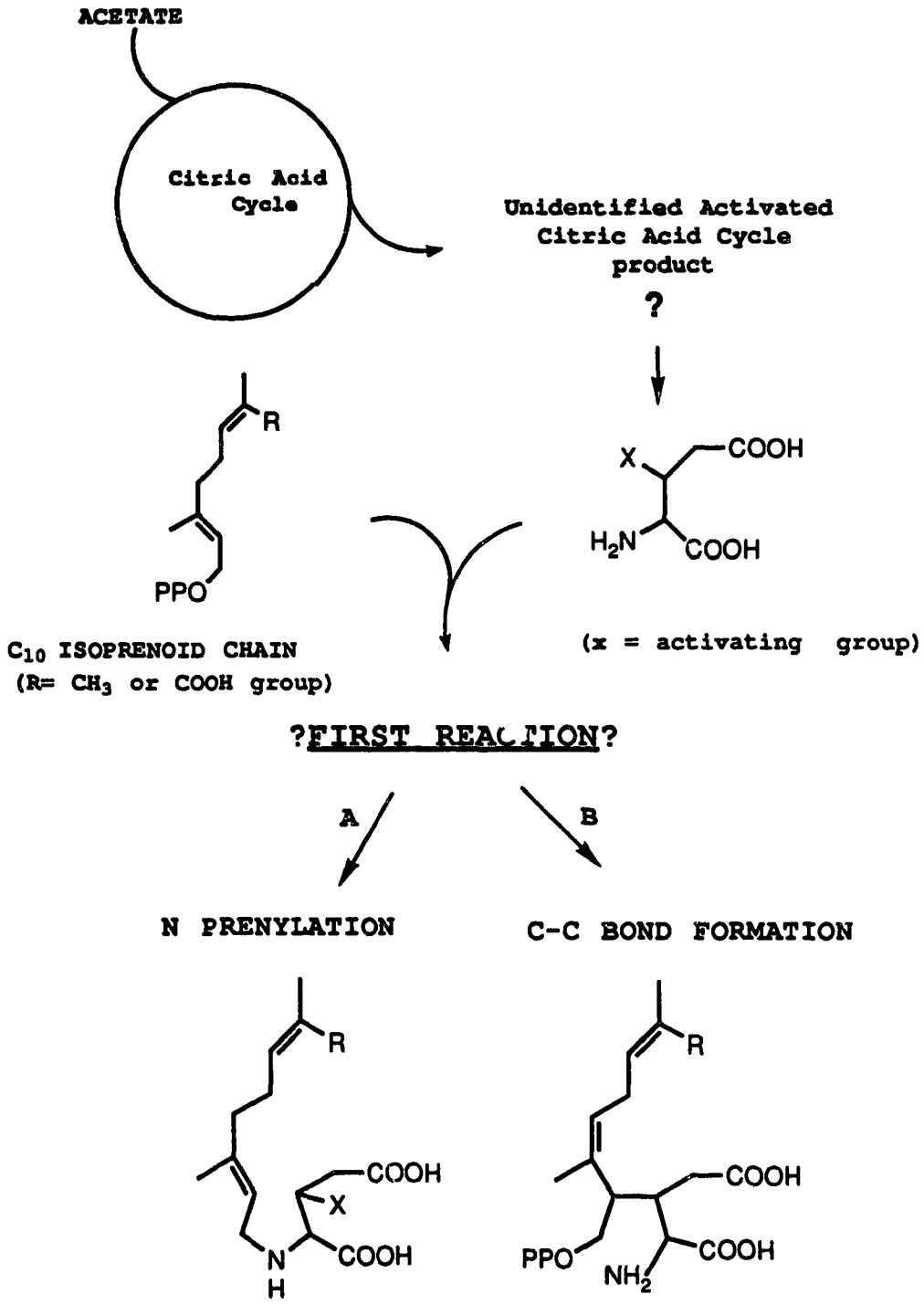

FIGURE 41: PUTATIVE STEPS IN DOMOIC ACID BIOSYNTHESIS

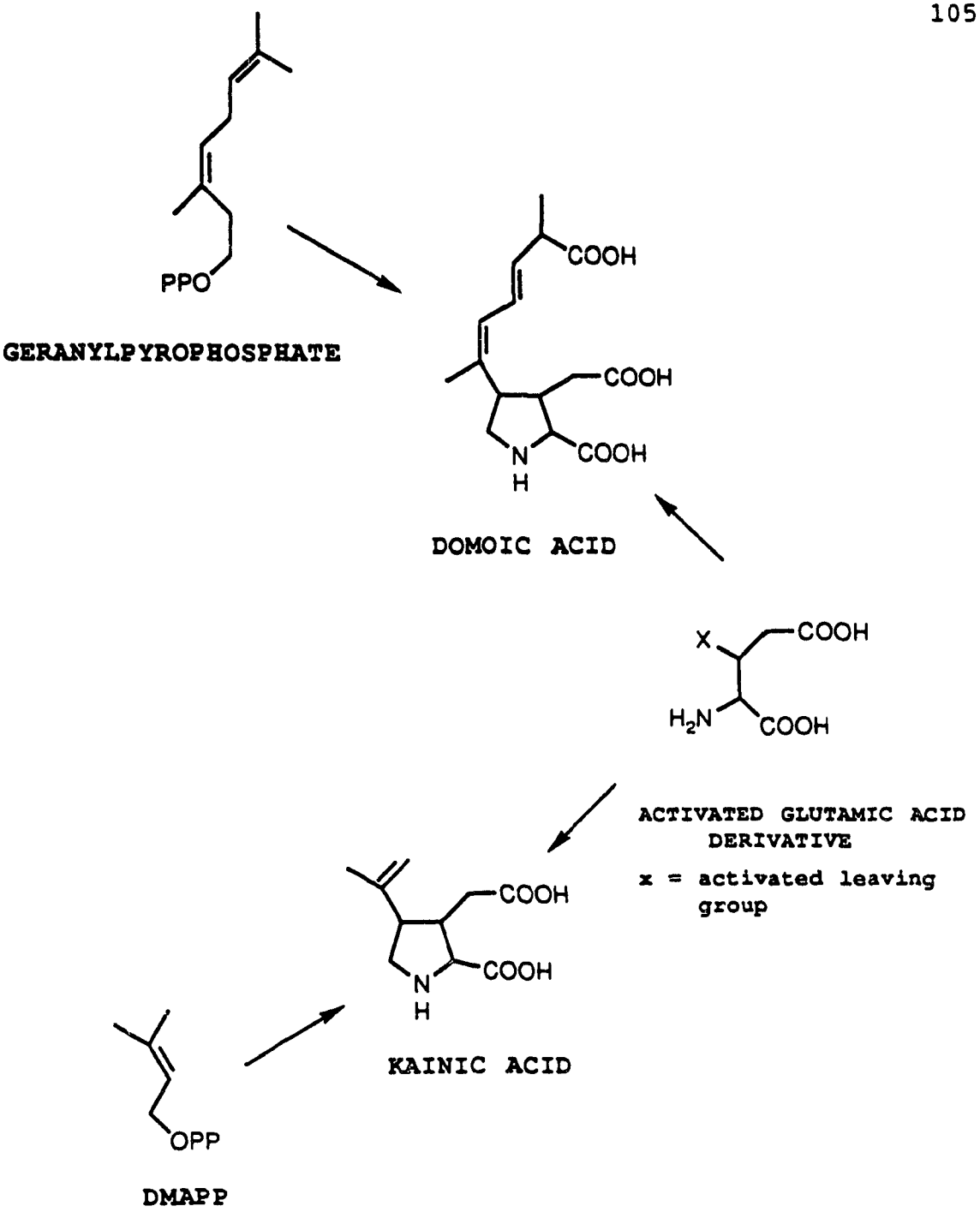

FIGURE 42: BIOGENESIS OF THE KAINOIDS

activated glutamic acid derivative (Fig. 43; Yamano and Shirahama, 1993). The recent isolation of a novel amino acid, L-N-[2-(3-pyridyl)ethyl]-glutamic acid from *C. acromelalga* may represent an intermediate in this pathway (Fig 43; Yamano and Shirahama, 1993). In this amino acid the glutamic acid appears to have condensed with stizolobic acid but the final reaction to form the proline ring has not occurred. A possible explanation for this result is the absence of the leaving group at the third carbon position of glutamic acid, believed necessary to activate this position and thus facilitate proline ring formation.

In the current work several isolates of the pennate diatom *Pseudonitzschia pungens* f. *multiseries*, a known producer of domoic acid, were examined for possible intermediates in the biosynthesis of domoic acid. In addition, isolates of the closely related *Pseudonitzschia pungens* f. *pungens*, which does not produce domoic acid, were also examined, since it is possible that this organism has a partially complete pathway for domoic acid biosynthesis and therefore produces only intermediates, but not the final product. The *Palmaria palmata* mutant, which produces kainic acid, was also examined for putative intermediates in kainic acid biosynthesis.

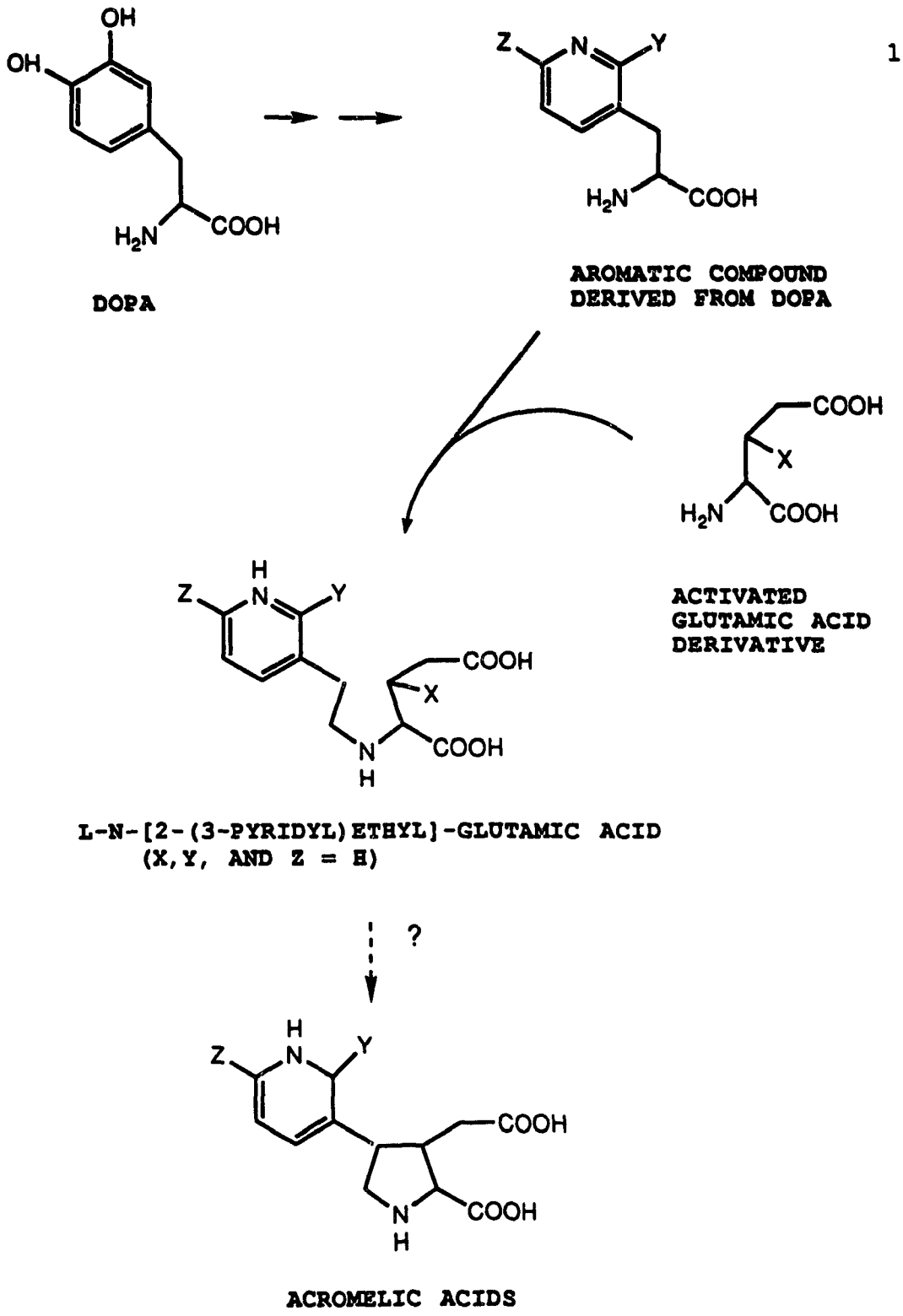

FIGURE 43: PUTATIVE PATHWAY OF ACROMELIC ACID BIOSYNTHESIS (modified from Yamano and Shirahama, 1993)

METHODS AND MATERIALS

ALGAL CULTURES

The axenic diatoms *Pseudonitzschia pungens* f. *multiseries* strain 13CC and *Pseudonitzschia australis* were cultured as described in Chapter One. In addition, several samples of harvested cells from xenic batch cultures of *Pseudonitzschia pungens* f. *multiseries* and *Pseudonitzschia pungens* f. *pungens* were provided by P. Cormier and J. Smith, Department of Fisheries and Oceans, Moncton, N.B. for subsequent amino acid analysis (Table 5). These strains were grown under the conditions described below (Cormier, 1994). The culture medium was artificial seawater supplemented with NaH_2PO_4 and vitamins as in F/2 media (Guillard, 1975), trace metals as in L-1 media (Guillard, 1975) and 428 µM Na_2SiO_3, with either 100 µM $NaNO_3$ or NH_4Cl added as the sole N source. Cultures were grown in Fernbachs at 16°C and an irradiance level of 100 µE s^{-1} m^{-1} with a 14:10 h light:dark cycle. Cells were filtered from the media on day 9 after entering the stationary phase of growth under nitrogen starvation conditions.

The *Palmaria palmata* mutant (GM) is a dwarf mutant produced on a normal frond of *P. palmata* already in culture from Grand Manan Island, Charlotte Co., New Brunswick (44°42'N, 66°47'W). Biomass of this *P. palmata* mutant was

TABLE 5: XENIC *PSEUDONITZSCHIA* SPP. CULTURES PROVIDED BY DR. J. SMITH, DEPARTMENT OF FISHERIES AND OCEANS, MONCTON (all strains isolated by K. Pauley at place and time listed)

STRAIN	LOCATION	NITROGEN SOURCE
Pseudonitzschia pungens f. multiseries		
KP72	New London Bay P.E.I.	$NaNO_3$
KP76	Nov. 20/91	NaNO3
KP82		$NaNO_3$
Pseudonitzschia pungens f. pungens		
KP42	Cardigan Bay Station V P.E.I.	$NaNO_3$ NH_4Cl
KP43	Oct 1/91	$NaNO_3$
KP55	New London Bay P.E.I.	$NaNO_3$
KP57	Oct 3/91	$NaNO_3$ NH_4Cl

provided by P. Shacklock, Sandy Cove Aquaculture Research Station, National Research Council, N.S. The alga was grown in an 8 L tank of aerated seawater maintained at 8-12°C. The nutrients NH_4NO_3 and $(NH_4)_2HPO_4$ were added to the tank twice a week to give a final N concentration of 1 mM (Mishra et al., 1993). The tank was flushed with fresh seawater at a rate of 10 volumes per day.

EXTRACTION OF FREE AMINO ACIDS FROM PLANKTON

Free amino acids were extracted from approximately 0.5 g wet weight biomass of axenic *Pseudonitzschia* spp. cells using 80% ethanol (10 mL) at 80°C for 2-3 min. The extract was centrifuged at 15,000 xg for 1 min and the supernatant dried by rotary evaporation. The residue was redissolved in 2 mL Beckman sodium citrate sample dilution buffer (pH 2.0) and analyzed on a Beckman automatic amino acid analyzer, model 6300 with a column temperature of 63°C. Primary amino acid were indicated by 570 nm absorbing-peaks while the secondary amino acids were indicated by 440 nm-absorbing peaks. The filter-harvested xenic cells of *Pseudonitzschia* spp. provided by Fisheries and Oceans, Moncton, were added to 70% ethanol (10 mL), sonicated and allowed to soak for 2.5 h before heating to 80°C for 2-3 min. The particulate material was then removed by filtering through a 0.2 µm Minisart Sartorius filter unit (Sartorius, CA) and the resulting supernatant

dried. The residue was resuspended in 100 µL of the Beckman sodium citrate sample dilution buffer and analyzed for free amino acids as described above.

An air-dried sample (0.5 g) of the *Palmaria palmata* mutant, ground to a fine powder in liquid nitrogen was extracted with 70% methanol (30 mL) at 80°C for 2-3 min. After centrifugation at 15,000 xg for 1 min, the supernatant was dried by rotary evaporation. The residues were redissolved in 1 mL Beckman sodium citrate sample dilution buffer (pH 2.0). The concentrated *P. palmata* sample was diluted 1/10 before being analyzed for amino acids on the Beckman automatic amino acid analyser with a column temperature of 55°C.

ISOLATION OF 1'-HYDROXYDIHYDROKAINIC ACID FROM *P. PALMATA*

Free amino acids from 1.5 kg of the *P. palmata* mutant (GM) were extracted in 80% methanol (5.2 L) at room temperature for 4 days. The extract was concentrated to approximately 250 mL by rotary evaporation, and adjusted to pH 2 with HCl. The extract was mixed with 100 g Dowex-AG50Wx8X (Sigma) cation exchange resin (H+ form; 200-400 mesh) in a beaker and stirred for several minutes before being transferred to a Buchner funnel and washed sequentially with 375 mL each of water, methanol (100%), and water. Amino acids

were eluted from the funnel with approximately 100 mL each of 1.0 M NH_4OH and water. Dowex-AG50Wx8X (100 g) was added to the water/methanol/water wash and the procedure repeated. The two NH_4OH eluates were then combined and concentrated to 115 mL.

The combined NH_4OH eluate was passed through a QAE-Sephadex column (A-25; 2.6 cm x 95 cm) and the resulting fractions were compared by High Voltage Paper Electrophoresis (HVPE) at pH 6.5 followed by staining of the paper with cadmium acetate/ninhydrin solution as previously described (Laycock et al., 1989). Fractions containing 1'-hydroxydihydrokainic acid were combined and further purified by preparative HVPE using an acetate-formate buffer, pH 1.8 (acetic acid, 89 mL/L; formic acid, 22 mL/L). Edges were cut off the electropherogram and stained with ninhydrin and zones corresponding to the yellow-staining bands on the edges were cut out from the rest of the electropherogram and eluted with water.

This eluate was dried by rotary evaporation and the blue residue (43 mg) dissolved in water (3 mL) and applied as thin bands on several sheets of washed Whatman 3MM chromatography paper for separation of the amino acids by descending paper chromatography (n-butanol: acetic acid: water; 4:1:1). Among the yellow-staining amino acids visualized with

ninhydrin, 1'-hydroxydihydrokainic acid was detected by amino acid analysis. Further purification required clean-up using a C18 column (J.T. Baker Inc. prepacked 6 mL, high capacity) and elution with increasing concentrations of aqueous acetonitrile containing 0.2% acetic acid. Fractions were analyzed by thin layer chromatography (TLC) on silica plates (n-butanol: acetic acid: water; 4:1:1) and those containing 1'-hydroxydihydrokainic acid were pooled and dried by rotary evaporation. The blue residue (24.8 mg) was dissolved in 80% methanol, and applied to a column of Sephadex LH-20 (Pharmacia; 1 x 50 cm), which was eluted with 80% methanol. The resulting fractions containing 1'-hydroxydihydrokainic acid on the basis of TLC analysis were pooled and dried.

In order to remove interfering cations associated with the material obtained from the LH20 column, the blue residue (20 mg) was dissolved in water (2 mL) and passed through a Chelex-100 column (Biorad; H^+ form, 100-200 mesh, 1 cm x 6 cm). The column was washed with equal volumes (8 mL) of water and 1 M NH_4OH solution and 1'-hydroxydihydrokainic acid (11.2 mg) was obtained in the fraction eluted with water. Metals bound to the compound were identified by analysis of the unknown compound using a Kevex 8000 energy-dispersive X-ray analyzer in a Jeol 35C scanning electron microscope (SEM) performed by D. O'Neil, Institute for Marine Biosciences, National Research Council, Halifax, N.S. In addition, the

Chelex-100 resin was compared by this same method before and after addition of the sample.

Final preparation was achieved by preparative reversed-phase HPLC (Capcell; 0.5% acetonitrile in water containing 0.1% trifluoracetic acid; flow rate 0.5 mL/min; monitored with a UV detector set at 210 nm). All fractions were collected and analyzed for 1'-hydroxydihydrokainic acid using the amino acid analyzer. The fraction containing 1'-hydroxydihydrokainic acid was dried (3 mg residue) and redissolved in 0.5 mL D_2O for subsequent NMR spectroscopy.

NUCLEAR MAGNETIC RESONANCE SPECTROSCOPY

Nuclear magnetic resonance spectroscopy was performed on a Bruker AMX-500 spectrometer at 125.77 MHz (^{13}C) and 500.14 MHz (^{1}H) using standard Bruker pulse sequences. Carbon-13 spectra (^{1}H-decoupled one pulse, DEPT 90° and DEPT 135°) were obtained from a solution acidified with DCl to pD 1.76 in 5mm tubes at 20°C. ^{1}H-detected phase-sensitive, ^{13}C-decoupled HMQC (heteronuclear multiple quantum correlation) spectra (Bax and Subramanian, 1986) and HMBC spectra (heteronuclear multiple bond correlation) of the same solution at pD 1.76, were obtained with the same spectrometer. Spectral widths were 3012 Hz (^{1}H dimension, acquisition time 0.085s) and 160 ppm (HMQC) or 173 ppm (HMBC) (^{13}C dimension, 512 t_1 increments).

Spectra were processed with weighting of each dimension with a 90°-shifted squared sine-bell function. 1D-^{1}H spectra, phase-sensitive 2D-NOESY and double-quantum filtered 2D-COSY spectra (Kessler et al., 1988) were obtained using solutions in D_2O at pD 1.76, which were then adjusted to pD 4.12 with NaOD. Standard Bruker pulse sequences were used with spectral widths 3012 Hz (pD 1.76) or 2564 Hz (pD 4.12) in each dimension, acquisition times 0.085s (pD 1.76) or 0.10 s (pD 4.12), number of t_1 increments 256 (COSY), 512 (NOESY pD 1.76) or 368 (NOESY pD 4.12). Spectra were processed by zero-filling the t_1 dimension to 512 points, and weighting as described above.

MASS SPECTROMETRY AND INFRARED SPECTROSCOPY

Mass spectrometric analyses were performed with a SCIEX (Thornhill, Ont., Canada) API III quadruple mass spectrometer in the ionspray and full-scan modes for negative ions. Mass spectra were acquired by flow injection analysis using aqueous acetonitrile (50:50) containing 0.1% ammonium acetate. Infrared spectroscopy was performed as described in Wright et al. (1989).

RESULTS

AMINO ACID PROFILES OF *PSEUDONITZSCHIA* SPP.

The amino acid profile of the axenic *Pseudonitzschia pungens* f. *multiseries* strain 13CC during late exponential growth before the onset of domoic acid production is shown in Fig. 44. An unknown 570 nm-absorbing amino acid (unknown A) was observed, with a retention time of approximately 6.5 min, between that of taurine and aspartic acid. The low concentration, however, precluded its isolation and identification. A peak with a similar retention time was also present in the amino acid profile of *Pseudonitzschia australis* analyzed during the late phase of exponential growth (Fig. 45).

The amino acid profiles of xenic *Pseudonitzschia pungens* f. *multiseries* strains KP72, KP76 and KP82, all isolated from the New London Bay, P.E.I., and grown in culture media with $NaNO_3$ as the sole nitrogen source, are shown in Figs. 46, 47 and 48. The concentration of glutamic acid appeared to be relatively constant between strains while levels of other amino acid such as aspartic acid, glycine, valine, isoleucine and tyrosine varied considerably. The profiles of strain KP76 and KP82 were very similar. Since these cells were harvested after the onset of the stationary phase of growth, domoic acid

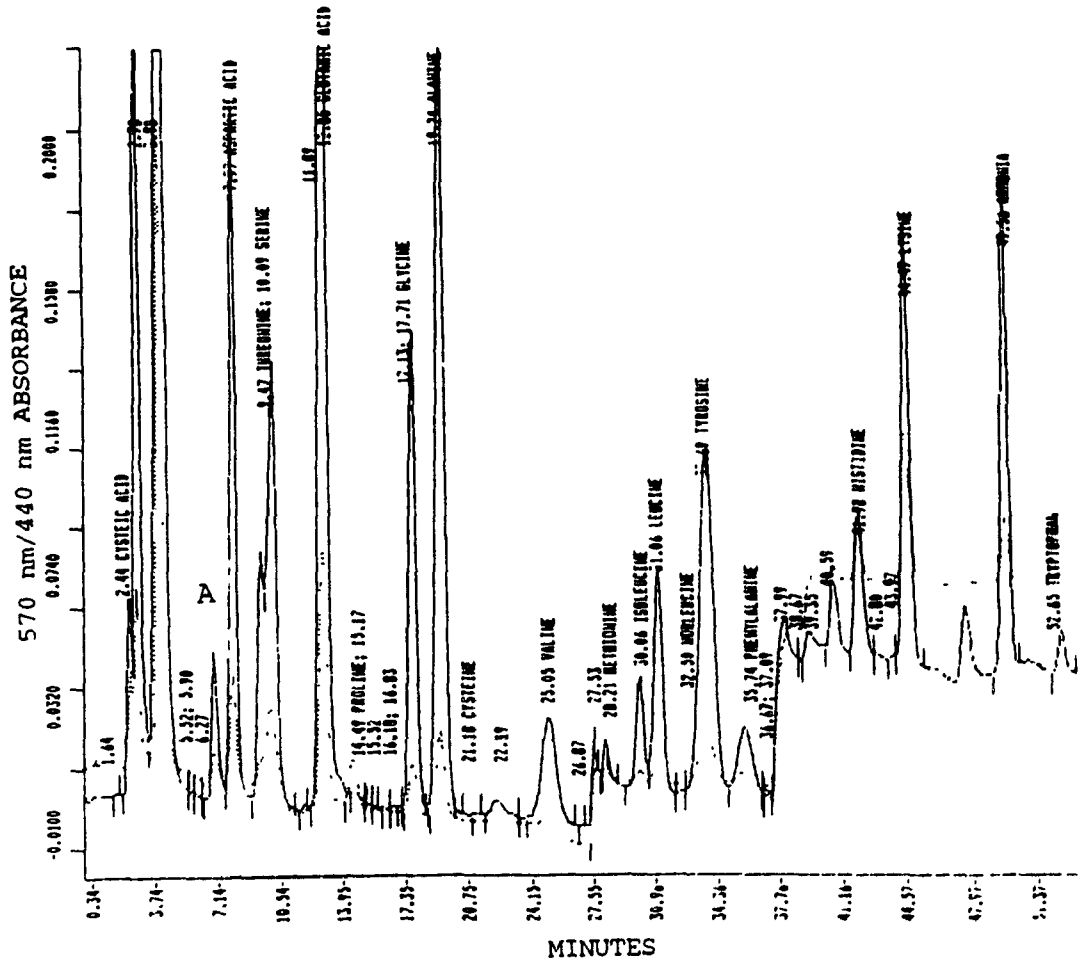

FIGURE 44: AMINO ACID PROFILE OF AXENIC *PSEUDONITZSCHIA PUNGENS* F. *MULTISERIES* STRAIN 13CC DURING LATE EXPONENTIAL GROWTH. (_____ represents 570 nm and ..... represents 440 nm; A represents first unknown amino acid of interest)

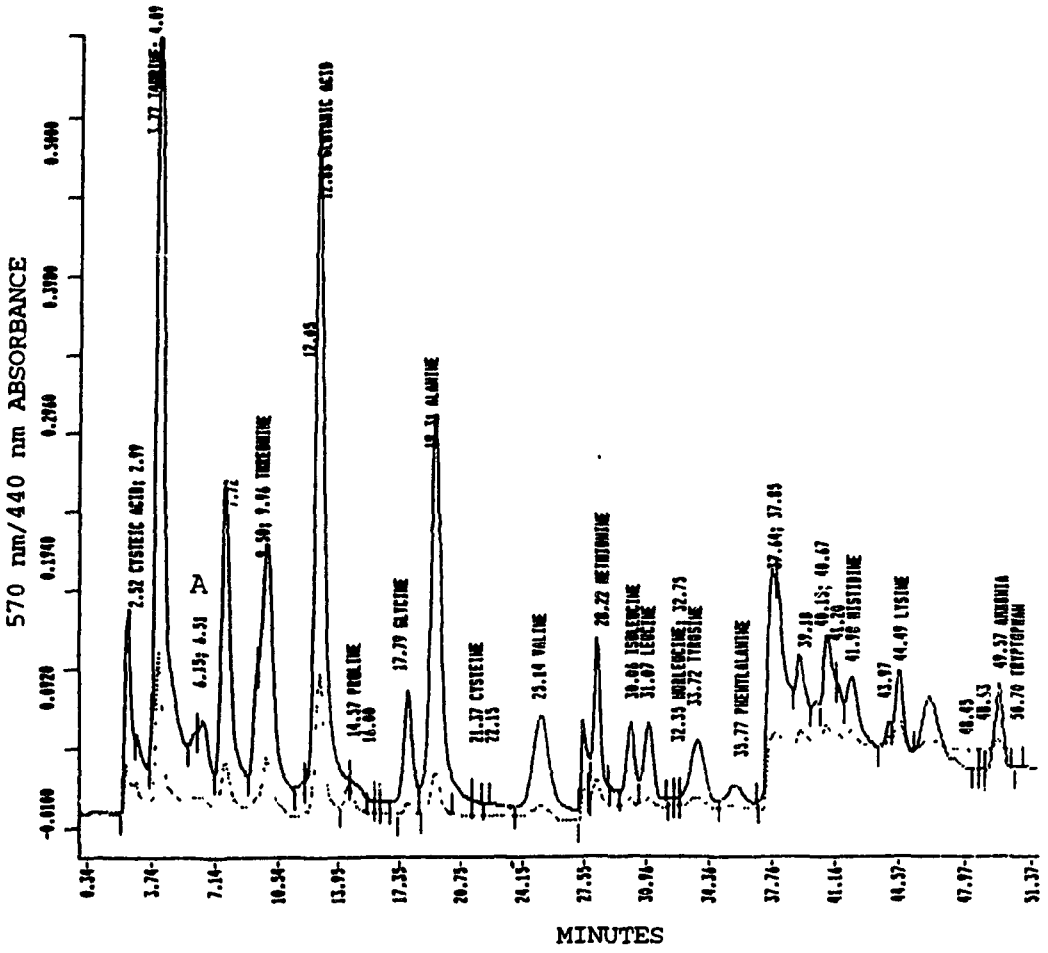

FIGURE 45: AMINO ACID PROFILE OF AXENIC *PSEUDONITZSCHIA AUSTRALIS* (_____represents 570 nm and ..... represents 440 nm; A represents first unknown amino acid of interest)

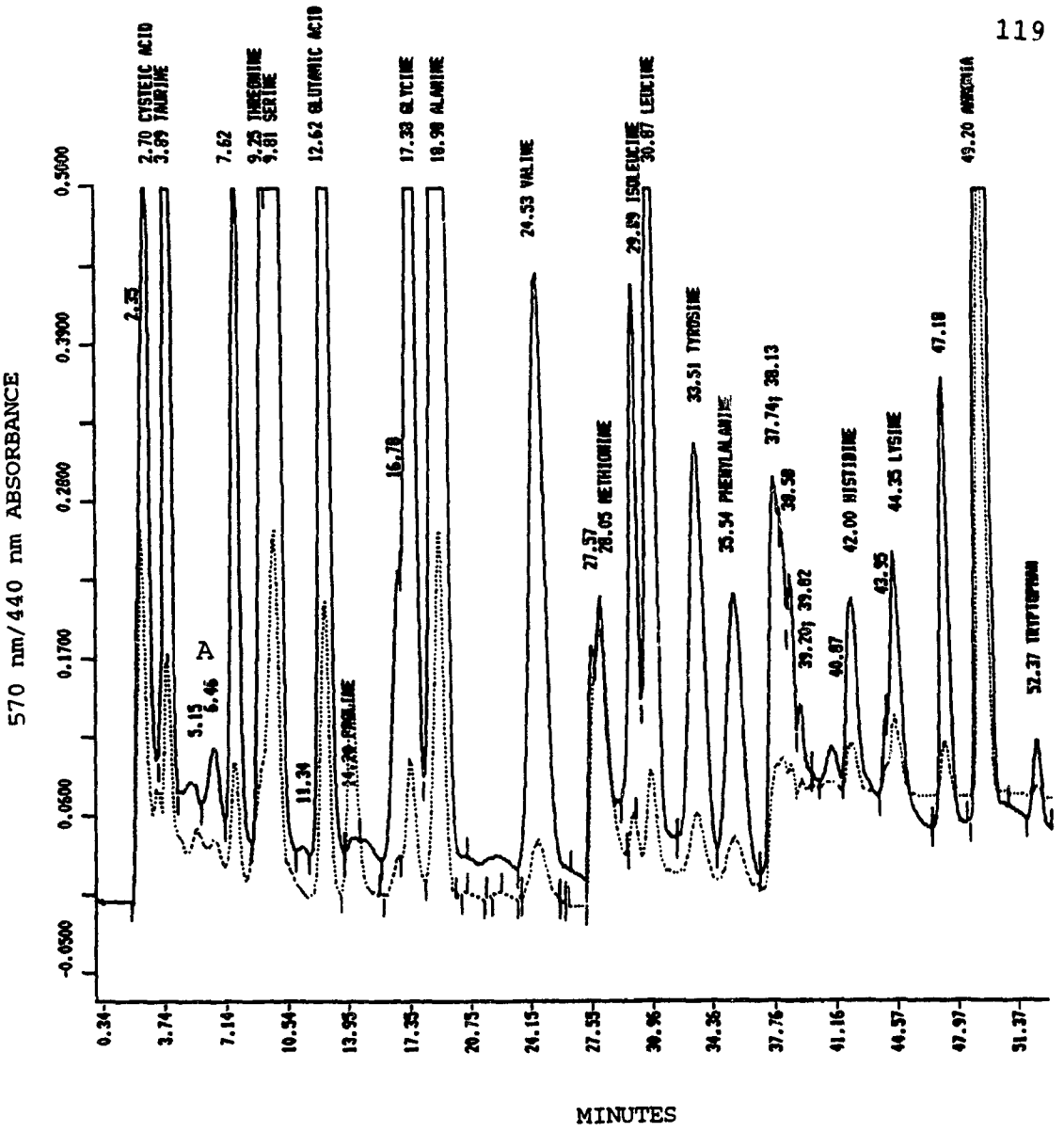

FIGURE 46: AMINO ACID PROFILE OF XENIC *PSEUDONITZSCHIA PUNGENS* F. *MULTISERIES* STRAIN KP72 GROWN WITH $NaNO_3$ AS THE SOLE N SOURCE(_____represents 570 nm and ..... represents 440 nm; A represents first unknown amino acid of interest)

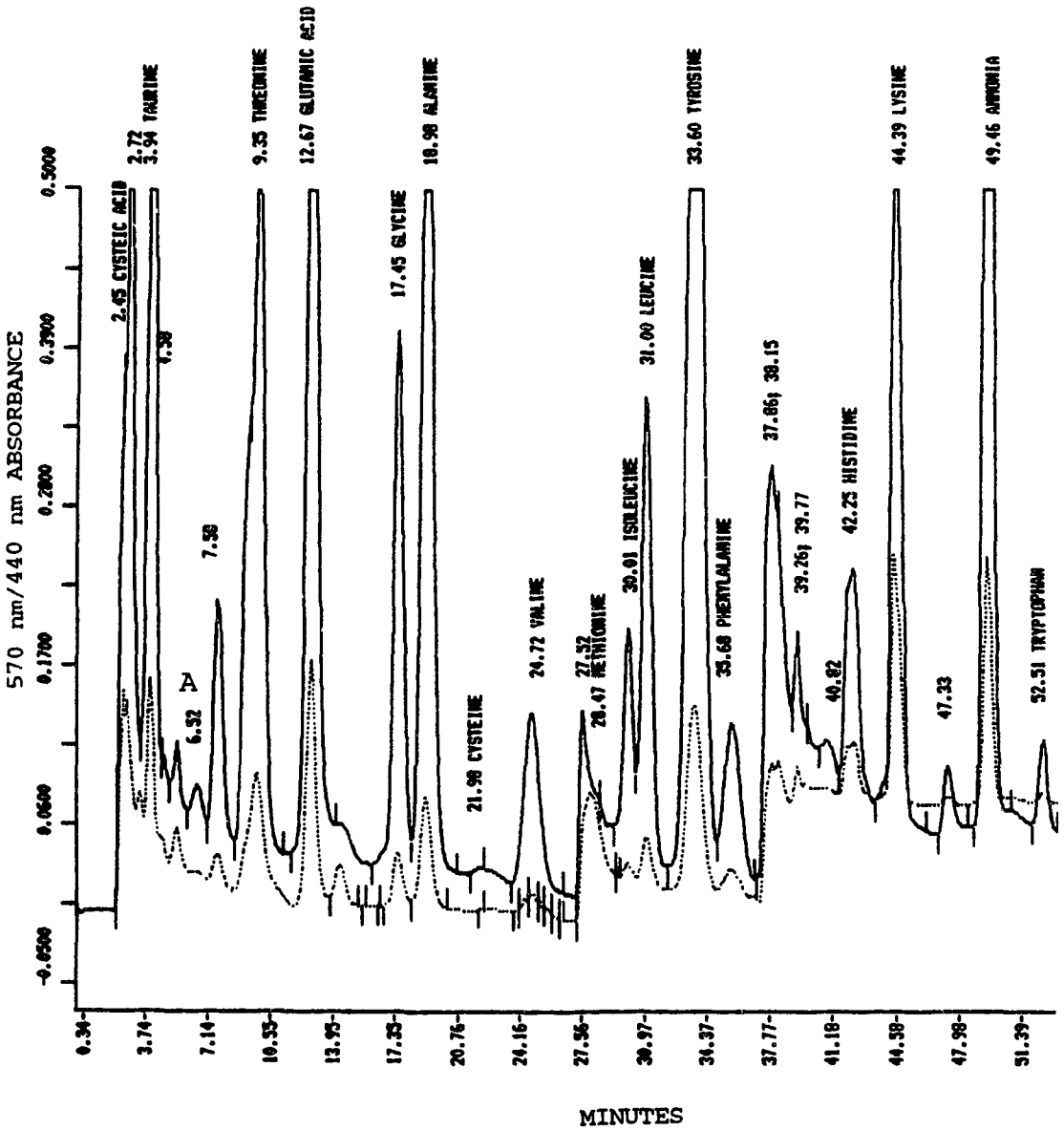

FIGURE 47: AMINO ACID PROFILE OF XENIC *PSEUDONITZSCHIA PUNGENS* F. *MULTISERIES* STRAIN KP76 GROWN WITH $NaNO_3$ AS THE SOLE N SOURCE(_____represents 570 nm and ..... represents 440 nm; A represents first unknown amino acid of interest)

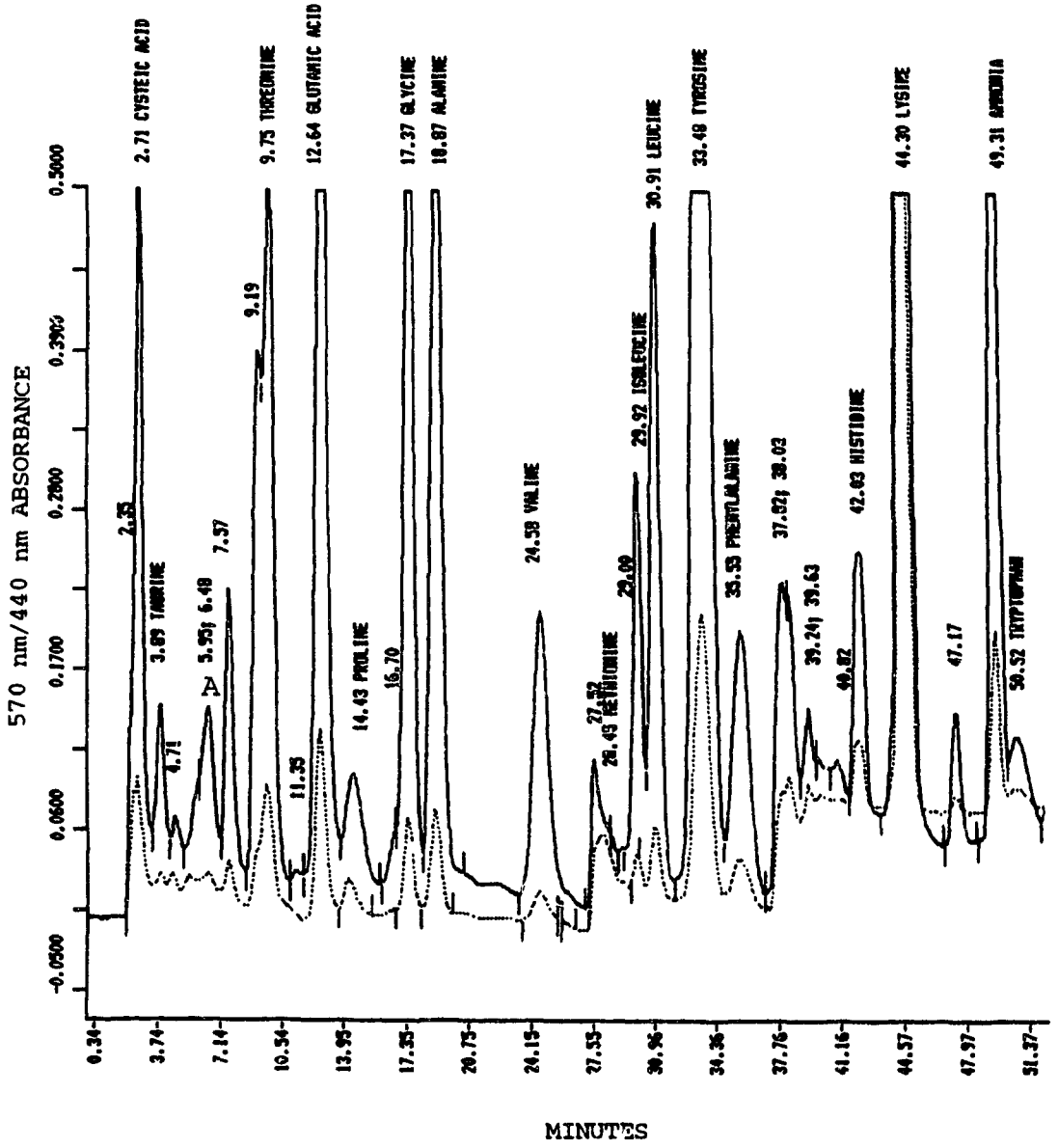

FIGURE 48: AMINO ACID PROFILE OF XENIC *PSEUDONITZSCHIA PUNGENS* F. *MULTISERIES* STRAIN KP82 GROWN WITH $NaNO_3$ AS THE SOLE N SOURCE(_____represents 570 nm and ..... represents 440 nm; A represents first unknown amino acid of interest)

was present in all the profiles examined, as shown by the 440 nm peak under methionine. The amino acid profiles of all three strains also revealed the presence of an unknown amino acid with a retention time of 6.5 min similar to unknown A seen previously in the axenic strains. Strain KP82 grown in media with NH_4Cl as the sole source of nitrogen had a similar profile to that grown in $NaNO_3$ (Fig. 49).

Several non-domoic acid-producing strains of *P. pungens* f. *pungens* were also analyzed for the presence of unusual amino acids. Strains KP42 and KP43, isolated from Cardigan Bay, P.E.I., and cultured in media with $NaNO_3$ as the sole nitrogen source, had similar amino acid profiles with less concentrated amino acids in strain KP43 (Figs. 50 and 51). A 440 nm-absorbing minor peak for an unknown amino acid (unknown B) was noted in both profiles with a retention time of approximately 9.2 min overlapping with the 570 nm-absorbing peak for threonine (Figs. 50 and 51). This peak was absent when KP42 was grown in media with NH_4Cl instead of $NaNO_3$ as the only nitrogen source (Fig. 52). Two other isolates, KP55 and KP57, from New London Bay, P.E.I., were grown in media with $NaNO_3$ as the sole nitrogen source. The amino acid profile of KP57 and to a lesser extent the profile of KP55, also showed a 440 nm-absorbing peak with the same retention time as unknown B (9.2 min), but in significantly greater concentrations than for KP42 and KP43 (Figs. 53 and 54).

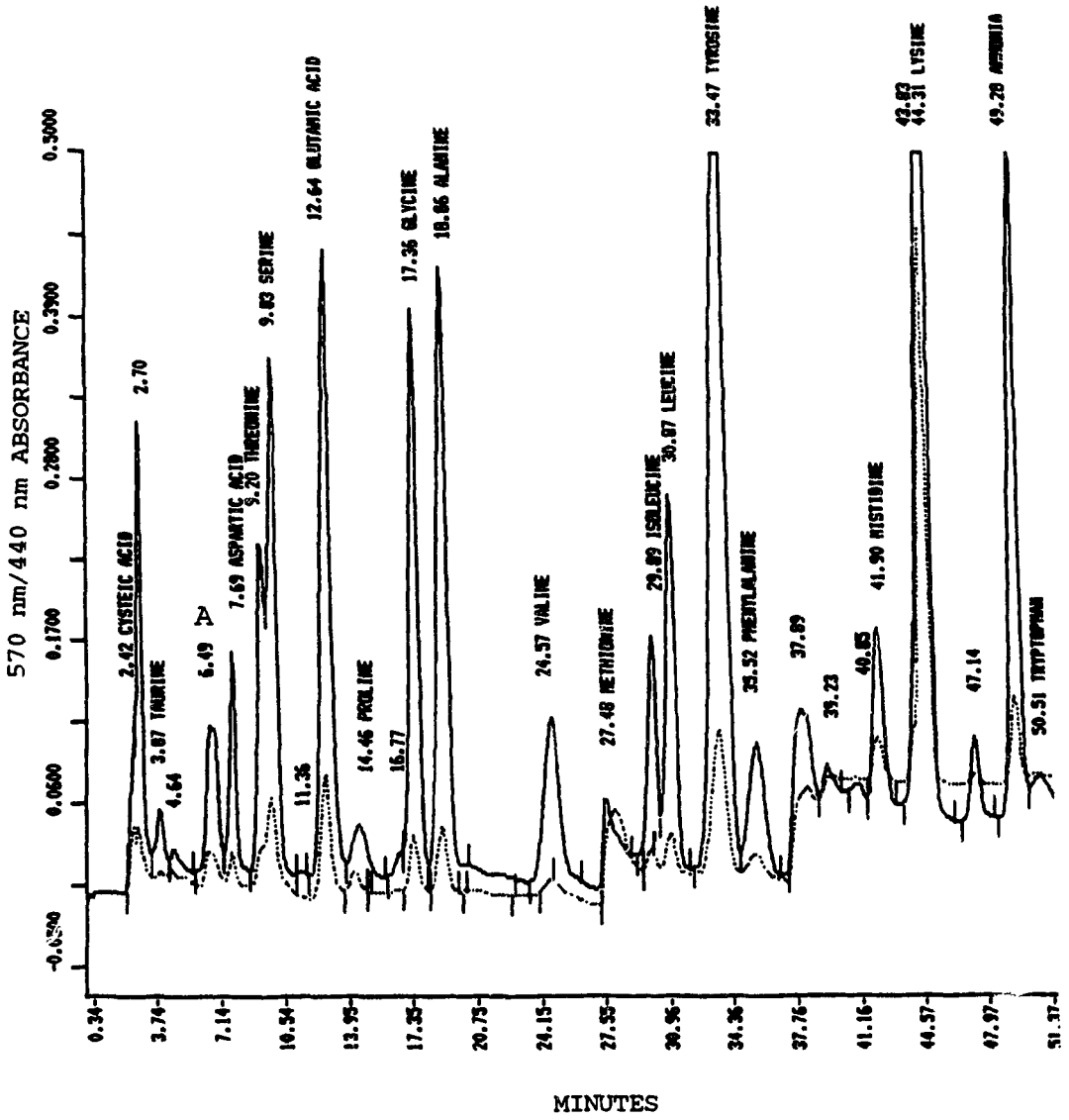

FIGURE 49: AMINO ACID PROFILE OF XENIC *PSEUDONITZSCHIA PUNGENS* F. *MULTISERIES* STRAIN KP82 GROWN WITH NH_4Cl AS THE SOLE N SOURCE(_____represents 570 nm and ..... represents 440 nm; A represents first unknown amino acid of interest)

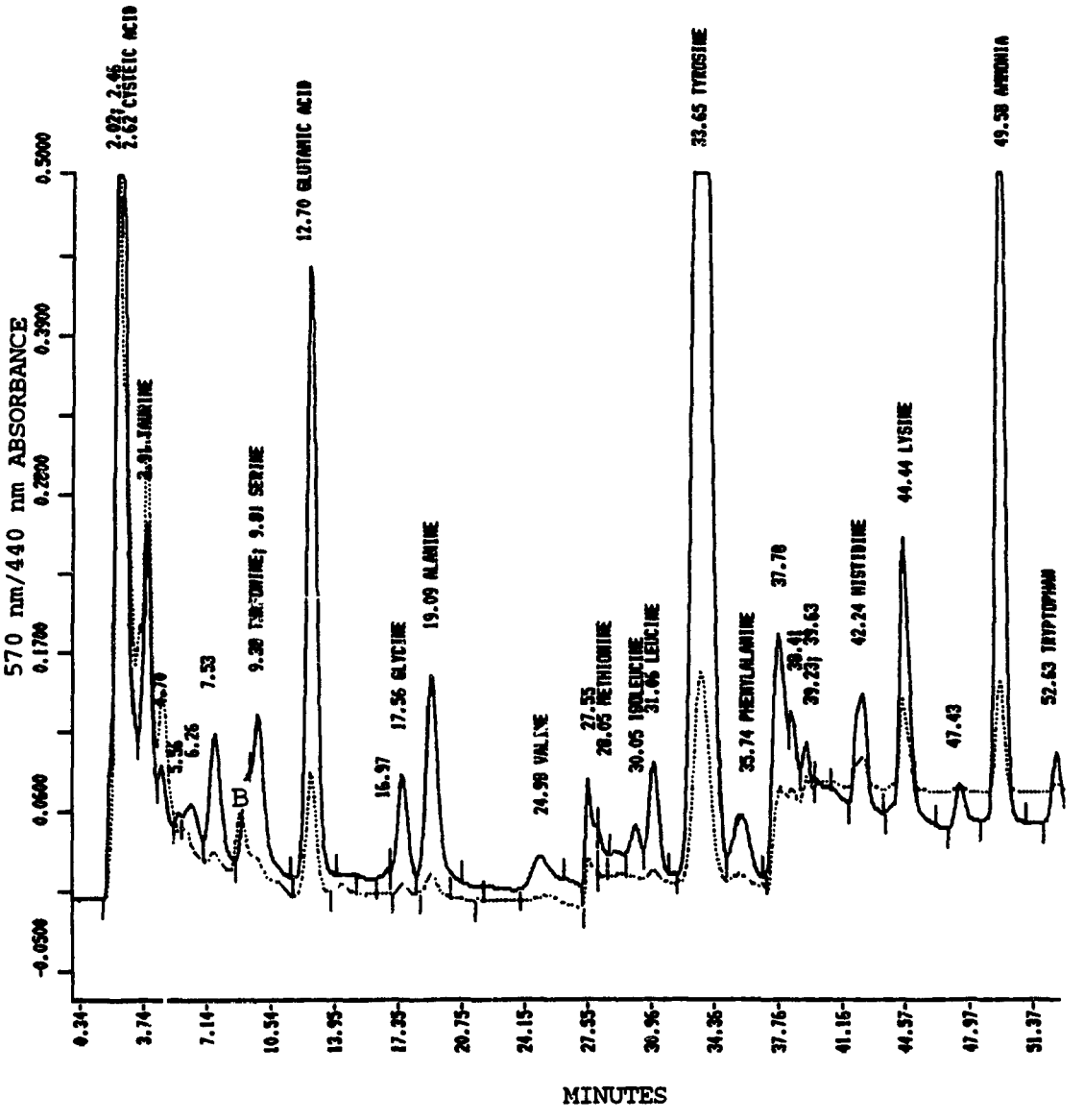

FIGURE 50: AMINO ACID PROFILE OF XENIC *PSEUDONITZSCHIA PUNGENS* F. *PUNGENS* STRAIN KP42 GROWN WITH $NaNO_3$ AS THE SOLE N SOURCE(_____represents 570 nm and ..... represents 440 nm; B represents second unknown amino acid of interest)

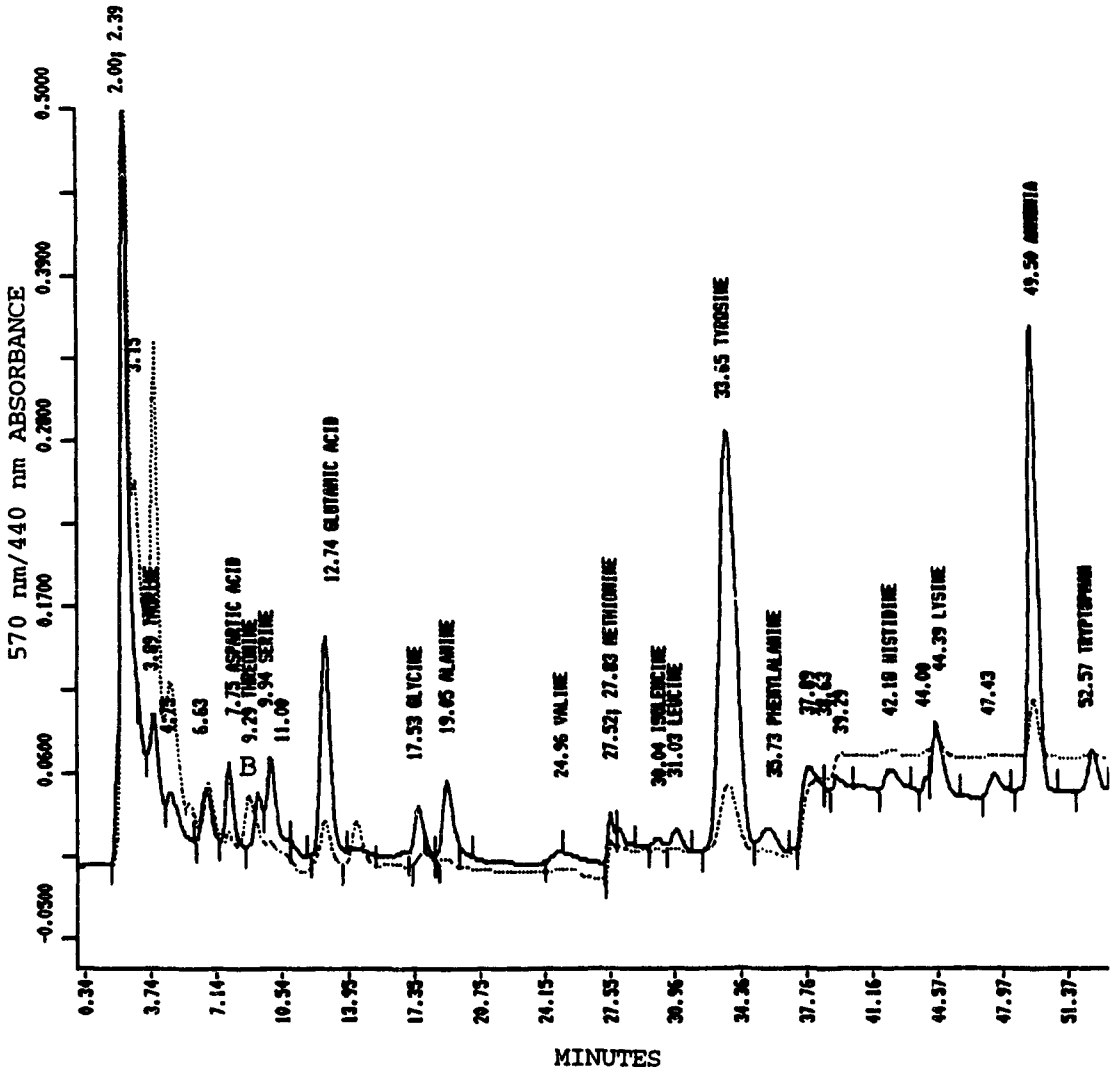

FIGURE 51: AMINO ACID PROFILE OF XENIC *PSEUDONITZSCHIA PUNGENS* F. *PUNGENS* STRAIN KP43 GROWN WITH $NaNO_3$ AS THE SOLE N SOURCE(_____represents 570 nm and ..... represents 440 nm; B represents second unknown amino acid of interest)

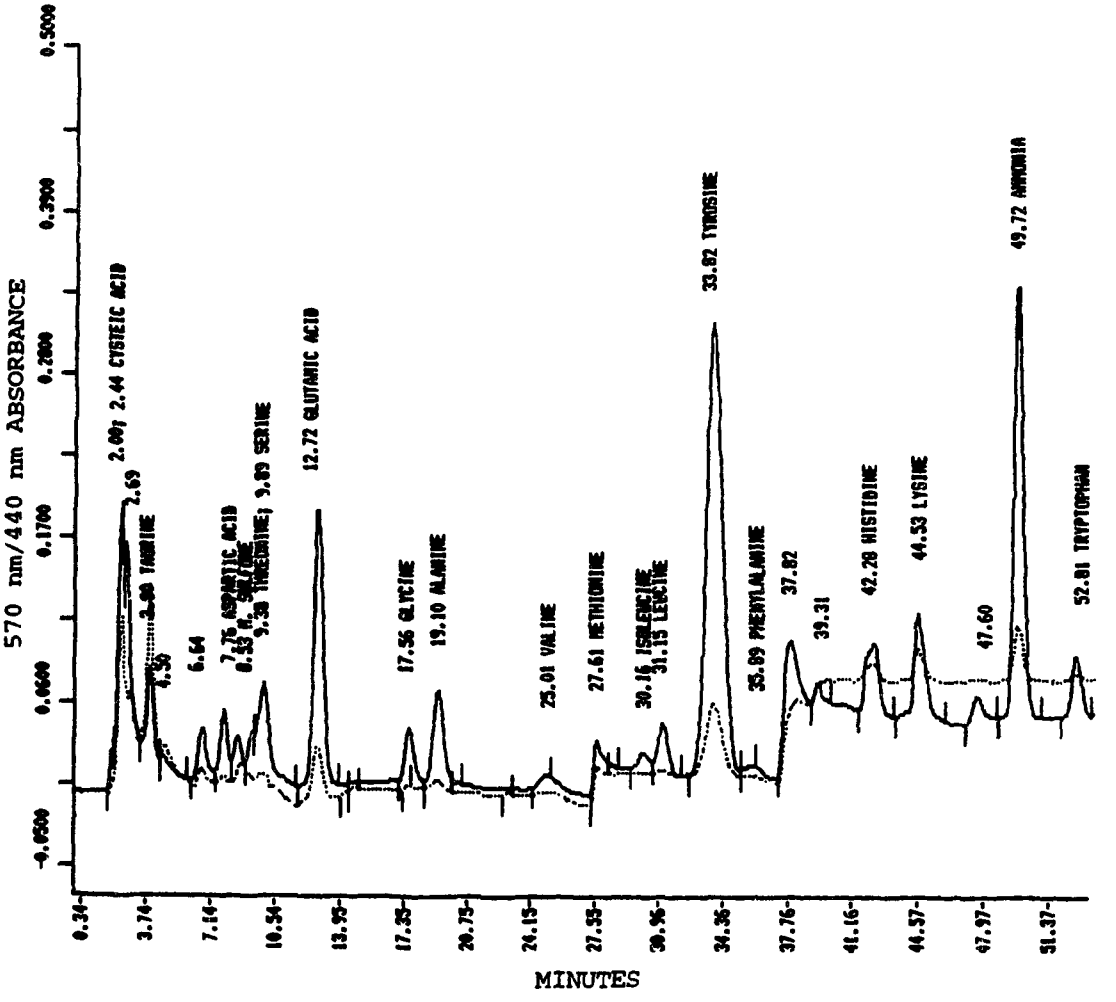

FIGURE 52: AMINO ACID PROFILE OF XENIC *PSEUDONITZSCHIA PUNGENS* F. *PUNGENS* STRAIN KP42 GROWN WITH NH_4Cl AS THE SOLE N SOURCE(_____represents 570 nm and ..... represents 440 nm)

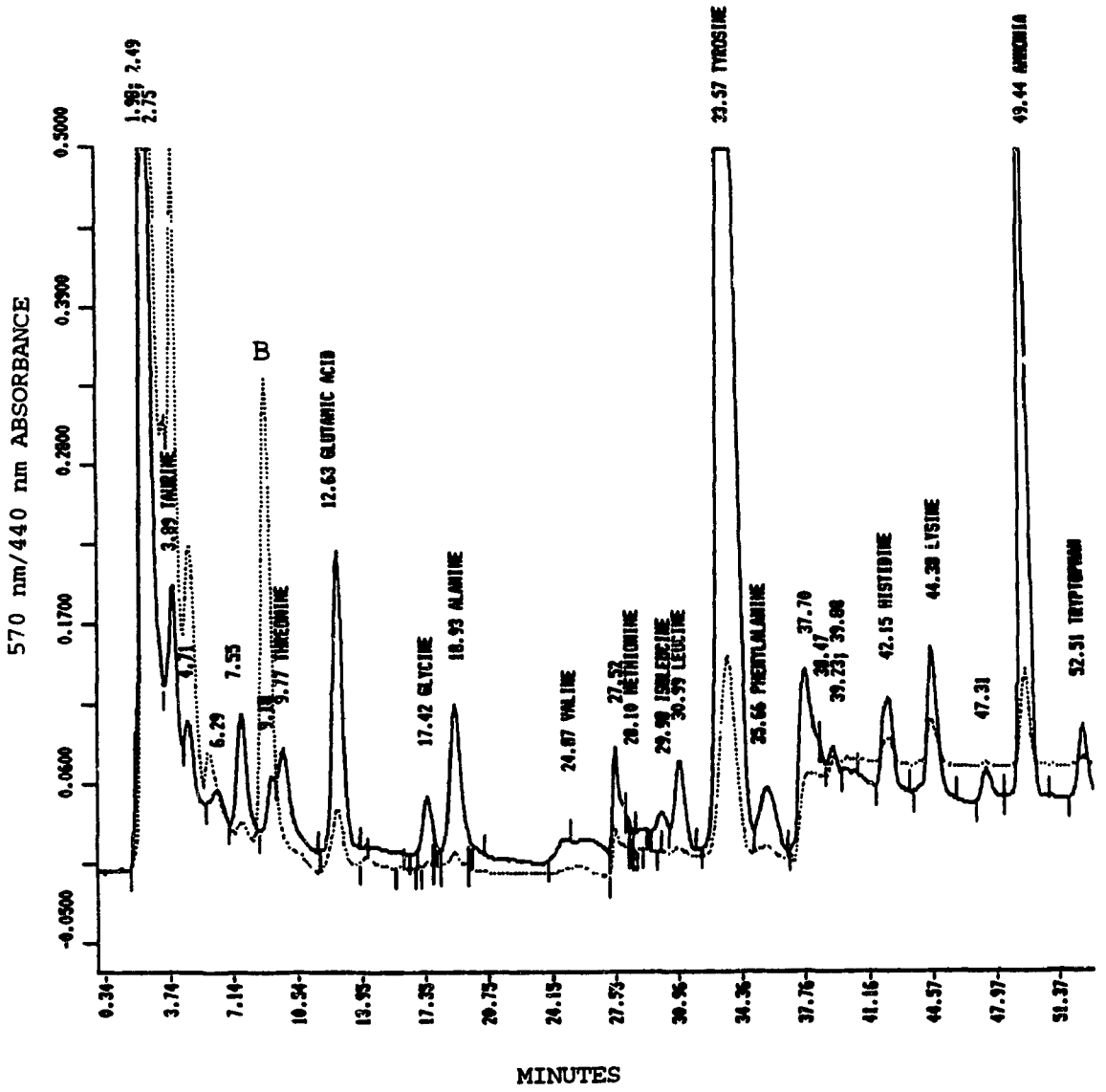

FIGURE 53: AMINO ACID PROFILE OF XENIC *PSEUDONITZSCHIA PUNGENS* F. *PUNGENS* STRAIN KP55 GROWN WITH $NaNO_3$ AS THE SOLE N SOURCE(_____represents 570 nm and ..... represents 440 nm; B represents second unknown amino acid of interest)

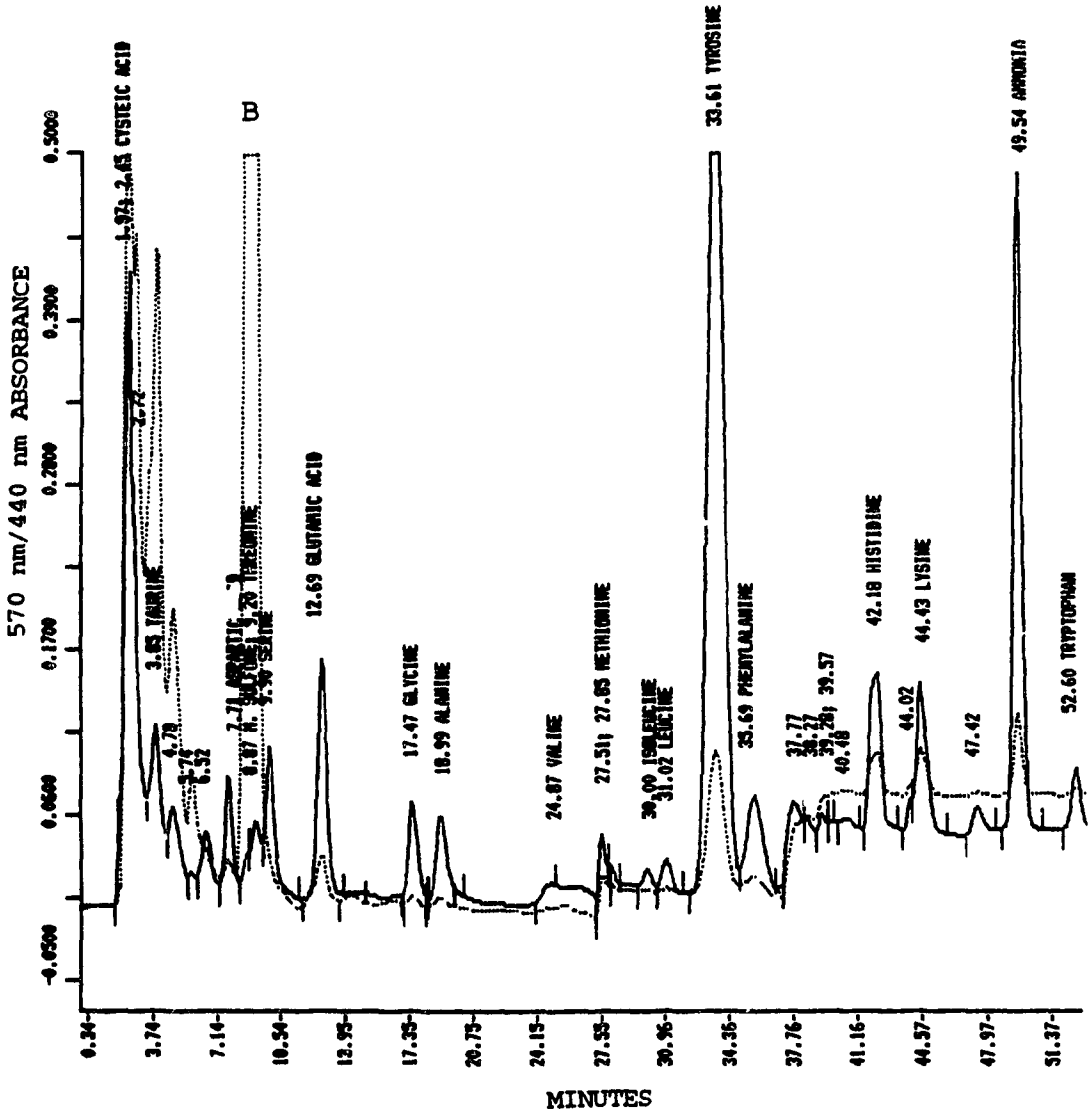

FIGURE 54: AMINO ACID PROFILE OF XENIC *PSEUDONITZSCHIA PUNGENS* F. *PUNGENS* STRAIN KP57 GROWN WITH $NaNO_3$ AS THE SOLE N SOURCE(_____represents 570 nm and ..... represents 440 nm; B represents second unknown amino acid of interest)

Strain KP57 grown with NH_4Cl instead of $NaNO_3$ showed a decrease in unknown B (Fig. 55). Strain KP57 was therefore grown in large-scale cultures in media containing $NaNO_3$ for the purpose of purifying this unknown amino acid. These cultures, upon amino acid analyses, unfortunately did not contain unknown B.

AMINO ACID PROFILE OF THE *PALMARIA PALMATA* MUTANT

The amino acid profile of the *Palmaria palmata* mutant (GM), a known producer of kainic acid (Laycock et al., 1989), was examined for unusual amino acids (Fig. 56). The presence of a 440 nm-absorbing unknown amino acid (unknown C) was noted, with a retention time of 8.3 min between that of aspartic acid and threonine. The presence of kainic acid was also revealed by the 440 nm peak under glycine.

ISOLATION AND IDENTIFICATION OF 1'-HYDROXYDIHYDROKAINIC ACID FROM *P. PALMATA*

Amino acid analyses of extracts of the *P. palmata* mutant revealed the presence of a previously unknown amino acid (C), shown (see below) to be 1'-hydroxydihydrokainic acid (RT 8.3 min). The absorption maximum of the ninhydrin product (440 nm) suggested a secondary amino acid and this interpretation was supported by its yellow colour on paper chromatograms stained with a cadmium acetate/ninhydrin solution. HVPE of

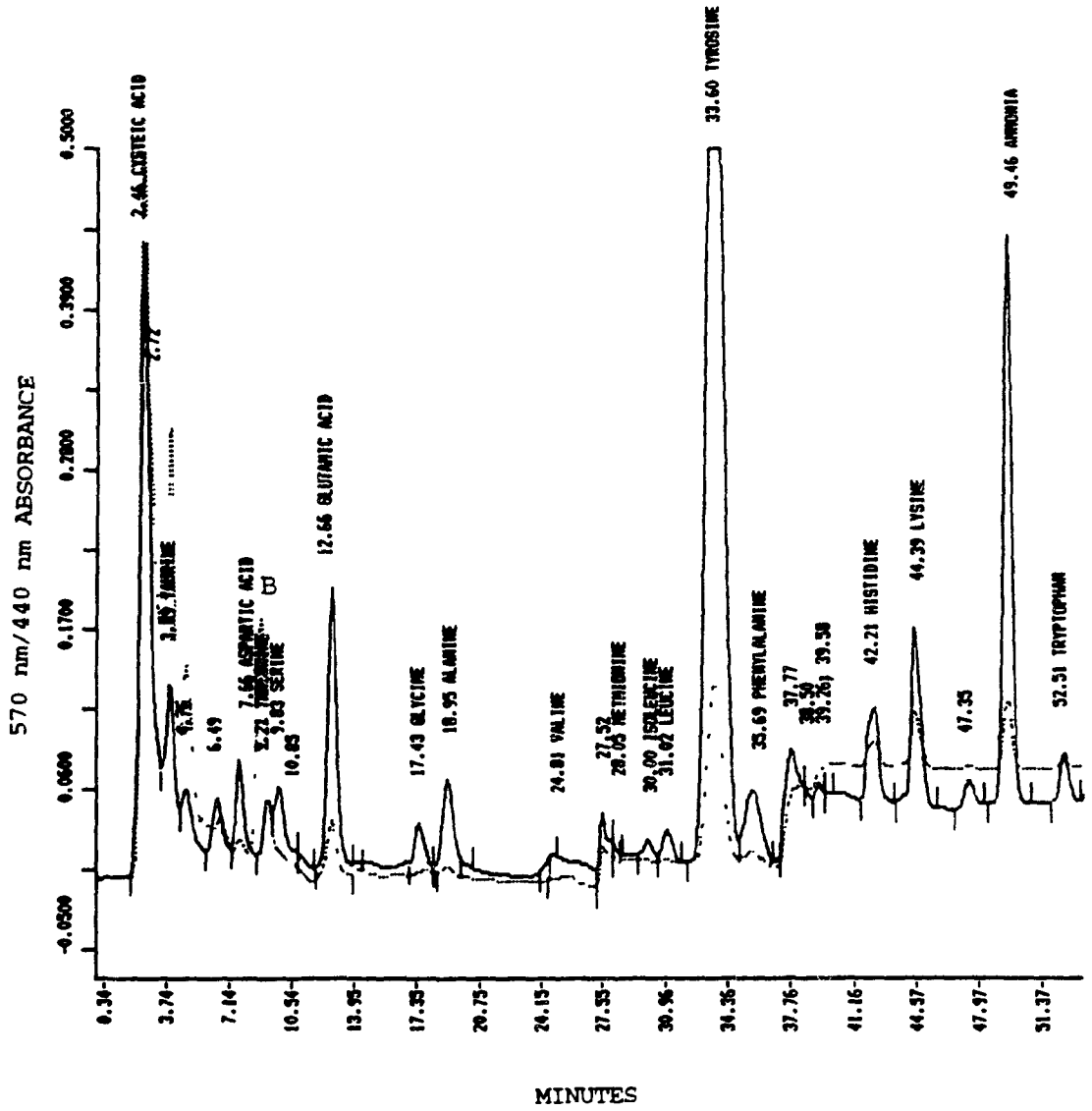

FIGURE 55: AMINO ACID PROFILE OF XENIC *PSEUDONITZSCHIA PUNGENS* F. *PUNGENS* STRAIN KP57 GROWN WITH NH_4Cl AS THE SOLE N SOURCE(_____represents 570 nm and ..... represents 440 nm; B represents second unknown amino acid of interest)

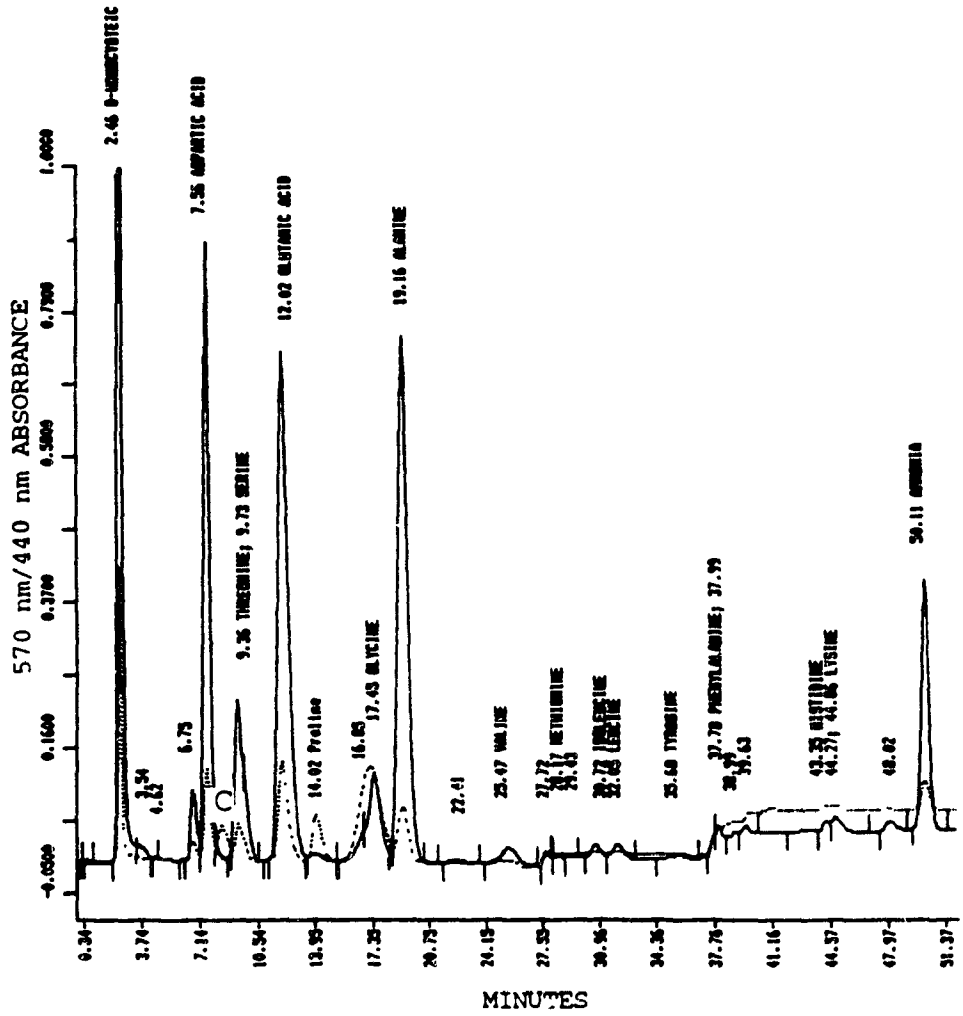

FIGURE 56: AMINO ACID PROFILE OF *PALMARIA PALMATA* MUTANT (GM) (_____represents 570 nm and ..... represents 440 nm; C represents third unknown amino acid of interest)

impure solutions of 1'-hydroxydihydrokainic acid indicated a neutral charge at pH 6.5. The pure compound, isolated as a white solid after extensive chromatographic clean up, had no UV spectrum, and displayed an ion at m/z 231 (LSIMS), consistent with a hydrated kainic acid derivative.

The broad peaks present in the early ^{1}H-NMR spectra suggested that the compound might be associated with a paramagnetic metal ion and a distinct blue colour of aqueous solutions supported this interpretation. The metals retained following passage through a Chelex-100 column were identified as Ca and Cu by X-ray SEM analyses. The Chelex-100 spheres were analyzed prior to the addition of 1'-hydroxydihydrokainic acid to the top of the column and after 1'-hydroxydihydrokainic acid was eluted from the column (Fig. 57). The presence of bound Ca and Cu was confirmed when the carbon planchet was compared with and without the addition of the pre-Chelex-100 1'-hydroxydihydrokainic acid (Fig. 58).

For NMR analysis 1'-hydroxydihydrokainic acid was dissolved in D_2O and acidified to pD 1.76 with DCl, in order to sharpen the resonances of the carbons near the carboxyl groups. The unknown amino acid displayed ten resonances in the ^{13}C-NMR spectrum and a DEPT experiment identified these as two methyl, two methylene, three methine and three quaternary carbons (Table 6; Fig. 59). The HMQC spectrum allowed the

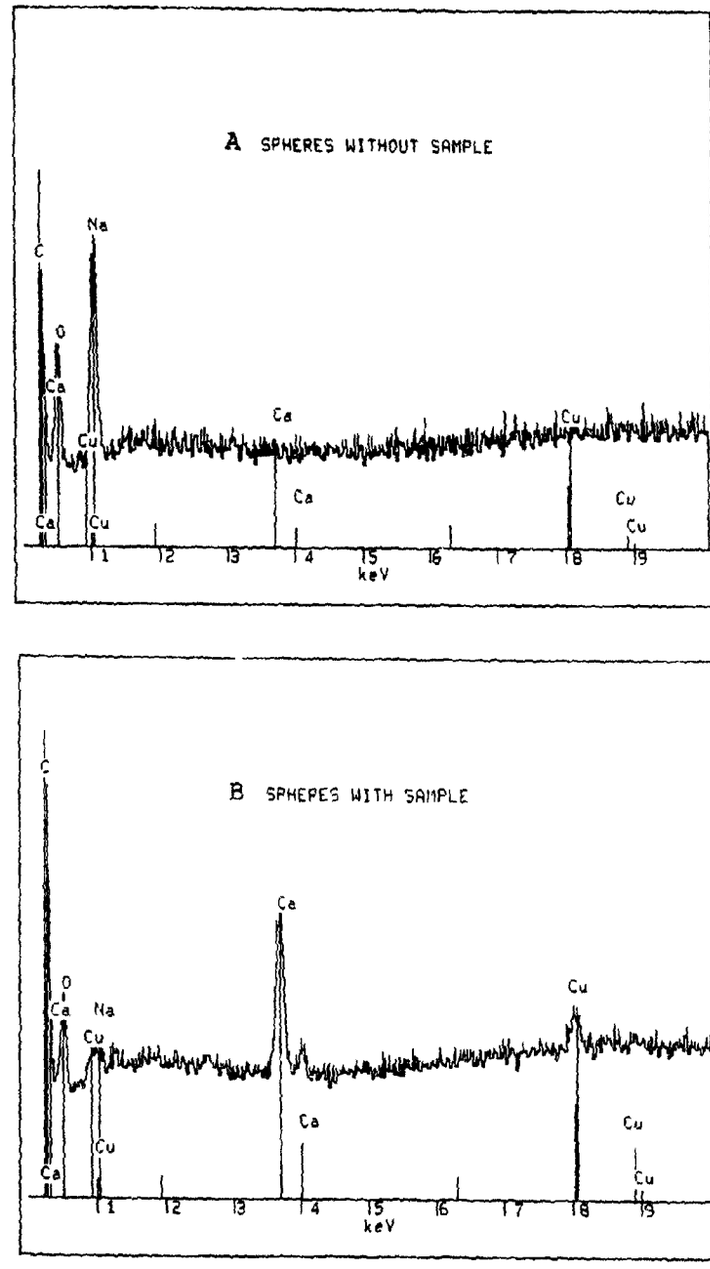

FIGURE 57: X-RAY SEM ANALYSES OF (A) THE CHELEX-100 SPHERES BEFORE 1'-HYDROXYDIHYDROKAINIC ACID WAS ADDED TO THE TOP OF THE COLUMN AND (B) THE RESULTING BLUE SPHERES AFTER 1'-HYDROXYDIHYDROKAINIC ACID WAS ELUTED.

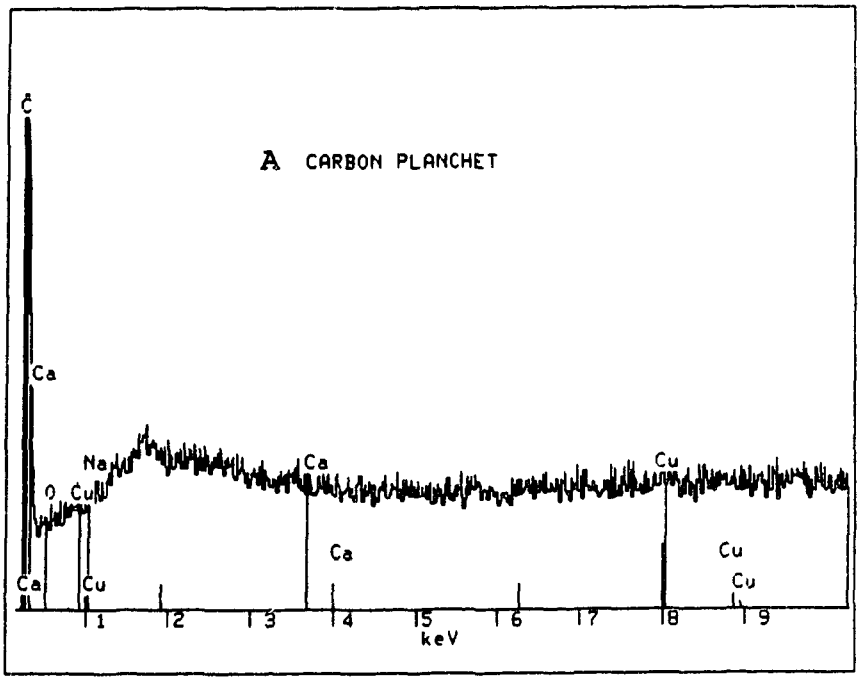

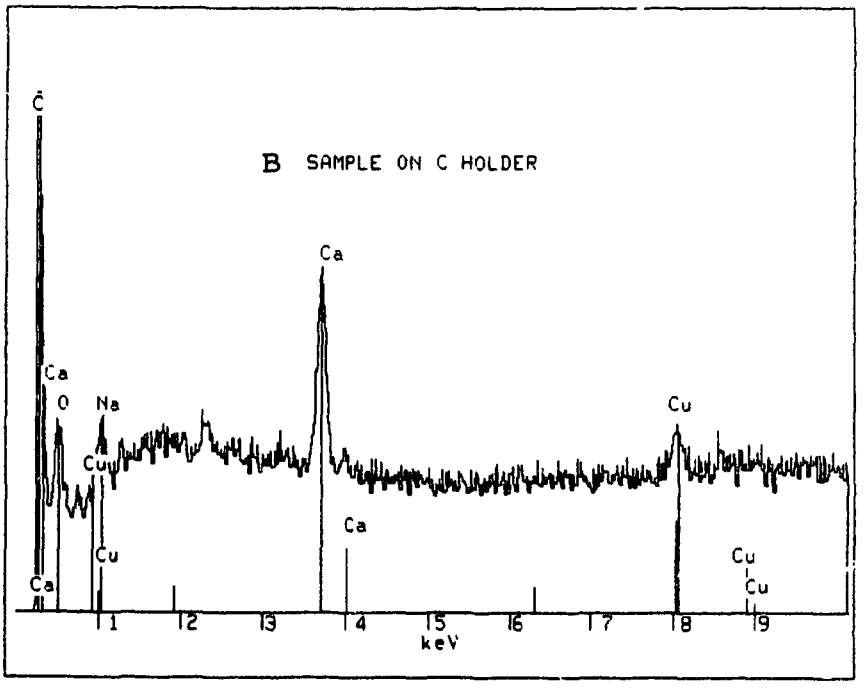

FIGURE 58: X-RAY SEM ANALYSES OF (A) THE CARBON PLANCHET SAMPLE HOLDER AND (B) THE CARBON PLANCHET WITH THE PRE-CHELEX-100 1'-HYDROXYDIHYDROKAINIC ACID ADDED

TABLE 6: NMR DATA FOR 1'-HYDRODIHYDROXYKAINIC ACID

Hydrogen Position	^{1}H-NMR Chemical Shifts (ppm) pD 1.76	Carbon Position	^{13}C-NMR Chemical Shifts (ppm) pD 1.76	DEPT pD 1.76
		2-COOH	174.08	-
2	4.18	2	69.67	CH
3	3.25	3	38.38	CH
4	2.88	4	44.97	CH
5α	3.32	5	47.76	CH_2
5β	3.80			
		6-COOH	176.37	-
6a	3.19	6	33.00	CH_2
6b	2.68			
		1'	85.00	-
1'-CH_3	1.52	1'-CH_3	29.93	CH_3
1'-CH_3	1.43	1'-CH_3	28.66	CH_3

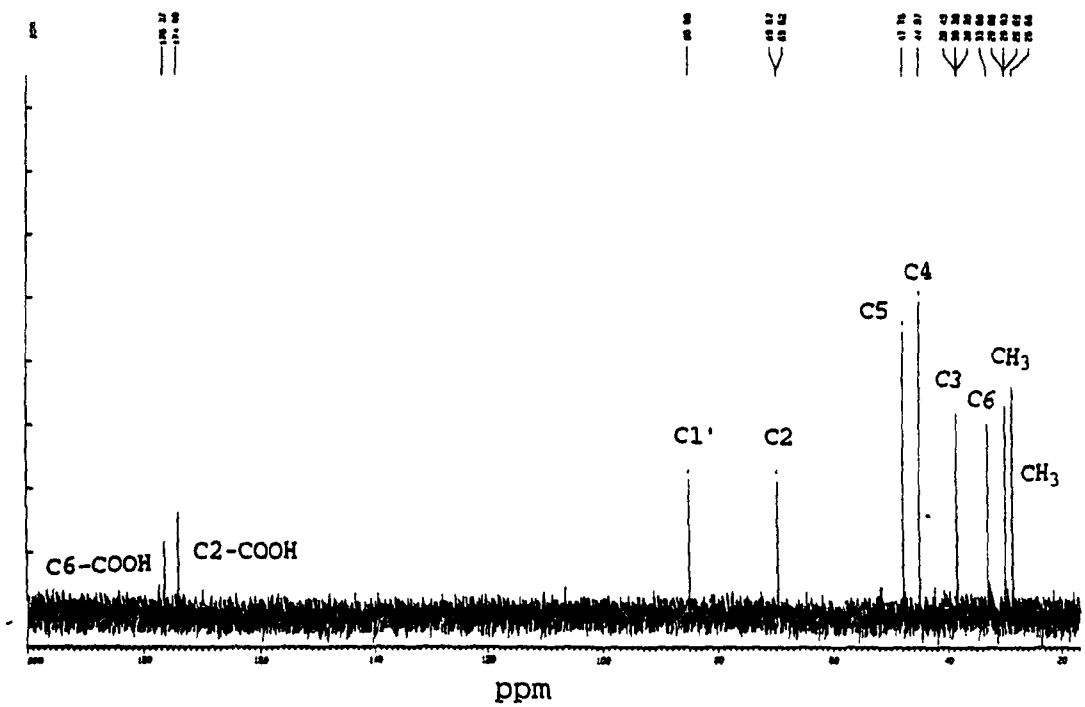

FIGURE 59: THE ^{13}C-NMR SPECTRUM OF
1'-HYDROXYDIHYDROKAINIC ACID AT pD 1.76

assignment of the proton resonances to the carbons in the structure (Fig. 60). The ^{1}H-NMR chemical shifts of 1'-hydroxydihydrokainic acid (spectrum shown in Fig. 61) after Chelex-100 treatment are listed in Table 7; these data revealed a close relationship to kainic acid (Laycock et al., 1989, Table 7). The 2D-COSY data (Fig. 62) at pD 1.76 showed that the proton at δ4.18 (H2) was coupled to a proton resonating at δ3.25 (H3), which in turn was coupled to two methylene protons resonating at δ2.68 and δ3.19 (H6). The H3 proton was also coupled to the methine proton at δ2.88 (H4) which in turn showed a COSY correlation to the methylene protons at δ3.32 and δ3.80 (H5). An HMBC correlation between the carbon resonance at δ174.08 and the proton resonance at δ4.18 (H2) indicated one carboxyl group at C2, and the correlation between the H6 methylene resonances (δ2.68 and δ3.19) and the carbon resonance at δ176.37 linked the second carboxyl group to C6 (Fig. 63). The two methyl singlets at δ1.43 and δ1.52 showed HMBC correlations to the quaternary carbon resonance at δ85.00 (C1'). The downfield chemical shift of this latter carbon suggested that it also carried an oxygen atom or hydroxyl group. HMBC correlation between the C4 carbon at δ44.97 and the two methyl singlets (δ1.43 and δ1.52) attached the side chain to C4 in the ring. Since 1'-hydroxydihydrokainic acid is a secondary amino acid, it was concluded from the ^{13}C resonances that C2 (δ69.67) and C5 (δ47.76) were attached to the sole imino group.

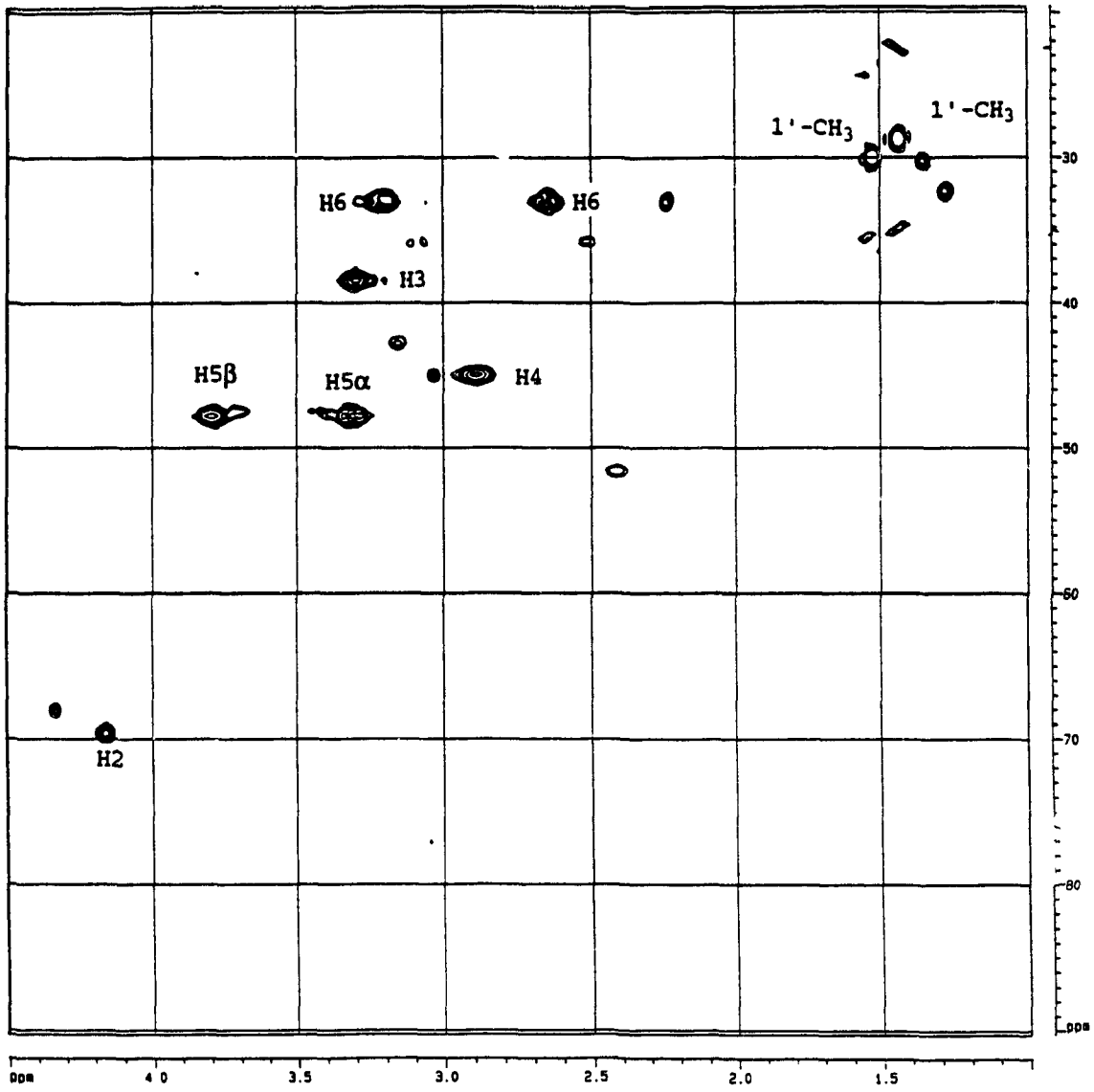

FIGURE 60: HMQC SPECTRUM OF 1'-HYDROXYDIHYDROKAINIC ACID AT pD 1.76

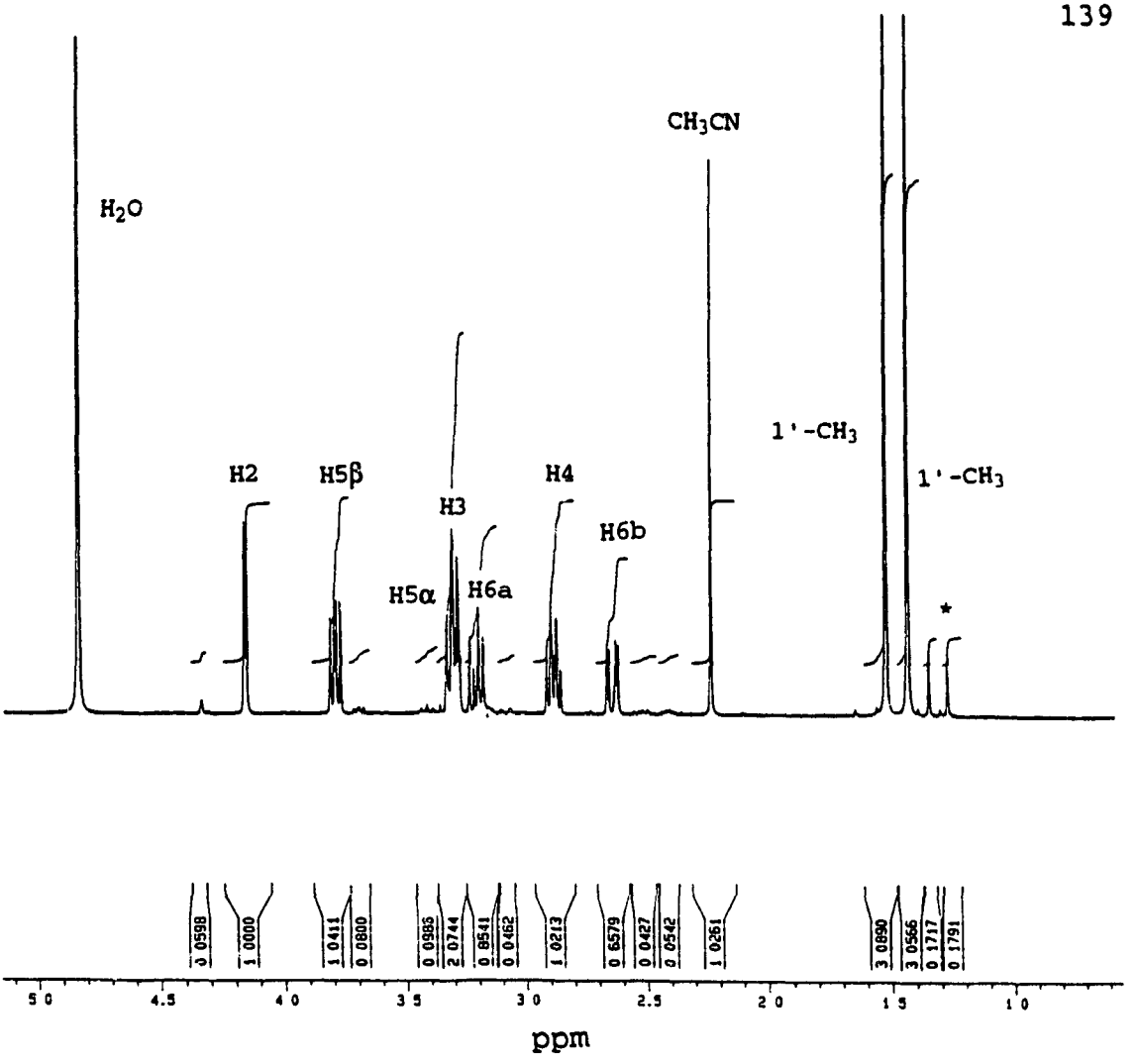

FIGURE 61: THE ^{1}H-NMR SPECTRUM OF 1'-HYDROXYDIHYDROKAINIC ACID AT pD 1.76 (CH_3CN used in final HPLC separation. Star refers to methyl peaks of contaminant (<5%) believed to be isomer of 1'-hydroxydihydrokainic acid).

TABLE 7: 1D-^{1}H NMR DATA FOR KAINIC ACID AND 1'-HYDROXYDIHYDROKAINIC ACID

Kainic Acid		**1'-Hydroxydihydrokainic Acid**			
Hydrogen Positions	^{1}H-NMR Chemical Shifts(ppm) pD 4.12	Hydrogen Positions	^{1}H-NMR Chemical Shifts(ppm) pD 4.12	Hydrogens coupled	Coupling constants (Hz) (a)
2	3.91	2	3.84	2,3	4.23
3	2.90	3	3.03	3,4	8.50
4	2.82	4	2.65	3,6a	9.20
5α	3.27	5α	3.09	3,6b	4.00
5β	3.46	5β	3.59	4,5α	11.80
6a	2.20	6a	3.01	4,5β	8.20
6b	2.09	6b	2.41	5α,5β	-12.20
1'CH_3	1.60	1'CH_3	1.33	6a,6b	-17.40
1'=CH_2	4.58,4.86	1'CH_3	1.24		

(a) Some coupling constants determined by simulation using Bruker PANIC program

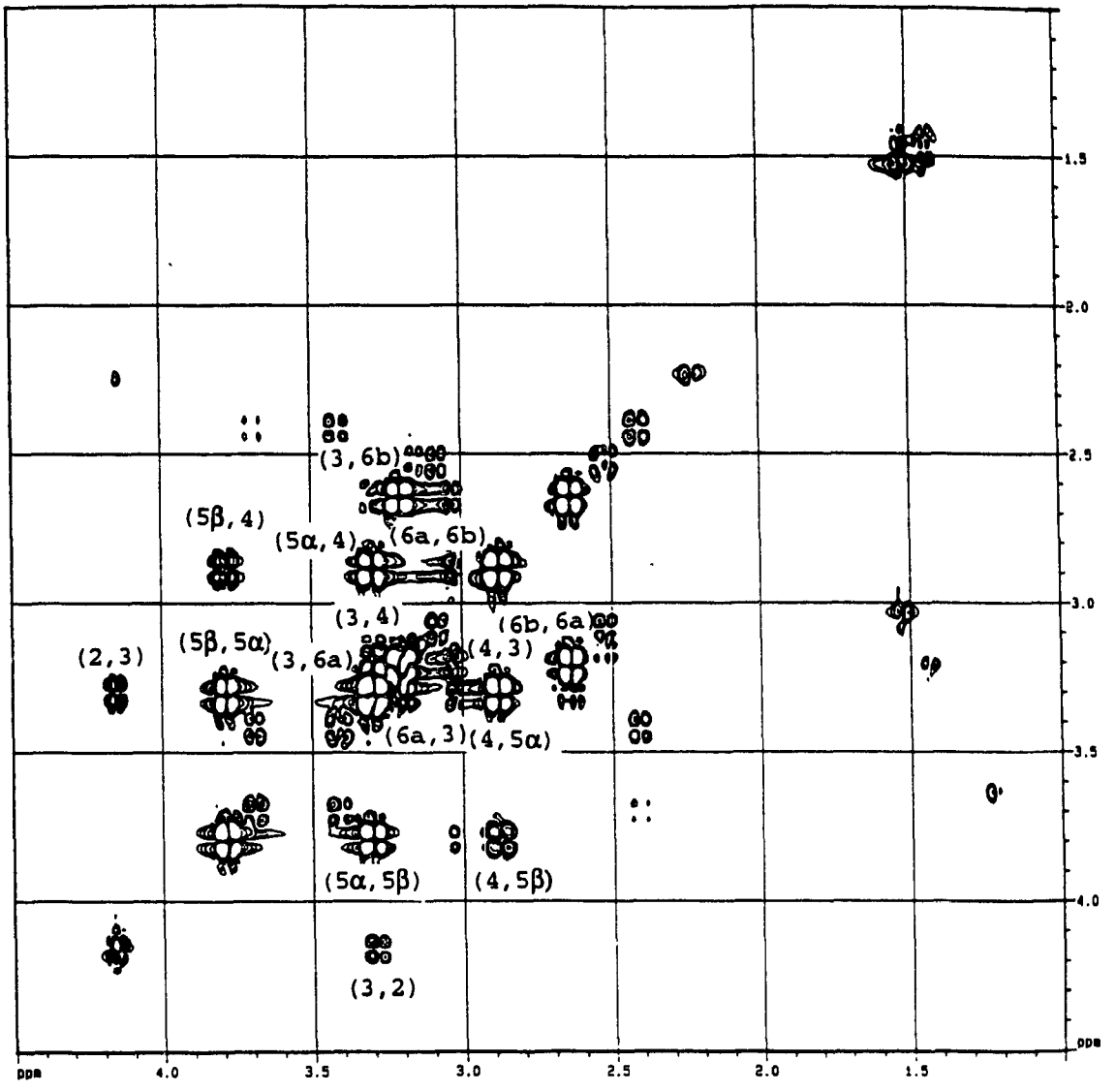

FIGURE 62: 2D-COSY NMR SPECTRUM OF
1'-HYDROXYDIHYDROKAINIC ACID AT pD 1.76

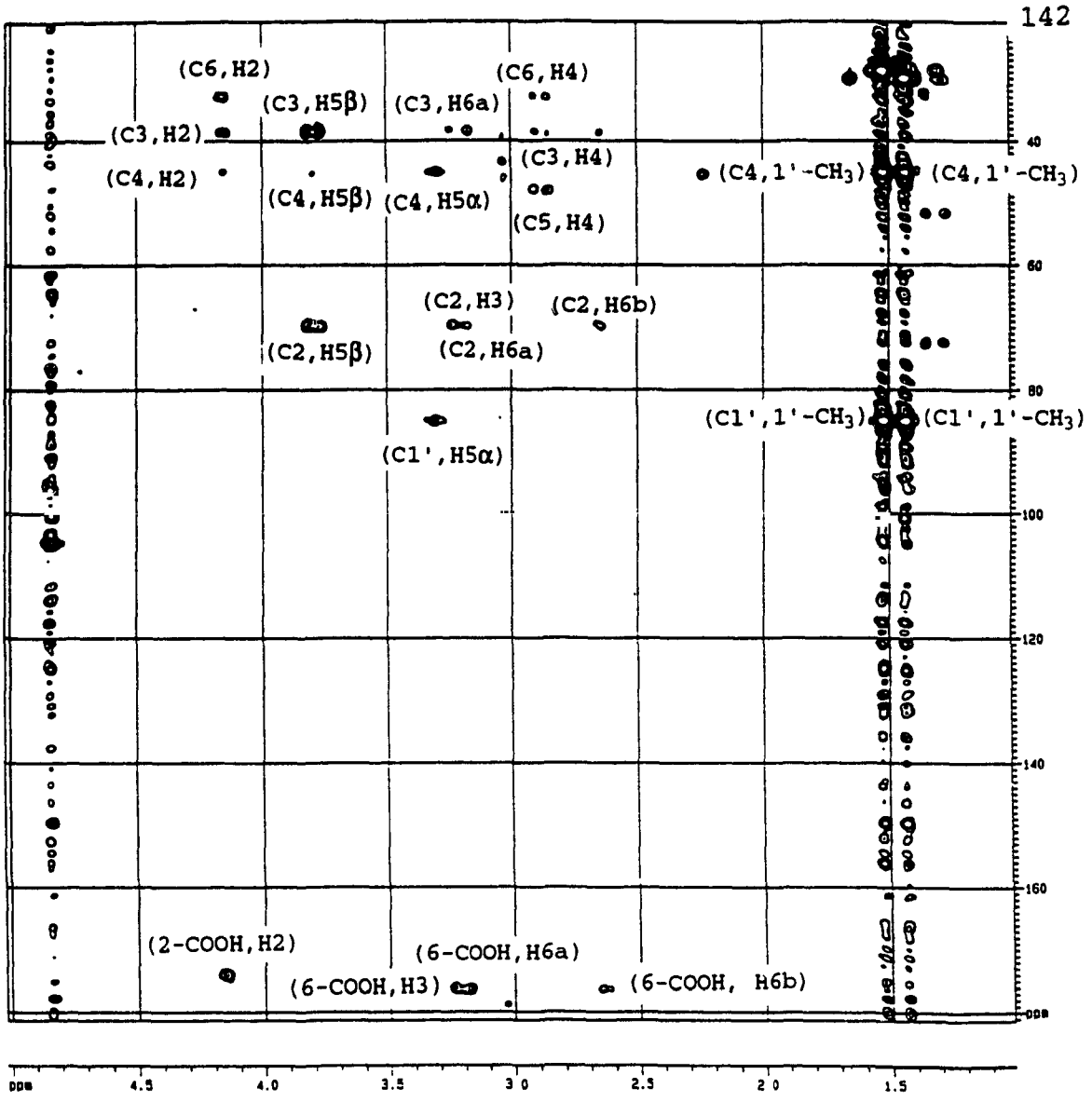

FIGURE 63: HMBC NMR SPECTUM OF
1'-HYDROXYDIHYDROKAINIC ACID AT pD 1.76

The pD was increased to 4.12 with NaOD to improve the resolution of the H4 resonance from those of H3, H5α and H6a, and thus facilitate the analysis of the 2D-NOESY data (Fig. 64). The resonances were assigned based on 2D-COSY also run at pD 4.12. The NOE between H3 and H4 in 1'-hydroxydihydrokainic acid confirmed the *cis* arrangement of these ring protons as found in kainic acid rather than the *trans* arrangement found in allo-kainic acid (Figs. 65 and 66). The NOESY correlation between H3 and one methyl group (δ1.33) and between the H5α proton and the other methyl group (δ1.24), suggested the orientation of the C4 side chain as shown in Figure 66. Neither the H6 protons, nor H2, showed any NOE interaction with the methyl groups. The lack of any NOE between H2 and H3, as well as between H2 and H4, was consistent with the orientation of the groups as found in kainic acid. As further proof, the coupling constant between the protons H3 and H4 (J_{34}=8.50 Hz; Table 7) for 1'-hydroxydihydrokainic acid is similar to the coupling constant reported between the same protons (J_{34}=8.40) in the domoic acid isomer 1 which also has been shown to possess a *cis* arrangement of the H3 and H4 ring protons (Fig. 65; Wright et al., 1990).

The infrared spectrum of 1'-hydroxydihydrokainic acid was consistent with the structure elucidated using NMR. The broad band with strong absorption in the infrared spectrum between

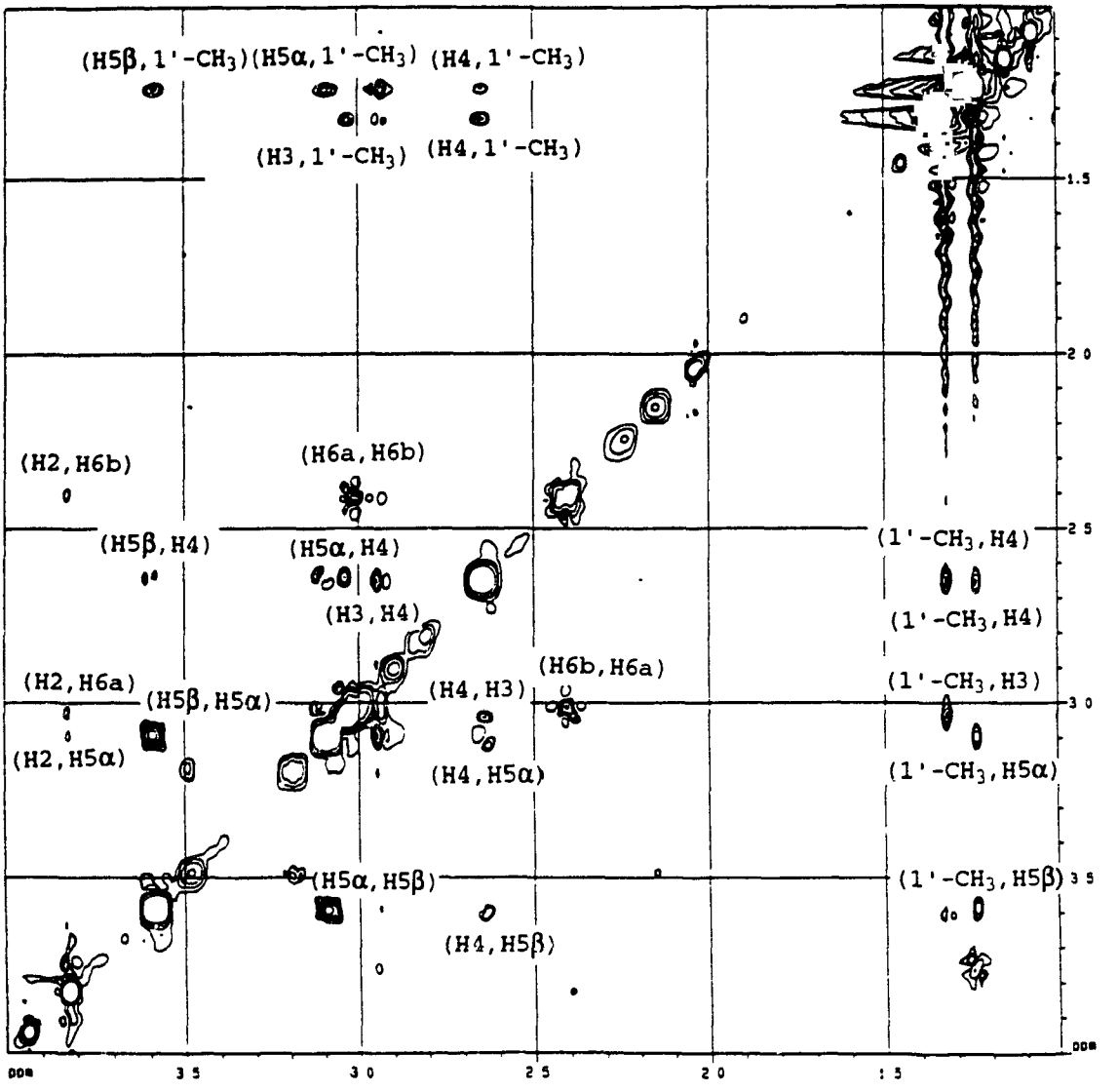

FIGURE 64: 2D-NOESY NMR SPECTRUM OF
1'-HYDROXYDIHYDROKAINIC ACID AT pD 4.12

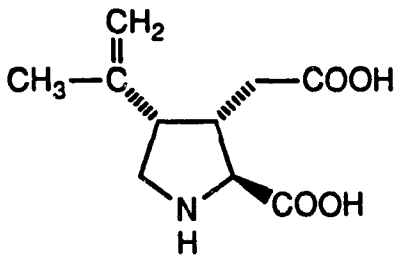

KAINIC ACID

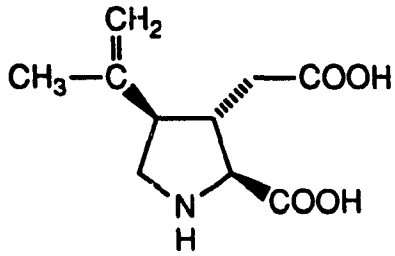

ALLO-KAINIC ACID

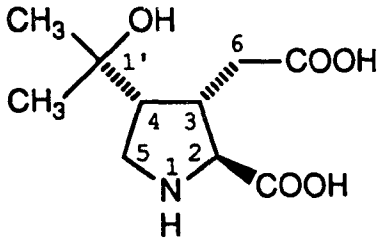

1'-HYDROXYDIHYDROKAINIC ACID

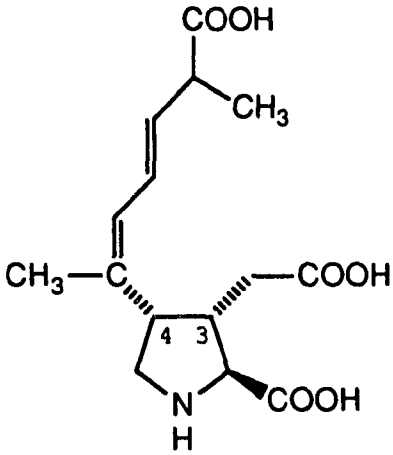

DOMOIC ACID ISOMER 1

FIGURE 65: SEVERAL KAINOID STRUCTURES

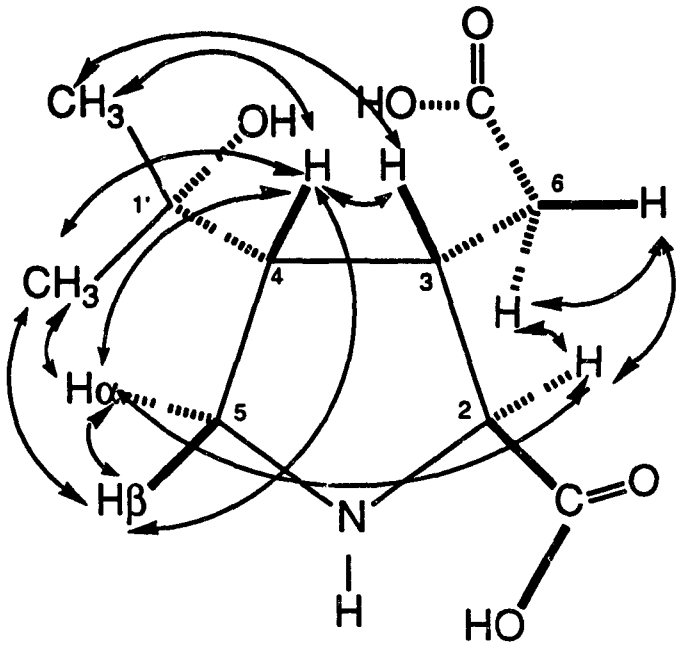

FIGURE 66: INTERACTIONS AMONG PROTONS OF 1'-HYDROXYDIHYDROKAINIC ACID BASED ON NOESY DATA AT pD 4.12

2500 cm^{-1} and 3600 cm^{-1} probably resulted from the stretching of several O-H bonds (Silverstein et al., 1981). Two sharp bands were noted at 1641 cm^{-1} and 1685 cm^{-1}, which correspond to the stretching of two C=O bonds within the two carboxyl groups (Silverstein et al., 1981). Three strong sharp bands were present at 1207 cm^{-1}, 1185 cm^{-1} and 1135 cm^{-1}; these may result from the stretching of C-O bonds (Silverstein et al., 1981).

DISCUSSION

The labelling studies described in Chapter One suggested the possibility of at least one intermediate in kainoid biosynthesis. Thus it was of interest to see if any unusual or unknown amino acids, corresponding to kainoid biosynthetic intermediates, were present in kainoid-producing organisms. Interestingly, the amino acid profile of axenic *P. pungens* f. *multiseries* strain 13CC and *P. australis* both showed the presence of an unknown primary amino acid (unknown A) with a retention time of approximately 6.5 minutes. A similar peak was also present in the xenic strains of *P. pungens* f. *multiseries* and in *P. pungens* f. *pungens* strain KP57. Whether these peaks all correspond to the same compound is not known. The unknown is present in the non-producing and producing strains during the stationary phase of growth in similar concentrations. The axenic nature of the *P. pungens* f. *multiseries* culture shows that unknown A is biosynthesized by the diatom. Whether this amino acid is a precursor in domoic acid production is unknown. Very low amounts of unknown A and the lack of a large biomass for extraction prohibited the isolation of unknown A.

Unknown B, a secondary amino acid with a retention time of approximately 9.2 minutes, was present only in the non-producer of domoic acid, *P. pungens* f. *pungens*. This unknown

may be synthesized either by the diatom or by the bacteria present since the cultures of *P. pungens* f. *pungens* examined were unialgal but not axenic. Unfortunately, *P. pungens* f. *pungens* strain KP57, the strain that produced the greatest amount of unknown B in small-scale cultures, did not produce unknown B when grown on a larger scale. The reason for the absence of unknown B after large-scale culturing is unclear, and indeed the involvement, if any, of unknown B in domoic acid biosynthesis is also not known.

Analysis of the free amino acids of the *Palmaria palmata* mutant (GM) indicated the co-occurrence of kainic acid and a third unknown (C). Unknown C was isolated and subsequently identified as 1'-hydroxydihydrokainic acid, which is probably formed by hydration of kainic acid itself and is therefore unlikely to be a precursor to kainic acid.

1'-Hydroxydihydrokainic acid is able to chelate divalent cations such as calcium and copper as demonstrated by X-ray SEM analyses. The conformation depicted in Figure 66 from the NOE data reveals the close proximity of the hydroxyl group of the side chain and the carboxymethyl group. The close proximity of these two groups provides a possible chelation site for metal ions. In support of this hypothesis there is no report of any similar chelation effect for kainic acid itself. In addition, 1'-hydroxydihydrokainic acid possessed

no net charge on HVPE at pH 6.5, but was acidic after removal of the bound metals with Chelex-100. The toxic effects of copper have been known for several years as exemplified by the use of copper sulfate to control blooms of nuisance algae (Clarke et al., 1987). Those organisms that have developed metal tolerance use two general mechanisms: they exclude the metal from the cell or detoxify it inside the cell. Internal detoxification may be accomplished by binding metal ions, making them unavailable to the cell (Twiss et al., 1993). Whether 1'-hydroxydihydrokainic acid functions in this capacity is not clear and requires further study.

CHAPTER THREE

PRELIMINARY ENZYME STUDIES IN THE BIOSYNTHESIS OF KAINOIDS

INTRODUCTION

The biosynthetic pathways of many prenylated products of both primary and secondary metabolism have been well characterized. A more recent area of interest is the group of enzymes called prenyltransferases, which catalyze the prenylation of these compounds. The general characteristics of those prenyltransferases that have been studied will be discussed in this chapter, which describes the assay for prenyltransferase activity in kainic acid biosynthesis, as well as the effects of specific enzyme inhibitors of protein prenylation on domoic acid production.

Many of the prenyltransferases involved in the prenylation of isoflavones and coumarins are associated with membrane systems (Schroder et al., 1979; Zahringer et al., 1981). The cellular localization of the prenyltransferases in glyceollin synthesis in soybeans and phaseollin synthesis in beans has been determined to be the envelope membrane of the chloroplast, based on both Percoll and sucrose gradients (Fig. 67; Biggs et al., 1990). The prenyltransferase involved in the prenylation of umbelliferone to produce 7-demethylsuberosin in the biosynthesis of furanocoumarins by *Ruta graveolens* was also predominantly localized in the chloroplast fraction (Fig. 68; Ellis and Brown, 1974; Dhillon

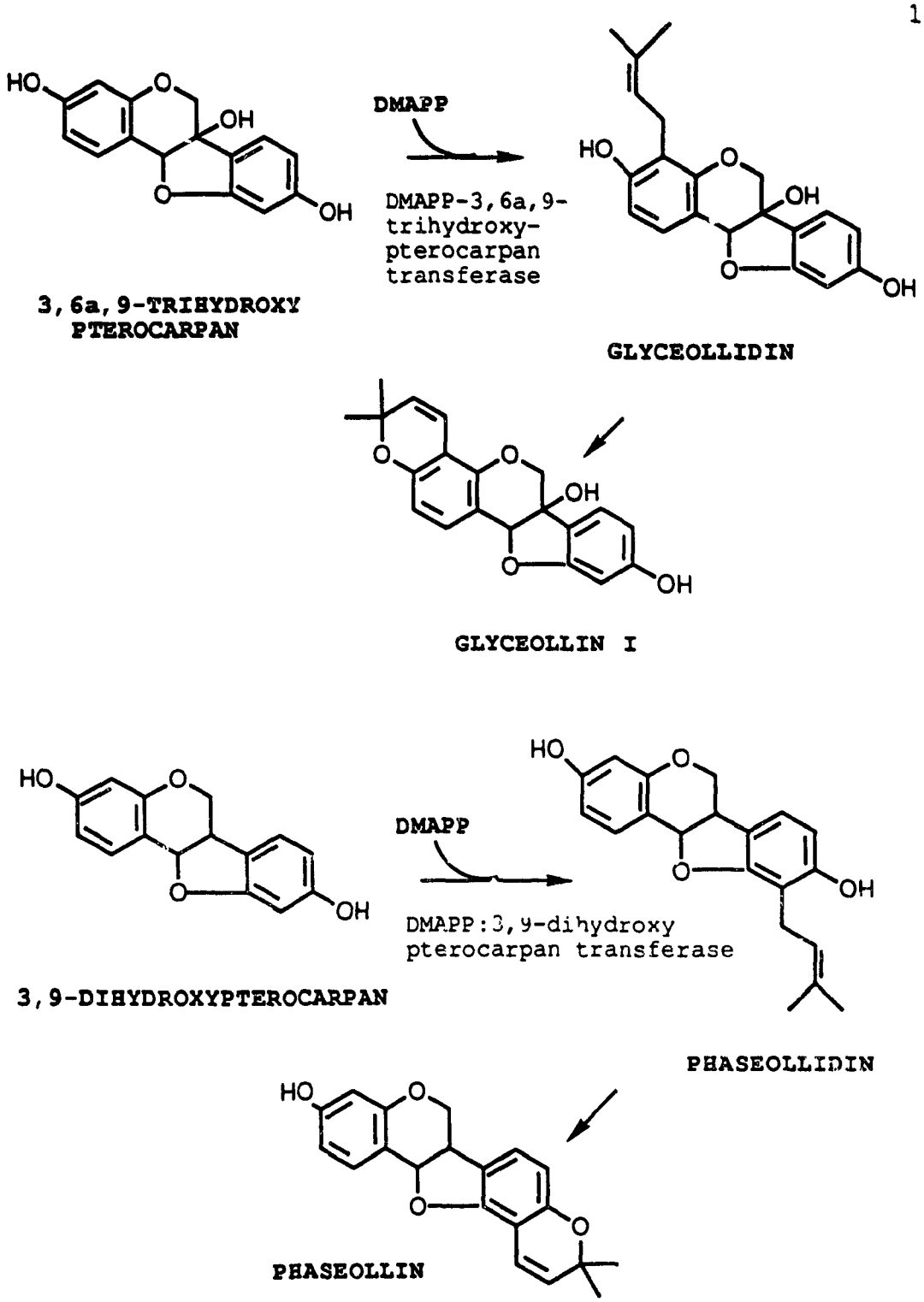

FIGURE 67: THE REACTIONS MEDIATED BY THE PRENYLTRANSFERASES IN GLYCEOLLIN AND PHASEOLLIN SYNTHESIS

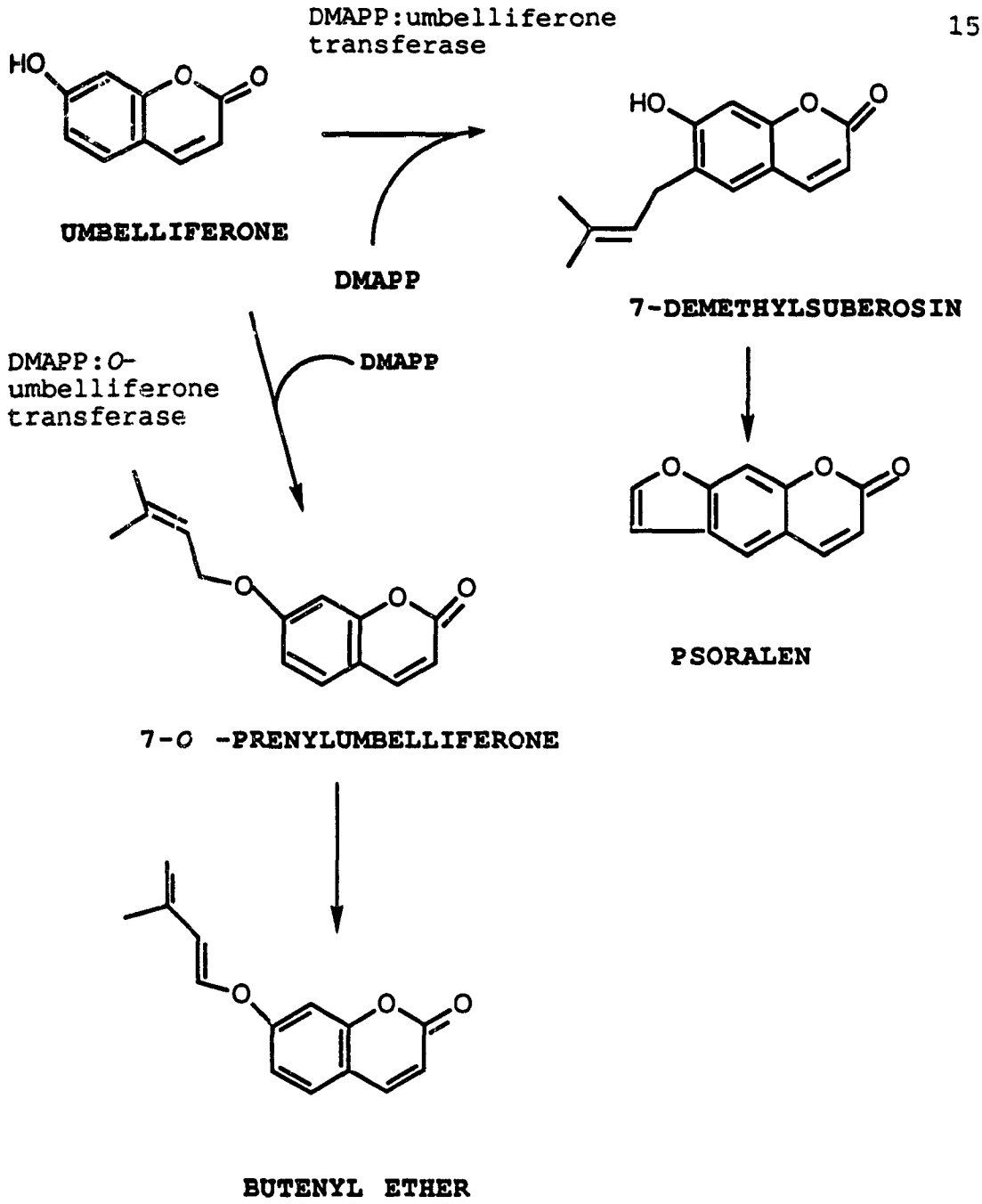

FIGURE 68: THE REACTIONS MEDIATED BY PRENYLTRANSFERASES IN THE SYNTHESIS OF FUROCOUMARINS AND *O*-PRENYLATED COUMARINS

and Brown, 1976; Hamerski and Matern, 1988). *Ammi majus* treated with extracts of *Alternaria carthami* Chowdhury or *Phytophthora megasperma* f.sp. *glycinea* produces furocoumarins from 7-demethylsuberosin, in addition to butenyl ethers from 7-O-prenylumbelliferone (Fig. 68; Hamerski and Matern, 1988). In *Ammi majus*, the prenyltransferases in both furanocoumarin and butenyl ether biosynthesis occur in the endoplasmic reticulum and not in the chloroplast (Hamerski and Matern, 1988). Treatment with detergent solubilizes the *O*-prenyltransferase, which suggests that it is a peripheral rather than an integral membrane protein (Hamerski et al., 1990b).

Within plant cells, prenylated adenosine residues of tRNA are produced in both the cytoplasm and the chloroplast and are possibly synthesized in the mitochondria (Goodwin and Mercer, 1983). The cytoplasmic tRNAs are transcribed from nuclear genes and are subsequently prenylated in the cytoplasm whereas the chloroplast tRNAs are transcribed from plastid genes and prenylated within the organelle stroma (Goodwin and Mercer, 1983).

In some cases prenyltransferases are induced by fungal extract as in the production of glyceollin by soybean when the latter is infected with *Phytophthora* f.sp. *glycinea* or a glucan derivative from the cell wall of this fungus (Welle and

Grisebach, 1988). In other cases, such as luteone synthesis, the prenyltransferase activity is constitutive (Schroder et al., 1979). Feedback inhibition is also variable. The prenyltransferase involved in furanocoumarin synthesis, purified from a cell culture of *Ruta graveolens,* is inhibited neither by 7-demethylsuberosin nor by the end-product of the pathway, psoralen (Fig. 68; Dhillon and Brown, 1976). The prenyltransferases used in the biosynthesis of glyceollin are also not affected by the presence of the intermediate glyceollidin or the other glyceollin isomers (Fig. 67; Biggs et al., 1987). However, other prenyltransferases are affected by feedback inhibition. For example the phaseollin prenyltransferase is competitively inhibited by 3,9-dihydroxypterocarpan, the intermediate phaseollidin, and by phaseollin itself (Fig. 67; Biggs et al., 1987).

In many cases enzyme activity has been established in cell-free extracts or partially purified fractions but the enzymes have not been purified. Those prenylating enzymes that have been purified include the DMAPP transferases in tRNA prenylation, the farnesyltransferases and geranylgeranyltransferases in protein prenylation, and the strictosidine synthase involved in indole alkaloid synthesis (Fig. 69). The DMAPP transferases of yeast and *Escherichia coli* have molecular weights of 33.5 and 34 kDa, respectively (Connolly and Winkler, 1989). These enzymes are similar in

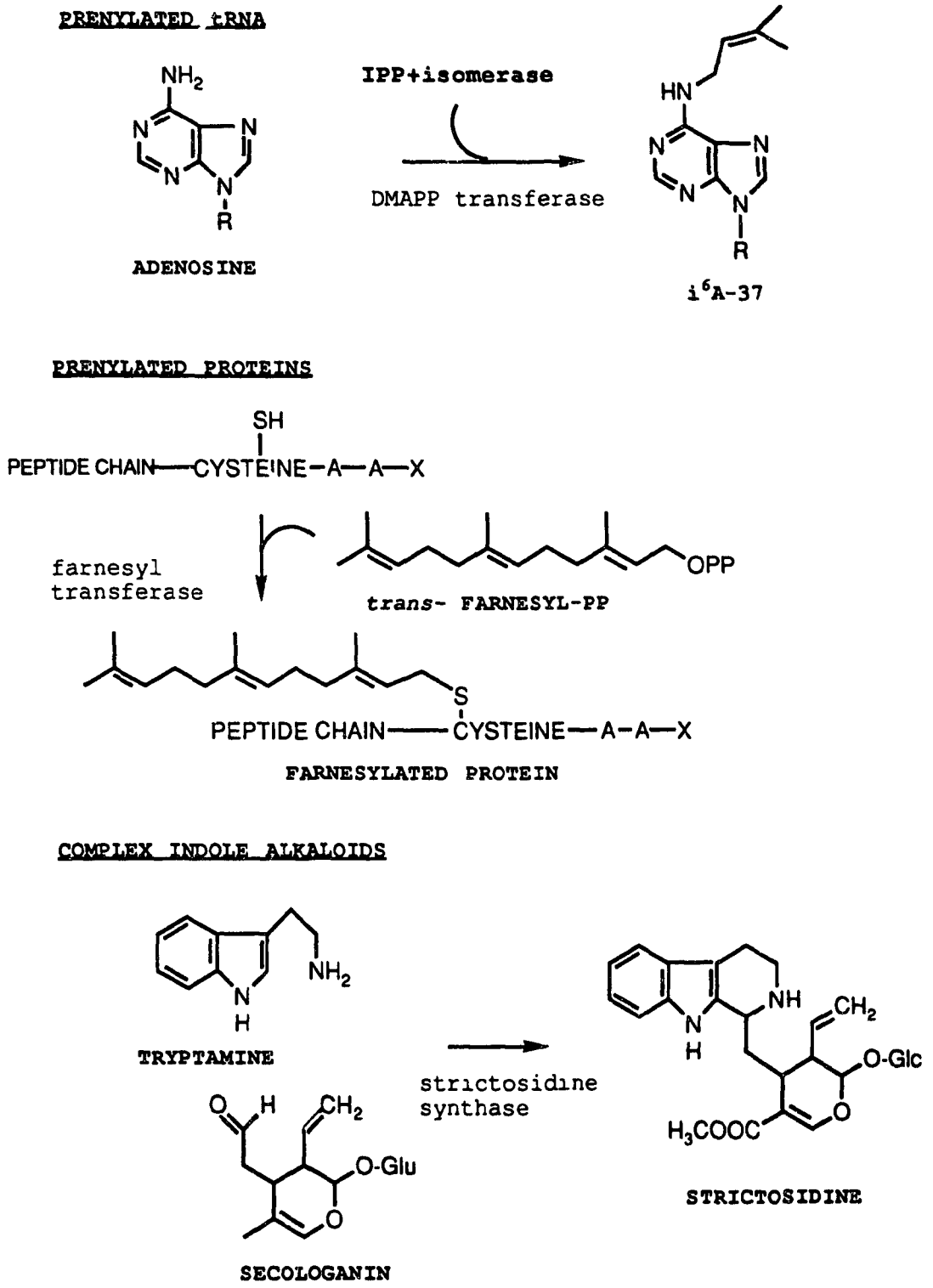

FIGURE 69: THE REACTIONS MEDIATED BY PRENYLTRANSFERASES IN THE PRENYLATION OF tRNA, PROTEINS AND IN STRICTOSIDINE SYNTHESIS

size to strictosidine synthase, which also has a molecular weight of 34 kDa (Bracher and Kutchan, 1992). Generally the farnesyltransferases known to be involved in protein prenylation are dimers with molecular weights of approximately 100 kDa. In rats the α- and β-subunits are 49 and 46 kDa, respectively (Clarke, 1992). These weights are similar to the *Ram1* and *Ram2* subunits for farnesyltransferase in yeast, which have molecular weights of 43 and 38 kDa, respectively (Goodman et al., 1990). One subunit of the dimer recognizes the carboxy-terminal protein sequence of CAAX, where C is cysteine, A is an aliphatic amino acid and X is the carboxy-terminal amino acid. The other subunit appears to recognize the pyrophosphate prenyl donor (Clarke, 1992). There are multiple forms of geranylgeranyltransferases (GGT) that recognize different terminal motifs: GGT-I recognizes the terminal sequence -CAAX, GGT-II recognizes -CC terminal sequences and GGT-III recognizes -CAC terminal sequences (Clarke, 1992; Sinensky and Lutz, 1992). In mammalian systems the GGT-1 enzyme is composed of the two subunits α and β with molecular weights of 48 and 43 kDa, respectively (Moomaw and Casey, 1992). There is evidence to suggest that the α-subunit of the mammalian farnesyltransferase is also associated with the mammalian GGT-1 (Clarke, 1992).

The Michaelis-Menten constant (K_m) values range from 1.5 μM to 3.4 mM for the isoprenoid substrate and from 1.4 μM to

2.3 mM for the non-isoprenoid substrate. Strictosidine synthase had the highest K_m values for both the cyclized isoprenoid secologanin and for the non-isoprenoid substrate tryptamine (Treimer and Zenk, 1979).

Most but not all of the prenyltransferases isolated require divalent cations such as Mg^{2+}, Mn^{2+}, or Zn^{2+} for activity. The prenyltransferases involved in the synthesis of the prenylated isoflavonoids glyceollin I, II and III and in the synthesis of the prenylated coumarin 7-demethylsuberosin require Mn^{2+} cations for activity (Zahringer et al., 1981; Ellis and Brown, 1974). The cation Mg^{2+} is generally required in the prenylation of tRNA and the farnesylation or geranylgeranylation of proteins (Bartz et al., 1970; Goodman et al., 1990; Moomaw and Casey, 1992). The Mg^{2+} or Mn^{2+} cations are postulated to be involved in the coordination of the phosphate groups of the prenyl diphosphate substrates in catalysis (Moomaw and Casey, 1992; Hamerski et al., 1990b). In bovine brain, in contrast, farnesyltransferase and geranylgeranyltransferase each requires both Mg^{2+} and Zn^{2+} for optimum activity (Moomaw and Casey, 1992). Both of these enzymes contain tightly bound Zn^{2+}, which appears to play a role in catalysis rather than a structural role in the enzyme, since the removal and readdition of the Zn^{2+} restores activity. It has been speculated that the Zn^{2+} is involved in the coordination of the incoming thiol group of cysteine, which is

the attachment site of the isoprenoid chain (Moomaw and Casey, 1992). The cation Zn^{2+} is also added in assays of protein prenylation in plants (Zhu et al., 1993). Metals are not required for activity of the prenyltransferase in strictosidine synthesis (Treimer and Zenk, 1979).

It has been suggested that the prenyltransferases involved in domoic acid and kainic acid biosynthesis may be alike due to the the structural similarity of these two metabolites. In Chapter One it was determined that domoic acid is biosynthesized by the condensation of a C10 isoprenoid chain with an activated citric acid cycle derivative. The presence of the carboxyl group at C7′ in domoic acid complicates the biosynthetic pathway since it is not clear whether oxidation of C7′ to a carboxyl group occurs before or after the condensation of the two units. In the proposed pathway of kainic acid biosynthesis a C5 isoprenoid unit condenses with the activated citric acid cycle derivative, without modification of the terminal carbon in the isoprenoid chain. An assay for the prenyltransferase involved in kainic acid biosynthesis would thus not be complicated by the oxidation of the sidechain.

Specific enzyme inhibitors are very useful in the study of enzyme structure and function (Tamanoi, 1993). Several inhibitors of protein prenylation have been reported,

including gliotoxin and (+)-limonene (Fig 70; Pyl et al., 1992; Tamanoi, 1993). Gliotoxin was originally isolated from a fungus and shown to affect the growth of fungi, bacteria and viruses (Pyl et al., 1992). It has also been shown to inhibit farnesyltransferase of Ras p21 proteins (Pyl et al., 1992). This inhibition does not appear to be specific to farnesyltransferases (Tamanoi, 1993). The mode of action of gliotoxin is unknown, but it does not appear to act as a substitute farnesyl substrate, nor does it act as a competitive inhibitor of the protein acceptor (Tamanoi, 1993). (+)-Limonene, a cyclized form of geranylpyrophosphate, also inhibits protein prenylation (Crowell et al., 1991). It has been shown to inhibit prenylation of a class of 21-26 kDa proteins including Ras p21 and other GTP-binding proteins in both NIH3T3 and human mammary epithelial cells. Inhibition of GGT-1 also occurs when (+)-limonene is added. In human mammary epithelial cells, (+)-limonene did not inhibit cholesterol biosynthesis, suggesting that its likely target is the protein prenyltransferase (Crowell et al., 1991).

This chapter describes the results of preliminary assays for prenyltransferase activity in kainic acid biosynthesis by the *Palmaria palmata* mutant (GM). DMAPP, the suggested C5 isoprenoid unit involved in kainic acid biosynthesis, was synthesized for use in the prenyltransferase assay. GPP was also synthesized for use in future

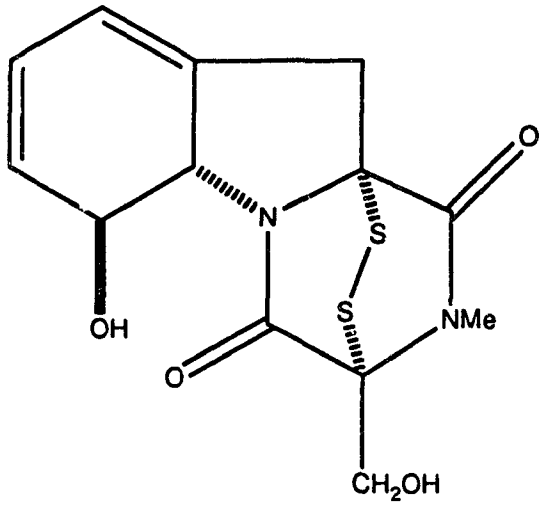

GLIOTOXIN

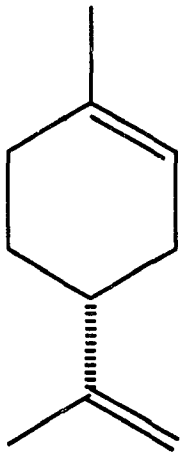

(+)-LIMONENE

FIGURE 73: STRUCTURES OF GLIOTOXIN AND (+)-LIMONENE

prenyltransferase assays in domoic acid biosynthesis. Three ^{14}C-labelled citric acid cycle intermediates were used in the assays as putative precursors to the activated citric acid cycle derivative involved in kainic acid biosynthesis. This Chapter also describes the effects of the protein prenyltransferase inhibitors, gliotoxin and (+)-limonene, on the growth and production of domoic acid by *Pseudonitzschia pungens* f. *multiseries*.

METHODS AND MATERIALS

DIMETHYLALLYLPYROPHOSPHATE AND GERANYLPYROPHOSPHATE SYNTHESIS AND PURIFICATION

Dimethylallylpyrophosphate (DMAPP) and geranyl pyrophosphate (GPP) were synthesised and purified according to the method of Davisson et al. (1985, 1986). The purity of both compounds was determined by ^{1}H-NMR at 500.13 MHz on a Bruker AMX-500 spectrometer (see Chapter One).

KAINIC ACID PRENYLTRANSFERASE ENZYME ASSAYS

Fresh biomass of the *Palmaria palmata* mutant GM was obtained from P. Shacklock, Sandy Cove Aquaculture Research Station, National Research Council, N.S. Approximately 2 g of biomass was placed in a 250 mL Erlenmyer flask with SWM-3 medium (100 mL) containing nutrients at half the original concentrations (McLachlan, 1973), the phosphate reduced to 5 µM, and without soil or liver extract added. The culture was aerated with filtered compressed air at 25°C with a 8:16 light:dark cycle until protein extraction. For the extraction *Palmaria palmata* (2 g) was placed in a sterile 12 mL polypropylene tube (Elkay, Shrewbury, MA) and 5 mL of extraction buffer was added [0.1 M Tris pH 7.0; 1 mM dithiothreitol (DTT; Sigma); 1 mM phenylmethylsulfonyl fluoride (PMSF; Sigma; dissolved in acetone); 10^{-7}M pepstatin A (Sigma; dissolved in dH_2O)]. The tube was placed on ice and

the algal biomass homogenized using a Brinkmann homogenizer (PT10/35, attachment PTA10; Brinkmann Instruments Co., Switzerland) for 2 min. The crude extract was then placed on ice until added to the enzyme assay. The quantity of protein was estimated by measuring the absorbance at 280 nm using a Beckman DU64 spectrophotometer (Beckman Instruments Inc., CA). In order to determine the activity of the crude protein extract a malate dehydrogenase assay was performed using the oxaloacetate reduction method (Kitto, 1969). A unit of malate dehydrogenase activity is defined as the amount of enzyme required to oxidize or reduce 1 μmole of coenzyme per minute (Kitto, 1969).

The L[1-^{14}C]-glutamate kainic acid prenyltransferase assay contained: 100 μL assay buffer (0.25 M Tris pH 7.4; 5 mM $MgCl_2$; 5 mM $MnCl_2$; 5 mM DTT), 20 nmoles DMAPP (5 μL), 0.2 nmoles L[1-^{14}C]-glutamate (0.5 μL; 15 nCi) and approximately 350 μg crude protein extract (20 μL). The [1-^{14}C]-α-ketoglutarate assay contained: 100 μL assay buffer as above, 20 nmoles DMAPP, 0.2 nmoles [1-^{14}C]-α-ketoglutarate (0.5 μL; 15 nCi), 0.1 mM β-nicotinamide-adenine dinucleotide, reduced (NADH, Boehringer Mannheim, Germany; 2 μL), 20 μL ferredoxin solution (final: 20 μM ferredoxin from *Porphyra umbilicalis*, Sigma); 14 mM sodium dithionite; 30 mM sodium bicarbonate, and approximately 350 μg crude protein extract (20 μL). The [1,5-^{14}C]-citric acid assay contained: 100 μL assay buffer as above,

20 nmoles DMAPP, 0.2 nmoles [1,5-^{14}C]-citric acid (0.5 µL; 20 nCi), 0.1 mM NADH (2 µL), 0.6 mM β-nicotinamide-adenine dinucleotide (NAD+, Sigma; 12 µL), 0.1 mM β-nicotinamide-adenine dinucleotide phosphate (NADP+, Sigma; 2 µL), 20 µL ferredoxin solution, and approximately 350 µg crude protein extract (20 µL). Final volumes in all cases were brought up to 200 µL with sterile water. Each assay was performed in triplicate. Two controls were also prepared concurrently for all three ^{14}C-experiments: one without DMAPP added and the second without DMAPP or the crude protein extract added.

The enzyme reactions were allowed to proceed for one hour at room temperature, then 5 µL from each tube were spotted onto a silica TLC plate. A 5 µL aliquot of kainic acid (Sigma) solution (5 mg/mL water) was spotted flanking either side of the applied samples. The plate was dried and placed in n-butanol:acetic acid: water (4:1:1) in a TLC tank and allowed to run for 2 h. The plate was dried and sprayed with a cadmium/ninhydrin solution (see Chapter Two). It was then wrapped in plastic wrap, placed in an X-ray cassette (Wolf X-ray Corporation, NY) with a Kodak X-OMAT AR X-ray film, and stored at -70°C for one week. The film was developed using the Kodak GBX developing system (Kodak Canada Inc., Toronto). The reaction product was again spotted on a silica TLC plate after 24 h at room temperature and treated as described above.

GLIOTOXIN AND (+)-LIMONENE EXPERIMENTS

Five axenic cultures of *Pseudonitzschia pungens* f. *multiseries* strain KP59/2 were grown until the stationary phase in 250 mL F/2 media with 4.1 mM Tris buffer in 500 mL Erlenmyer flasks with the light intensity and temperature as described in Chapter One. Routine samples (5 mL) were taken for % transmittance readings and then frozen at -20°C for later domoic acid analysis (see Chapter One for conversion of % transmittance to optical density and method of domoic acid analysis). Gliotoxin (5 mg; Sigma) was dissolved in ethanol (95%; 1.05 mL) and aliquots (70 µL) removed with a syringe and added to each of the three cultures on day 9, during the onset of the stationary phase, giving a final concentration in the medium of 5 µM. The two remaining flasks were treated as controls and only ethanol (95%; 70 µL) was added.

In a second series of experiments, thirty 125 mL flasks containing F/2 media (50 mL) and 4.1 mM Tris buffer were inoculated with *Pseudonitzschia pungens* f. *multiseries* strain KP59/2 and grown until stationary phase was reached. Routine samples (5 mL) were removed, % transmittance was measured and then the samples were frozen at -20°C for later domoic acid analyses. A small aliquot (11.2 µL) of the above gliotoxin solution was removed with a syringe and serially diluted with

ethanol. Aliquots (100 µL) of the diluted gliotoxin were added to the culture flasks on day 13, during the onset of the stationary phase of growth, to give final concentrations in the media of 0.5 µM, 0.05 µM, 0.005 µM, and 0.0005 µM. Triplicate flasks were maintained at each concentration of gliotoxin. Three control flasks were treated with 100 µL ethanol only. In a parallel (+)-limonene experiment, a small aliquot (3.3 µL) of (+)-limonene was removed with a sterile pipetman and serially diluted with ethanol. Each culture received 100 µL diluted (+)-limonene to give final concentrations in the media of 0.5 µM, 0.05 µM, 0.005 µM, and 0.0005 µM. Triplicate flasks were maintained at each concentration of (+)-limonene. Ethanol (100 µL) was added to each of three control flasks. Two days after the addition of gliotoxin or (+)-limonene a sample (5 mL) was removed from each flask and the % transmittance was measured. The samples were then placed at -20°C for later domoic acid analyses.

RESULTS

DMAPP AND GPP SYNTHESIS AND PURIFICATION

The ^{1}H-NMR spectra of purified DMAPP and GPP are shown in Figs. 71 and 72. The chemical shifts and the coupling constants are similar to those reported (Davisson et al., 1985). The ^{1}H-NMR spectrum for GPP shows a resonance at δ4.5 corresponding to H1 which is downfield from H5 and H4 (δ2.11) due to the presence of the pyrophosphate group on C1. A resonance at δ4.5 is also present in the spectrum of DMAPP where it also corresponds to H1.

KAINIC ACID PRENYLTRANSFERASE ENZYME ASSAYS

The autoradiographs of the kainic acid prenyltransferase enzyme assays with L[1-^{14}C]-glutamate, [1-^{14}C]-α-ketoglutarate or [1,5-^{14}C]-citric acid added as putative precursors are shown in Figs. 73 and 74 for reaction times of 1 h and 24 h, respectively. After one hour the L[1-^{14}C]-glutamate-containing assay showed a radioactive spot (R_f 0.24) in the triplicate assay samples (G1-G3) and the negative controls without DMAPP (G4) or without DMAPP and the enzyme extract (G5). The TLC plate stained with ninhydrin revealed purple spots (G1-G4) with a similar R_f value of 0.24. No radioactive

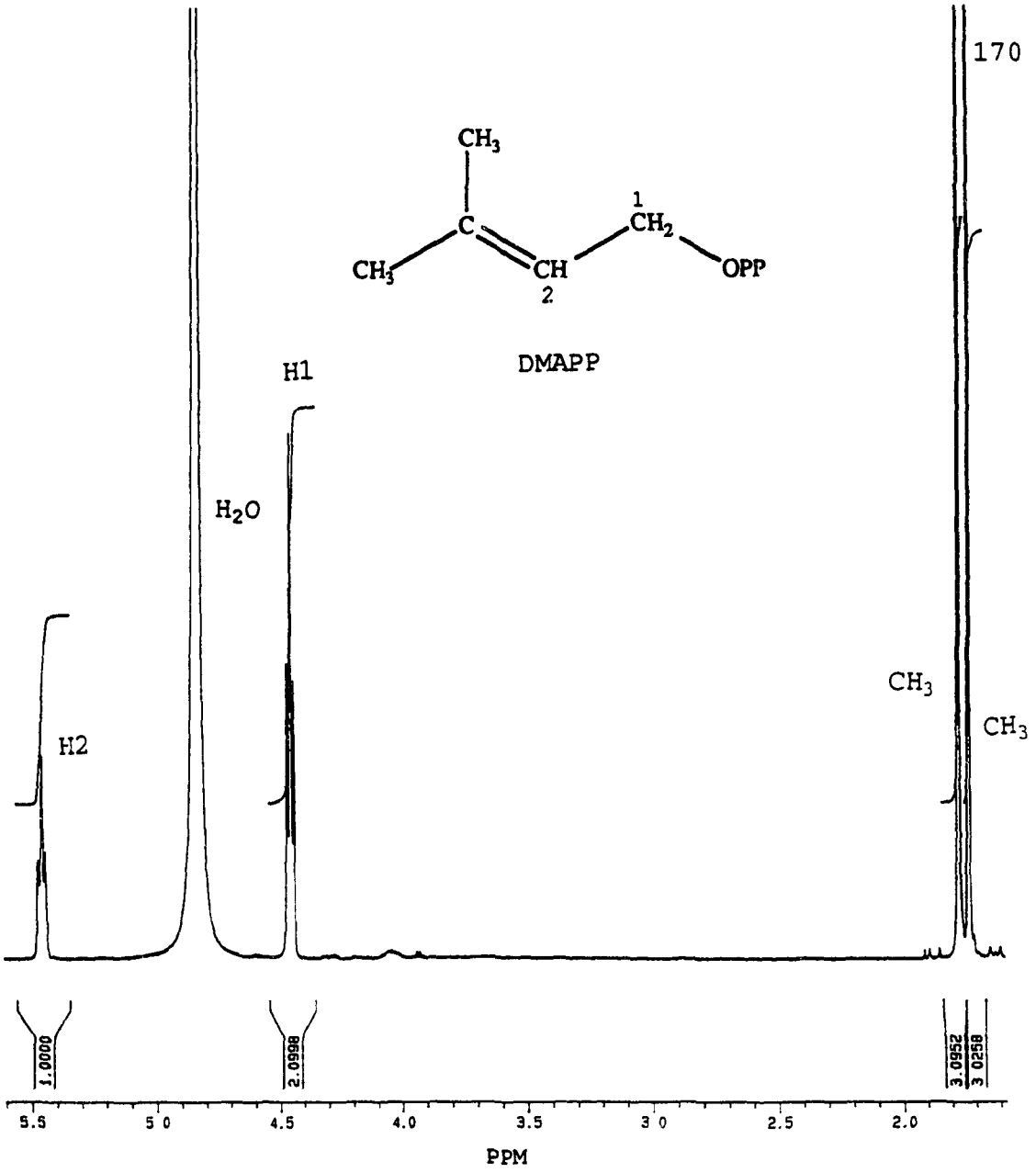

FIGURE 71: ^{1}H-NMR SPECTRUM OF PURIFIED DMAPP

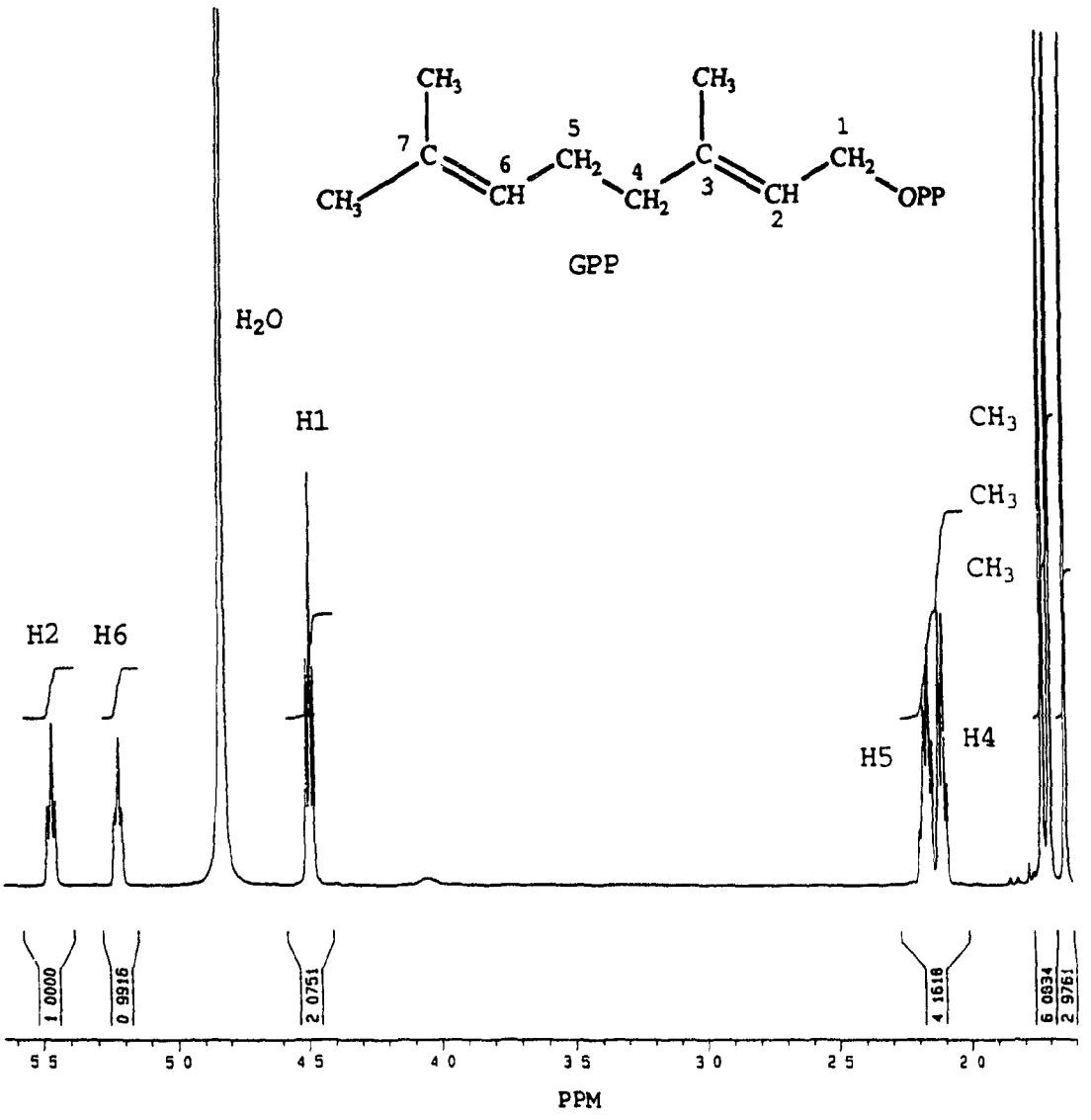

FIGURE 72: ^{1}H-NMR SPECTRUM OF PURIFIED GPP

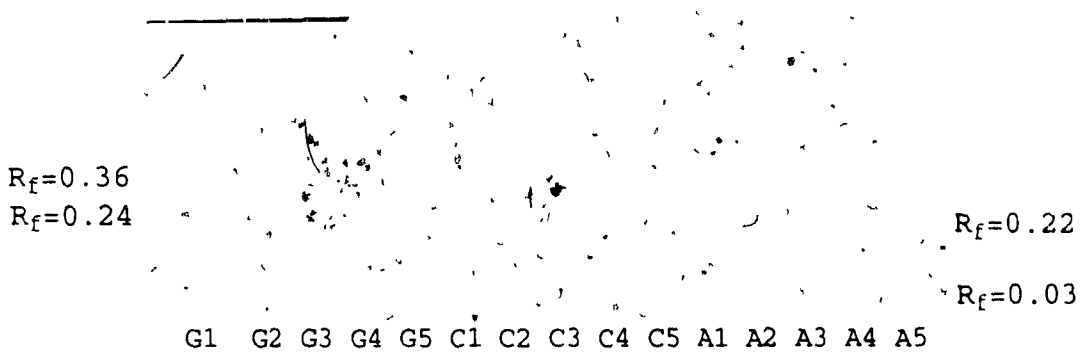

FIGURE 73: THE AUTORADIOGRAPH OF THE KAINIC ACID PRENYLTRANSFERASE ASSAY AFTER 1 h. (G = L[1-^{14}C]-GLUTAMATE; C = [1,5-^{14}C]-CITRIC ACID; A = [1-^{14}C]-α-KETOGLUTARATE; 1-3 ARE THE TRIPLICATE ASSAYS FOR EACH PRECURSOR; 4 IS THE CONTROL WITHOUT DMAPP; 5 IS THE CONTROL WITHOUT DMAPP AND THE CRUDE PROTEIN EXTRACT)

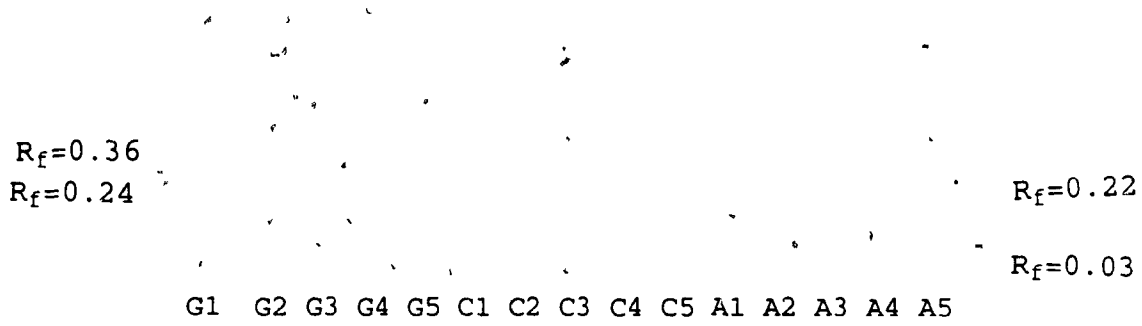

FIGURE 74: THE AUTORADIOGRAPH OF THE KAINIC ACID PRENYLTRANSFERASE ASSAY AFTER 24 h. (G = L[1-^{14}C]-GLUTAMATE; C = [1,5-^{14}C]-CITRIC ACID; A = [1-^{14}C]-α-KETOGLUTARATE; 1-3 ARE THE TRIPLICATE ASSAYS FOR EACH PRECURSOR; 4 IS THE CONTROL WITHOUT DMAPP; 5 IS THE CONTROL WITHOUT DMAPP AND THE CRUDE PROTEIN EXTRACT)

kainic acid (R_f 0.36) was present (Fig. 73). After 24 h the radioactive spot (R_f 0.24) was weaker in the control G4 and to a lesser extent in G5 but was considerably weaker in the assay samples (G1-G3) (Fig. 74).

After both 1 h and 24 h reactions the kainic acid prenyltransferase assay with [1,5-^{14}C]-citric acid added showed a radioactive spot close to the origin (R_f 0.03) in the triplicate assays (C1-C3) as well as in the controls without DMAPP (C4) or without DMAPP and the crude protein extract (C5) (Fig. 73). In addition, a second very faint radioactive spot (R_f 0.14) was noted in C1-C5 at both 1 h and 24 h. Neither spots (R_f 0.03 or R_f 0.14) corresponded to ninhydrin-stained products on the TLC plate. After 24 h, a very faint radioactive spot (R_f 0.24) was observed in the triplicate assays C1-C3 and the control C4, but was not present in the second control without the crude extract (C5). A purple-staining ninhydrin product on the TLC plate with the same R_f value of 0.24 was also noted in C1-C4. No radioactive kainic acid (R_f 0.36) was noted at either 1 h or 24 h.

The kainic acid prenyltransferase assay with [1-^{14}C]-α-ketoglutarate added revealed a radioactive spot with an R_f value of 0.22 in the three triplicate assays (A1-A3) and in the negative controls without DMAPP (A4) and without DMAPP and the crude protein extract (A5) after 1 h reaction (Fig. 73).

This spot did not correspond to a ninhydrin-staining product on the TLC plate. A1-A4 contained another radioactive spot at R_f 0.24 after 1 h that was less intense in the control without the crude protein extract. In A1-A4 this spot corresponded to a ninhydrin-staining (purple) product on the TLC plate (Figs. 73 and 74). After 24 h of reaction A1-A4 contained a radioactive spot (Rf 0.24) that corresponded to a ninhydrin-staining product. The control without the crude protein extract (A5) still contained a radioactive spot (Rf 0.22) after 24 h. A fainter signal was also present in A1-A5 with an R_f value of 0.03 at both 1 h and 24 h. No radioactive kainic acid (R_f 0.36) was noted at either 1 h or 24 h.

The general activity of the crude protein extract was assayed using an oxaloacetate reduction assay for malate dehydrogenase activity. The crude protein extract contained 0.08 units/mL of malate dehydrogenase activity.

GLIOTOXIN AND (+)-LIMONENE EXPERIMENTS

The optical densities and domoic acid levels of *Pseudonitzschia pungens* f. *multiseries* strain KP59/2 with gliotoxin added to a final concentration of 5 µM on day 9 during the stationary phase of growth are shown in Figs. 75 and 76. Two controls, without gliotoxin added, are also shown in Figs. 75 and 76. The cultures with gliotoxin added on day

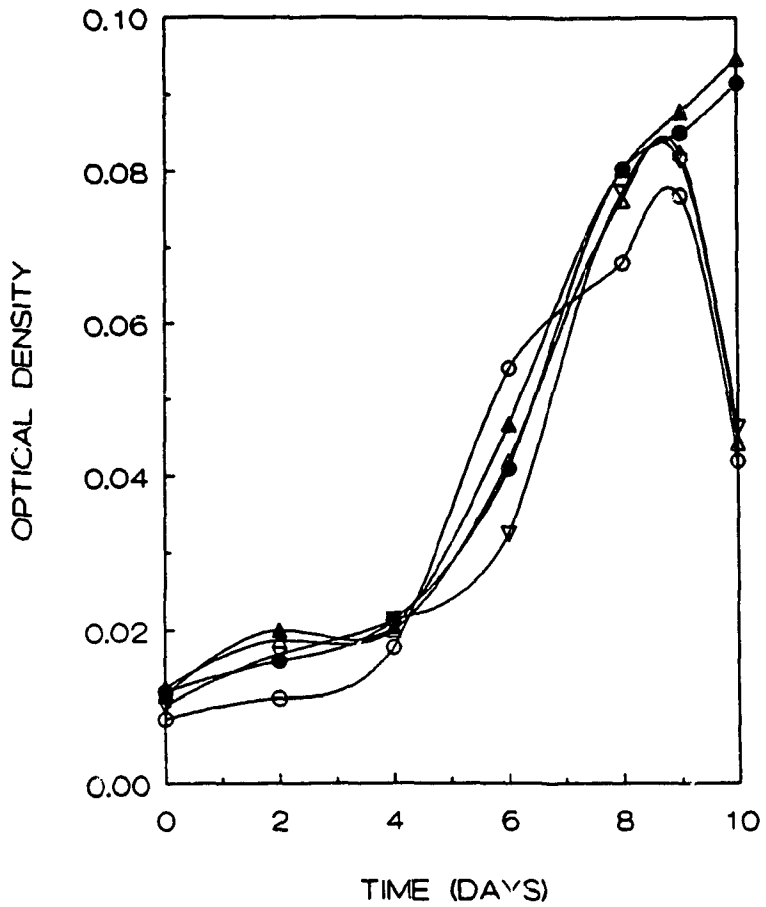

FIGURE 75: THE EFFECT OF GLIOTOXIN ON THE GROWTH OF *PSEUDONITZSCHIA PUNGENS* F. *MULTISERIES* STRAIN KP59/2 (the open symbols represent the triplicate samples with gliotoxin added on day 9 to a final concentration of 5 µM; the solid symbols represent the two control samples)

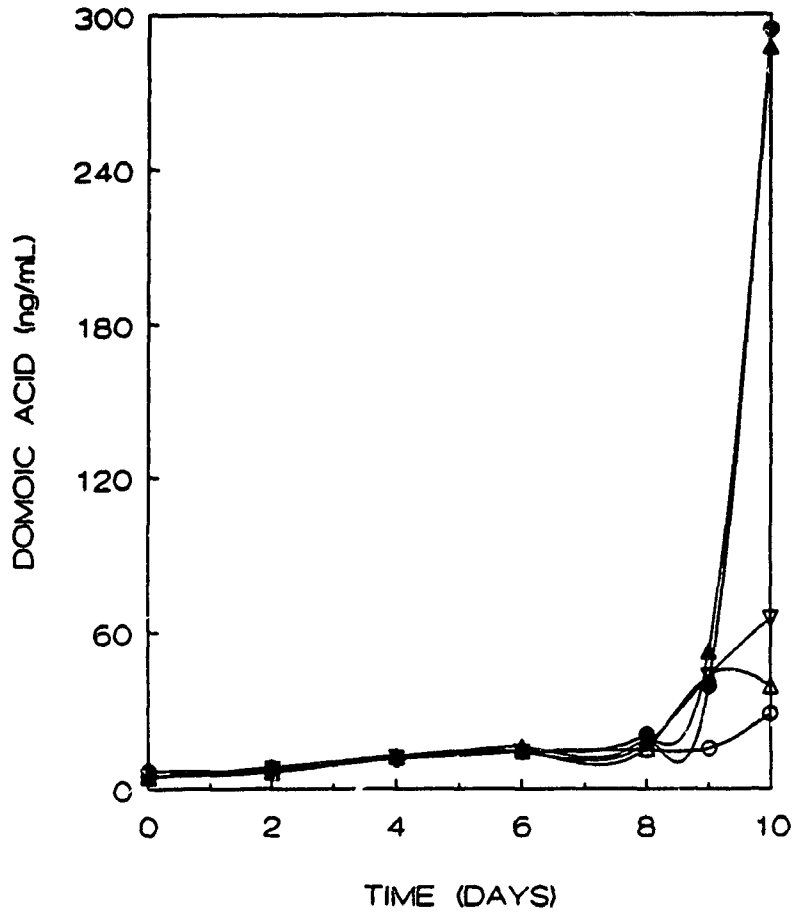

FIGURE 76: THE EFFECT OF GLIOTOXIN ON DOMOIC ACID PRODUCTION BY *PSEUDONITZSCHIA PUNGENS* F. *MULTISERIES* STRAIN KP59/2 (the open symbols represent the triplicate samples with gliotoxin added on day 9 to a final concentration of 5 µM; the solid symbols represent the two control samples)

9 showed a marked decrease in optical density and a cessation of domoic acid production on day 10 (Figs. 75 and 76). This is in contrast to the two control cultures, which showed an increase in optical density and a dramatic increase in domoic acid production between days 9 and 10.

Cultures of *Pseudonitzschia pungens* f. *multiseries* strain KP59/2 with gliotoxin added on day 13 during the stationary phase of growth to final concentrations of 0.5 µM and 0.05 µM showed a significant decrease in optical density two days later in comparison to control cultures without gliotoxin added (Table 8). Cultures with final concentrations of gliotoxin of 0.005 µM and 0.0005 µM did not differ significantly in optical density from the control cultures. Levels of domoic acid did not differ significantly between the cultures with gliotoxin added to final concentrations of 0.5 µM, 0.05 µM, 0.005 µM and 0.0005 µM when compared with the control cultures (Table 9).

When (+)-limonene was added to cultures of *Pseudonitzschia pungens* f. *multiseries* strain KP59/2 on day 13 during the stationary phase of growth to final concentrations of 0.5 µM, 0.05 µM, and 0.005 µM, a significant decrease was noted in optical density two days later when compared to the control without (+)-limonene added (Table 10). No significant difference was noted between cultures containing 0.0005 µM

TABLE 8: THE EFFECTS OF GLIOTOXIN ON THE GROWTH OF *PSEUDONITZSCHIA PUNGENS* F. *MULTISERIES* STRAIN KP59/2 (T = number of days of culture growth when a sample was removed for analysis; Gliotoxin was added on day 13).

Final media concentration of gliotoxin	OPTICAL DENSITIES T=9 AVG	T=9 STD	T=13 AVG	T=13 STD	T=15 AVG	T=15 STD
0.5 µM	0.056	0.014	0.068	0.005	0.043	0.003
0.05 µM	0.050	0.014	0.064	0.009	0.056	0.002
0.005 µM	0.063	0.012	0.077	0.004	0.074	0.003
0.0005 µM	0.059	0.015	0.081	0.006	0.082	0.007
CONTROL	0.056	0.016	0.065	0.006	0.075	0.006

PAIRWISE T-TEST FOR OPTICAL DENSITY AT T=15:

0.5 µM	CONTROL	SIGNIFICANT
0.05 µM	CONTROL	SIGNIFICANT
0.005 µM	CONTROL	NOT SIGNIFICANT
0.0005 µM	CONTROL	NOT SIGNIFICANT

TABLE 9: THE EFFECTS OF GLIOTOXIN ON DOMOIC ACID PRODUCTION BY *PSEUDONITZSCHIA PUNGENS* F. *MULTISERIES* STRAIN KP59/2 (T = number of days of culture growth when a sample was removed for analysis; Gliotoxin was added on day 13).

Final media concentration of gliotoxin	DOMOIC ACID LEVELS (ng/mL)					
	T=9		T=13		T=15	
	AVG	STD	AVG	STD	AVG	STD
0.5 µM	26.0	2.1	204.1	38.3	211.8	39.3
0.05 µM	27.5	2.9	195.0	28.0	196.9	17.1
0.005 µM	35.9	14.4	204.7	11.3	266.2	32.6
0.0005 µM	30.8	5.5	201.2	67.3	260.1	61.5
CONTROL	30.7	1.8	209.7	39.5	265.5	41.9

PAIRWISE T-TEST OF DOMOIC ACID LEVELS AT T=15:

0.5 µM	CONTROL	NOT SIGNIFICANT
0.05 µM	CONTROL	NOT SIGNIFICANT
0.005 µM	CONTROL	NOT SIGNIFICANT
0.0005 µM	CONTROL	NOT SIGNIFICANT

TABLE 10: THE EFFECTS OF (+)-LIMONENE ON THE GROWTH OF *PSEUDONITZSCHIA PUNGENS* F. *MULTISERIES* STRAIN KP59/2 (T = number of days of culture growth when a sample was removed for analysis; (+)-Limonene was added on day 13).

Final media concentration of limonene	OPTICAL DENSITIES T=9 AVG	T=9 STD	T=13 AVG	T=13 STD	T=15 AVG	T=15 STD
0.5 µM	0.073	0.005	0.081	0.006	0.072	0.002
0.05 µM	0.049	0.027	0.078	0.007	0.072	0.009
0.005 µM	0.023	0.030	0.067	0.017	0.078	0.006
0.0005 µM	0.025	0.012	0.076	0.006	0.083	0.003
CONTROL	0.015	0.004	0.087	0.002	0.090	0.004

PAIRWISE T-TEST FOR OPTICAL DENSITY AT T=15:

0.5 µM	CONTROL	SIGNIFICANT
0.05 µM	CONTROL	SIGNIFICANT
0.005 µM	CONTROL	SIGNIFICANT
0.0005 µM	CONTROL	NOT SIGNIFICANT

(+)-limonene when compared to the control. Domoic acid levels were not significantly different between the control and the cultures with 0.05 µM, 0.005 µM and 0.0005 µM (+)-limonene. However, a significant increase in domoic acid was observed in the culture with 0.5 µM (+)-limonene added in comparison to the control (Table 11).

TABLE 11: THE EFFECTS OF (+)-LIMONENE ON DOMOIC ACID PRODUCTION BY *PSEUDONITZSCHIA PUNGENS* F. *MULTISERIES* STRAIN KP59/2
(T = number of days of culture growth when a sample was removed for analysis; (+)-Limonene was added on day 13).

Final media concentration of limonene	DOMOIC ACID LEVELS (ng/mL) T=9 AVG	T=9 STD	T=13 AVG	T=13 STD	T=15 AVG	T=15 STD
0.5 µM	35.4	2.7	239.5	26.6	292.4	39.0
0.05 µM	48.9	37.4	222.2	104.3	279.0	45.2
0.005 µM	18.7	5.2	127.2	105.1	182.8	106.3
0.0005 µM	24.9	3.3	147.0	26.5	266.3	80.7
CONTROL	24.5	5.9	86.7	61.9	223.9	16.7

PAIRWISE T-TEST OF DOMOIC ACID LEVELS AT T=15:

0.5 µM	CONTROL	SIGNIFICANT INCREASE
0.05 µM	CONTROL	NOT SIGNIFICANT
0.005 µM	CONTROL	NOT SIGNIFICANT
0.0005 µM	CONTROL	NOT SIGNIFICANT

DISCUSSION

In each kainic acid prenyltransferase assay with a different ^{14}C-labelled precursor added, intense radioactive spots were observed in the control without the crude extract; these resulted from the exogenous ^{14}C-labelled precursor added. With L[1-^{14}C]-glutamate, [1,5-^{14}C]-citrate, and [1-^{14}C]-α-ketoglutarate the major spots had R_f values of 0.24, 0.03, and 0.22, respectively. The spot with an R_f value of 0.24 also corresponded to a purple ninhydrin-staining product and had a similar R_f value to that reported for glutamic acid using the same TLC system (Pataki, 1968). In the prenyltransferase assay with [1-^{14}C]-glutamate added, the reduced signal of this spot (R_f 0.24) after 24 h in the triplicate samples and the control without DMAPP may result from the loss of ^{14}C as $^{14}CO_2$ due to enzymes present in the crude extract. The stronger signal in the control without DMAPP and the crude extract (G5) supports this argument.

In the kainic acid prenyltransferase assay with [1,5-^{14}C]-citrate added, a faint radioactive spot (R_f 0.24) was noted after 24 h in the triplicate samples and the control without DMAPP but was not present in the control without DMAPP and the crude extract. This R_f value is similar to that of glutamic acid, indicating that the [1,5-^{14}C]-citric acid may have been converted to ^{14}C-labelled glutamic acid. The common pathway

of conversion of citric acid to glutamic acid requires the activity of the citric acid cycle enzymes aconitase and isocitrate dehydrogenase in addition to one of several possible transaminating enzymes.

In the third prenyltransferase assay with [1-^{14}C]-α-ketoglutarate added, a radioactive spot (R_f 0.24) was present after 1 h, indicating the possible presence of glutamic acid. This spot was more intense in the triplicate assay samples and the control without DMAPP, which all contained the crude extract. This suggests that enzymes present in the crude protein extract resulted in the transamination of [1-^{14}C]-α-ketoglutarate to produce ^{14}C-labelled glutamic acid. After 24 h the R_f 0.22 spot disappeared while the R_f 0.24 spot increased in intensity in all those samples with the crude extract included. In addition, the Rf 0.24 spot corresponded to a ninhydrin staining product possibly that of glutamic acid. The control without the protein extract (A5) contained the original spot (R_f 0.22). It was difficult to distinguish these two spots (R_f 0.22 and R_f 0.24), due to their similar Rf values, suggesting that future assays may require a different solvent system.

Clearly the crude protein extract contained active enzymes as shown by the conversion of citrate and α-ketoglutarate to glutamate. In addition, malate

dehydrogenase in the extract converted oxaloacetate to malate with the concurrent oxidation of NADH to NAD+. The lack of activity of the kainic acid prenyltransferase suggests that the conditions of the assays were not optimal. Temperature, pH, buffer type and concentration, and metal types and concentrations were determined for use in the preliminary kainic acid prenyltransferase assay based on published prenyltransferase assays in plant extracts (Biggs et al., 1987; Hamerski et al., 1990a, Lee et al., 1976; Schroder et al., 1979; Zahringer et al., 1981). Unknown cofactors not present may be required for activity (Eisenthal and Danson, 1992; Scopes, 1987). A crude extract was used in the assay for the prenyltransferase involved in kainic acid biosynthesis since several of the purified prenyltransferases are associated with membrane systems (Hamerski et al., 1990b; Schroder et al., 1979; Zahringer et al., 1981). The crude extract, however, may contain inhibitors of the prenyltransferase in kainic acid biosynthesis. Many of these considerations can be dealt with by varying each condition and assaying for activity. A greater problem is the lack of knowledge of the specific substrates required by the enzyme. Although the domoic acid biosynthetic studies in Chapter One revealed that an activated citric acid cycle product was involved, the specific compound is unknown. The ^{14}C-labelled metabolites added to the assay may not be identical to or readily convertible to the substrates required by the kainic

acid prenyltransferase. Modifications of the precursors by other enzymes may also be required before the prenyltransferase will recognize the precursor and catalyze the reaction. The use of labelled DMAPP or GPP instead of labelled citric acid cycle intermediates may prove more successful.

Gliotoxin, in final culture concentrations of 5 µM, 0.5 µM and 0.05 µM, had a negative effect on the growth of *P. pungens* f. *multiseries* strain KP59/2, as indicated by the significant decrease in optical density when compared to the control cultures. A significant decrease in domoic acid production was only noted at the final gliotoxin concentration of 5 µM when growth of the culture was severely affected. At the lower concentrations when growth was not affected, gliotoxin did not appear to inhibit domoic acid biosynthesis. This lack of inhibition of domoic acid biosynthesis may result from differences between the process of prenylation in domoic acid and proteins. In domoic acid biosynthesis a N atom is supposedly prenylated with a C10 isoprenoid chain, whereas in protein prenylation a S atom is prenylated by a C15 or C20 chain. Further understanding of the mechanism of gliotoxin inhibition in protein prenylation may provide insights into why the compound does not inhibit the process in domoic acid synthesis.

(+)-Limonene, in final concentrations of 0.5 µM, 0.005 µM and 0.005 µM also significantly decreased the growth of *P. pungens* f. *multiseries* strain KP59/2. A significant increase in domoic acid production was noted in the culture with a final (+)-limonene concentration of 0.5 µM when compared to the control cultures. Many secondary metabolites are produced at higher levels under conditions of stress (Vining, 1990); alternately, (+)-limonene may somehow trigger an increase in the synthesis of the activated citrate intermediate.

(+)-Limonene appears to target the prenyltransferase in protein prenylation instead of acting as a substitute isoprenoid (Crowell et al., 1991). The lack of inhibition of domoic acid biosynthesis by (+)-limonene suggests that the prenyltransferase involved is significantly different from that involved in protein prenylation. Isolation of the prenyltransferase utilized in domoic acid biosynthesis would confirm if this is in fact the case.

CONCLUSION

The pathway of domoic acid biosynthesis in the diatom *Pseudonitzschia pungens* f. *multiseries* was investigated using both ^{13}C- and ^{14}C-labelled putative precursors. The labelling patterns of domoic acid resulting when [1,2-^{13}C]-acetate was fed to *P. pungens* f. *multiseries* strain 13CC from Galveston, TX, led to the conclusion that domoic acid is biosynthesized by condensation of an isoprenoid chain with a product of the citric acid cycle. A similar [1,2-^{13}C]-acetate-derived labelling pattern in domoic acid produced by *P. pungens* f. *multiseries* strain KP59/2 from Cardigan Bay, P.E.I. confirmed that the pathway was similar in the two geographically separated strains.

The time of addition of the [1,2-^{13}C]-acetate to the culture did not affect the labelling pattern, revealing that isoprenoid synthesis occurs at the same time as the synthesis of the citric acid cycle product. The labelling pattern in the citric acid cycle-derived portion of domoic acid showed that the ^{13}C-labelled acetate had gone through multiple rounds of the citric acid cycle. The only organelle that appears to have a complete citric acid cycle is the mitochondrion (Chen and Gadal, 1990; Graham, 1980), which suggests that the citric acid cycle product was synthesized in this organelle. The consistently lower level of ^{13}C enrichment and the presence of

single label due to scrambling in the isoprenoid sidechain implied that the acetate used in isoprenoid synthesis originated from a different pool than that used for the citric acid cycle product. Many isoprenoid compounds in plants are synthesized in the chloroplast (Kleinig and Beyer, 1985), suggesting this organelle as a possible site of synthesis of the isoprenoid chain in domoic acid biosynthesis by *Pseudonitzschia* spp. The lower levels of ^{13}C enrichment possibly result from slower transport rates of ^{13}C-labelled acetate through the four membranes surrounding the chloroplast or dilution of the labelled acetate with a larger natural abundance pool that is used by other biosynthetic pathways. The localization of domoic acid synthesis within the cell may provide interesting insights into the source of both the isoprenoid chain and the citric acid cycle derivative.

The [2-^{13}C,$^{2}H_3$]-acetate labelling experiment revealed that the hydroxyl group of isocitrate was oxidized to a ketone before the transamination reaction, suggesting that the citric acid cycle product that condenses with the isoprenoid chain may be an activated glutamate derivative. The ^{14}C-labelled citrate, α-ketoglutarate and glutamate feeding experiments also showed that glutamate may be a more direct precursor than citrate, but the low levels of enrichment precluded further experiments using these compounds labelled with ^{13}C. The low level of incorporation of these precursors into domoic acid

may result from the inaccessibility of the enzymes involved in domoic acid biosynthesis, or through loss of the ^{14}C-label as $^{14}CO_2$ during multiple rounds of the citric acid cycle. This latter explanation would also account for the wide variation in ^{14}C-labelled domoic acid noted between the Fernbachs for each putative precursor added.

In the search for intermediates in kainic acid biosynthesis an unknown secondary amino acid was observed, purified, and identified as 1'-hydroxydihydrokainic acid. This compound is probably formed by hydration of kainic acid and is not an intermediate in kainic acid biosynthesis. 1'-Hydroxydihydrokainic acid is able to chelate calcium and copper. Whether this compound plays a detoxifying role in the cell is unknown and requires further study.

Gliotoxin and (+)-limonene, known inhibitors of protein prenyltransferases, did not inhibit domoic acid production when diluted below the concentration that affects the growth of the cells of *P. pungens* f. *multiseries* strain KP59/2. (+)-Limonene, at a more dilute concentration, actually resulted in an increase in domoic acid levels. This may result from stress to the cells, or (+)-limonene may somehow stimulate the production of the citric acid cycle precursor. The lack of inhibition suggests that the prenyltransferase in domoic acid synthesis is significantly different from that

involved in protein prenylation. Purification of the domoic acid prenyltransferase would allow the determination of the role of (+)-limonene in domoic acid production.

Preliminary kainic acid prenyltransferase assays with [1,5-^{14}C]-citrate, [1-^{14}C]-α-ketoglutarate or [1-^{14}C]-glutamate added as putative precursors did not produce radioactive kainic acid. The conditions of the assays may not have been optimal for activity of the enzyme or these compounds may not be direct precursors of kainic acid. Future research in this area should involve an investigation of the enzyme assay conditions, and should include the use of other precursors, such as ^{14}C-DMAPP or ^{14}C-GPP. An assay for the prenyltransferase involved in domoic acid biosynthesis may also prove more successful.

APPENDIX

THE CONSTRUCTION OF A cDNA LIBRARY FROM *PSEUDONITZSCHIA PUNGENS* F. *MULTISERIES* STRAIN 13CC

A cDNA library from the pennate diatom *Pseudonitzschia pungens* f. *multiseries* 13CC was constructed for use in future isolation of the genes involved in domoic acid biosynthesis.

Total RNA was isolated from mid- and late-log axenic *Pseudonitzschia pungens* f. *multiseries* strain 13CC cells and from late-log axenic cells of *Pseudonitzschia pungens* f. *pungens* Brud C using the following method. Culture conditions and cell harvest method used are described in Chapter One. The cells were lysed in a lysis buffer [25 mL final volume; 25 mM tris, pH 8.5, 120 mM NaCl, 10 mM (ethylenedinitrilo)tetraacetic acid pH 7.0, 2% sodium dodecyl sulphate and 0.1 mg/mL proteinase K] at room temperature for 30 min. The sample was then extracted twice with phenol (25 mL) followed by a chloroform/isoamyl alcohol solution (25 mL) as outlined in Sambrook et al. (1989). The nucleic acids were precipitated by the addition of 5 M NaCl (1 mL) and 100 % isopropanol (15.6 mL). After overnight at -20°C the sample was centrifuged at 10,000 xg for 30 min. The pellet was resuspended in sterile dH_2O (5 mL) and 4M LiCl (5 mL) was added. After 12 h at 4°C the sample was centrifuged at 10,000 xg for 10 min and the resulting pellet was then resuspended in 3 mL sterile dH_2O. Following the addition of 5 M NaCl

(120 µL) and 95% ethanol (6 mL) to the sample, it was placed overnight at -20°C. The sample was centrifuged at 10,000 xg for 10 min, air-dried and the RNA precipitated by the addition of 2.5 M sodium acetate (0.24 mL) and 95% ethanol (4 mL). The RNA was stored at -70°C. Yields were approximately 3 mg/ 5 g cells. Poly A mRNA was isolated from the total RNA of the mid- and late-log *Pseudonitzschia pungens* f. *multiseries* strain 13CC cells using the Invitrogen Fast Track mRNA isolation kit (Invitrogen, CA) with final yields of 11 µg and 13 µg, respectively. A cDNA library from *P. pungens* f. *multiseries* strain 13CC late-log mRNA was constructed using the Stratagene ZAP-cDNA synthesis kit (Stratagene, CA). The total cDNA library size is 7.9 x 10^5 recombinants of which 2.5[illegible] x 10^5 recombinants have inserts of 1 kilobase (Kb) or larger and 5.3 x 10^5 recombinants have inserts of 0.5 to 1 Kb.

BIBLIOGRAPHY

Anderson, D.M. 1989. Toxin variability in *Alexandrium* species. In Graneli, E., B. Sundstrom, L. Edler and D.M. Anderson [ed.] Toxic marine phytoplankton. Proceedings of the fourth international conference on toxic marine phytoplankton, Lund, Sweden June 26-30, 1989. pp. 41-51.

Aune, T. and M. Yndestad. 1993. Diarrhetic shellfish poisoning. In I.R. Falconer [ed.] Algal toxins in seafood and drinking water. Academic Press, Toronto. pp. 87-104.

Austin, D.J. and S.A. Brown. 1973. Furanocoumarin biosynthesis in *Ruta graveolens* cell cultures. Phytochemistry 12: 1657-1667.

Baden, D.G. and V.L. Trainer. 1993. Mode of action of toxins of seafood poisoning. In I.R. Falconer [ed.] Algal toxins in seafood and drinking water. Academic Press, Toronto. pp. 49-74.

Balansard, G., A. Gayte-Sorbier, C. Cavalli and M. Dani. 1982. Acides amines de Corse *Alsidium helminthocorton* Kutzing, de *Jania rubens* Lamx. et de *Corallina officinalis* L. Ann. Pharmaceutiques Francaises 40: 527-534.

Bartz, J.K., L.K. Kline and D. Soll. 1970. N^6-(2-isopentenyl)adenosine: biosynthesis *in vitro* in transfer RNA by an enzyme purified from *Escherichia coli*. Biochem. Biophys. Res. Comm. 40: 1481-1487.

Bates, S.S., C.J. Bird, R.K. Boyd, A.S.W. deFreitas, M. Falk, R.A. Foxall, L.A. Hanic, W.D. Jamieson, A.W. McCulloch, P. Odense, M.A. Quilliam, P.G. Sim, P. Thibault, J.A. Walter and J.L.C. Wright. 1988. Investigations on the source of domoic acid responsible for the outbreak of amnesic shellfish poisoning (ASP) in eastern Prince Edward Island. Atlantic Research Laboratory, Halifax, N.S. Technical Report 57. 59 pp.

Bates, S.S., C.J. Bird, A.S.W. deFreitas, R. Foxall, M. Gilgan, L.A. Hanic, G.R. Johnson, A.W. McCulloch, P. Odense, R. Pocklington, M.A. Quilliam, P.G. Sim, J.C. Smith, D.V. Subba Rao, E.C.D. Todd, J.A. Walter and J.L.C. Wright. 1989a. Pennate diatom *Nitzschia pungens* as the primary source of domoic acid, a toxin in shellfish from eastern Prince Edward Island, Canada. Can. J. Aquat. Sci. 46: 1203-1215.

Bates, S.S., A. deFreitas, R. Pocklington, M. Quilliam and J.C. Smith. 1989b. Factors influencing the production and release of domoic acid by the diatom *Nitzschia pungens*:

nutrient and light limitation In S.S. Bates and J. Worms [ed.] Proceedings of the first Canadian workshop on harmful marine algae. Gulf Fisheries Centre, Moncton, N.B. September 27-28, 1989. Can. Tech. Rep. Fish. Aquat. Sci. 1712: 13.

Bax, A. and S. Subramanian. 1986. Sensitivity-enhanced two-dimensional heteronuclear shift correlation NMR spectroscopy. J. Mag. Reson. 67: 565-569.

Biggs, D.R., R. Welle, F.R. Visser and H. Grisebach. 1987. Dimethylallylpyrophosphate:3,6-dihydroxypterocarpan 10-dimethylallyl transferase from *Phaseolus vulgaris*. FEBS Lett. 220: 223-226.

Biggs, D.R., R. Welle and H. Grisebach. 1990. Intracellular localization of prenyltransferases of isoflavonoid phytoalexin biosynthesis in bean and soybean. Planta 181: 244-248.

Bracher, D. and T.M. Kutchan. 1992. Strictosidine synthase from *Rauvolfia serpentina*: analysis of a gene involved in indole alkaloid biosynthesis. Arch. Biochem. Biophys. 294: 717-723.

Burckle, L.H. 1978. Marine Diatoms. In Haq. B.U. and A. Boersma [ed.]. Introduction to marine micropaleontology. Elsevier Biomedical, New York. pp. 245-266.

Cembella, A.D. and E. Todd. 1993. Seafood toxins of algal origin and their control in Canada. In I.R. Falconer [ed.] Algal toxins in seafood and drinking water. Academic Press, Toronto. pp. 129-144.

Chang, F.H., L. Mackenzie, D. Till, D. Hannah and L. Rhodes. 1993. The first toxic shellfish outbreaks and the associated phytoplankton blooms in early 1993 in New Zealand. Sixth International Conference on Toxic Marine Phytoplankton. Nantes, France. October 18-22, 1993.

Chen, R. and P. Gadal. 1990. Structure, functions and regulation of NAD and NADP dependent isocitrate dehydrogenases in higher plants and in other organisms. Plant Physiol. Biochem. 28: 411-427.

Chiang, M.T., M. Bittner, M. Silva, A. Mondaca, R. Zemelman and P.G. Sammes. 1982. A prenylated coumarin with antimicrobial activity from *Haplopappus multifolius*. Phytochemistry 21: 2753-2755.

Chou, H. and Y. Shimizu. 1987. Biosynthesis of brevetoxins. Evidence for the mixed origin of the backbone carbon chain and the possible involvement of bicarboxylic acids. J. Am. Chem. Soc. 109: 2184-2185.

Clarke, S. 1992. Protein isoprenylation and methylation at carboxyl-terminal cysteine residues. Annu. Rev. Biochem. 61: 355-386.

Clarke, S.E., J. Stuart and J. Sanders-Loehr. 1987. Induction of siderophore activity in *Anabaena* spp. and its moderation of copper toxicity. Appl. Environ. Microbiol. 53: 917-922.

Connolly, D.E. and M.E. Winkler. 1989. Genetic and physiological relationships among the *miaA* gene, 2-methylthio-N^6-(2-isopentenyl)-adenosine tRNA modification, and spontaneous mutagenesis in *Escherichia coli* K-12. J. Bacteriol. 171: 3233-3246.

Cormier, P. 1994. M.Sc. Thesis. In progress.

Crowell, P.L., R.R. Chang, Z. Ren, C.E. Elson and M.N. Gould. 1991. Selective inhibition of isoprenylation of 21-26 kDa proteins by the anticarcinogen *d*-limonene and its metabolites. J. Biol. Chem. 266: 17679-17685.

Davisson, V.J., A.B. Woodside and C.D. Poulter. 1985. Synthesis of allylic and homoallylic isoprenoid pyrophosphates. Methods in Enzymol. 110: 130-144.

Davisson, V.J., A.B. Woodside, T.R. Neal, K.E. Stremler, M. Muehlbacher and C.D. Poulter. 1986. Phosphorylation of isoprenoid alcohols. J. Org. Chem. 51: 4768-4779.

Debonnel, G., M. Weiss and C. de Montigny. 1990. Neurotoxic effect of domoic acid: mediation by kainate receptor electrophysiological studies in the rat. In I. Hynie and E.C.D. Todd [ed.] Proceedings of a symposium on domoic acid toxicity. Ottawa, Ont. April 11-12, 1989. Canada Diseases Weekly Report 16S1E: 59-68.

Dhillon, D.S. and S.A. Brown. 1976. Localization, purification, and characterization of dimethylallylpyrophosphate :umbelliferone dimethylallyltransferase from *Ruta graveolens*. Arch. Biochem. Biophys. 177: 74-83.

Dickey, R.W., G.A. Fryxell, H.R. Granade and D. Roelke. 1992. Detection of the marine toxins okadaic acid and domoic acid in shellfish and phytoplankton in the Gulf of Mexico. Toxicon 30: 355-359.

Douglas, D.J. and S.S. Bates. 1992. Production of domoic acid, a neurotoxic amino acid, by an axenic culture of the marine diatom *Nitzschia pungens* f. *multiseries* Hasle. Can. J. Fish. Aquat. Sci. 49: 85-90.

Ege, S. 1989. Organic chemistry. 2nd Edition. D.C. Heath and Company, Toronto.

Eisenthal, R. and M.J. Danson. 1992. Enzyme assays, a practical approach. IRL Press, New York.

Ellis, B.E and S.A. Brown. 1974. Isolation of dimethylallyl pyrophosphate:umbelliferone dimethylallyltransferase from *Ruta graveolens*. Can. J. Biochem. 52: 734-738.

Fessenden, R.S. and J.S. Fessenden. 1982. Organic chemistry. 2nd edition. Willard Grant Press, Boston.

Flugge, U. and H. W. Heldt. 1991. Metabolite translocators of the chloroplast envelope. Annu. Rev. Plant Physiol. Mol. Biol. 42: 129-144.

Forbes, J.R. and R. Chiang. 1994. Geographic and temporal variability of domoic acid in samples collected for seafood inspection in British Columbia, 1992-1994. Abstract. Fourth Canadian Workshop on Harmful Marine Algae. Sydney, B.C. May 3-5, 1994.

Fritz, L., M.A. Quilliam, J.A. Walter, J.L.C. Wright, A.M. Beale and T.M. Work. 1992. An outbreak of domoic acid poisoning attributed to the pennate diatom *Pseudonitzschia australis*. J. Phycol. 28: 439-442.

Fryxell, G.A., M.E. Reap and D.L. Valencic. 1990. *Nitzschia pungens* Grunow f. *multiseries* Hasle: observations of a known neurotoxic diatom. Nova Hedwigia Beih. 100: 171-178.

Garrison, D.L., S.M. Conrad, P.P. Eilers and E.M. Waldron. 1992. Confirmation of domoic acid production by *Pseudonitzschia australis* (Bacillariophyceae) cultures. J. Phycol. 28: 604-607.

Garson, M.J. 1993. The biosynthesis of marine natural products. Chem. Rev. 93: 1699-1733.

Goodman, L.E., S.R. Judd, C.C. Farnsworth, S. Powers, M.H. Gelb, J.A. Glomset and F. Tamanoi. 1990. Mutants of *Saccharomyces cerevisiae* defective in the farnesylation of Ras proteins. Proc. Natl. Acad. Sci. USA 87: 9665-9669.

Goodwin, T.W. and E.I. Mercer. 1983. Introduction to plant biochemistry. 2nd edition. Pergamon Press, New York.

Graham, D. 1980. Effects of light on "dark" respiration. The biochemistry of plants 2: 525-579.

Grundon, M.F. 1988. Quinoline, acridone, and quinazoline

alkaloids: chemistry, biosynthesis, and biological properties. Alkaloids: chemical and biological perspectives. 6: 339-522.

Guillard, R.R.L. 1975. Culture of phytoplankton for feeding marine invertebrates. In W.L. Smith and M.H. Chanley [ed.] Culture of marine invertebrate animals. Plenum Press, New York, NY. p. 29-60.

Gupta, S., M. Norte and Y. Shimizu. 1989. Biosynthesis of saxitoxin analogues: the origin and introduction mechanism of the side-chain carbon. J. Chem. Soc., Chem. Commun. 1989: 1421-1424.

Hamerski, D. and U. Matern. 1988. Elicitor-induced biosynthesis of psoralens in *Ammi majus* L. suspension cultures. Eur. J. Biochem. 171: 369-375.

Hamerski, D., R.C. Beier, R.E. Kneusel, U. Matern and K. Himmelspach. 1990a. Accumulation of coumarins in elicitor-treated cell suspension cultures of *Ammi majus*. Phytochemistry 29: 1137-1142.

Hamerski, D., D. Schmitt and U. Matern. 1990b. Induction of two prenyltransferases for the accumulation of coumarins in elicitor-treated *Ammi majus* cell suspension cultures. Phytochemistry 29: 1131-1135.

Hampson, D.R., C.J. Dechesne and R.J. Wenthold. 1990. The molecular characterization of a putative kainic acid receptor. In I. Hynie and E.C.D. Todd [ed.] Proceedings of a symposium on domoic acid toxicity. Ottawa, Ont. April 11-12, 1989. Canada Diseases Weekly Report 16S1E: 69-71.

Horner, R.A. J.R. Postel and S.E. Hinds. 1994. Blooms of *Pseudonitzschia* spp. in western Washington waters. Abstract. American Society of Limnology and Oceanography and the Phycological Society of America conference, Miami, Florida. June 12-16, 1994.

Impellizzeri, G., S. Mangiafico, G. Oriente, M. Piatelli, S. Sciuto, E. Fattorusso, S. Magno, C. Santacroce and D. Sica. 1975. Amino acids and low molecular weight carbohydrates of some marine red algae. Phytochemistry 14: 1549-1557.

Kao, C.Y. 1993. Paralytic shellfish poisoning. In I.R. Falconer [ed.] Algal toxins in seafood and drinking water. Academic Press, Toronto. pp. 75-86.

Kessler, H., M. Gehrke and C. Grieringer. 1988. Two dimensional NMR spectroscopy: background and overview of the experiments. Agnew. Chem. Int. Ed. Engl. 27: 490-536.

Kitto, G.B. 1969. Intra- and extramitochondrial malate dehydrogenases from chicken and tuna heart. Methods in Enzymol. 8: 106-116.

Kleinig, H. and P. Beyer. 1985. Carotene synthesis in spinach (*Spinacia oleracea* L.) chloroplasts and daffodil (*Narcissus pseudonarcissus* L.) chromoplasts. Methods in Enzymol. 110: 267-273.

Konno, K., K. Hashimoto, Y. Ohfune, H. Shirahama and T. Matsumoto. 1988. Acromelic acids A and B. Potent neuroexcitory amino acids isolated from *Clitocybe acromelalga*. J. Am. Chem. Soc. 110: 4807-4815.

Kutchan, T.M., H. Dittrich, D. Bracher and M.H. Zenk. 1991. Enzymology and molecular biology of alkaloid biosynthesis. Tetrahedron 47: 5945-5954.

Laycock, M.V., A.S.W. deFreitas and J.L.C. Wright. 1989. Glutamate agonists from marine algae. J. Applied. Phycol. 1: 113-122.

Lee, S., H.G. Floss and P. Heinstein. 1976. Purification and properties of dimethylallylpyrophosphate: tryptophan dimethylallyl transferase, the first enzyme of ergot alkaloid biosynthesis of *Claviceps*. Arch. Biochem. Biophys. 177: 84-94.

Lee, M.S., D.J. Repeta and K. Nakanishi. 1986. Biosynthetic origins and assignments of ^{13}C NMR peaks of brevetoxin B. J. Am. Chem. Soc. 108: 7855-7856.

Lee, M.S., G. Qin, K. Nakanishi and M.G. Zagorski. 1989. Biosynthetic studies of brevetoxins, potent neurotoxins produced by the dinoflagellate *Gymnodinium breve*. J. Am. Chem. Soc. 111: 6234-6241.

Lehner, K. and H.W. Heldt. 1978. Dicarboxylate transport across the inner membrane of the chloroplast envelope. Biochim. Biophys. Acta 501: 531-544.

Letham, D.S. and L.M.S. Palni. 1983. The biosynthesis and metabolism of cytokinins. Annu. Rev. Plant Physiol. 34: 163-197.

Lincoln, R.A., S. Kazimierz and J.M. Walker. 1990. Biologically active compounds from diatoms. Diatom Research 5: 337-349.

Lundholm, N., J. Skov, R. Pocklington, and O. Moestrup. 1994. Toxic and potentially toxic *Pseudonitzschia* in Danish coastal waters. Abstract. Fourth Canadian Workshop on Harmful Marine Algae. Sydney, B.C. May 3-5, 1994.

Maeda, M., T. Kodama, T. Tanaka, Y. Ohfune, K. Nomoto, K. Nishimura and T. Fujita. 1984. Insecticidal and neuromuscular activities of domoic acid and its related compounds. J. Pesticide Sci., 9: 27-32.

Mann, J. 1987. Secondary Metabolism. Second Edition. Clarendon Press, Oxford.

Marshall, J.L. 1983. Carbon-carbon and carbon-proton NMR couplings: applications to organic stereochemistry and conformational analysis. In A.P. Marchand [ed.] Methods in Stereochemical analysis. Vol. 2. Verlag Chemie International, Florida. pp. 1-218.

Martin, J.L., K. Haya and D.J. Wildish. 1993. Distribution and domoic acid content of *Nitzschia pseudodelicatissima* in the Bay of Fundy. In T.J. Smayda and Y. Shimizu [ed.] Toxic phytoplankton blooms in the sea. Fifth international conference on toxic marine phytoplankton. Newport. R.I., Oct 28 - Nov 1, 1991. Elsevier Science Publishers, New York. pp. 613-618.

McLachlan, J. 1973. Growth media - marine. In J.R. Stein [ed.] Handbook of phycological methods. Cambridge University Press, Cambridge. pp. 25-51.

Mishra, V.K., F. Temelli, B. Ooraikul, P.F. Shacklock and J.S. Craigie. 1993. Lipids of the red alga, *Palmaria palmata*. Botanica Marina 36: 169-174.

Mosmaw, J.F. and P.J. Casey. 1992. Mammalian protein geranylgeranyltransferase. J. Biol. Chem. 267: 17438-17443.

Murakami, S., T. Takemoto, Z. Shimizu and K. Daigo. 1953. Effective principle of *Digenea*. Jpn. J. Pharm. Chem. 25: 571-574.

Murata, M. A.M. Legrand, Y. Ishibashi, M. Fukui and T. Yasumoto. 1990. Structures and configurations of ciguatoxin for the moray eel *Gymnothorax javanicus* and its likely precursor from the dinoflagellate *Gambierdiscus toxicus*. J. Am. Chem. Soc. 112: 4380-4386.

Nitta, I., H. Watase and Y. Tomile. 1958. Structure of kainic acid and its isomer, allokainic acid. Nature (London) 181: 761-762.

Norte, M., A. Padilla and J.J. Fernandez. 1994. Studies on the biosynthesis of the polyether marine toxin dinophysistoxin-1 (DTX-1). Tetrahedron Lett. 35: 1441-1444.

Olney, J.W. 1990. Excitotoxicity: an overview. In I. Hynie and

E.C.D. Todd [ed.] Proceedings of a symposium on domoic acid toxicity. Ottawa, Ont. April 11-12, 1989. Canada Diseases Weekly Report 16S1E: 47-58.

Parrish, C.C., A.S.W. deFreitas, G. Bodennec, E.J. Macpherson and R.G. Ackman. 1990. Unusual fatty acid composition of the toxic marine diatom *Nitzschia pungens*. Bull. Aquacul. Assoc. Canada 90-4: 15-18.

Pataki, G. 1968. Techniques of thin-layer chromatography in amino acid and peptide chemistry. Ann Arbor Science Publishers, Inc., Ann Arbor. pp. 65-97.

Perl, T.M., L. Bedard, T. Kosatsky, J.C. Hockin, E.C.D. Todd, L.A. McNutt and R.S. Remis. 1990. Amnesic shellfish poisoning: a new clinical syndrome due to domoic acid. In I. Hynie and E.C.D. Todd [ed.] Proceedings of a symposium on domoic acid toxicity. Ottawa, Ont. April 11-12, 1989. Canada Diseases Weekly Report 16S1E: 7-8.

Pei-Gen, X. and F. Shan-Lin. 1986. Traditional antiparasitic drugs in China. Parasitology Today 2: 353-355.

Pocklington, R., J.E. Milley, S.S. Bates, C.J. Bird, A.S.W. deFreitas and M.A. Quilliam. 1990. Trace determination of domoic acid in seawater and phytoplankton by high-performance liquid chromatography of the fluorenylmethoxycarbonyl (FMOC) derivative. Int. J. Environ. Anal. Chem. 38: 351-368.

Pyl, D. Van der, J. Inokoshi, K. Shiomi, H. Yang, H. Takeshima and S. Omura. 1992. Inhibition of farnesyl-protein transferase by gliotoxin and acetylgliotoxin. J. Antibiot. 45: 1802-1805.

Quilliam, M.A., P.G. Sim, A.W. McCulloch and A.G. McInnes. 1989. High-performance liquid chromatography of domoic acid, a marine neurotoxin, with application to shellfish and plankton. Int. J. Environ. Anal. Chem. 36: 139-154.

Quilliam, M.A. and J.L.C. Wright. 1989. The amnesic shellfish poisoning mystery. Anal. Chem. 61: 1053A-1060A.

Rao, D.V.S., M.A. Quilliam and R. Pocklington. 1988. Domoic acid - a neurotoxic amino acid produced by the marine diatom *Nitzschia pungens* in culture. Can. J. Fish. Aquat. Sci. 45: 2076-2079.

Rilling, H.C., E. Bruenger, W.W. Epstein and A.A. Kandutsch. 1989. Prenylated proteins: demonstration of a thioether linkage to cysteine of proteins. Biochem. Biophys. Res. Commun. 163: 143-148.

Robinson, T. 1981. The biochemistry of alkaloids. Molecular

Biology, Biochemistry and Biophysics. 2nd edition. 3: 137-140.

Roessler, P.G. 1988. Effects of silicon deficiency on lipid composition and metabolism in the diatom *Cyclotella cryptica*. J. Phycol. 24: 394-400.

Round, F.E., R.M. Crawford, and D.G. Mann. 1990. The diatoms: biology and morphology of the genera. Cambridge University Press, New York.

Sambrook, J., E.F. Fritsch and T. Maniatis. 1989. Molecular cloning. 2nd Edition. Cold Spring Harbor Laboratory Press, Cold Spring Harbor.

Schmitz, F.J. and T. Yasumoto. 1991. The 1990 Unites States-Japan seminar on bioorganic marine chemistry, meeting report. J. Nat. Prod. 54: 1469-1490.

Schroder, G., U. Zahringer, W. Heller, J. Ebel and H. Grisebach. 1979. Biosynthesis of antifungal isoflavonoids in *Lupinus albus*. Enzymatic prenylation of genistein and 2'-hydroxygenistein. Arch. Biochem. Biophys. 194: 635-636.

Scopes, R.K. 1987. Protein purification, principles and practice. 2nd Edition. Springer-Verlag, New York.

Sedgwick, B. and J.W. Cornforth. 1977. The biosynthesis of long-chain fatty acids. Stereochemical differentiation in the enzymic incorporation of chiral acetates. Eur. J. Biochem. 75: 465-479.

Shimizu, Y., M. Norte, A. Hori, A. Genenah and M. Kobayashi. 1984. Biosynthesis of saxitoxin analogues: the unexpected pathway. J. Am. Chem. Soc. 106: 6433-6434.

Shimizu, Y. 1988. The chemistry of paralytic shellfish toxins. In A.T. Tu [ed.] Handbook of natural toxins. Vol 3. Marine toxins and venoms. Marcel Dekker, Inc. New York. pp. 63-85.

Shimizu, Y. 1993. Microalgal metabolites. Chem. Rev. 93: 1685-1698.

Shinozaki, H., M. Ishida and T. Okamoto. 1986. Acromelic acid, a novel excitatory amino acid from a poisonous mushroom: effects on the crayfish neuromuscular junction. Brain Research 399: 395-398.

Silverstein, R.M., G.C. Bassler and T.C. Morrill. 1981. Spectrometric identification of organic compounds. 4th Edition. John Wiley and Sons, New York. pp. 95-138.

Sinensky, M. and R.J. Lutz. 1992. The prenylation of proteins.

Bioessays 14: 25-31.

Smayda, T.J. 1989. The global epidemic of harmful phytoplankton blooms in the sea: apparent causes and consequences. In S.S. Bates and J. Worms [ed.] Proceedings of the first Canadian workshop on harmful marine algae. Gulf Fisheries Centre, Moncton, N.B. September 27-28, 1989. Can. Tech. Rep. Fish. Aquat. Sci. 1712: 9.

Smayda, T.J. 1990. Novel and nuisance phytoplankton blooms in the sea: evidence for a global epidemic. In Graneli, E., B. Sundstrom, L. Edler and D.M. Anderson [ed.] Toxic marine phytoplankton. Proceedings of the fourth international conference on toxic marine phytoplankton, Lund, Sweden June 26-30, 1989. pp. 29-40.

Smith, J.C., R. Angus, K. Pauley, P. Cormier, S.Bates, L. Hanic, J. Worms and T. Sephton. 1989. Toxic blooms of the domoic acid-containing diatom *Nitzschia pungens* in eastern Prince Edward Island in the fall of 1988 and late summer of 1989. In S.S. Bates and J. Worms [ed.] Proceedings of the first Canadian workshop on harmful marine algae. Gulf Fisheries Centre, Moncton, N.B. September 27-28, 1989. Can. Tech. Rep. Fish. Aquat. Sci. 1712: 11.

Stoessl, A., J.B. Stothers and E.W.B. Ward. 1978. Biosynthetic studies of stress metabolites from potatoes: incorporation of sodium acetate-$^{13}C_2$ into 10 sesquiterpenes. Can. J. Chem. 56: 645-653.

Stumpf, P.K. 1980. Biosynthesis of saturated and unsaturated fatty acids. The biochemistry of plants 4: 177-204.

Taguchi, S., J.A. Hirata and E.A. Laws. 1987. Silicate deficiency and lipid synthesis of marine diatoms. J. Phycol. 23: 260-267.

Takemoto, T. and K. Daigo. 1958. Constituents of *Chondria armata* and their pharmacological effects. Chem. Pharm. Bull. 6: 578-580.

Tamanoi, F. 1993. Inhibitors of Ras farnesyltransferases. Trends in Biol. Sci. 18: 349-353.

Treimer, J.F. and M.H. Zenk. 1979. Purification and properties of strictosidine synthase, the key enzyme in indole alkaloid formation. Eur. J. Biochem. 101: 225-233.

Twiss, M.R., P.M. Welbourn and E. Schwartzel. 1993. Laboratory selection for copper tolerance in *Scenedesmus acutus* (Chlorophyceae). Can. J. Bot. 71: 333-338.

Vederas, J.C. 1987. The use of stable isotopes in biosynthetic studies. Nat. Prod. Reports 4: 277-337.

Vining, L.C. 1990. Functions of secondary metabolites. Annu. Rev. Microbiol. 44: 395-427.

Waldichuk, M. 1989. Amnesic shellfish poison. Mar. Poll. Bull. 20: 359-360.

Walter, J.A., D.M. Leek and M. Falk. 1992. NMR study of the protonation of domoic acid. Can. J. Chem. 70: 1156-1161.

Welle, R. and H. Grisebach. 1988. Induction of phytoalexin synthesis in soybean: enzymatic cyclization of prenylated pterocarpans to glyceollin isomers. Arch. Biochem. Biophys. 263: 191-198.

Werner, D. 1978. Regulation of metabolism by silicate in diatoms. In G. Bendz, I. Lindqvist [ed.] Biochemistry of silicon and related problems. Plenum Press, New York, 149-176.

Whyte, J.N.C., N.G. Ginther and L.D. Townsend. 1994. Seasonal variation in content and distribution of domoic acid in the razor clam, *Siliqua patula*, from different geographic locations in British Columbia. Abstract. Fourth Canadian Workshop on Harmful Marine Algae. Sydney, B.C. May 3-5, 1994.

Wiskich, J.T. 1977. Mitochondrial metabolite transport. Annu. Rev. Plant Physiol. 28: 45-69.

Wiskich, J.T. 1980. Control of the Krebs cycle. The biochemistry of plants 2: 243-278.

Work, T.M., A.M. Beale, L. Fritz, M.A. Quilliam, M. Silver, K. Buck and J.L.C. Wright. 1993. Domoic acid intoxication of brown pelicans and cormorants in Santa Cruz, California. In T.J. Smayda and Y. Shimizu [ed.] Toxic phytoplankton blooms in the sea. Fifth international conference on toxic marine phytoplankton. Newport. R.I., Oct 28 - Nov 1, 1991. Elsevier Science Publishers, New York. pp. 643-649.

Wright, J.L.C. 1992. Domoic acid on the west coast of America, a brief history. In J.C. Therriault and M. Levasseur [ed.] Proceedings of the third Canadian workshop on harmful marine algae. Maurice Lamontagne Institute, Mont-Joli, Quebec, May 12-14, 1992. Can Tech Rep. Fish. Aqua. Sci. 1893: 24.

Wright, J.L.C., R.K. Boyd, A.S.W. deFreitas, M. Falk, R.A. Foxall, W.D. Jamieson, M.V. Laycock, A.W. McCulloch, M.A. Quilliam, M.A. Ragan, P.G. Sim, P. Thibault, J.A. Walter, M. Gilgan, D.J.A. Richard and D. Dewar. 1989. Identification of domoic acid, a neuroexcitory amino acid, in toxic mussels from

eastern Prince Edward Island. Can J. Chem. 67: 481-490.

Wright, J.L.C., M. Falk, A.G. McInnes and J.A. Walter 1990. Identification of isodomoic acid D and two new geometrical isomers of domoic acid in toxic mussels. Can. J. Chem. 68: 22-25.

Yamano, K. and H. Shirahama. 1993. Isolation of L-N-[2-(3-pyridyl)ethyl]-glutamic acid from the poisonous mushroom *Clitocybe acromelalga*, a possible intermediate in the biogenesis of acromelic acids. Chem. Soc. Japan., Chem. Lett. 1993: 21-24.

Zahringer, U., E. Schaller and H. Grisebach. 1981. Induction of phytoalexin synthesis in soybean. Structure and reactions of naturally occurring and enzymatically prepared prenylated pterocarpans from elicitor-treated cotyledons and cell cultures of soybean. Z. Naturforsch. 36c: 234-241.

Zhu, J., R.A. Bressan and P.M. Hasegawa. 1993. Isoprenylation of the plant molecular chaperone ANJ1 facilitates membrane association and function at high temperature. Proc. Natl. Acad. Sci. 90: 8557-8561.

Zou, J.Z., M.J. Zhou and C. Zhang. 1993. Ecological features of toxic *Nitzschia pungens* Grunow in Chinese coastal waters. In T.J. Smayda and Y. Shimizu [ed.] Toxic phytoplankton blooms in the sea. Fifth international conference on toxic marine phytoplankton. Newport. R.I., Oct 28 - Nov 1, 1991. Elsevier Science Publishers, New York. pp. 651-656.